University of Missouri, St. Louis
IRL @ UMSL

Dissertations | UMSL Graduate Works

12-17-2010

ROLE OF AMYLOID BETA ASSEMBLY STATE IN THE HUMAN IMMUNE RESPONSE

Deepa Viswanathan
University of Missouri-St. Louis, viswanathand@missouri.edu

Follow this and additional works at: https://irl.umsl.edu/dissertation

 Part of the Chemistry Commons

Recommended Citation
Viswanathan, Deepa, "ROLE OF AMYLOID BETA ASSEMBLY STATE IN THE HUMAN IMMUNE RESPONSE" (2010). *Dissertations*. 444.
https://irl.umsl.edu/dissertation/444

This Dissertation is brought to you for free and open access by the UMSL Graduate Works at IRL @ UMSL. It has been accepted for inclusion in Dissertations by an authorized administrator of IRL @ UMSL. For more information, please contact marvinh@umsl.edu.

ROLE OF AMYLOID BETA ASSEMBLY STATE

IN THE HUMAN IMMUNE RESPONSE

by

DEEPA VISWANATHAN
M.S., Biochemistry, University of Missouri-St.Louis, 2006
M.S., Biochemistry, Kasturba Medical College-India, 1994
B.S., Chemistry, Bharathiar University-India, 1991

A DISSERTATION

Submitted to the Graduate School of the

UNIVERSITY OF MISSOURI- ST. LOUIS
In partial Fulfillment of the Requirements for the Degree

DOCTOR OF PHILOSOPHY

in

CHEMISTRY
with an emphasis in Biochemistry

September, 2009

Advisory Committee

Michael R. Nichols, PhD
Chairperson
Cynthia M. Dupureur, PhD
Keith J. Stine, PhD
Chung F. Wong, PhD

Dedication

This dissertation is dedicated to

My husband, Ajit

My kids, Aditi and Tejazaditya

My extended family and all of my friends

I am thankful to you all for all the love and support

ACKNOWLEDGEMENTS

I would like to express my grateful thanks to the many people who contributed to this research work. First and foremost, I would like to express my sincere gratitude to my advisor Dr. Michael R. Nichols for his unconditional support and persistent motivation right from the day I joined the PhD program. Thank you for being an excellent advisor. I would like to thank members of my committee Dr. Cynthia M. Dupureur, Dr. Keith J. Stine and Dr. Chung F. Wong for their valuable insights and comments. I would like to thank the faculty of Department of Chemistry and Biochemistry for all their support during my days as a graduate student.

I appreciate the support I had received from Dr. Philip Fraundorf and Mr. Sam (Suhan) Lin during my training days at the Center for Nanoscience. I would also like to thank Dr. Dan Zou and Dr. David Osborn for all their help with microscopy studies.

My labmates Maria L Udan, Nikkilina Crouse, Geeta Paranjape and Laura Williams made sure we had some very exciting moments in the laboratory. Thank you all for the stimulating discussions and good times we had together.

My deepest gratitude goes to my family for their untiring love and support throughout. I am indebted to my husband Ajit for keeping me always motivated towards achieving my goal. I owe immensely to my wonderful kids Aditi and Tejazaditya for trekking this path along with me!

I would also like to thank my mother-in-law Leela and my mother Rema for their emotional support throughout. Last, I would like to thank all my friends and well-wishers, both within and outside of UMSL, for their suggestions and moral support. I dedicate this to you all!

TABLE OF CONTENTS

LIST OF TABLES

LIST OF FIGURES

LIST OF ABBREVIATIONS

Aβ	Amyloid beta
AD	Alzheimer's Disease
ADDL	Aβ-derived diffusible ligands
AFM	Atomic force microscopy
APP	Amyloid precursor protein
APTES	3 Aminopropyl triethoxy Silane
BACE1	Beta-site APP-cleaving enzyme
CNS	Central nervous system
CSF	Cerebrospinal fluid
DC	Dendritic cells
DMSO	Dimethyl sulfoxide
DS	Down's syndrome
ELISA	Enzyme-linked immunosorbent assay
EM	Electron microscopy
FAD	Familial Alzheimer's disease
FBS	Fetal bovine serum
Fn	Fibronectin
FTIR	Fourier transform infrared spectroscopy
HEK	Human embryonic kidney
HFIP	Hexafluoroisopropanol
IgG	Immunoglobulin G

iNOS	Inducible nitric oxide synthase
LBP	Lipoprotein Binding Protein
LMW	Low molecular weight
LPS	Lipopolysaccharide
LTP	Long Term Potentiation
MAC	Membrane Attack Complex
MS	Mass spectrometry
MTT	3-(4,5-dimethylthiazol-2-yl)-2,diphenyltetrazolium bromide
MVB	Multivesicular bodies
NFT	Neurofibrillary tangles
NMR	Nuclear magnetic resonance
NO	Nitric oxide
NSAID	Non-steroidal anti-inflammatory drug
PAMP	Pathogen-associated molecular pattern
PBS	Phosphate buffered saline
PBS/T	Phosphate buffered saline in Tween
PMA	Phorbol 12-myristate 13-acetate
PMS	Phenazine methosulfate
PMX-B	Polymyxin-B sulfate
PRR	Pattern recognition receptor
PS1	Presennilin 1
PS2	Presennilin 2
PTFE	Polytetrafluoroethylene

PVDF	Polyvinylidene difluoride
QLS	Quasielastic light scattering spectroscopy
RAGE	Receptor for advanced glycation end products
R_H	Hydrodynamic radius
rIgG	Rat immunoglobulin G
ROS	Reactive oxygen species
RSV	Respiratory Synctytial Virus
SAD	Sporadic Alzheimer's Disease
sAPPα	soluble APP cleaved by α secretase
sAPPβ	soluble APP cleaved by β secretase
SD	Standard deviation
SDS	Sodium dodecyl sulfate
SE	Standard error
SEC	Size exclusion chromatography
SPR	Surface plasmon responance
Tg	Transgenic
ThT	Thioflavin-T
TLR	Toll-like receptor
TNFα	Tumor necrosis factor alpha
WT	Wildtype
XTT	2,3-bis(2-methoxy-4-nitro-5-sulfophenyl)-2H-tetrazolium-5-carboxanilide

ABSTRACT

Deepa Viswanathan (Ajit) . University of Missouri-Saint Louis, September 2009. Role of Amyloid Beta Assembly State in the Human Immune Response.

Major Professor: Michael R. Nichols

Alzheimer's disease (AD) is a slowly progressing neurodegenerative disease that leads to dementia. Histopathological hallmarks that characterize AD are senile plaques formed by extracellular deposition of Amyloid beta (Aβ) peptide and intracellular aggregates of hyperphosphorylated tau protein. The plaques, which are found in the brain parenchyma, comprise both 40 and 42 residue Aβ. Aggregation of Aβ is an established pathogenic mechanism in AD, but little is known about the initiation of this process *in vivo*. Several studies have revealed significant inflammatory markers such as activated microglia and cytokines surrounding the plaques. Plaques are a hallmark of AD, but they are only part of an array of Aβ aggregate morphologies observed *in vivo*. Structural polymorphism is a prominent feature of Aβ aggregation both *in vitro* and *in vivo.* The molecular relationship between the different forms of Aβ remains to be determined. Inflammatory processes are believed to contribute to AD pathophysiology, and may play an important role in the disease progression. Not all Aβ deposits evoke a proinflammatory response, making it all the more important to probe into structural details of the Aβ aggregation pathway. This research was aimed at investigating what Aβ morphology or aggregation species induce the strongest proinflammatory response in human THP-1 monocytes as a model system. Our results indicate that an intermediate fibrillar aggregation species formed when Aβ(1-42) is reconstituted in water (100 μM, pH 3.6) and incubated at 4°C under quiescent conditions was capable of stimulating maximum tumor necrosis factor alpha (TNFα). Modulating conditions that accelerated or increased Aβ(1-42) fibril formation such as temperature, peptide concentration, or pH diminished the ability to activate the cells. Immunodepletion of Aβ(1-42) solution with fibril specific antibody (OC immune serum) reduced the ability to induce TNFα production. Characterization by SEC showed an included peak that appeared immediately after the void volume and stimulated the maximum proinflammatory response. We have also shown that the shorter peptide Aβ(1-40) could not stimulate a proinflammatory response under similar aggregation conditions. Overall, the data suggest that an intermediate Aβ(1-42) fibrillar precursor species is optimal for inducing maximum proinflammatory activity in THP-1 monocytes.

BIOCHEMISTRY
including biophysical chemistry & molecular biology
Article

Biochemistry **2009,** *48,* 9011–9021 9011
DOI: 10.1021/bi9003777

Amyloid-β(1−42) Fibrillar Precursors Are Optimal for Inducing Tumor Necrosis Factor-α Production in the THP-1 Human Monocytic Cell Line[†]

Deepa Ajit, Maria L. D. Udan, Geeta Paranjape, and Michael R. Nichols*

Department of Chemistry and Biochemistry and Center for Nanoscience, University of Missouri, St. Louis, Missouri 63121

Received March 5, 2009; Revised Manuscript Received August 13, 2009

ABSTRACT: Pathological studies have determined that fibrillar forms of amyloid-β protein (Aβ) comprise the characteristic neuritic plaques in Alzheimer's disease (AD). These studies have also revealed significant inflammatory markers such as activated microglia and cytokines surrounding the plaques. Although the plaques are a hallmark of AD, they are only part of an array of Aβ aggregate morphologies observed *in vivo*. Interestingly, not all of these Aβ deposits provoke an inflammatory response. Since structural polymorphism is a prominent feature of Aβ aggregation both *in vitro* and *in vivo*, we sought to clarify which Aβ morphology or aggregation species induces the strongest proinflammatory response using human THP-1 monocytes as a model system. An aliquot of freshly reconstituted Aβ(1−42) in sterile water (100 μM, pH 3.6) did not effectively stimulate the cells at a final Aβ concentration of 15 μM. However, quiescent incubation of the peptide at 4 °C for 48−96 h greatly enhanced its ability to induce tumor necrosis factor-α (TNFα) production, the level of which surprisingly declined upon further aggregation. Imaging of the Aβ(1−42) aggregation solutions with atomic force microscopy indicated that the best cellular response coincided with the appearance of fibrillar structures, yet conditions that accelerated or increased the level of Aβ(1−42) fibril formation such as peptide concentration, temperature, or reconstitution in NaOH/PBS at pH 7.4 diminished its ability to stimulate the cells. Finally, depletion of the Aβ(1−42) solution with an antibody that recognizes fibrillar oligomers dramatically weakened the ability to induce TNFα production, and size-exclusion separation of the Aβ(1−42) solution provided further characterization of an aggregated species with proinflammatory activity. The findings suggested that an intermediate stage Aβ(1−42) fibrillar precursor is optimal for inducing a proinflammatory response in THP-1 monocytes.

The Alzheimer's disease (AD)[1] brain is decorated by a wide array of polymorphic aggregated amyloid-β (Aβ) species. The parenchymal deposits exist as a range of species from dense core neuritic plaques containing fibrillar structures to wispy, loose, and granular diffuse deposits (*1*), yet the conditions that produce these structures *in vivo* are not well understood. Furthermore, these diverse Aβ morphologies do not appear to provoke the same *in vivo* response. For example, cytopathology, such as dystrophic neurites and inflammation, is seen surrounding the plaques (*2*) in the brains of human patients (*3*) and those in AD transgenic mouse models (*4*). Inflammatory markers such as activated microglia (*4*) stained with proinflammatory cytokines (*5*) are part of the environment surrounding the plaques, while diffuse deposits are devoid of inflammatory cytopathology (*1*). A chronic inflammatory state induced by accumulated Aβ has been suggested as one of the underlying mechanisms of progressive neurodegeneration in AD (*6*) and may in fact exacerbate Aβ deposition (*7*). The plaque-associated activated microglia do not efficiently clear the deposits (*4*) unless further stimulated by infusion of anti-Aβ antibodies (*8*).

In vitro aggregation studies of Aβ have been very useful for understanding fibrillogenesis mechanisms and the structural properties of monomers, soluble intermediates, and mature fibrils. These studies have identified a continuum of Aβ species in the assembly process which vary in size, length, solubility, and morphology (*9*−*13*). Monomeric, oligomeric, protofibrillar, fibrillar, and amorphous species possess distinct toxic and biological activities and potencies (*14*−*18*).

The *in vivo* inflammatory response to Aβ has been recapitulated in numerous *in vitro* cell model systems, including both microglial and monocytic cells (*19*−*21*). Several receptors have been shown to mediate Aβ-stimulated proinflammatory cytokine production, including the receptor for advanced glycation end products (RAGE) (*22*), a multireceptor complex comprising the scavenger receptor class B (SR-B) receptor CD36, $\alpha_6\beta_1$-integrin, CD47 (*23*), and Toll-like receptors (TLR) 2 and 4 (*24*−*26*). Furthermore, the SR-A receptor has been shown to mediate Aβ-induced production of reactive oxygen species (*27*). In all of these studies, induction of an inflammatory response appeared to favor a fibrillar Aβ conformation, although different assembly states were not always investigated. Since activated microglial cells are

[†]This work was supported by Grant NIRG-06-27267 (M.R.N.) from the Alzheimer's Association, by Grant R15AG033913 (M.R.N.) from the National Institute on Aging, and by a University of Missouri-St. Louis Dissertation Fellowship (M.L.D.U.).

*To whom correspondence should be addressed: Department of Chemistry and Biochemistry, University of Missouri, St. Louis, MO 63121. Telephone: (314) 516-7345. Fax: (314) 516-5342. E-mail: nicholsmic@umsl.edu.

[1]Abbreviations: AD, Alzheimer's disease; Aβ, amyloid-β; AFM, atomic force microscopy; BSA, bovine serum albumin; FBS, fetal bovine serum; HFIP, hexafluoroisopropanol; HRP, horseradish peroxidase; IP, immunoprecipitation; LPS, lipopolysaccharide; PBS, phosphate-buffered saline; RAGE, receptor for advanced glycation end products; SR, scavenger receptor; ThT, thioflavin T; TLR, Toll-like receptor; TNFα, tumor necrosis factor-α; TEM, transmission electron microscopy.

© 2009 American Chemical Society

Published on Web 08/20/2009

typically observed clustered around the dense core plaques as opposed to the diffuse Aβ deposits (*1*), their activation appears to be selective for a particular Aβ morphology. We have previously reported that aggregated Aβ(1−42) induces TNFα production from a human monocytic cell line via TLRs (*24*). Here we further explore the optimal Aβ aggregation state for this process.

MATERIALS AND METHODS

Cell Culture. THP-1 cells were obtained from ATCC (Manassas, VA) and maintained in RPMI-1640 culture medium (HyClone, Logan, UT) containing 2 mM L-glutamine, 25 mM HEPES, 1.5 g/L sodium bicarbonate, 10% fetal bovine serum (FBS) (HyClone), 50 units/mL penicillin, 50 μg/mL streptomycin (HyClone), and 50 μM β-mercaptoethanol at 37 °C in 5% CO_2. For cellular assays, THP-1 monocytes were centrifuged, washed, and resuspended in reduced FBS (2%) growth medium. Cells were added to individual wells of a 48-well or 96-well sterile culture plate at a final concentration of 8.5×10^5 cells/mL prior to treatment with 15 μM Aβ and/or sterile water control. In some experiments, polymyxin B sulfate (Sigma, St. Louis, MO) was included to verify the proinflammatory signal was not due to lipopolysaccharide (LPS) contamination. Following incubation of the cells at 37 °C for 6−24 h, the content of each well was removed and centrifuged at 2500*g* for 10 min, and the supernatant was frozen at −20 °C for subsequent analysis.

Preparation of Aβ Peptides. Aβ(1−42) peptides (rPeptide, Bogarth, GA) were dissolved in 100% hexafluoroisopropanol (HFIP) (Sigma) for 1 h, aliquoted into sterile microcentrifuge tubes, dried in a vacuum centrifuge, and stored at −20 °C. For experiments, the lyophilized peptides were resuspended in sterile water or treated with 100 mM NaOH at 2 mM Aβ and diluted into phosphate-buffered saline (PBS, HyClone) (6.7 mM phosphate and 150 mM NaCl). Final Aβ concentrations were 100 μM, and the solutions were incubated at 4 °C unless otherwise stated. THP-1 monocytes were exposed to a final Aβ(1−42) concentration of 15 μM. Commercial Aβ lots were endotoxin-tested by several methods as previously described (*24*). Centrifugation of Aβ solutions was conducted on either a Beckman-Coulter Microfuge 18 at 18000*g* for 10 min in a 4 °C cold room, a Sorvall RC5B refrigerated centrifuge with an SS-34 rotor at 50000*g* for 1 h at 4 °C, or a refrigerated Beckman-Coulter Optima Max ultracentrifuge with a TLA120.1 rotor at 50000−150000*g* for 1 h at 4 °C. Some centrifugation experiments utilized 0.2 μm polytetrafluoroethylene (PTFE) spin filters (Millipore, Billerica, MA) at 12000*g* for 3 min to separate small aliquots (~100 μL) of Aβ aggregation solutions. Further separation was achieved via size-exclusion chromatography (SEC). SEC columns were sanitized with 0.5 M NaOH and pretreated with 1 mg of bovine serum albumin (BSA) in running buffer to block nonspecific binding to the resin. The 18000*g* Aβ(1−42) supernatants were eluted on a Superdex 75 HR 10/30 column (GE Healthcare) in 50 mM Tris-HCl (pH 8.0) at a rate of 0.5 mL/min. Collection of fractions (0.5 mL) was initiated after 2 mL of elution volume. Aβ(1−42) concentrations from SEC were determined by absorbance using an extinction coefficient of 1450 cm^{-1} M^{-1} as previously described (*28*). In some cases, Aβ concentrations were determined by the Bradford method (*29*). Some Aβ aggregation solutions were monitored by thioflavin T (ThT) fluorescence as described previously (*30*). Briefly, Aβ aliquots were removed and diluted 5-fold (20 μM) into a 5 μM ThT solution prepared in the same solution used for Aβ(1−42) reconstitution (water or PBS). In some cases, Aβ(1−42) reconstituted and aggregated in water was monitored with 5 μM ThT in 50 mM Tris-HCl (pH 8.0). ThT fluorescence emission scans (460−520 nm) were conducted on a Cary Eclipse fluorescence spectrophotometer using an excitation wavelength of 450 nm and integrated from 470 to 500 nm to produce ThT fluorescence values. When necessary, the pH was determined in Aβ solutions using a small volume microelectrode (Thermo Scientific Orion).

Determination of TNFα Levels. Measurements of the amount of secreted TNFα in the supernatants were taken by an ELISA. Briefly, 100 μL of 2−4 μg/mL monoclonal anti-human TNFα/TNFSF1A capture antibody (R&D Systems, Minneapolis, MN) was added to 96-well plates for overnight incubation at room temperature. Wells were washed with PBS (HyClone) containing 0.05% Tween 20 and blocked with 300 μL of PBS containing 1% BSA, 5% sucrose, and 0.05% NaN_3 for 1 h at room temperature. After the samples had been washed, successive treatments with washing between them were done with 50 μL samples or standards for 2 h, 100 μL of biotinylated polyclonal anti-human TNFα/TNFSF1A detection antibody (R&D Systems) in 20 mM Tris with 150 mM NaCl and 0.1% BSA for 2 h, 100 μL of streptavidin-horseradish peroxidase (HRP) (R&D Systems) diluted 200 times with PBS containing 1% BSA for 20 min, and 100 μL of equal volumes of 3,3′,5,5′-tetramethylbenzidine and hydrogen peroxide (KPL, Gaithersburg, MD) for 30 min. The reaction was stopped by the addition of a 1% H_2SO_4 solution. The optical density of each sample was analyzed at 450 nm with a reference reading at 630 nm using a SpectraMax 340 absorbance plate reader (Molecular Devices, Union City, CA). A standard curve was constructed by sequential dilution of a TNFα standard from 2000 to 15 pg/mL. The concentration of TNFα in the experimental samples was calculated from a TNFα standard curve of 15−2000 pg/mL. When necessary, samples were diluted to fall within the standard curve.

Dynamic Light Scattering (DLS). Hydrodynamic radius (R_H) measurements were taken at room temperature with a DynaPro Titan instrument (Wyatt Technology, Santa Barbara, CA). Samples (30 μL) were placed directly into a quartz cuvette, and light scattering intensity was collected at a 90° angle using a 10 s acquisition time. Particle diffusion coefficients were calculated from autocorrelated light intensity data and converted to R_H with the Stokes−Einstein equation. Data regularization with Dynamics (version 6.7.1) generated histograms of percent mass versus R_H. Intensity-weighted mean R_H values were derived from the regularized histograms.

Atomic Force Microscopy (AFM). Aβ(1−42) aggregation solutions (100 μM) were diluted to 1 μM in water. Grade V1 mica (Ted Pella, Inc., Redding, CA) was cut into 11 mm circles and affixed to 12 mm metal disks. Aliquots (50 μL) were applied to freshly cleaved mica, allowed to adsorb for 15 min, washed twice with water, air-dried, and stored in a container with desiccant. For imaging of Aβ(1−42) aggregates that were SEC-separated in 50 mM Tris-HCl, mica surfaces were pretreated with 1% 3-aminopropyl triethoxysilane (APTES) in 1 mM acetic acid for 10 min, washed with water, and air-dried prior to application of sample. Images were obtained with a Nanoscope III multimode atomic force microscope (Digital Instruments, Santa Barbara, CA) in TappingMode. Height analysis was performed using Nanoscope III software on flattened height mode images.

Transmission Electron Microscopy. Aβ aggregation solutions were diluted to 20 μM in water, and 10 μL was applied to a 200-mesh Formvar-coated copper grid (Ted Pella, Inc.). Samples were allowed to adsorb for 10 min at 25 °C, followed

by removal of the excess sample solution with a tissue wipe. Grids were washed three times by being placed sample side down on a droplet of water. Heavy metal staining of the samples was conducted in a similar manner by incubation on a droplet of 2% uranyl acetate (Electron Microscopy Sciences, Hatfield, PA) for 5 min, removal of excess solution, and air drying. Affixed samples were visualized with a JEOL JEM-2000 FX transmission electron microscope operated at 200000 eV.

OC Immunodepletion of Aβ(1−42) Solutions. Fibrillar oligomers were immunoprecipitated (IP) by addition of OC antisera (2 μL, 1:300 dilution) (gift from R. Kayed, University of Texas Medical Branch, Galveston, TX) directly to Aβ aggregation solutions (60 μL, 100 μM) and incubation without agitation for 1 h at 4 °C. Protein G-Sepharose beads (10 μL) (Sigma) were then added to the solution and incubated with slow mixing for an additional 1 h at 4 °C. The solution was centrifuged for 15 min at 18000*g*, and the supernatant (45 μL) was used to treat THP-1 monocytes.

Dot Blot Analysis. All steps in the dot blot assay were conducted at 25 °C and were modified from those in ref *31*. Briefly, 5 μL of Aβ(1−42) was applied to moist nitrocellulose, allowed to stand for 20 min, and then blocked with 10% milk in PBS with 0.2% Tween 20 (PBST). Following a wash step with PBST, the membrane was incubated with OC serum (1:5000) or Ab9 antibody (1:5000) (gift from T. Rosenberry, Mayo Clinic Jacksonville, Jacksonville, FL) for 1 h with gentle shaking, washed, and incubated with a 1:1000 dilution of an anti-rabbit IgG (OC) or anti-mouse IgG (Ab9) HRP conjugate (R&D Systems) for 1 h. After being washed, the nitrocellulose membrane was then incubated with ECL substrate and exposed to film.

XTT Cell Viability Assay. Cell viability was monitored using an XTT [2,3-bis(2-methoxy-4-nitro-5-sulfophenyl)-2*H*-tetrazolium-5-carboxanilide] cell assay (*32*). Cell metabolic activity was probed by mitochondrial-mediated reduction of XTT (Sigma). Briefly, control cells and cells exposed to Aβ for a given period of time were further incubated with final concentrations of 0.33 mg/mL XTT and 8.3 μM phenazine methosulfate (PMS) (Acros, Morris Plains, NJ) for 3 h at 37 °C. The extent of XTT reduction was determined by absorbance measurements of the reduced form of XTT at 467 nm.

RESULTS

Aβ(1−42)-Induced TNFα Production Is Dependent on Aggregation State. The amount of TNFα, a key product of the proinflammatory response, is measurably increased in postmortem AD brain sections (*5*) and microvessels (*33*), and cerebrospinal fluid (*34*) of clinically diagnosed AD patients. The THP-1 human monocytic cell line is an excellent model system for inflammatory studies, exhibits responses to stimuli similar to those of microglia, and is a particularly valuable system for studying cell activation and cytokine production by Aβ (*19*−*21*). To gain further information about the most favorable aggregation state of Aβ for inducing TNFα production, freshly reconstituted solutions of Aβ(1−42) (100 μM) were aged at 4 °C and periodically tested for their ability to stimulate TNFα production from THP-1 monocytes. Figure 1 shows that immediately upon reconstitution Aβ(1−42) induced a varying but relatively small amount of TNFα. Aging of the peptide for 48−72 h caused a dramatic increase in the level of TNFα production (Figure 1, lines 1−4). Surprisingly, further aging reduced, and ultimately abolished, the proinflammatory response (Figure 1, lines 3 and 4).

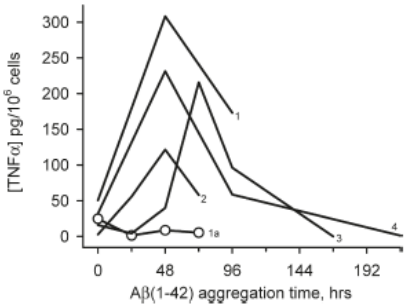

FIGURE 1: Dependence of the Aβ (1−42)-induced proinflammatory response on aggregation progression. Aβ(1−42) was reconstituted in sterile water (100 μM) and incubated at 4 °C. At various time points, aliquots were removed and incubated with THP-1 monocytes for 6 h at a final Aβ(1−42) concentration of 15 μM. The amount of secreted TNFα was measured in cell supernatants with an ELISA. Lines 1−4 represent separate 100 μM Aβ(1−42) aggregation experiments. Line 1a (○) represents a 1.2 mM Aβ(1−42) aggregation solution incubated at 25 °C prepared and tested within the same experiment as line 1.

The results from multiple experiments suggested that an intermediate Aβ(1−42) aggregation structure may be preferred for inducing TNFα production in THP-1 monocytes. Furthermore, the data demonstrate that continued aggregation from that point diminished the response.

The idea that later-stage Aβ(1−42) aggregation species were not effective inducers of TNFα production was tested further by modulating Aβ(1−42) aggregation kinetics. The initial peptide concentration was increased 12-fold, thereby accelerating aggregation. Aβ assembly occurs via a nucleation-dependent polymerization process (*35*). One of the tenets of this type of kinetics is that an increased peptide concentration can significantly shorten the lag time for nucleation which is then followed by rapid polymerization and fibril formation. In addition to an increased peptide concentration, elevated temperature also accelerates Aβ aggregation (*11*). The more concentrated solution of Aβ(1−42) (1.2 mM) was incubated at 25 °C, and aliquots were added to THP-1 monocytes the same final concentration (15 μM) as that used for the 100 μM solutions was maintained. Although a small amount of TNFα was induced at 0 h, the remaining Aβ(1−42) aggregation age time points had no stimulatory activity [Figure 1 (○)].

An Intermediate Aggregation State Correlates with Proinflammatory Activity. AFM analysis of an Aβ(1−42) aggregation time course was done to visualize morphologies that corresponded to periods of TNFα production shown in Figure 1. Upon reconstitution of Aβ(1−42) in sterile water, images primarily showed a dense field of small punctate species with heights of < 2 nm as reported previously (*24*)(Figure 2A). Dynamic light scattering analysis of the freshly reconstituted Aβ(1−42) showed a predominant peak (95% mass) with an R_H of 1.0 nm representing monomeric Aβ and a small population (5% mass) of oligomeric species with an R_H of 5.7 nm (Figure 2B). Incubation of the Aβ(1−42) solution at 4 °C produced fibrillar structures by 48 h (Figure 2C). The 48 h image in Figure 2C is representative of the intermediate Aβ(1−42) aggregation state that typically stimulated maximal TNFα production (see Figure 1). Height analysis of the 48 h fibrils produced a mean height and standard deviation (SD) of 4.2 ± 1.4 nm with lengths ranging from 1 to 3 μm. We have described these features previously in the context of Toll-like receptor activation (*24*).

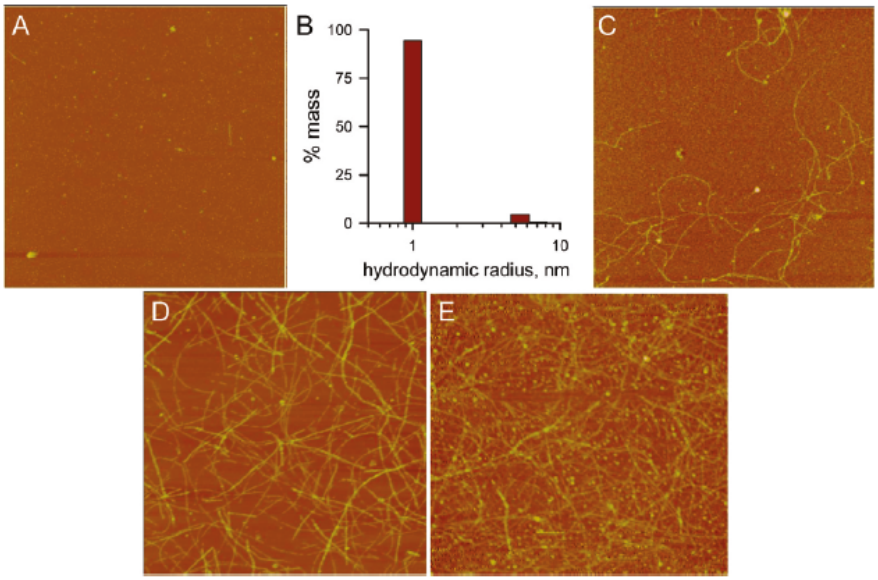

FIGURE 2: Morphological changes during the Aβ(1−42) aggregation time course. An Aβ(1−42) aggregation solution (100 μM) was prepared as described in the legend of Figure 1 and incubated at 4 °C. Aliquots were removed, diluted to 1 μM in water, and imaged by AFM at 0 (A), 48 (C), and 216 h (D). DLS measurements were obtained for the 0 h solution as described in Materials and Methods, and a histogram of percent mass vs R_H is shown in panel B. A separate 1.2 mM Aβ(1−42) solution was prepared and imaged at 24 h (E). All AFM images are 5 μm × 5 μm and shown in "height" mode.

The fibril height values did not change significantly after incubation for 216 h (4.5 ± 1.4 nm) (Figure 2D), and lengths were only slightly greater. The most notable change was in the density of fibrils (fibrils per square micrometer) which increased from approximately 1 fibril/μm^2 after incubation for 48 h to 6 fibrils/μm^2 by 216 h. ThT fluorescence measurements of the Aβ(1−42) solution indicated no fluorescence at 0 h, although a longer incubation time gradually increased the fluorescence [Figure 5 (○)]. A more concentrated Aβ(1−42) solution (1.2 mM) showed accelerated aggregation and fibril production after 24 h at 25 °C (Figure 2E). This accelerated aggregation was also reflected in ThT fluorescence levels which were 10−20 times higher in the 1.2 mM solutions than in the 100 μM solutions (data not shown). Treatment of the THP-1 monocytes with the more concentrated sample in Figure 2E at a final Aβ(1−42) concentration of 15 μM did not induce TNFα production (data not shown), consistent with the results shown in Figure 1.

The aggregation rate of the 100 μM Aβ(1−42) solution was accelerated by incubation at higher temperatures. Three solutions of 100 μM Aβ(1−42) were prepared and incubated at 4, 25, or 37 °C. Incubation at higher temperatures significantly weakened the ability of the solution to induce TNFα production. AFM images showed differences in the extent of aggregation at 96 h (Figure 3A−C), yet only the sample incubated at 4 °C stimulated TNFα production in THP-1 monocytes (Figure 3D). As in Figure 2, the AFM image of the Aβ(1−42) sample incubated at 4 °C contained long flexible fibril structures with a mean height of 5.5 ± 1.6 nm (SD) along with numerous globular species. The Aβ(1−42) sample at 25 °C showed a greater number of fibril structures and also a greater dispersity in measured fibril heights (6.9 ± 2.1 nm). The Aβ(1−42) sample at 37 °C was very different as determined by AFM imaging. Although the fibril heights were similar (6.1 ± 1.6 nm), a smaller amount of total Aβ(1−42) species was evident in the image, possibly due to decreased adsorption of the Aβ(1−42) fibrils formed at 37 °C to the mica surface. Furthermore, the smaller globular species were no longer observed. Separate experiments measuring ThT fluorescence found much higher levels for Aβ(1−42) incubated at 37 °C (470 arbitrary units) compared to incubation at 25 °C (80 units) or 4 °C (40 units) (data not shown). Aβ(1−42) samples were taken from the three solutions depicted in Figure 3A−C and tested for induction of THP-1 monocyte TNFα production. The dependence of TNFα production on Aβ(1−42) aggregation state for the sample incubated at 4 °C [Figure 3D (○)] showed the same profile as in Figure 1, while Aβ(1−42) solutions incubated at higher temperatures were ineffective at inducing an inflammatory response. The cumulative data demonstrated that Aβ(1−42)-induced TNFα production correlated with initial formation of an intermediate fibrillar species yet continued, accelerated, or increased fibril formation abolished the ability of Aβ(1−42) to stimulate the monocyte response.

Two possible explanations for the loss of Aβ(1−42) proinflammatory activity at the later stages of fibril formation were solubility (fibril precipitation) and fibril toxicity to the monocytes, particularly at later stages when significant numbers of fibrils are present. The first possibility was explored, and it was observed that many of the late-stage fibrillar species formed in water remained in solution after centrifugation of the sample at 18000*g* for 10 min based on AFM images pre- and postcentrifugation (data not shown). This result indicated the fibrils were not easily precipitating out of solution. The toxicity of Aβ(1−42) to the monocytes at both intermediate and late aggregation stages was tested using an XTT cell viability assay. Aβ(1−42) was not toxic to the cells at two stages of aggregation as mitochondrial-mediated reduction of XTT was not affected (Figure 4).

The pH of the Aβ(1−42) aqueous solutions was determined to be 3.6 using a microelectrode. Acidic pH has been shown previously to enhance single-fibril formation (*11*). We hypothesized

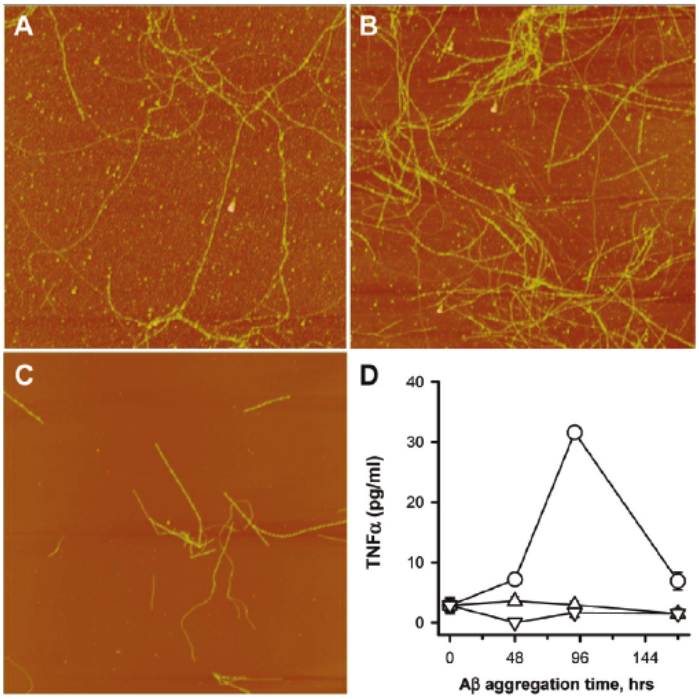

FIGURE 3: Increased incubation temperature accelerates Aβ(1−42) aggregation and weakens its ability to induce a proinflammatory response. A solution of Aβ(1−42) (100 μM) was separated into three tubes, and each tube was incubated at different temperatures. At various times, aliquots were removed for both AFM imaging and treatment of the THP-1 monocytes as described in Materials and Methods. (A−C) AFM images (5 μm × 5 μm) were obtained as described in the legend of Figure 2 from each Aβ(1−42) solution at 96 h prior to cell treatment. Images shown are representative of the solutions incubated at 4 (A), 25 (B), and 37 °C (C). (D) Secreted TNFα levels (SE, $n = 3$ measurements) were determined at each time point for Aβ(1−42) solutions incubated at 4 (○), 25 (△), and 37 °C (▽).

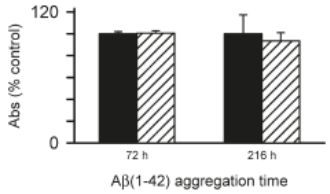

FIGURE 4: Monocyte viability is not compromised by aggregated Aβ(1−42). Aβ(1−42) solutions were prepared and incubated as described in the legend of Figure 1. After Aβ aggregation for 72 and 216 h, THP-1 monocytes were treated with 15 μM Aβ(1−42) for 6 h. Cell viability was assessed using an XTT assay as described in Materials and Methods. XTT reduction was assessed by the absorbance at 467 nm for both control cells treated with sterile water vehicle (black bars) and Aβ-treated cells (hatched bars). Error bars for each condition represent the standard error for six trials in two experiments. Absorbance values are presented as the percent of control cells for each experiment.

that Aβ(1−42) at higher ionic strengths and buffered at neutral pH may form structures with different proinflammatory stimulating activity. Aβ(1−42) was either reconstituted in water or treated with 100 mM NaOH followed by dilution into PBS. Both solutions were prepared at a final Aβ concentration of 100 μM and incubated at 4 °C. The Aβ(1−42)/PBS solution (pH 7.4) achieved a higher degree of aggregation based on ThT fluorescence measurements compared to the Aβ(1−42)/water solution (Figure 5A), yet Aβ(1−42) incubated in PBS did not stimulate TNFα production to the same extent as Aβ(1−42) incubated in water (Figure 5B). Initially, the Aβ(1−42)/water solutions were monitored by ThT prepared in water which maintained the acidic pH. This method resulted in very low ThT fluorescence (data not shown) and did not accurately reflect the extent of Aβ(1−42) aggregation. Analysis of the (1−42)/water solutions with ThT prepared in Tris-HCl (pH 8.0) [Figure 5A (○)] or glycine (pH 8.0) (data not shown) produced similar ThT fluorescence values that were both significantly higher than when ThT fluorescence was measured under acidic conditions. Microscopy was utilized to discern morphological differences between Aβ(1−42) incubated in water and PBS. Difficulty was encountered in attempting to adsorb Aβ(1−42) aggregates formed in PBS to mica grids for AFM; therefore, TEM was used for morphological evaluation of the two Aβ(1−42) solutions. TEM images obtained of each sample showed that both preparations contained significant fibrillar material. Compared to the Aβ(1−42)/water solution, the Aβ(1−42)/PBS solution possessed more laterally associated fibrils (Figure 5C,D) and a greater number of fibrils when a lower magnification was used to observe a larger field (data not shown).

Aβ(1−40) Does Not Have the Same Proinflammatory Activity as Aβ(1−42) under Similar Aggregation Conditions. The data to this point indicated that Aβ(1−42) incubated in water at 4 °C formed a species that acted as a proinflammatory stimulus. It was of interest to determine if Aβ(1−40) could form the same species under similar conditions. Solutions of Aβ(1−42) and Aβ(1−40) (100 μM in water) were prepared. The Aβ(1−42) solution was incubated at 4 °C, while the Aβ(1−40) solution was

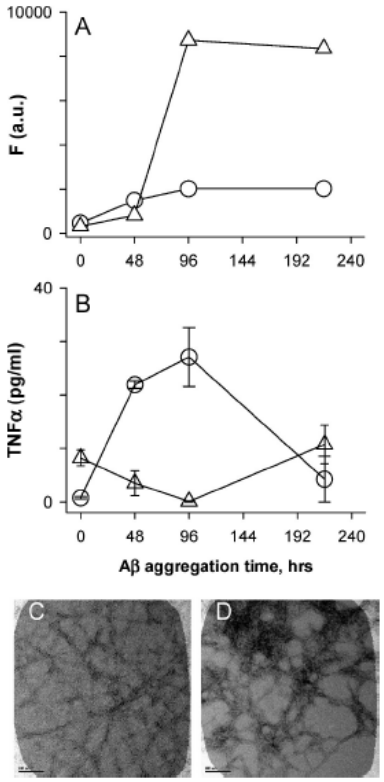

FIGURE 5: Ionic strength and pH influence Aβ(1−42) proinflammatory activity. Two lyophylized Aβ(1−42) aliquots were reconstituted in either sterile water (○) or 100 mM NaOH followed by 20-fold dilution into sterile phosphate-buffered saline (PBS) (△) at a concentration of 100 μM. Both solutions were incubated at 4 °C. ThT fluorescence was measured at different time points as described in Materials and Methods (A). For the same time points, THP-1 cells were treated with 15 μM Aβ(1−42) from each solution and secreted TNFα was measured in cell supernatants as described in the legend of Figure 1 (B). Error bars represent the standard error for three trials. (C and D) Aliquots were removed from each sample at 96 h and imaged by TEM as described. Images are of Aβ(1−42) reconstituted in water (C) and NaOH/PBS (D). Scale bars represent 100 nm.

incubated at three temperatures (4, 25, and 37 °C). AFM imaging indicated that even at 4 °C Aβ(1−40) did form fibrils (Figure 6A−C), albeit at a much slower rate compared to Aβ(1−42). The Aβ(1−40) fibrils were much longer (> 5 μm) than those formed by Aβ(1−42), and their measured heights were slightly greater. Aβ(1−40) fibrils presented in panels B and C of Figure 6 had average heights of 5.9 ± 1.7 nm (SD) with very little change in the fibril morphology from 96 to 216 h. Concurrent treatment of THP-1 monocytes with aliquots from the Aβ solutions revealed that, under these conditions, only Aβ(1−42) effectively stimulated TNFα production (Figure 6D). Incubation of Aβ(1−40) at an increased temperature produced more numerous fibrils as observed by AFM (data not shown) yet did not produce a proinflammatory Aβ species.

The Proinflammatory Aβ(1−42) Species Formed in Water Is Soluble and Can Be Recognized by an Antibody Specific for Fibrillar Oligomers. The data in Figure 1 demonstrated that, upon Aβ(1−42) reconstitution in sterile water, a period of incubation is necessary before an aggregated species conducive for inducing secretion of TNFα from THP-1 monocytes is formed. The fact that continued aggregation diminished proinflammatory activity indicated that an intermediate Aβ-(1−42) species was optimal. To better characterize this species, we subjected an Aβ(1−42) solution incubated for 72 h at 4 °C to centrifugation at speeds up to 150000*g* for 1 h at 4 °C. This treatment failed to significantly suppress the ability of the supernatant to induce TNFα production (Figure 7A) yet was effective at removing many of the Aβ(1−42) fibrils from solution at 150000*g* (Figure 7B,C). Centrifugal filter units with a 0.2 μm PTFE membrane were used to separate fibrillar material from Aβ(1−42) aggregation solutions. This was effectively done as the filtrate was devoid of fibrils (Figure 8B). Concentration measurements of the Aβ(1−42) solution pre- and postfiltering determined the filters removed 65% of the Aβ concentration with 35% remaining in the filtrate (data not shown). Separate control filtering experiments with monomeric Aβ indicated only a small loss (~10%) due to nonspecific adsorption. Monocyte activation experiments comparing the total solution with the filtrate showed that 0.2 μm filtering of the Aβ(1−42) solution completely abolished the ability of Aβ(1−42) to induce proinflammatory activity (Figure 8C). It has been previously reported that Aβ-(1−40) protofibrils will pass through a 0.2 μm filter (*36*), although in these studies no protofibrillar material was observed in the filtrate (Figure 8B).

The morphology, solubility, and transient appearance of the proinflammatory Aβ(1−42) species suggested similarities to protofibrils or fibrillar oligomers that have been described previously (*10*, *37*). Fibrillar oligomers are conformationally related to fibrils but have been observed across a broad size distribution. Their size appears to overlap with that of prefibrillar oligomers, yet the structural characteristics of the two oligomeric species are distinct. The ability to distinguish between these structural characteristics has been previously demonstrated with OC antisera, which recognize an epitope common to fibrils and oligomeric fibrillar precursors of varying size (*37*). We used an OC immune serum in this study to investigate whether fibrillar oligomers were involved in the Aβ(1−42)-induced proinflammatory response. Aβ(1−42) solutions were immunodepleted of OC-positive species as described in Materials and Methods and examined for remaining OC-positive material by dot blot. Although there was significant Aβ remaining in the supernatant, as detected by a sequence-specific Aβ antibody that is not dependent on conformation (Ab9), very little of it was OC-positive (Figure 9A). AFM analysis of the Aβ(1−42) supernatant after OC IP and centrifugation indicated a loss of both diffuse and fibrillar material (Figure 9B,C). Subsequent experiments looked at the ability of the OC-immunodepleted supernatants to stimulate TNFα production from THP-1 monocytes. Reprobing of the OC-immunodepleted supernatants with OC antisera again showed the amount of OC-positive Aβ(1−42) material was greatly reduced in the Aβ(1−42) solution after OC IP and centrifugation compared to just centrifugation or IP treatment with a rabbit IgG control (Figure 10A). Immunodepletion of OC-positive material in the Aβ(1−42) solution severely diminished the Aβ(1−42) proinflammatory activity compared to untreated 72 h Aβ(1−42) samples, 18000*g* supernatants, or supernatants after IP with rabbit IgG and centrifugation (Figure 10B).

Separation techniques such as SEC allow separation of differently sized aggregates but may also suffer a preferential loss of a particular hydrophobic species due to adsorption to the

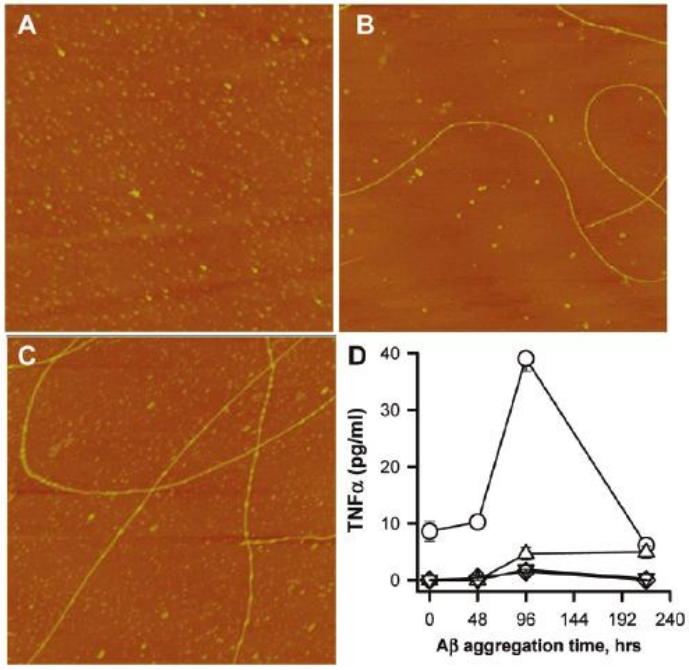

FIGURE 6: Aβ(1−40) is not as effective as Aβ(1−42) in inducing a proinflammatory response. Aβ(1−42) and Aβ(1−40) were reconstituted in sterile water at the same concentration (100 μM). Aβ(1−42) was incubated at 4 °C (○), while Aβ(1−40) was incubated at multiple temperatures. Aliquots were removed for both AFM imaging and incubation with THP-1 monocytes. (A−C) AFM images (5 μm × 5 μm) of Aβ(1−40) incubated at 4 °C are shown for 0 (A), 96 (B), and 216 h (C). (D) TNFα production was measured as described and is plotted for Aβ(1−42) incubated at 4 °C (○) and Aβ(1−40) incubated at either 4 (△), 25 (▽), or 37 °C (◇).

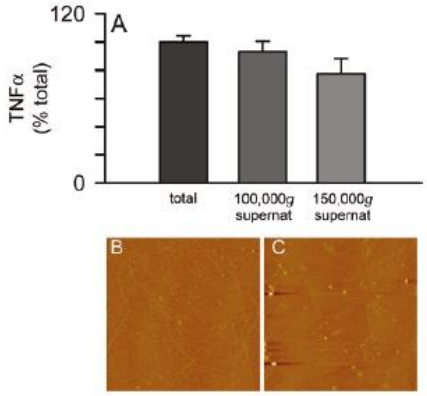

FIGURE 7: Solubility of the proinflammatory Aβ(1−42) species. Aβ(1−42) was reconstituted in sterile water (100 μM) and incubated at 4 °C for 72 h. Separate aliquots of the same Aβ(1−42) solution were subjected to centrifugation for 1 h at 4 °C and 100000*g* and 150000*g*. Equal volumes of the supernatants and the precentrifuge sample (total) were incubated with THP-1 monocytes for 24 h, and the amount of secreted TNFα was measured as described in the legend of Figure 1. AFM images (5 μm × 5 μm) were obtained for the precentrifuged total (B) and the 150000*g* supernatant (C).

column matrix or dilution-induced dissociation during column purification. OC-positive Aβ species elute across a broad size spectrum on SEC (*37*). To further support the ultracentrifugation studies that showed sedimentation of a significant percentage of

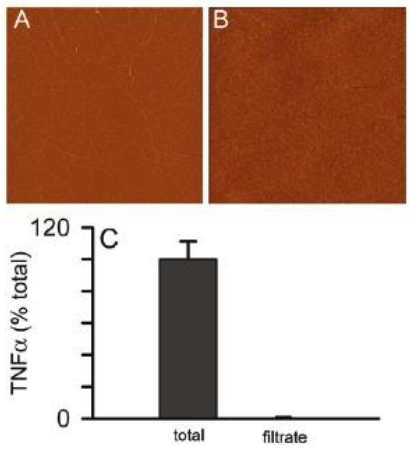

FIGURE 8: Filtering of the Aβ(1−42) aggregation solution removes the proinflammatory ability. Aβ(1−42) was reconstituted in sterile water (100 μM) and incubated at 4 °C for 72 or 96 h. An aliquot from the solution was applied to a 0.2 μm PTFE centrifugal filter unit and centrifuged for 3 min at 12000*g* and 4 °C. AFM images (5 μm × 5 μm) were obtained for the prefilter total (A) and the filtrate (B). (C) Equal volumes of the prefilter sample (total) and the filtrate were incubated with THP-1 monocytes for 6 h, and the amount of secreted TNFα was measured as described in the legend of Figure 1. TNFα is represented as a percentage of the TNFα induced by the prefilter sample. Secreted TNFα averaged 92 pg/mL in two experiments. Error bars represent the standard error for six measurements over two experiments.

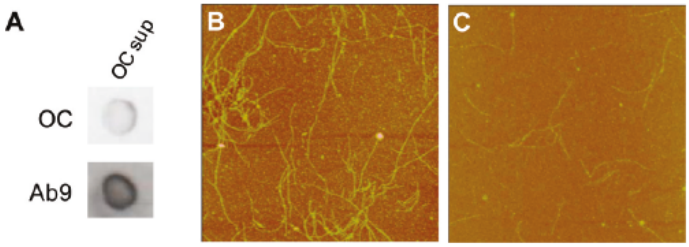

FIGURE 9: Immunoprecipitation with OC antisera depletes fibrillar oligomers and fibrils from an Aβ(1−42) solution. Aβ(1−42) was reconstituted in sterile water (100 μM) and stored at 4 °C for 72 h. The Aβ(1−42) solution was immunodepleted with OC antisera as described in Materials and Methods, and the remaining supernatant was re-examined by dot blot and AFM analysis. (A) Dot blot analysis of the 72 h Aβ(1−42) solution supernatant probed with OC antisera and the Ab9 antibody following OC IP. (B and C) AFM images (5 μm × 5 μm) of an untreated 72 h Aβ(1−42) solution (total) and the supernatant after immunodepletion with OC antisera (OC sup).

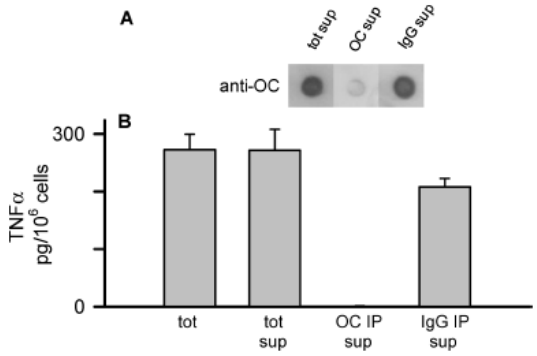

FIGURE 10: Immunodepletion with an antifibrillar oligomer antibody reduces the Aβ(1−42)-induced proinflammatory response. Aβ(1−42) was reconstituted in sterile water (100 μM) and stored at 4 °C for 72 h. The Aβ(1−42) solution was immunodepleted with OC antisera or rabbit IgG as described in the legend of Figure 9. The IP supernatants were then re-examined for OC-reactive species by dot blot analysis and also applied to THP-1 monocytes. (A) Dot blot probed with OC antisera of the 72 h Aβ(1−42) 18000*g* centrifugation supernatant (tot sup), OC IP supernatant (OC IP sup), and rabbit IgG IP supernatant (IgG IP sup). (B) Equal volumes of an untreated 72 h Aβ(1−42) solution (tot) and 18000*g* centrifugation supernatant (tot sup) and the OC- and rabbit IgG-immunodepleted supernatant (OC IP sup and IgG IP sup, respectively) were incubated with THP-1 monocytes for 24 h, and the amount of secreted TNFα was measured as described in the legend of Figure 1.

fibrils without a concomitant loss of cellular activity, an Aβ-(1−42)/water solution was incubated for 96 h at 4 °C and centrifuged at 18000*g*, and the supernatant was chromatographed via SEC (Figure 11A). Multiple peaks were observed by UV absorbance, including elution peaks at the void volume (V_o), multiple included volumes (peaks 2 and 3), and monomer volume. Selected fractions were assessed for OC reactivity (Figure 11B) using dot blot analysis. OC-positive material was found in all tested peaks except for monomer. The OC-positive fractions were then tested for their ability to induce a proinflammatory response which showed that the included peak 2 induced the highest levels of secreted TNFα from THP-1 monocytes (Figure 11C). Subsequent SEC separations of Aβ-(1−42) aggregated for 72−96 h were analyzed by DLS, and higher-molecular weight fractions 11−14 showed an expected decrease in size (R_H) from 100 to 10 nm as the elution volume increased. The fractions with the highest proinflammatory activity corresponded to R_H values between 10 and 30 nm and exhibited significant ThT fluorescence (data not shown). AFM images of a fraction from included peak 2 showed a significant population of short rodlike structures between 100 and 200 nm in length with a mean diameter (height) of 5.4 ± 1.6 nm (SD) for 116 measurements.

DISCUSSION

It has been postulated for some time that a sustained inflammatory response to aggregated Aβ may contribute to progressive neurodegeneration in AD (*6*). This idea emanated from pathology studies, which revealed inflammatory markers such as dystrophic neurites (*2*), activated microglia (*3*), and proinflammatory cytokines (*5*) surrounding Aβ lesions in the human AD brain (*15*). Interestingly, even though a vast array of Aβ aggregate morphologies ranging from dense core neuritic plaques to granular diffuse wispy Aβ deposits are observed in the AD brain, only the plaques appear to provoke this particular inflammatory response (*1*). A recent report by Meyer-Luehmann et al. (*4*) highlighted this phenomenon whereupon rapid plaque formation, and an equally rapid microglial response, was observed in an AD transgenic mouse model. Microglia were observed surrounding only the dense core plaques as opposed to the diffuse Aβ deposits.

THP-1 human monocytes have been used extensively to investigate the Aβ-induced proinflammatory response and display a pattern of activation similar to that of microglial cells (*19*−*21*). Many of the monocyte/macrophage and microglial studies have utilized preformed fibrillar Aβ, and some of those studies included costimulators such as interferon-γ (*38*) or lipopolysaccharide (*39*) along with the Aβ treatment. In this study, we correlated the time-dependent aggregation of Aβ with the ability to induce secretion of TNFα from human THP-1 monocytes. We observed that an intermediate Aβ(1−42) species formed under acidic (pH 3.6−4) aqueous conditions was optimal for stimulating the response. While the peak cellular response coincided with the appearance of Aβ(1−42) fibrils, the cell response did not correlate with fibrillar species based on the observation that increased production of Aβ(1−42) fibrils, Aβ-(1−40) fibrils, and Aβ(1−42) fibrils formed in PBS at neutral pH was not an effective inducer of TNFα secretion. This observation in combination with the OC immunodepletion studies and SEC separation in Figures 10 and 11, respectively, suggested that small fibrillar precursors were transient species that rapidly progressed to fibrils upon their formation. The neutral pH and increased ionic strength conditions in PBS accelerated Aβ(1−42) fibril formation but weakened the peptide's ability to stimulate a

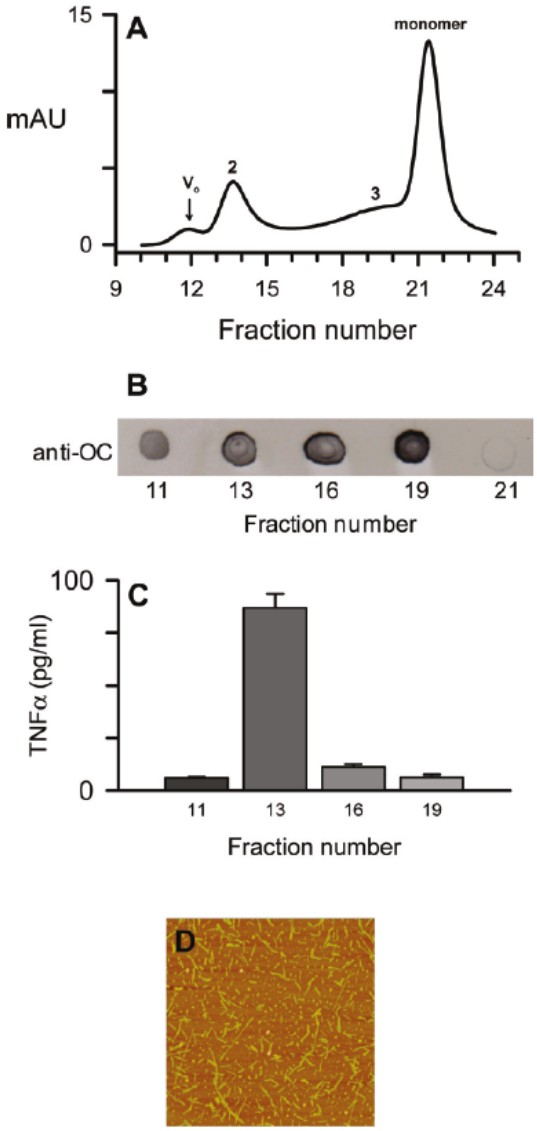

FIGURE 11: SEC separation of aggregated Aβ(1−42). Aβ(1−42) reconstituted in sterile water was allowed to incubate for 96 h at 4 °C before centrifugation at 18000*g* and separation of the supernatant on a Superdex 75 column as described in Materials and Methods. (A) The 280 nm absorbance elution profile of an aggregated Aβ(1−42)/water solution. Tick marks for fractions (0.5 mL) represent the beginning of elution collection for each fraction tube. Aβ concentrations determined by absorbance for the peak maxima were 1.4 μM for the void volume (V_o) and 5.7, 3.5, and 18.3 μM for the included volumes (peak 2, peak 3, and monomer, respectively). (B) Dot blot probed with OC antisera for the fractions listed above (without dilution). (C) THP-1 monocytes were treated with 90 μL from the OC-positive fractions in a total volume of 300 μL for 6 h at 37 °C, and TNFα production was measured as described in the legend of Figure 1. (D) AFM height mode image (3 μm × 3 μm) of a fraction from SEC-separated included peak 2 prepared without dilution.

proinflammatory response. There is some physiological support for Aβ(1−42) aggregates formed under acidic conditions. Although much of the attention is focused on the extracellular neuritic Aβ plaques, a significant amount of research now indicates that Aβ(1−42) aggregates may also form intracellularly in an acidic endosomal environment (*40*). These aggregates, if secreted, may form the structural basis for fibrils that are recognized by phagocytic cells and optimally induce proinflammatory events.

Significant structural polymorphism within Aβ fibrils at the molecular level has been demonstrated *in vitro*. Solid state NMR measurements revealed that Aβ(1−42), Aβ(1−40), and Aβ(10−35) fibrils contained in-register, parallel β-sheets (*41*, *42*), while fibrils formed by the shorter peptides Aβ(16−22), Aβ(34−42), and Aβ(11−25) adopted antiparallel β-strand alignments (*43*−*45*). The scope was expanded further by the observation that pH (*45*) and physical aggregation conditions (*46*) could also alter fibril structure and neuronal toxicity (*46*). Our finding that pH and ionic strength could alter Aβ(1−42) fibril morphology and its proinflammatory properties was consistent with these observations.

Structural differences at the molecular level are not always obvious in imaging techniques such as AFM and EM which are able to survey dimensional and architectural properties of aggregated Aβ. Recently, conformation-specific antibodies have been used to identify structural similarities between amyloid fibrils (*47*) and soluble oligomers (*48*) formed from different proteins. These antibodies are able to recognize a particular assembly state and can distinguish structural differences between monomeric, oligomeric, and fibrillar Aβ species (*37*, *47*). OC antisera recognize fibrils and fibrillar oligomers, which have been described as small soluble aggregates that are conformationally related to mature fibrils (*37*). Prefibrillar oligomers, which are recognized by the A11 antibody, but not OC, are structurally distinct from fibrillar oligomers (*37*). The immunodepletion studies in this report demonstrate that selective removal of fibrillar oligomers from an Aβ(1−42) solution by OC antibodies significantly lowered the THP-1 monocyte proinflammatory response to the peptide (Figure 10). This result indicated that an aggregated Aβ(1−42) species with inherent components of fibril structure is necessary to induce TNFα secretion, but smaller units of this structure induce the best response. This possibility is supported by the observation that continued, or accelerated, Aβ(1−42) aggregation diminished the monocyte response (Figures 1 and 3). Furthermore, the time course suggests that the fibrillar oligomers are transient and appear almost simultaneously with fibrils but rapidly disappear as they likely elongate to form additional fibrils. Fibrillar oligomers may be precursors to protofibrils (*10*−*12*) and have similar structural properties, although further investigation will be needed to make a careful comparison. The inability of Aβ(1−40) to stimulate a proinflammatory response under the same conditions as Aβ(1−42) tested in this study may be due to a lower nucleation propensity which would produce a substantially lower concentration of fibrillar oligomers.

Numerous studies suggest that small Aβ(1−42) oligomers may cause early and significant alterations in synaptic function, and then as fibrillar structures are formed, concomitant inflammatory responses appear (reviewed in ref *49*). This description of the progression of Aβ(1−42) aggregation toward an inflammatory species is consistent with the data in this report demonstrating that a soluble fibrillar precursor or nuclei are optimal for inducing an inflammatory response in a human monocyte cell line. Plaques consist of fibrillar Aβ at the core (*50*), although the complexities of plaque composition appear to be quite

significant. Hyman and colleagues have characterized Aβ plaques as a reservoir of bioactive molecules and proposed that soluble Aβ species surround the plaques (*4*). New evidence now indicates a halo of oligomeric Aβ surrounding the plaques based on immunostaining with an NAB61 antibody (*51*). NAB61 is able to recognize both oligomeric and fibrillar pathologic forms of Aβ but does not effectively stain diffuse Aβ (*52*). These studies make a case that different Aβ aggregation states exist not only throughout the brain parenchyma but also within the plaque area. Our studies in a human monocyte cell line show that soluble fibrillar Aβ(1−42) precursors are optimal for triggering an inflammatory response. These findings provide further information about the complexities of Aβ aggregation, inflammation, and the most favorable Aβ structure for interacting with cell surface receptors.

ACKNOWLEDGMENT

We greatly appreciate the gift of OC antisera from Dr. Rakez Kayed (George and Cynthia Mitchell Center for Neurodegenerative Diseases, Department of Neurology, University of Texas Medical Branch) and the Ab9 antibody from Dr. Terrone Rosenberry (Mayo Clinic Jacksonville). We thank the Microscopy Image and Spectroscopy Technology Laboratory in the Center for Nanoscience at the University of Missouri for technical assistance and equipment.

REFERENCES

1. Selkoe, D. J. (2004) Cell biology of protein misfolding: The examples of Alzheimer's and Parkinson's diseases. *Nat. Cell Biol. 6*, 1054–1061.
2. Selkoe, D. J. (1998) The cell biology of β-amyloid precursor protein and presenilin in Alzheimer's disease. *Trends Cell Biol. 8*, 447–453.
3. McGeer, P. L., Itagaki, S., Tago, H., and McGeer, E. G. (1987) Reactive microglia in patients with senile dementia of the Alzheimer type are positive for the histocompatibility glycoprotein HLA-DR. *Neurosci. Lett. 79*, 195–200.
4. Meyer-Luehmann, M., Spires-Jones, T. L., Prada, C., Garcia-Alloza, M., de Calignon, A., Rozkalne, A., Koenigsknecht-Talboo, J., Holtzman, D. M., Bacskai, B. J., and Hyman, B. T. (2008) Rapid appearance and local toxicity of amyloid-β plaques in a mouse model of Alzheimer's disease. *Nature 451*, 720–724.
5. Dickson, D. W., Lee, S. C., Mattiace, L. A., Yen, S. H. C., and Brosnan, C. (1993) Microglia and cytokines in neurological disease, with special reference to AIDS and Alzheimer disease. *Glia 7*, 75–83.
6. McGeer, E. G., and McGeer, P. L. (1998) The importance of inflammatory mechanisms in Alzheimer disease. *Exp. Gerontol. 33*, 371–378.
7. Golde, T. E. (2002) Inflammation takes on Alzheimer disease. *Nat. Med. 8*, 936–938.
8. Bacskai, B. J., Kajdasz, S. T., Christie, R. H., Carter, C., Games, D., Seubert, P., Schenk, D., and Hyman, B. T. (2001) Imaging of amyloid-β deposits in brains of living mice permits direct observation of clearance of plaques with immunotherapy. *Nat. Med. 7*, 369–372.
9. Harper, J. D., Wong, S. S., Lieber, C. M., and Lansbury, P. T. Jr. (1997) Observation of metastable Aβ amyloid protofibrils by atomic force microscopy. *Chem. Biol. 4*, 119–125.
10. Walsh, D. M., Lomakin, A., Benedek, G. B., Condron, M. M., and Teplow, D. B. (1997) Amyloid β-protein fibrillogenesis: Detection of a protofibrillar intermediate. *J. Biol. Chem. 272*, 22364–22372.
11. Harper, J. D., Wong, S. S., Lieber, C. M., and Lansbury, P. T. Jr. (1999) Assembly of Aβ amyloid peptides: An *in vitro* model for a possible early event in Alzheimer's disease. *Biochemistry 38*, 8972–8980.
12. Walsh, D. M., Hartley, D. M., Kusumoto, Y., Fezoui, Y., Condron, M. M., Lomakin, A., Benedek, G. B., Selkoe, D. J., and Teplow, D. B. (1999) Amyloid β-protein fibrillogenesis: Structure and biological activity of protofibrillar intermediates. *J. Biol. Chem. 274*, 25945–25952.
13. Stine, W. B. J., Dahlgren, K. N., Krafft, G. A., and LaDu, M. J. (2003) *In vitro* characterization of conditions for amyloid-β peptide oligomerization and fibrillogenesis. *J. Biol. Chem. 278*, 11612–11622.
14. Deshpande, A., Mina, E., Glabe, C., and Busciglio, J. (2006) Different conformations of amyloid β induce neurotoxicity by distinct mechanisms in human cortical neurons. *J. Neurosci. 26*, 6011–6018.
15. Lorenzo, A., and Yankner, B. A. (1994) β-Amyloid neurotoxicity requires fibril formation and is inhibited by Congo red. *Proc. Natl. Acad. Sci. U.S.A. 91*, 12243–12247.
16. Pike, C. J., Walencewicz, A. J., Glabe, C. G., and Cotman, C. W. (1991) *In vitro* aging of β-amyloid protein causes peptide aggregation and neurotoxicity. *Brain Res. 563*, 311–314.
17. Dahlgren, K. N., Manelli, A. M., Stine, W. B. Jr., Baker, L. K., Krafft, G. A., and LaDu, M. J. (2002) Oligomeric and fibrillar species of amyloid-β peptides differentially affect neuronal viability. *J. Biol. Chem. 277*, 32046–32053.
18. Walsh, D. M., Klyubin, I., Fadeeva, J. V., Cullen, W. K., Anwyl, R., Wolfe, M. S., Rowan, M. J., and Selkoe, D. J. (2002) Naturally secreted oligomers of amyloid β protein potently inhibit hippocampal long-term potentiation *in vivo*. *Nature 416*, 535–539.
19. Klegeris, A., Walker, D. G., and McGeer, P. L. (1997) Interaction of Alzheimer β-amyloid peptide with the human monocytic cell line THP-1 results in a protein kinase C-dependent secretion of tumor necrosis factor-α. *Brain Res. 747*, 114–121.
20. Yates, S. L., Burgess, L. H., Kocsis-Angle, J., Antal, J. M., Dority, M. D., Embury, P. B., Piotrkowski, A. M., and Brunden, K. R. (2000) Amyloid β and amylin fibrils induce increases in proinflammatory cytokine and chemokine production by THP-1 cells and murine microglia. *J. Neurochem. 74*, 1017–1025.
21. Combs, C. K., Karlo, J. C., Kao, S. C., and Landreth, G. E. (2001) β-Amyloid stimulation of microglia and monocytes results in TNFα-dependent expression of inducible nitric oxide synthase and neuronal apoptosis. *J. Neurosci. 21*, 1179–1188.
22. Yan, S. D., Chen, X., Fu, J., Chen, M., Zhu, H., Roher, A., Slattery, T., Zhao, L., Nagashima, M., Morser, J., Migheli, A., Nawroth, P., Stern, D., and Schmidt, A. M. (1996) RAGE and amyloid-β peptide neurotoxicity in Alzheimer's disease. *Nature 382*, 685–691.
23. Bamberger, M. E., Harris, M. E., McDonald, D. R., Husemann, J., and Landreth, G. E. (2003) A cell surface receptor complex for fibrillar β-amyloid mediates microglial activation. *J. Neurosci. 23*, 2665–2674.
24. Udan, M. L., Ajit, D., Crouse, N. R., and Nichols, M. R. (2008) Toll-like receptors 2 and 4 mediate Aβ(1−42) activation of the innate immune response in a human monocytic cell line. *J. Neurochem. 104*, 524–533.
25. Fassbender, K., Walter, S., Kuhl, S., Landmann, R., Ishii, K., Bertsch, T., Stalder, A. K., Muehlhauser, F., Liu, Y., Ulmer, A. J., Rivest, S., Lentschat, A., Gulbins, E., Jucker, M., Staufenbiel, M., Brechtel, K., Walter, J., Multhaup, G., Penke, B., Adachi, Y., Hartmann, T., and Beyreuther, K. (2004) The LPS receptor (CD14) links innate immunity with Alzheimer's disease. *FASEB J. 18*, 203–205.
26. Walter, S., Letiembre, M., Liu, Y., Heine, H., Penke, B., Hao, W., Bode, B., Manietta, N., Walter, J., Schulz-Schuffer, W., and Fassbender, K. (2007) Role of the Toll-like receptor 4 in neuroinflammation in Alzheimer's disease. *Cell. Physiol. Biochem. 20*, 947–956.
27. El Khy, J., Hickman, S. E., Thomas, C. A., Cao, L., Silverstein, S. C., and Loike, J. D. (1996) Scavenger receptor-mediated adhesion of microglia to β-amyloid fibrils. *Nature 382*, 716–719.
28. Nichols, M. R., Moss, M. A., Reed, D. K., Lin, W. L., Mukhopadhyay, R., Hoh, J. H., and Rosenberry, T. L. (2002) Growth of β-amyloid-(1−40) protofibrils by monomer elongation and lateral association. Characterization of distinct products by light scattering and atomic force microscopy. *Biochemistry 41*, 6115–6127.
29. Bradford, M. M. (1976) A rapid and sensitive method for the quantitation of microgram quantities of protein utilizing the principle of protein-dye binding. *Anal. Biochem. 72*, 248–254.
30. Nichols, M. R., Moss, M. A., Reed, D. K., Cratic-McDaniel, S., Hoh, J. H., and Rosenberry, T. L. (2005) Amyloid-β protofibrils differ from amyloid-β aggregates induced in dilute hexafluoroisopropanol in stability and morphology. *J. Biol. Chem. 280*, 2471–2480.
31. Parvathy, S., Rajadas, J., Ryan, H., Vaziri, S., Anderson, L., and Murphy, G. M. (2008) Aβ peptide conformation determines uptake and interleukin-1α expression by primary microglial cells. *Neurobiol. Aging* (in press).
32. Scudiero, D. A., Shoemaker, R. H., Paull, K. D., Monks, A., Tierney, S., Nofziger, T. H., Currens, M. J., Seniff, D., and Boyd, M. R. (1988) Evaluation of a soluble tetrazolium/formazan assay for cell growth and drug sensitivity in culture using human and other tumor cell lines. *Cancer Res. 48*, 4827–4833.
33. Grammas, P., and Ovase, R. (2001) Inflammatory factors are elevated in brain microvessels in Alzheimer's disease. *Neurobiol. Aging 22*, 837–842.

34. Tarkowski, E., Andreasen, N., Tarkowski, A., and Blennow, K. (2003) Intrathecal inflammation precedes development of Alzheimer's disease. *J. Neurol., Neurosurg. Psychiatry 74*, 1200–1205.
35. Jarrett, J. T., and Lansbury, P. T. Jr. (1993) Seeding "one-dimensional crystallization" of amyloid: A pathogenic mechanism in Alzheimer's disease and scrapie? *Cell 73*, 1055–1058.
36. Lashuel, H. A., and Grillo-Bosch, D. (2005) In vitro preparation of prefibrillar intermediates of amyloid-β and α-synuclein. *Methods Mol. Biol. 299*, 19–33.
37. Kayed, R., Head, E., Sarsoza, F., Saing, T., Cotman, C. W., Necula, M., Margol, L., Wu, J., Breydo, L., Thompson, J. L., Rasool, S., Gurlo, T., Butler, P., and Glabe, C. G. (2007) Fibril specific, conformation dependent antibodies recognize a generic epitope common to amyloid fibrils and fibrillar oligomers that is absent in prefibrillar oligomers. *Mol. Neurodegener. 2*, 18.
38. Meda, L., Cassatella, M. A., Szendrei, G. I., Otvos, L. Jr., Baron, P., Villalba, M., Ferrari, D., and Rossi, F. (1995) Activation of microglial cells by β-amyloid protein and interferon-γ. *Nature 374*, 647–650.
39. Lorton, D., Kocsis, J. M., King, L., Madden, K., and Brunden, K. R. (1996) β-Amyloid induces increased release of interleukin-1β from lipopolysaccharide-activated human monocytes. *J. Neuroimmunol. 67*, 21–29.
40. Laferla, F. M., Green, K. N., and Oddo, S. (2007) Intracellular amyloid-β in Alzheimer's disease. *Nat. Rev. Neurosci. 8*, 499–509.
41. Tycko, R. (2003) Insights into the amyloid folding problem from solid-state NMR. *Biochemistry 42*, 3151–3159.
42. Burkoth, T. S., Benzinger, T. L. S., Urban, V., Morgan, D. M., Gregory, D. M., Thiyagarajan, P., Botto, R. E., Meredith, S. C., and Lynn, D. G. (2000) Structure of the β-amyloid$_{(10-35)}$ fibril. *J. Am. Chem. Soc. 122*, 7883–7889.
43. Balbach, J. J., Ishi, Y., Antzutkin, O. N., Leapman, R. D., Rizzo, N. W., Dyda, F., Reed, J., and Tycko, R. (2000) Amyloid fibril formation by Aβ_{16-22}, a seven-residue fragment of the Alzheimer's β-amyloid peptide, and structural characterization by solid state NMR. *Biochemistry 39*, 13748–13759.
44. Lansbury, P. T. Jr., Costa, P. R., Griffiths, J. M., Simon, E. J., Auger, M., Halverson, K. J., Kocisko, D. A., Hendsch, Z. S., Ashburn, T. T., Spencer, R. G., Tidor, B., and Griffin, R. G. (1995) Structural model for the β-amyloid fibril based on interstrand alignment of an antiparallel-sheet comprising a C-terminal peptide. *Nat. Struct. Biol. 2*, 990–998.
45. Petkova, A. T., Buntkowsky, G., Dyda, F., Leapman, R. D., Yau, W. M., and Tycko, R. (2004) Solid state NMR reveals a pH-dependent antiparallel β-sheet registry in fibrils formed by a β-amyloid peptide. *J. Mol. Biol. 335*, 247–260.
46. Petkova, A. T., Leapman, R. D., Guo, Z., Yau, W. M., Mattson, M. P., and Tycko, R. (2005) Self-propagating, molecular-level polymorphism in Alzheimer's β-amyloid fibrils. *Science 307*, 262–265.
47. O'Nuallain, B., and Wetzel, R. (2002) Conformational Abs recognizing a generic amyloid fibril epitope. *Proc. Natl. Acad. Sci. U.S.A. 99*, 1485–1490.
48. Kayed, R., Head, E., Thompson, J. L., McIntire, T. M., Milton, S. C., Cotman, C. W., and Glabe, C. G. (2003) Common structure of soluble amyloid oligomers implies common mechanism of pathogenesis. *Science 300*, 486–489.
49. Haass, C., and Selkoe, D. J. (2007) Soluble protein oligomers in neurodegeneration: Lessons from the Alzheimer's amyloid β-peptide. *Nat. Rev. Mol. Cell Biol. 8*, 101–112.
50. Terry, R. D., Gonatas, N. K., and Weiss, M. (1964) Ultrastructural studies in Alzheimer's presenile dementia. *Am. J. Pathol. 44*, 269–297.
51. Koffie, R. M., Meyer-Luehmann, M., Hashimoto, T., Adams, K. W., Mielke, M. L., Garcia-Alloza, M., Micheva, K. D., Smith, S. J., Kim, M. L., Lee, V. M., Hyman, B. T., and Spires-Jones, T. L. (2009) Oligomeric amyloid β associates with postsynaptic densities and correlates with excitatory synapse loss near senile plaques. *Proc. Natl. Acad. Sci. U.S.A. 106*, 4012–4017.
52. Lee, E. B., Leng, L. Z., Zhang, B., Kwong, L., Trojanowski, J. Q., Abel, T., and Lee, V. M. (2006) Targeting amyloid-β peptide (Aβ) oligomers by passive immunization with a conformation-selective monoclonal antibody improves learning and memory in Aβ precursor protein (APP) transgenic mice. *J. Biol. Chem. 281*, 4292–4299.

CHAPTER 1

INTRODUCTION

1.1 Protein Misfolding and Amyloid Formation

Proteins are involved in virtually every biological process in the living system. The amino acids in the protein must fold into the native three-dimensional structures, and these structures are characteristic of individual proteins (Voet, 1995). The folding of a protein is influenced by its amino acid sequence, and the cellular environment around the amino acid chain (Anfinsen, 1973, Horwich et al., 1999). The folding and unfolding of proteins is associated with a wide range of cellular processes from the trafficking of molecules to specific organelles to the regulation of the cell cycle and the immune response (Radford and Dobson, 1999, Stefani and Dobson, 2003). These observations led to the conclusion that the failure to fold correctly, or to remain folded correctly, leads to many different types of biological malfunctions and hence to many different forms of diseases (Radford and Dobson, 1999). In the case of incompletely folded proteins, some regions of the structure that are actually buried in the native state will be exposed to the solvent. Hence, these proteins are prone to inappropriate interaction with other molecules within the crowded environment of the cell (Ellis, 2001). Therefore living systems have evolved strategies to prevent unwanted interactions. The cell has evolved the chaperone

system, and some chaperones interact with the nascent proteins as they emerge out of the ribosomes, while others are involved in guiding later stages of the folding process (Bukau and Horwich, 1998, Hartl and Hayer-Hartl, 2002), and hence prevent aggregation. Furthermore, unfolded proteins that escape the chaperone system are degraded by the proteasome. However, there is a gradual decrease in the efficiency of the system with age that could lead to late onset disorders.

Failure of a specific peptide or protein to adopt, or remain in, its native functional conformational state results in a broad range of human diseases termed as protein folding disorders (Chiti and Dobson, 2006). Abnormal physiological concentrations and mutations are believed to destabilize the native three-dimensional state, thereby deviating the protein from its normal folding pathway (Dobson, 1999, Hetz and Soto, 2003). The largest group of misfolding diseases is associated with the conversion of specific peptides or proteins from their soluble functional states ultimately into highly organized fibrillar aggregates (Lansbury, 1999). The fact that only select groups of proteins are found in the disease-associated fibrils suggest that these proteins are subject to abnormally high expression to such an extent that the chaperone and the proteosome system are temporarily overwhelmed (Lansbury, 1999). These structures are generally described as amyloid fibrils or plaques when they accumulate extracellularly. The term "intracellular inclusions" has been suggested when fibrils that are morphologically and structurally related to extracellular amyloid form inside the cell (Westermark et al., 2005). Current focus in studying the structural aspects of amyloid aggregation states is due to their crucial role in disorders such as Alzheimer's disease, Parkinson's disease, Huntington's disease (Table 1), and diverse systemic amyloidosis (Walker and LeVine, 2000, Selkoe

and Podlisny, 2002, Selkoe, 2003). Despite the ability of many proteins to form amyloid fibrils, not much is known about their structures or the factors that govern their formation. A principal unanswered question about these disorders is the nature in which the natively soluble proteins of different primary structures undergo partial unfolding and aberrant refolding to produce highly stable oligomers and polymers. The partially folded forms have exposed hydrophobic regions and are therefore prone to self-aggregation (Selkoe, 2003). An understanding of how this aggregation process happens and how the resultant aggregates initiate cell dysfunction will offer valuable information that is essential in the development of new therapeutic strategies for specific molecular interventions, and treatment modalities for these disorders.

1.2 Alzheimer's Disease (AD)

AD is the most common cause of dementia in the elderly, and is a progressive neurodegenerative disorder that gradually destroys cognitive function and eventually causes death. AD currently affects nearly 2% of the population in industrialized countries (Mattson, 2004). As the life expectancy of individuals has extended considerably, these diseases are of a major concern (Glenner, 1989), and it is estimated that about 22 million people will be afflicted globally by 2025 [St George- Hyslop 2000]. This statistics emphasizes the need for novel and effective treatments. During the last decade there has been expansive research in the field of AD. Microscopic studies have revealed a loss of neurons in hippocampus, a center for memory, and the cerebral cortex,

Disease	Protein	Locus
Alzheimer's disease	Amyloid beta protein Tau	Extracellular plaques Tangles in neuronal cytoplasm
Frontotemporal dementia with parkinsonism	Tau	Tangles in neuronal cytoplasm
Parkinson's disease; dementia with Lewy bodies	α-synuclein	Neuronal cytoplasm
Creutzfeldt-Jakob disease: Mad cow disease	Prion protein PrP^{SC}	Extracellular plaques Oligomers inside and outside neurons
Polyglutamine disease; Huntigton's disease, spino cerebellar ataxias	Long glutamine stretches within certain proteins	Neuronal nuclei and cytoplasm
Amyotrophic lateral sclerosis	Superoxide dismutase	Nueronal cytoplasm

Table1.1 Some human brain diseases characterized by protein misfolding and aggregation Figure adapted from Selkoe. D.J., (2003) *Nature*, 426: 900-904

which is the center for reasoning memory and other thought processes. Hallmark lesions of AD include amyloid deposits neurofibrillary tangles (NFTs) and dystrophic neuritis (Glenner, 1989, Ballatore et al., 2007).

Immunocytochemsitry revealed that one of the earliest pathological changes include a population of neurons packed with swollen lysosomal granules (Nixon et al., 1992). These lysosomes or granules also stain with antibodies against Aβ (Gouras et al., 2000, D'Andrea et al., 2001). Extracellular heparan sulfate (Perry et al., 1991, Cummings et al., 1993) immunoreactivity, advanced glycation end products (Smith et al., 1994, Vitek et al., 1994), racemic amino acids and isopeptide bonds (Shapira et al., 1988, Roher et al., 1993) are found associated with senile plaques, NFTs, and dystrophic neurites. Activated microglia are found along the margins of senile plaques (Wisniewski et al., 1989). Key markers of inflammation are also associated with amyloid deposits (Rozemuller et al., 1989, Dickson et al., 1993). A broad spectrum of pathological events are associated with AD, and recent studies have indicated the possibility of AD representing a spectrum of diseases (Hyman, 1996). These studies have also revealed genetic causes of the disease in addition to cellular and molecular mechanisms that are linked to AD. Until recently post mortem analysis of the brain tissue was the only way to study the pathological features of AD. This limitation prompted research on biochemical markers of AD in serum and cerebrospinal fluid that will be able to complement clinical approaches and help in early diagnosis (Khachaturian, 2002). It was initially assumed that extracellular amyloid fibrils were responsible for exerting cytotoxic effects. Over the past decade data from cell culture models, β-amyloid precursor transgenic mice, and studies on the human brain suggest that prefibrillar, diffusible assemblies of amyloid beta

was also deleterious. This has opened up a wide avenue for further probing the mechanisms of AD.

1.3 AD Pathology

The characteristic neuropathology of AD was first described by a German psychiatrist, Alois Alzheimer, in 1907. Two hallmark pathological findings in the brains of AD patients are extracellular amyloid plaques, and intracellular neurofibrillary tangles (NFTs). However, there is evidence that suggests that apart from the plaques and the neurofibrillary tangles, a third of the AD patients will exhibit significant cerebrovascular pathology. Cerebral amyloid angiopathy, micro vascular degeneration that affects the cerebral endothelium and smooth muscle cells, hyalinosis and fibrosis are also seen in AD (Vinters et al., 1996, Attems, 2005, Thal et al., 2008).

1.3.1 Extracellular Plaques

Extracellular amyloid plaques mainly constitute diffuse and neuritic plaques. The neuritic plaques are intimately surrounded by dystrophic axons and dendrites, reactive astrocytes and activated microglia (Selkoe, 2001). Neuritic plaques are brain lesions that are generally found in large numbers in limbic and association cortices (Dickson, 1997). The main protein constituent of plaques is amyloid beta (Aβ) peptide. Aβ peptide is a 39-43 amino acid proteolytic product of amyloid precursor protein (APP) and forms long insoluble amyloid fibrils which accumulate as spherical microscopic deposits known as

senile plaques. These plaques consist of a central amorphous core which can be identified by histological amyloid stains such as Congo red (Klunk et al., 1989) and Thioflavin T or S (Sage et al., 1983). Plaques are surrounded by dystrophic neurites (Glenner, 1989, Dickson, 1997) reactive astrocytes (Pike et al., 1995) and microglia (Perlmutter et al., 1990) that are thought to release complement factors and cytokines (McGeer and McGeer, 2001) and cause inflammatory reactions around the plaques.

Studies have established that much of the fibrillar Aβ found in neuritic plaques is the 42 amino acid peptide Aβ(1-42). This peptide is more hydrophobic, and more prone to aggregation than the shorter Aβ(1-40) peptide (Jarrett et al., 1993a). In the late 1980s experimental data confirmed the presence of diffuse amyloid plaques in the same brain region that contained many neuritic plaques (Tagliavini et al., 1988, Joachim et al., 1989). However, further research on the diffuse plaques showed that they were the sole form found in brain regions that lacked neuritic dystrophy, glial changes, and neurofibrillary tangles. In the case of healthy aged human, free of AD or other dementing processes, studies have shown the presence of solely diffuse plaques in the limbic and association cortices. AD patients on the other hand showed mixtures of diffuse and neuritic plaques (Fig 1.1). It was therefore hypothesized that these diffuse plaques represent precursor lesions of neuritic plaques (Selkoe, 2001). This hypothesis is best illustrated by studies on Down's syndrome. Patients with Down's syndrome have little or no Aβ deposition in the first decade of life, but by around 12 years of age one begins to see diffuse plaques containing Aβ(1-42) and not Aβ(1-40). More and more Down's subjects develop such plaques during the second and third decade of life (Lemere et al., 1996). After the age of 30, amyloid fibril formation is seen and there is associated

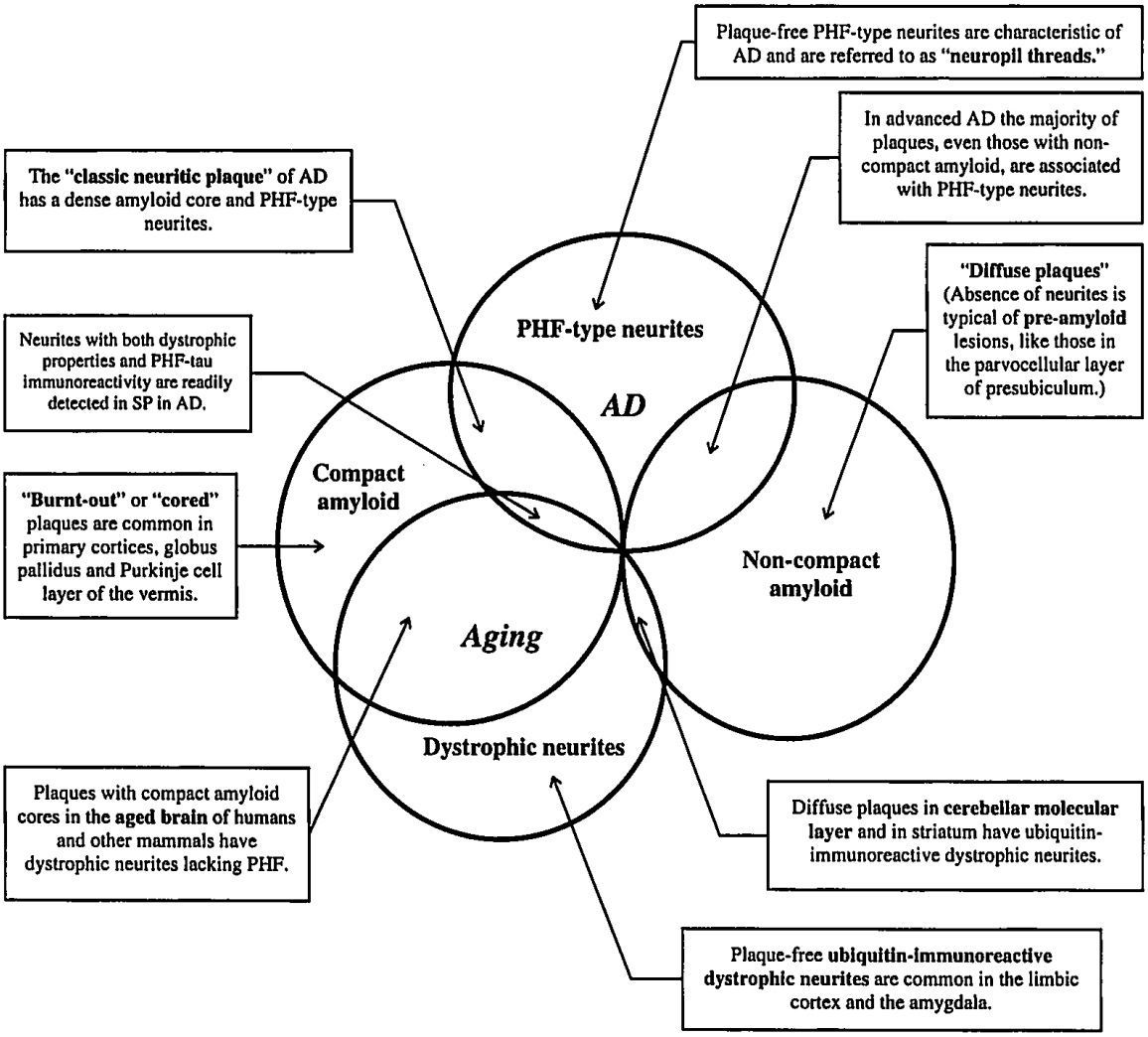

Figure 1.1.**Types of Plaques** Diagram showing the relationship between the subsets of senile plaques based on the morphology of the amyloid and whether or not they are associated with PHF type or dystrophic neurites. (Figure adapted from Dickson W D, 1997, *J Neuropathol Exp Neurol*, 56:321-339)

microgliosis, astrocytosis and some neuritic dystrophy. These neuritic plaques then become more prevalent over the next 2 decades of life.

1.3.2 Neurofibrillary Tangles

The healthy neurons in the brain are connected by axons. Microtubules are support structures present inside the axons that aid in the transport of molecules and nutrients into and out of the cell. Tau is a microtubule-associated protein and the hyperphosphorylation of this protein leads to detachment of tau from the microtubules, which results in the formation of neurofibrillary tangles and neurophil threads. The three main types of neurofibrillary lesions (NFLs) based on their localizations in nerve cells are: (i) neurofibrillary tangles (NFTs) in the cell body and apical dendrites of neurons, (ii) neurophil threads (NTs) in distal dendrites and (iii) dystrophic neurites associated with neuritic plaques (Tolnay and Probst, 1999). NFLs contain bundles of abnormal fibers that consist of pairs of ~10 nm filaments wound into helices (paired helical filaments or PHFs) as a major fibrous component, and straight 10 nm to 15 nm filaments (SFs) as a minor component (Selkoe, 2001). Most of these filaments are highly insoluble and resistant to detergent such as sodium dodecyl sulfate (Selkoe et al., 1982). In AD, the hyperphosphorylated tau decreases the ability to promote the microtubule assembly and instead aggregates into paired helical filaments (PHFs) in the cytoplasm of the degenerating neurons (Buee et al., 2000). Neurofibrillary pathology is also found in other neurodegenerative disorders like FTDP-17 (fronto temporal dementia and Parkinsonism linked to chromosome 17) (Lewis et al., 2001).

1.3.3 Relationship Between Aβ and Tau

Pathophysiological mechanisms underlying AD have been controversial. The most dominant theory of AD etiology and pathogenesis is amyloid cascade hypothesis. The hypothesis states that overproduction of Aβ, or defect in the peptide clearance, leads to amyloid deposition, which produces tangles that may lead to cell death, resulting in memory impairment in AD (Hardy and Gwinn-Hardy, 1998, Selkoe, 2001). There is strong evidence suggesting that Aβ is critically involved at an early stage in the pathogenesis of AD (Vassar, 2004), and that Aβ accumulation precedes and promotes tau pathology. PHF formation in AD is not due to mutations in the tau gene but is due to cellular cascade triggered by Aβ, which causes the abnormal phosphorylation of tau proteins, and their assembly to filaments (Gouras et al., 2000, Greenfield et al., 2000, Gotz et al., 2001, Lewis et al., 2001). This statement has been supported by data that showed presence of Aβ in the vicinity of the neurons enhanced tau phophorylation *in vitro* and *in vivo* (Busciglio et al., 1995). Double transgenic mice expressing mutant human tau gene (P301L) and mutant APP developed neurofibrillary tangles and degeneration in cortical and subcortical brain regions (Lewis et al., 2001). Further studies on 3xTg-AD mouse harboring mutations in APP, Tau and presenilin showed that intraneural Aβ accumulation in cell bodies preceded tau hyperphosphorylation (Oddo et al., 2003, Billings et al., 2005). Injection of Aβ(1-42) into the brains of P30IL mutant tau transgenic mice resulted in an increase in the number of NFTs by a factor of five. The increase in the numbers were seen in the amygdale from where the neurons project into

the injection sites (Gotz et al., 2001). These data support the fact that Aβ is the primary cause for the disease.

1.4 Overview of Amyloid Beta (Aβ) Peptide

1.4.1 Aβ Generation from Amyloid Precursor Protein (APP)

Amyloid beta is derived from a larger precursor protein, amyloid precursor protein (APP), a type-I integral transmembrane glycoprotein. APP contains an extracellular N-terminus and a short C-terminal region that lies in the cytoplasm APP is present in a variety of tissues but predominantly in the brain (Mattson, 1997). It is encoded by a gene located on chromosome 21 (Masters et al., 1985). Splicing of the APP gene gives rise to at least three transcripts that encode proteins of 695, 751 and 770 amino acids (Hardy, 1997, Selkoe, 1999). All of the APP isoforms contain the 39/43 amino acids long Aβ domain. The 695 amino acids are the main isoform expressed in neurons (Golde et al., 1990). At present the physiological function of APP in the brain remains unclear, although it has been proposed to have functions in transmembrane signal transduction (Nishimoto et al., 1993), calcium regulation (Mattson et al., 1993) and cell proliferation and adhesion (Saitoh et al., 1989). A characteristic feature of APP is its proteolytic cleavage by group of enzymes or enzyme complexes, the α-, β- and γ-secretases (Selkoe, 2001). The differential actions of these secretases lead either to the non-amyloidogenic or amyloidogenic pathway. Three enzymes, ADAM 9, ADAM 10 and ADAM 17 (also known as tumor necrosis factor converting enzyme), all with α-

secretase activity, have been identified. These belong to the ADAM family, a disintergrin and metalloproteinase enzyme (Allinson et al., 2003). The α-secretase cleaves APP within the Aβ region to produce the large amino N-terminal ectodomain, the soluble sAPP that is subsequently secreted into the extracellular medium (Kojro and Fahrenholz, 2005), and the 83-residue COOH-terminal fragment C83 (Sisodia et al., 1990). The C83 fragment is retained in the membrane, and subsequently cleaved by γ-secretase to form the short segment p3 (Sisodia et al., 1990). The α-cleavage pathway is considered as default, non-amyloidogenic pathway, since the cleavage occurs in the Aβ region, thereby precluding formation of Aβ. In the amyloidogenic pathway, initial proteolysis is mediated by β-secretase, a type I integral membrane protein of the pepsin family of aspartyl proteases (Vassar et al., 1999). The β-secretase cleavage produces a 99-residue COOH-terminal fragment C99 within the membrane and soluble β-APPs, in the extracellular space (Vassar, 2004). These fragments are processed by γ-secretase to produce p3 from C83 or Aβ from C99 (Fig 1.2). γ-secretase cleavage is not sequence specific resulting in Aβ peptides of varying length ranging from 39-43 amino acids. (Selkoe, 2001).

1.4.2 Aβ Fibrillogenesis

Monomeric Aβ formed from APP cleavage is unstructured (Suzuki et al., 1994), and can self- assemble via non-covalent nucleation dependent polymerization process (Jarrett and Lansbury, 1993, Lomakin et al., 1996). Aβ is thought to start accumulating in vivo as low molecular weight species (LMW Aβ) that consists primarily of monomers

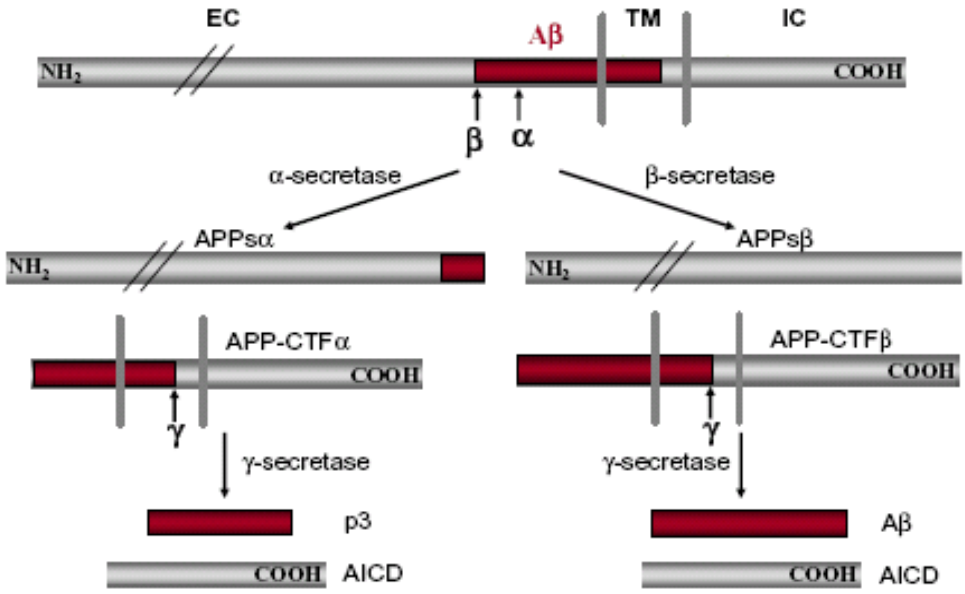

Figure 1.2 Schematic representation of formation of Aβ from APP by the action of secretases. EC: extracellular; TM: transmembrane; IC: intracellular. Aβ domain is highlighted in red. Only one cleavage site is shown for each enzyme. Figure adapted from Zheng.H and Koo H.E, 2006, *Mol Neurodegen*, 1:5.

that are constitutively secreted from the brain cells (Hartley et al., 1999). Formation of Aβ consists of a change from random coil or α-helix into a β-strand. The conformational change of β-amyloid is in part due to the hydrophobic collapse of the very hydrophobic C-terminal region of Aβ. This limits the rate of nucleation, and the hydrophobic interaction is further maximized by β-sheet conformation (Tycko, 2003). Although Aβ(1-40) residue is present in higher concentrations in the human body, elevated levels of Aβ(1-42) residue with additional hydrophobic I41 and A42 are found to be associated with familial forms of AD. Furthermore, it has been reported that Aβ(1-42) is the major component of the immature senile plaques and cerebrovascular amyloid deposits (Roher et al., 1993, Iwatsubo et al., 1994). *In vitro*, Aβ(1-42) forms fibrils rapidly even at much lower concentration than Aβ(1-40) (Jarrett et al., 1993b, Harper et al., 1997a). Hence, identification of the slowest or rate-determining step in the overall process is the key to understanding the rate of amyloid formation.

1.4.3 Nucleation-Dependent Polymerization of Aβ

In vitro, Aβ fibrillogenesis is proposed to occur via nucleation-dependent polymerization process. This model consists of a nucleation or lag phase and an extension phase. Monomers undergo a slow nucleation phase or lag phase, which comprise a series of association steps to form an oligomeric nucleus. This step is thermodynamically unfavorable, representing the rate-limiting step in amyloid fibril formation. Once the nucleus has been formed, further addition of monomers becomes

thermodynamically favorable, resulting in a growth phase in which the nucleus grows rapidly to form large polymers. This is followed by a steady state phase, in which the aggregate and the monomer appear to be at equilibrium (Fig 1.3A) (Jarrett and Lansbury, 1993, Harper and Lansbury, 1997). In nucleation dependent polymerization, polymer formation is observed only if the monomer exceeds a certain level known as the critical concentration. Beyond the critical concentration, the polymer concentration increases but the monomer concentration remains the same (Harper and Lansbury, 1997). The *in vivo* concentration of Aβ in the CSF is in the low nanomolar range (Nitsch et al., 1995, van Gool et al., 1995). However, the critical concentration of Aβ measured *in vitro* is 3-4 orders of magnitude greater than the average brain concentration, thereby suggesting a local super saturation mechanism for Aβ nucleus formation and growth (Harper and Lansbury, 1997, Klunk et al., 1994). The proposed mechanism suggests that the Aβ gets supersaturated transiently in a cellular compartment. During this period a slight increase in the concentration results in intracellular aggregation. Also, the length of time that Aβ is locally supersaturated is very critical. If Aβ is released from the supersaturated state before nucleus is formed, there will be no amyloid formation as in normal conditions. In AD, it is hypothesized that the duration of supersaturated state is lengthened thereby leading to nucleation and amyloid fibril formation (Harper and Lansbury, 1997, Jarrett and Lansbury, 1993, Lomakin et al., 1996), Lomakin et al., 1997). In a typical nucleation-dependent polymerization oligomerization is not observed until the monomer concentration exceeds the critical concentration. During the lag phase protein associates in a supersaturated solution to form ordered soluble oligomeric nuclei, and during this period there are no detectable fibers. Addition of preformed protein nuclei during the lag

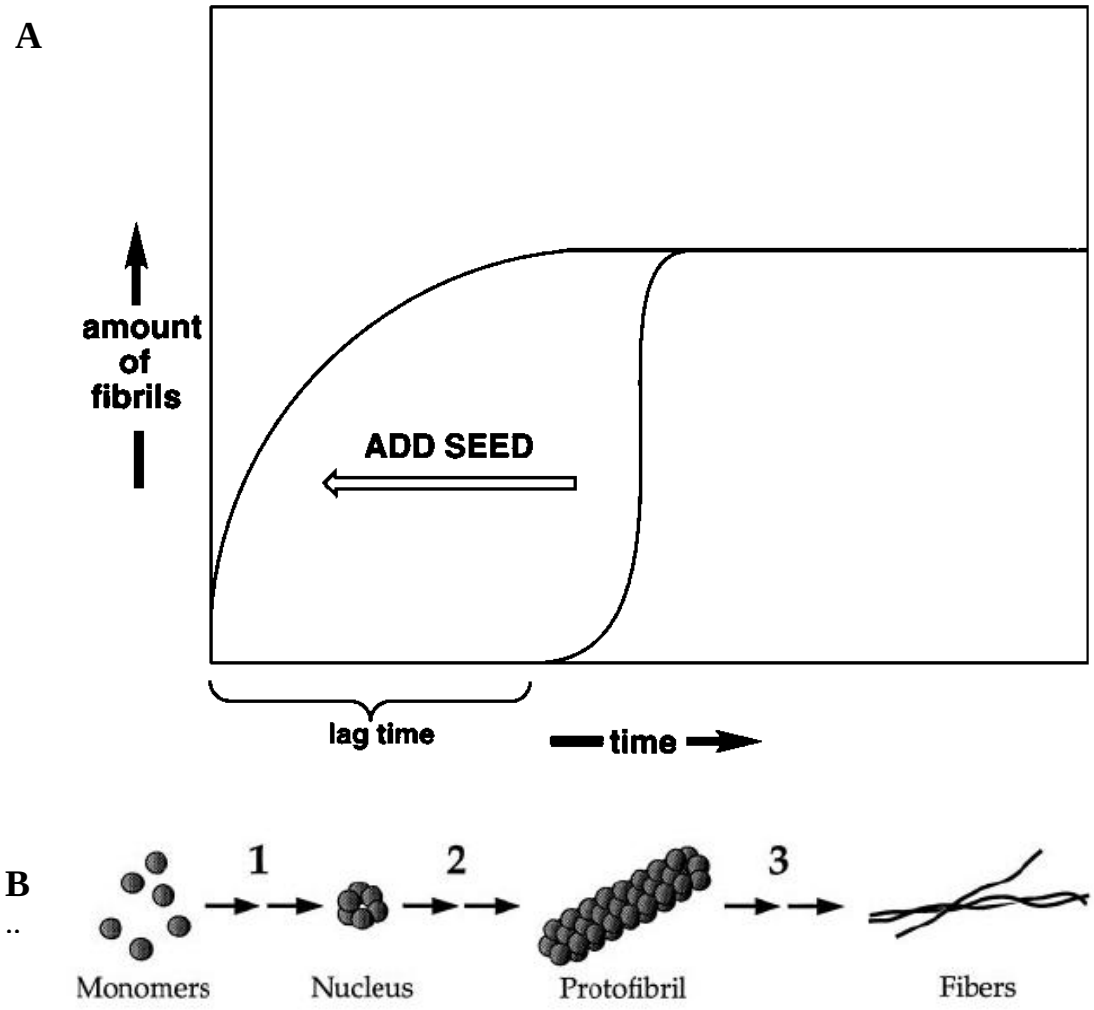

Figure 1.3. Schematic representation of nucleation dependent polymerization
(A) Monomers undergo slow nucleation to form the nucleus (lag phase). Once the nucleus is formed there is rapid aggregation to form fibrils. The lag phase can be overcome by the addition of preformed seeds, or by manipulating the aggregation conditions like peptide concentration, temperature, pH and ionic strength. (**B**) Once critical concentration is achieved, monomers undergo nucleation to form nucleus, and this proceeds to form the protobrils and then the mature fibrils. (Fig 1.3A adapted from Harper. J.D., and Lansbury, P.T. Jr., 1997, *Ann Rev Biochem*, 66:387-407. 1.3 B adapted from Walsh, D.M., et al 1997, *J Biol Chem*, 272:22364-22372).

time results in immediate polymerization, a process known as seeding (Harper et al., 1997a). Once the oligomeric nuclei are formed, the aggregates grow rapidly (elongation phase) until a thermodynamic equilibrium between the aggregate and monomer is reached (Harper et al., 1997a, Walsh et al., 1997). Studies have shown that small elongated oligomers appear early in the fibril formation pathway, and measure 2.7 to 4.2 nm in diameter and < 200 nm in length. These structures disappeared with longer incubation time, and were replaced by full length fibrils (Kowalewski and Holtzman, 1999). Radiochemical immunological assays have shown the existence of short lived species prior to the formation of protofibrils, that progress to form the mature fibrils (Walsh et al., 1997). Intermediate protofibril structures were about ~40% the height of the mature fibril, and are believed to appear very early in the process and disapears as the fibrils appear (Koo et al., 1999). These findings support the idea that protofibrils acts as a center for the formation of mature fibril. Several models exist that shows the proposed coversion of protofibrils to mature fibrils. One is the end to end association of protofibrils but,this was considered unlikely due to the kinetic barriers associated with proper allignment of protofibril ends (Walsh et al., 1997). Alternatively, protofibrils could also associate laterally followed by an end-end annealing to form mature fibrils (Nichols et al., 2002).

The longer peptide Aβ(1-42) was shown to nucleate faster than Aβ(1-40) (Harper and Lansbury, 1997). Transgenic mice that secrete high levels of Aβ(1-42) in the absence of APP over expression, show greater extent of amyloid pathology in contrast to

transgenic Aβ(1-40) mice (McGowan et al., 2005). These experiments highlighted the importance of Aβ(1-42) in amyloid deposition, and it was suggested that Aβ(1-42) is required for the nucleation *in vivo*. The exact nature of the nucleation seed *in vivo* is not known. It is hypothesized that in the crowded environment inside neurons or in the brain parenchyma, Aβ binds to other proteins or lipids and contributes to seeding (Hoozemans et al., 2006). One such example that supports this hypothesis is the binding of Aβ to ganglioside GM1, leading to a conformation change that likely acts as a seed for aggregation, thereby increasing the fibril formation (Hayashi et al., 2004).

1.5 Fibril Structural Assembly

Amyloid fibrils are noncrystalline and insoluble making it difficult for structural studies by the two principal experimental approaches to structure determination – X-ray crystallography and solution-state nuclear magnetic resonance (NMR). However, X-ray fiber diffraction studies indicate a cross β' orientation in amyloid fibrils. Intense synchrotron X-ray beams were used to obtain high-resolution diffraction patterns from a range of different ex vivo and synthetic amyloid fibrils. Amyloid fibrils were isolated from patients with monoclonal λ immunoglobulin light chain amyloidosis, reactive systemic amyloid A protein amyloidosis and Val30Met transthyretin amyloid, synthetic fibrils were isolated from residues 10-19 of transthyretin, and peptide was isolated from residues 20-29 of islet–associated polypeptide (1APP) (Inouye et al., 1993, Sunde et al., 1997). High resolution patterns from these samples were dominated by cross beta reflections, and the diffraction patterns showed similarities in spite of the fact that the samples were from different peptides. This suggested the presence of a common core

molecular structure at least at the level of protofilament. Extensive biophysical studies were done on transthyretin, a tetrameric protein that is the backup transporter of thyroxine and the main transporter of retinol binding protein (Blake et al., 1978). One model that was extensively studied was the Val30Met transthyretin amyloid (Blake and Serpell, 1996), and this model represented the basic structural elements of the other amyloid fibrils that were studied in Sunde et al, (1997). Structure prediction studies have indicated that C –terminal 10 residues and residues 17-21 are highly hydrophobic. Residues 28 onwards had high probability for β-sheet structure (Kirschner et al., 1987)

The fiber diffraction studies cannot determine the chemical details required to understand the fibrillogenesis, especially details regarding parts of the sequence that form β-strands, and the specific amino acid residues that interact. Solid state NMR studies (Petkova et al., 2002) have revealed that the cross-β motif in full length Aβ fibrils is comprised of in-register parallel –β sheets. These studies have shown that the first 10 residues of Aβ(1-40) are structurally disordered in the fibrils. Further probe into the structural aspects revealed that the residues 12-24 and 30-40 (Fig 1.4B) form two β -strand segments that are separated by a "bend" segment with non-β -strand conformation at G25, S26 and G29. The bend enables the two strands to form parallel β-sheets that are in contact via the side chains. The resulting structure is a parallel, in register, cross β structure with a hydrophobic core and one hydrophobic face. Fibrillization of amyloid is generally considered to driven by hydrophobic rather than electrostatic interactions (Halverson et al., 1990, Hilbich et al., 1991, Hilbich et al., 1992). All full-length Aβ and Aβ fragment fibrils studied so far have been found to possess structures that maximize hydrophobic contacts within a β -sheet. Thus, hydrophobic interactions appear to play a.

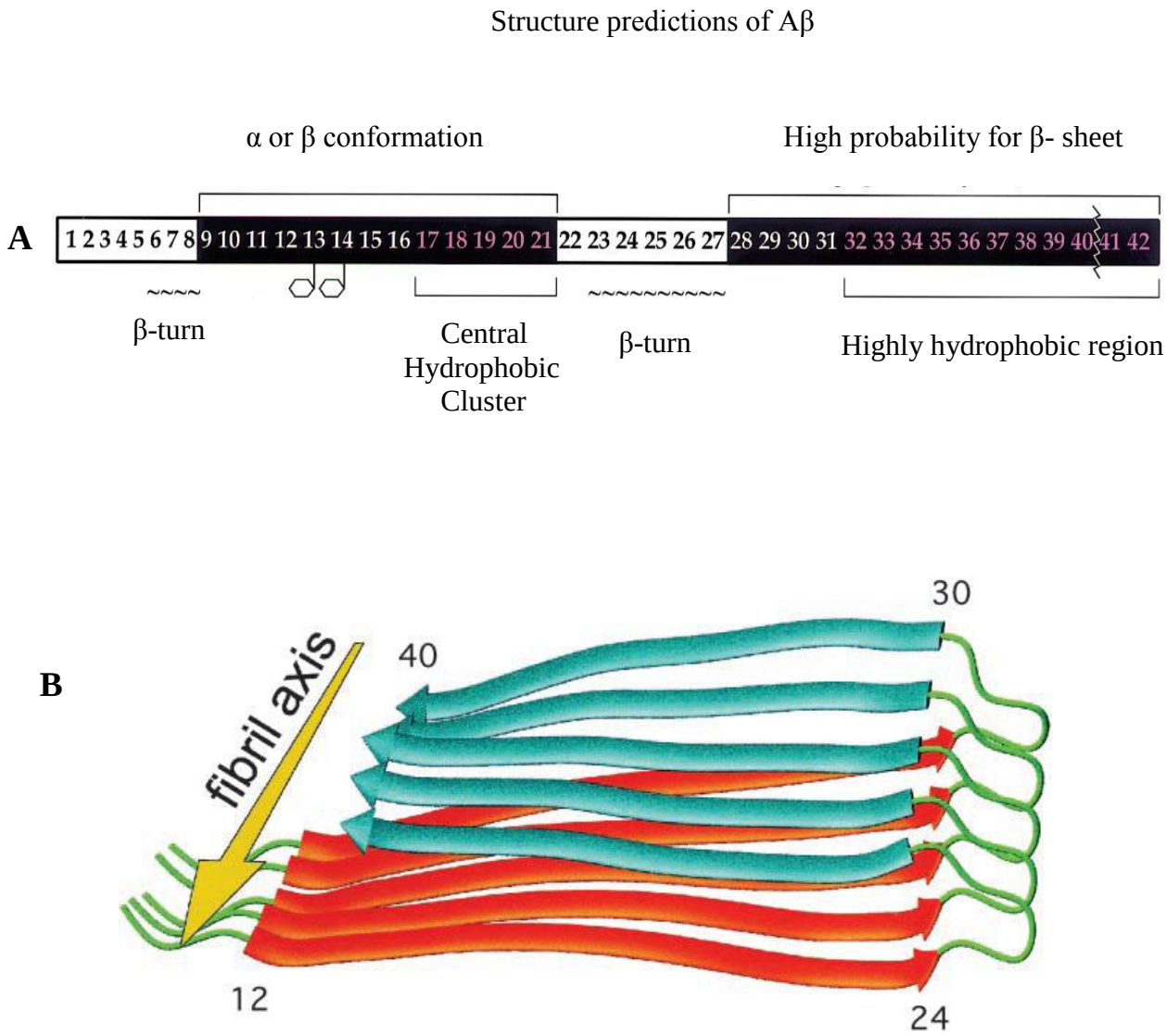

Figure 1.4 (A) Structural prediction showing the region with a high propensity for β-sheet (shown in black). The hydrophobic clusters are shown in pink. Figure adapted from Serpell (2000) Biochim Biophys Acta 1502:16-30. **(B)** Structural model of Aβ(1-40) schematic representation of a single molecular layer, or cross-β unit. The yellow arrow indicates the direction of the long axis of the fibril, which coincides with the direction of intermolecular backbone hydrogen bonds. The cross-β unit is double-layered structure, with in-register parallel β-sheets formed by residues 12–24 (red ribbons) and 30–40 (blue ribbons). Figure adapted from Petkova.et al (2002) *Proc.Natl.Acad.Sci*.USA, 99:16742-16747.

large role in stabilizing amyloid fibril structures (Halverson et al., 1990, Hilbich et al., 1991, Hilbich et al., 1992, Harper et al., 1999)

1.6 Classification of AD

Although AD is predominantly a disease of late life, there are two broad types of AD – the familial AD (FAD) and the sporadic AD (SAD). About 5% of AD cases are 'familial' and occur due to mutations in the APP or in the presenilin genes. Sporadic AD cases are thought to be chiefly associated with lack of Aβ clearance from the brain, unlike familial AD that shows increased Aβ production (Winklhofer et al., 2008). In FAD, the disease segregates in families, following an autosomal dominant inheritance pattern. In SAD, no clear family history is indicated and the disease usually occurs above 60 years of age (Price and Sisodia, 1998). Because of the variation in age at onset, AD is also categorized into early onset and late onset forms. Both the early-onset (familial) and the late-onset (mostly sporadic) forms of the disease have similar neurological and histopathological changes, suggesting that the different forms of the disease have a common pathophysiology and shared etiology (Pimplikar, 2009).

1.6.1 Genetic Mutations Linked with Early Onset AD

Three different genes have been implicated in the pathology of familial Alzheimer's disease. They are: APP (mAPP) gene on chromosome 21 (Goate et al., 1989, Levy et al., 1990), mutations in the presenilin 1 (PS1) gene on chromosome 14 and

mutations in the presenilin 2 (PS2) gene on chromosome 1 (St George-Hyslop, 2000, Tanzi and Bertram, 2001). Mutation in the APP gene was the first mutation associated with FAD. Involvement of APP in FAD was suspected due to the fact that the genes resided on chromosome 21, and people with Down's syndrome developed the symptoms of AD by the age of 40 (Selkoe and Podlisny, 2002). Presenilins are transmembrane proteins localized mainly in the endoplasmic reticulum and Golgi membranes of neuronal and non-neuronal cells **(**De Strooper et al., 1998**)**. Precise functions of presenilins are unclear. Several studies indicate that PS1 and PS2 are catalytic components of γ-secretases (Haass and De Strooper, 1999, Sisodia et al., 1999). *In vitro* studies demonstrated that the pathogenic mutations in the APP and presenilin genes are associated with abnormal processing of APP. The processing sites are either located adjacent to the Aβ domain in APP at the β- and γ- secretase cleavage sites (Nilsberth et al., 2001) or within the Aβ sequence at the α-secretase cleavage site. Either of these lead to increased production and elevated plasma levels of Aβ, especially Aβ(1-42) or increased ratio between Aβ(1-42) and Aβ(1-40) (Mullan et al., 1992, Citron et al., 1994, Suzuki et al., 1994). The only known mutation near to the β-secretase cleavage site is the Swedish double mutation KM → NL. This mutation increases the level of total Aβ by increasing Aβ(1-40) and the levels of Aβ(1-42), though the increase is less in the case of the latter. Mutations near the γ- secretase cleavage site results in an increased production of Aβ(1-42) (Scheuner et al., 1996). However, the V715M mutation (French) results in reduction of Aβ(1-40) levels without affecting the Aβ(1-42) levels (Ancolio et al., 1999), suggesting that the increase in Aβ(1-42) : Aβ(1-40) ratio is important rather than the absolute amount of Aβ(1-42).

Intra-Aβ mutations are associated with amyloid accumulation in the cerebral blood vessels in addition to the amyloid plaque formation. E693Q (Dutch) mutations are associated with intracerebral hemorrhages (Levy et al., 1990). A692G (Flemish) mutation manifest with intracerebral hemorrhages but these patients may survive to develop a progressive AD-like dementia (Hendriks et al., 1992). The E693G (Arctic) mutation is associated with a decrease in Aβ(1-42) concentration in media from cells that were transfected with APP_{E693G}. Also, the plasma levels of both Aβ(1-42) and Aβ(1-40) were low in mutation carriers compared to healthy family members. *In vitro* studies have shown that the carriers of E693G (Arctic) mutation have a high propensity to form protofibrils (Nilsberth et al., 2001).

Transgenic (Tg) animals carrying mutations in amyloid precursor protein and presenilin genes displayed enhanced production and progressive aggregation of Aβ. Mouse models have shown that Aβ(1-42) is essential for Aβ deposition not only in parenchyma but also in vessels (Borchelt et al., 1997, Holcomb et al., 1998). These models have established that when APP/Sw mice (producing both Aβ(1-40) and Aβ(1-42) are bred with mice expressing mutant PS1 (that increases brain Aβ(1-42)/Aβ(1-40) ratio), the crossbred mice have drastically increased amyloid deposition in parenchyma and vessels compared to single transgenic controls. However, no significant tau pathology or extensive neuron loss, as found in AD brain, was detected in these transgenic animals (Games et al., 1995, Hsiao et al., 1996). Studies on mutations in APP, PS1 and PS2 genes have provided important insights for understanding some of the key underlying biological mechanisms of AD. All these genetic mutations lead to

Gene (and protein)	Chromosomal location	Relevance to AD pathogenesis
Amyloid Precursor Protein (APP)	21q21.3	Increase in Aβ production or Aβ(1-42)/Aβ(1-40) ratio; mutations in the Aβ sequence or close to the β and γ-secretase site of APP [need beta symbols for Abeta]
Presenilin 1 PSEN1	14q24.3	Increase in Aβ(1-42)/Aβ(1-40) ratio; mutations throughout molecule; enzymatic role in γ-secretase complex
Presenilin 2 PSEN2	1q31–42	Increase in Aβ(1-42)/Aβ(1-40) ratio; mutations throughout molecule; enzymatic role in γ-secretase complex

Table 1.2 Three genes implicated in the pathology of early onset AD

Intra Aβ mutations

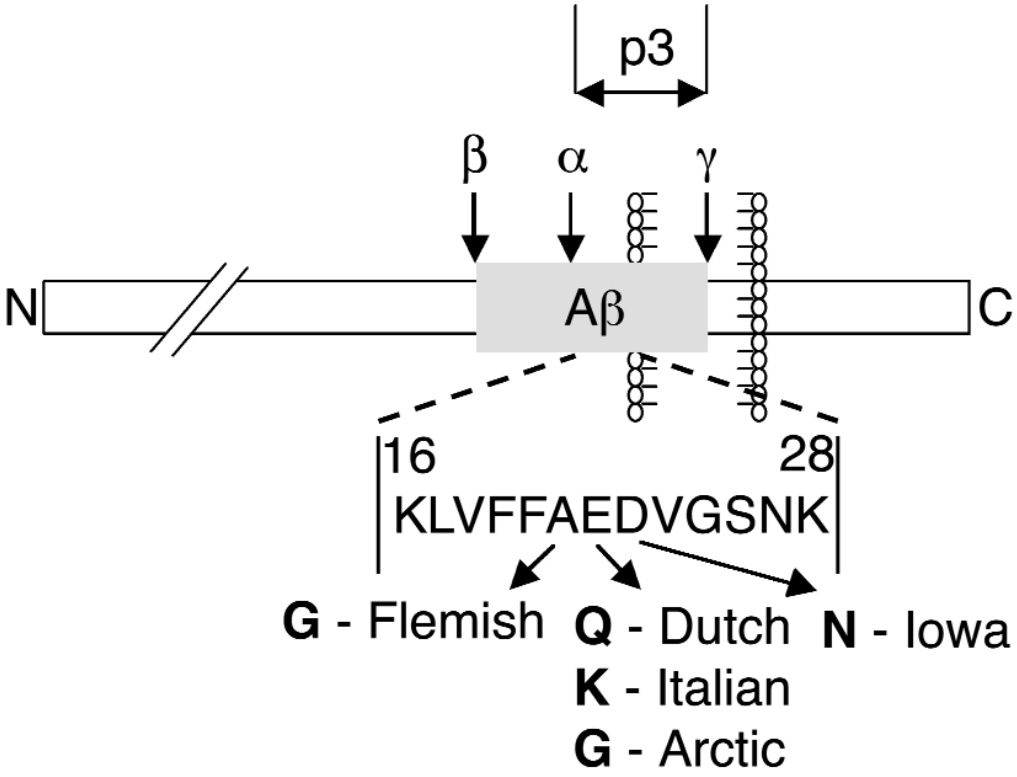

Figure 1.5 Intra Aβ mutations. Schematic representation of APP molecule illustrating the sites of cleavage by α-, β-, γ-secretases. Localization of Aβ and p3 proteins containing the intra Aβ mutations. [Figure adapted from Nilsberth C, et al, 2001, *Nat Neurosci*, 4:887-893.]

overproduction of Aβ(1-42) in the brain before AD symptoms arise, indicating accumulation of Aβ(1-42) as initiating factor in the pathogenesis of Alzheimer's disease. APP or presenilin mutations cause chronic increase in the Aβ(1-42) levels in the brain extracellular fluid, and inside neurons that slowly leads to the oligomerization and, eventually, forms fibrils that deposit and later forms the mature plaques (Selkoe and Podlisny, 2002). FAD genetics and other mouse studies have been very useful in research on early onset AD. However, vast majority of AD cases occur late in life, and are influenced by both genetic and environmental factors (Bertram and Tanzi, 2008, Bu, 2009). These include the ε4 allele of the apolipoprotein E (ApoE) gene (Blacker et al., 1998, Bu, 2009). ApoE was identified as a risk factor or a susceptibility gene for AD in 1993 (Strittmatter et al., 1993). ApoE plays a major role in lipoprotein metabolism and cholesterol homeostasis, in the brain (Mahley, 1988). The other genetic factors are, proteinase inhibitor α2-macroglobulin gene on chromosome 12 (Pericak-Vance et al., 1997, Blacker et al., 1998), insulin degrading enzyme on chromosome 10 (Olson, 1998, Vekrellis et al., 2000), low density lipoprotein receptor related protein and angiotensin converting enzyme (Olson, 1998, Kehoe et al., 1999). So far, 20 mutations in the APP gene, 124 mutations in the PS1gene and 8 mutaions in PS2 gene have been described worldwide. Therefore gene-targeting strategies will help clarify the *in vivo* functions of genes linked to AD. The transgenic mouse model studies will offer new opportunities to study the evolution and character of AD-type cellular dysfunction in addition to biochemical and cellular mechanisms of the disease. These models will also be very useful to test the various treatment strategies for the disease.

1.7 Amyloid Cascade Hypothesis

The amyloid cascade hypothesis was formulated more than a decade ago and states that the neurodegenerative process comprises of series of events triggered by the abnormal processing of the amyloid precursor protein. The main tenet of the hypothesis is that the increased production or decreased clearance of Aβ peptides causes the disease (Hardy and Higgins, 1992, Hardy and Selkoe, 2002). In either case there is accumulation of Aβ(1-40) and Aβ(1-42) peptides that result in aggregation and formation of insoluble plaques, triggering a series of deleterious changes that results in death of the neuronal cells. Since Aβ(1-42) levels are found to be higher in AD patients, it was proposed that increased levels of Aβ(1-42) triggered the cascade of events resulting in AD (Younkin, 1995). Over the years the hypothesis has changed with regards to the type of pathogenic Aβ species that initiates deleterious events resulting in AD. Two primary reasons led to this alteration in the hypothesis. First, the plaque load does not correlate with the degree of dementia in humans (Terry et al., 1991). Also, many mouse models of AD show memory deficits long before appearance of plaques in the brain (Lesne et al., 2008). Second, *in vivo* neuroimaging techniques have shown the presence of plaques in cognitively normal people (Nordberg, 2008, Villemagne et al., 2008). It is possible that these people may have high risk of AD. These observations suggest that insoluble plaques are not responsible for the pathologic cascade of events, and may in fact be benign or even protective in nature (Caughey and Lansbury, 2003).

1.8 Modified Amyloid Cascade Hypothesis

Intracellular Aβ is assumed to be an early event in AD pathogenesis (Fig 1.6) prior to extracellular Aβ deposition (Wirths et al., 2004). There is evidence for intracellular accumulation of Aβ, in both mouse models and human AD brains, that could contribute to disease progression (Gouras et al., 2000). The focal point is mainly on the soluble aggregates of Aβ termed oligomers. Oligomers were observed to occur intracellularly (Walsh et al., 2000). Furthermore, Aβ(1-42) oligomers were found to be potent neurotoxins in neuronal cultures at nanomolar concentrations (Lambert et al., 1998). These oligomers were termed as Aβ derived diffusible ligands (ADDLs), and were found to be capable of inhibiting hippocampal long term potentiation thereby disrupting synaptic plasticity (Lambert et al., 1998, Walsh et al., 2002b). Primary neuronal cultures from APP transgenic mice have shown that oligomeric Aβ(1-42) redistributes from the outer membrane of the multivesicular bodies (MVB) to the inner membranes of the abnormal endosomal organelles and microtubules, and oligomeric forms have been observed in abnormal processes and synaptic components in the human AD brain (Takahashi et al., 2002, Takahashi et al., 2004). Sodium dodecyl sulfate (SDS) soluble dimeric Aβ was found to accumulate in lipid rafts in the brain tissue of APP transgenic mice. These dimers were found to appear early on as memory impairments become obvious, and provide a further link to the assumption that Aβ oligomers are tightly linked to memory dysfunction in AD (Kawarabayashi et al., 2004). Dimeric oligomeric species have been isolated from human AD brains even in the absence of protofibrils, or fibrils (Walsh et al., 2002a, Shankar et al., 2008), and the dimers were found to inhibit long–term potentiation. A number of other poorly characterized but

Modified β-Amyloid Cascade

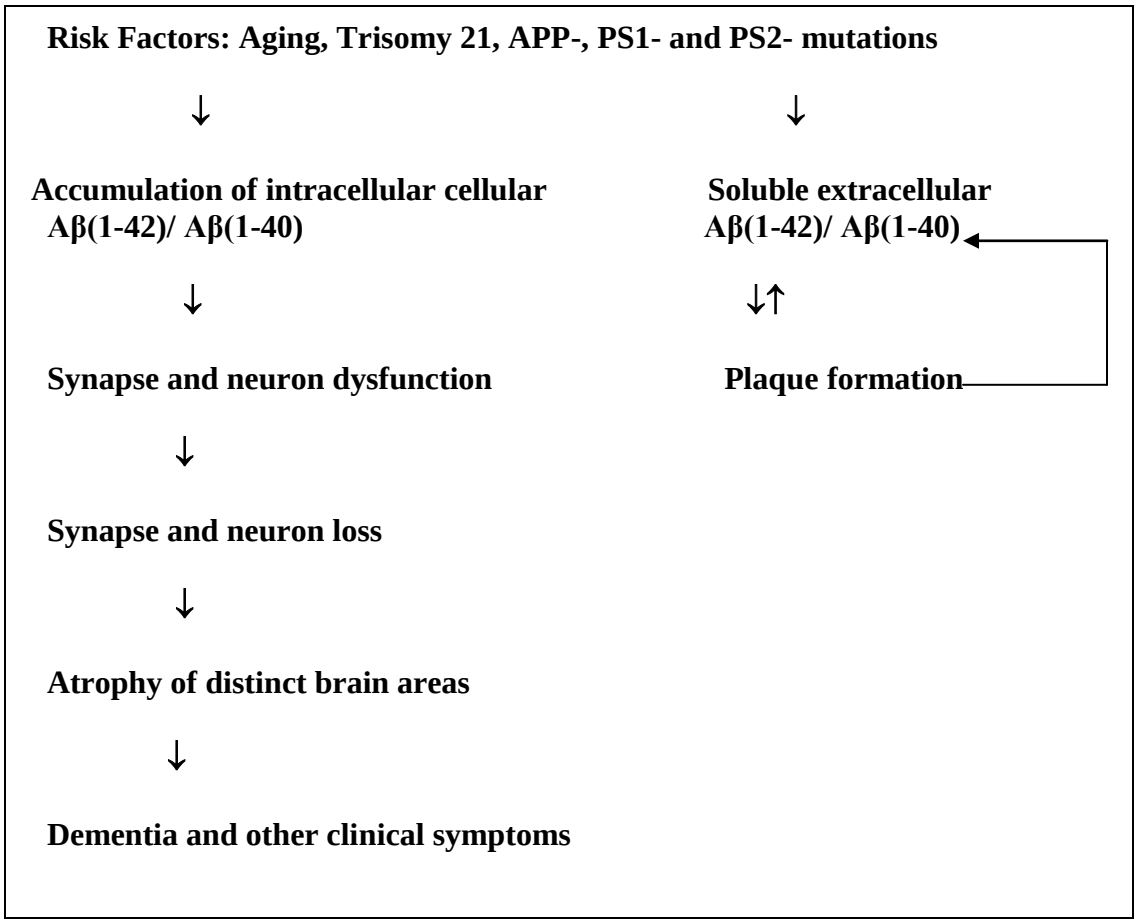

Figure 1.6. Scheme showing the modified Aβ amyloid hypothesis. Ageing, Down syndrome and mutant APP, PS-1 or PS-2 causes an increase in intraneuronal Aβ(1-42) levels causing it to accumulate, leading to synaptic and neuronal dysfunction and degeneration in brain areas responsible for distinct memory functions. In parallel, increased secretion and deposition of Aβ(1-42) leads to extracellular plaque formation. Aβ(1-42) plaques are dynamic structures, and can also be internalized again, thereby increasing the intraneuronal pool of Aβ(1-42), which in turn increases the neurotoxic intracellular events. (Adapted from Wirths.O 2004, *J Neuchem*, 91: 513-520)

biochemically distinct forms of Aβ oligomers have been identified. These aggregation species have demonstrated toxicity effects *in vivo* and *in vitro* model systems (Klein et al., 2001, Walsh and Selkoe, 2004, Glabe, 2005, Walsh and Selkoe, 2007). Fibrillar and pre-fibrillar oligomer species formation have been reported by (Kayed et al., 2007). The new hypothesis suggests that Aβ formation activates the microglial cells which in turn release neurotoxic substances such as nitric oxide, proinflammatory cytokines, complement proteins and other inflammatory mediators leading to tau phosphorylation and neurodegenerative changes (Akiyama et al., 2000, McGeer and McGeer, 2001).

1.9 Microglia

Microglia represent the macrophage-derived cells in the nervous system that are capable of responding rapidly to various types of insults (Davalos et al., 2005, Nimmerjahn et al., 2005). They are derived from a myeloid lineage and are the immune effector cells in the brain. Microglia represent approximately 5-10% of all the glia found in the brain and are distributed throughout the gray and white matter of the nervous system. At rest, they are believed to play supportive roles for neurons. An inflammatory stimulus will activate the microglia causing them to migrate to sites of injury and subsequently transform into a macrophage-like phenotype (Bamberger and Landreth, 2001). Transformation of microglia into activated form is accompanied by the up regulation of cell surface molecules that are involved in immune responses, secretion of cytokines and acute phase proteins (Kalaria, 1999). Deposition of fibrillar amyloid deposits leads to activation of microglia, and this has been supported by a number of

animal studies. Transgenic (Tg2576) mice overexpressing APP were generated and they developed extensive amyloid plaques, mostly in the hippocampus and in the cortex. Analyses of these animals revealed the presence of activated microglia surrounding the plaques (Benzing et al., 1999, Mehlhorn et al., 2000). Aβ accumulation leads to a site-specific activation of glia resulting in the secretion of pro-inflammatory cytokines (Akiyama et al., 2000, Cooper et al., 2000). The inflammatory response can be considered as an attempt to clear the Aβ, however, an overwhelming accumulation of Aβ will lead to a chronic proinflammatory response (Blasko et al., 2004) which causes the defect in neuronal function.

A 'microglia dysfunction' theory (Streit, 2004) has been proposed recently. The theory states that many of the microglia in the AD brains are dystrophic and apoptotic due to presence of Aβ and cellular debris, and are unable to carry out their normal function of phagocytosis and neuroprotection. The activation of microglia in AD reflects the ongoing pathology. Experimental data have shown that reactive microglia occur within Aβ deposits that are associated with tissue injury and dementia (neuritic plaques), and not with diffuse plaques (clinically benign Aβ deposits) (Perlmutter et al., 1992, Giulian et al., 1995, Giulian, 1999). Selectivity in the distribution of reactive microglia suggests that a specific signal within the neuritic and core plaques triggers the brain inflammation. Moreover the pattern of microglia distribution in AD is unique to the disease, suggesting a very crucial role for brain inflammatory responses in the etiology of the disease. In AD, it is believed that plaques serve as stable irritants that sets the CNS in a chronic state of inflammation, promoting the activation and recruitment of microglia, which in turn secretes neurotoxins (Giulian, 1999). Two *in vitro* models support this

hypothesis. First, plaque fragments are engulfed within few minutes after they were placed in cultures of human microglia (Giulian et al., 1995). The morphology changes from resting ramified forms to reactive, amoeboid shapes. Data also suggest that plaque activated, and not resting microglia, secrete neurotoxic substances. Second, plaque fragments do not show direct toxic effects on microglia depleted neuron cultures. About 50-µl to 100-µl spots of highly aggregated Aβ are placed on the floor of a cell culture well to mimic the Aβ deposits of AD. Cultured microglia from rapid brain autopsies of subjects with or without AD are then seeded into the well. Within days, there is a pronounced activation of the microglia as well as clear chemotaxis to the Aβ spots. The activated microglia, within weeks, completely cover the Aβ deposits and begin to phagocytose them, a process that can be measured quantitatively (Rogers and Lue, 2001). These findings support the fact that immune cells of the brain are necessary to mediate the plaque related injury to the neurons. Activated glia contributes to neurotoxicity through the induction of inflammatory mediators such as interleukin (IL)-1and tumor necrosis factor-alpha (TNF α). In addition, these cytokines also mediate the expression of the inflammatory enzyme-inducible nitric-oxide synthase (iNOS) (Akama and Van Eldik, 2000).

1.10 Aβ Induced Inflammatory Response

The brain was believed to be immunologically privileged by virtue of two factors. One is the blood-brain barrier, which hinders entry of humoral immune elements into the brain. Second, it was assumed that the nervous system was unable to mount an intrinsic

inflammatory response. However, it is now widely recognized that brain immunologic privilege may be limited since antibodies and humoral immune cells do penetrate the brain, (Wekerle, 2002). Innate, intrinsic, microlocalized, chronic inflammatory responses are clearly evident in multiple neurologic disorders, especially AD (Akiyama et al., 2000, Griffin, 2006). *In vitro* models have facilitated elucidation of mechanisms underlying microglial migration, colocalization, and scavenging of Aβ deposits (Rogers and Lue, 2001). Several groups have identified a number of inflammation-related receptors expressed on microglia. Among the many receptors that have been identified, macrophage scavenger receptors (El Khoury et al., 2003), Formyl chemotactic receptors (Lorton et al., 2000), receptor of advanced glycation end products (RAGE) (Yan et al., 1996), are probable important ones since they can have Aβ as a ligand. Studies have also confirmed that Aβ induces glial activation *in vivo* (Weldon et al., 1998, Ishii et al., 2000). The fibrillar conformation of Aβ seems to be a crucial feature for such cell activating effects (Ishii et al., 2000). Alternative and classical complement pathways have been implicated in AD pathogenesis (Rogers et al., 2002b), Akiyama et al., 2000). Fibrillar Aβ can bind C1q, the first classical pathway component. This leads to sequential activation of other components of the classic pathway with the release of anaphylatoxin (C4a and C3a) and opsonizing (C3b and iC3b) fragments (Rogers, 2008) that enhance inflammatory mechanisms. Another mechanism of complement-mediated inflammatory responses is the formation of C5b-9, the membrane attack complex (MAC), targeted at cellular membranes. This assembly creates a transmembrane channel that facilitates the diffusion of ions to and from the cytoplasm, leading to disruption of cell homeostasis. Sufficient assembling of MAC complexes on the cell surface leads to cell lysis.

Immunohistochemical staining of C1q was shown to be colocalized with aggregated Aβ deposits in the AD brain, but is absent in the non demented brain (Rogers et al., 1992). A certain degree of aggregation is required for the activation of the complement system. The amino acids 14-26 of the antibody- independent binding site of C1q contain five cationic side chains that are likely to become charge-coupled to four anionic side chains within residues 1 to 16 of N-terminus of Aβ peptide (Jiang et al., 1994). Along with this charge coupling, the hexameric structure of C1q appears to align well with adjacent C1q binding sites when Aβ is in its aggregated cross-β-pleated sheet configuration, the configuration that is predominant in the aggregated Aβ deposit. Once C1q has been activated by Aβ, subsequent activation of the full classic cascade may ensue, and this has been widely reported in Aβ -rich areas of the AD brain (Webster et al., 1995). CD14, the receptor for lipopolysaccharide (LPS) interacts with fibrillar Aβ (Fassbender et al., 2004) and microglia kill the Aβ(1-42) damaged neuron by a CD14 dependent process (Bate et al., 2004). The involvement of CD14 in Aβ induced microglia activation strongly supports the hypothesis that innate immunity is linked with AD pathology (Fassbender et al., 2004, Eikelenboom et al., 2006).

1.10.1 Neuroinflammation and AD Pathogenesis

One of the mechanisms underlying neurodegeneration in AD is a significant inflammatory response to Aβ plaques. Inflammatory response to Aβ plaques are observed in the brains of human patients (McGeer et al., 1987), and in AD transgenic mouse models (Meyer-Luehmann et al., 2008). Neuropathological studies in human brains have

demonstrated activation of microglial cells (McGeer et al., 1996), and these results have been corroborated by *in vitro* studies in which microglial cells exposed to aggregated Aβ have shown an overproduction of proinflamamtory cytokines that trigger the neurodegenerative cascade in the neurons (Quintanilla et al., 2004, Orellana et al., 2005). Further support for this concept came from data showing that individuals consuming nonsteroidal anti-inflammatory drugs (NSAIDS) have a lower risk of AD (McGeer et al., 2006). NSAIDS have also shown protective mechanism in animal models of AD (Yan et al., 2003). Patients receiving systemic NSAIDS developed significantly less symptoms of AD, suggesting that controlling inflammation in the brain helps prevent or slow down the onset of AD (McGeer et al., 1996, Rojo et al., 2008). However, this effect is restricted to only certain (NSAIDS) drugs (Maccioni et al., 2009). Neuroinflammation is characterized by generation of proinflammatory mediators that are locally produced by the host cells, thereby indicating the involvement of the innate immune system.

Inflammation associated with the brain (neuroinflammation) is different from the peripheral inflammation. AD can be thought to be autotoxic disease in which an innate immune system uses local phagocytes, microglia, as an effector (Maccioni et al., 2009). *In vitro* studies have shown that Aβ fibrils result in microglial activation (Giulian et al., 1996, McDonald et al., 1997). The plaque-associated microglia have dilated intracellular channels of smooth endoplasmic reticulum containing amyloid fibrils (Wisniewski et al., 1989, Wisniewski et al., 1992). These findings indicate the role of microglia in clearing the Aβ by phagocytosis, which normally takes place in health (Wisniewski et al., 1991). In AD, the microglia, found clustered around the amyloid deposits, become dysfunctional and unable to clear the amyloid deposits (Rogers et al., 2002a), (Meyer-Luehmann et al.,

2008). While the activated microglia fail to clear Aβ, their presence results in neuronal damage and cognitive decline due to release of cytokines (Edison et al., 2008). Infusion of anti-Aβ antibodies stimulates the plaque-associated activated microglia to clear the deposits (Bacskai et al., 2001).

1.11 Modeling of Alzheimer's Disease

Several *in vivo* models have been developed that were aimed at being a replica to the AD symptoms, and to model certain aspects of neurodegeneration, or amyloid deposition. Mouse models that express wild type APP, APP fragments, Aβ and FAD-linked mutant APP and PS1 were produced. Mice expressing both mutant PS1 and mutant APP were shown to develop Aβ amyloidosis in the central nervous system. Co-expression of the human A246E mutant PS1 and APPswe have displayed elevated levels of Aβ in the brain, and these mice developed several amyloid deposits, dystrophic neurites and glial responses in the hippocampus and cortex (Borchelt et al., 1997). Further, these studies have demonstrated that APP, PS1 and BACE1 are colocalized in the neurites immediately proximal to the sites of Aβ formation in the brain. These findings strengthen the concept of a neuronal origin for Aβ (Wong et al., 2002). The triple transgenic model (3xTg-AD) (Oddo et al., 2003), harbors $PS1_{M146V}$, APP (Swe) and tau_{P301L} transgenes, and exhibit deficits in synaptic plasticity, long term potentiation, and deficits in long-term synaptic plasticity correlate with the accumulation of intraneuronal Aβ. Besides, data from 3xTg-AD model suggest that Aβ pathology precedes tau pathology by several months. *In vitro* models have been very useful since they constitute

models that are able to serve as approximations of a disease. *In vitro* models allow detailed study of pathological factors, and make characterization possible at a cellular level. Rat primary septal cultures (Zheng et al., 2002) and human neuroblastoma cells (Misonou et al., 2000) have been used to study the pathophysiological mechanisms that are hypothesized to contribute to AD. Non transfected cell lines like differentiated PC-12 cells have been treated with Aβ(1-42) to study Aβ neurotoxicity (Bergamaschini et al., 2002). Human SH-SY5Y cells exposed to aggregated synthetic beta-amyloid peptide Aβ(1-42), caused a decreased solubility of tau along with the generation of PHF-like tau-containing filaments that correlates with amyloid cascade (Ferrari et al., 2003).

1.11.1 *In vitro* and *In vivo* Studies on Inflammation and AD

The *in vivo* inflammatory response to Aβ has been mirrored in numerous *in vitro* cell model systems including both microglial and monocytic cells (Klegeris et al., 1997, Misonou et al., 2000, Yates et al., 2000, Combs et al., 2001). Aβ is deposited in the cerebral cortex in the AD brains, and studies have shown the presence of fibrillar Aβ (fAβ) associated with the dystrophic neuritis (Mirra et al., 1991). Geula et al have shown that injection of plaque equivalent concentrations (200pg) of fAβ to the cerebral cortex of aged Rhesus or marmoset monkeys resulted in a significant neuronal loss, and induced hyperphosphorylation of tau. Further, it was also reported that injections of fAβ in the aged primates also resulted in the recruitment and activation of large population of microglia (Geula et al., 1998). Recent studies have shown that low concentrations of fAβ induced massive activation of microglia in aged rhesus cortex in addition to neuronal loss

(Leung et al., 2009). Fibrillar Aβ serves as a ligand for both the scavenger receptor class A (El Khoury et al. 1996; Paresce et al. 1996) and receptor for advanced glycation end products (Yan et al. 1996).

1.12 Human Immune Response

The mammalian immune system is comprised of two branches: innate (cellular), and adaptive immune systems. Innate immune system is the first line of host defense against the pathogens, and is mediated by phagocytes, including the macrophages and the dendritic cells. Innate immunity does not require prior exposure to foreign antigens to get stimulated. Adaptive immunity is dependent upon the signals provided by the innate immune system, which in turn facilitates expansion of antigen specific T and B lymphocytes that can recognize infinite number of potential antigens (Kielian, 2006). Host-defense has been based on the ability to recognize pathogen structures (Akira et al., 2006). The innate immune system recognizes pathogens via a predetermined subset of germ line encoded receptors, thereby limiting the ability to recognize every possible antigen. The innate immune system focuses on few highly conserved structures that are unique and expressed by a large group of microorganisms (Kielian, 2006). The conserved structural motifs are called pathogen-associated molecular patterns (PAMPS). These bind via a limited number of germ-line encoded pattern recognition receptors (PRRs) (Akira et al., 2006, Danilova, 2006). This attribute enables the immune system to distinguish between self and nonself (Medzhitov and Janeway, 1997). Further, PAMPS are essential for the microbial survival, and any mutaion or loss of pattern can be very

lethal. Hence, these patterns are less likely to be subjected to high mutation rates (Medzhitov and Janeway, 1997). Among the various PAMPS available, (Fig 1.7) the TLR-family members are pattern recognition receptors (PRRs) that collectively recognize lipid, carbohydrate, peptide and nucleic acid structures expressed by different microorganisms.

1.12.1 Toll Like Receptors (TLRs) as Pattern Recognition Receptors

Toll-like receptors (TLRs) are evolutionarily conserved from the worm Caenorhabditis elegans to mammals (Hoffmann, 2003, Akira and Takeda, 2004, Beutler, 2004). TLRs are the primary mediators of the innate immune response and belong to a class of type-1 integral membrane glycoproteins. Depending on the primary sequences, TLRs are further divided into subfamilies. TLR1, TLR2 and TLR6 recognize lipids, while TLR7, TLR8 and TLR9 recognize nucleic acids. TLR4 is known to recognize a collection of different ligands, each having a different structure, such as, lipopolysaccharides (LPS), plant diterpene pactlitaxel, fusion protein of respiratory synctytial virus (RSV), fibronectin and heat shock protein (Akira et al., 2006). TLRs are expressed on various immune cells, including macrophages, dendritic cells (DCs), B cells, specific types of T cells, and even on nonimmune cells such as fibroblasts and epithelial cells. Expressions of TLRs are modulated rapidly in response to a variety of cytokines and environmental stresses. Certain TLRs (TLRs 1, 2, 4, 5, and 6) are expressed on the cell surface, others (TLRs 3, 7, 8, and 9) are found almost exclusively in intracellular compartments such as endosomes. The most extensively studied PAMP is

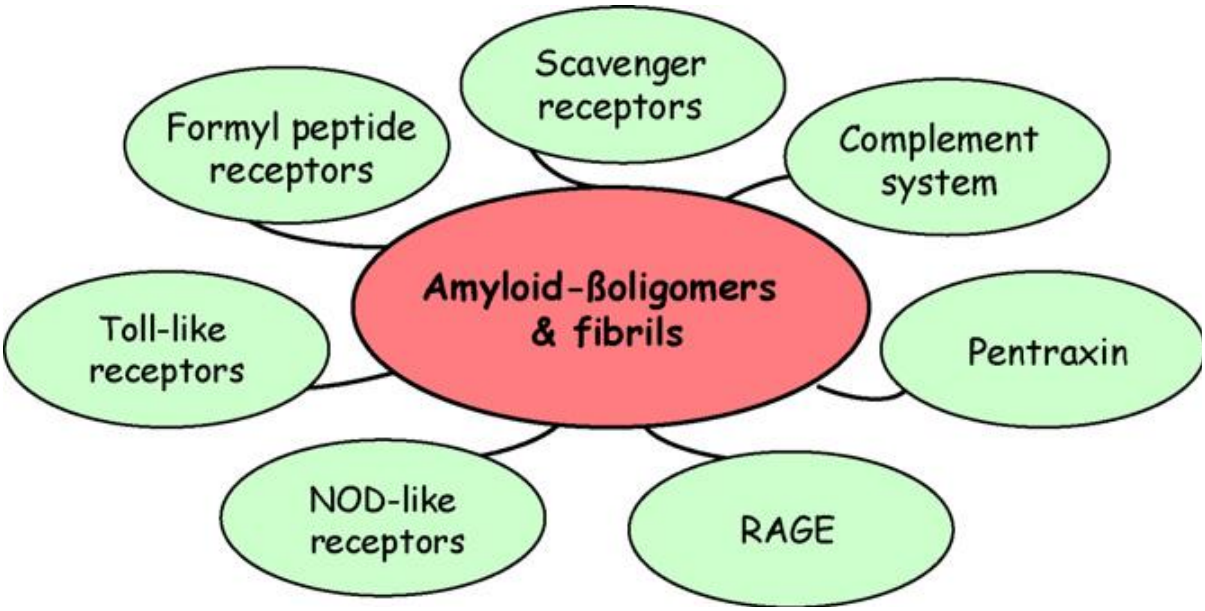

Figure 1.7 Pattern Recognition Receptors (PRRs) Pattern recognition receptors involved in the innate immunity mediated host defence against amyloid-beta oligomers and fibrils in brain. Figure adapted from Salminen A et al, 2009, *Pro Neubiol*, 87:187-194

the bacterial lipopolysaccahride (LPS), an outer membrane component of Gram-negative bacteria. LPS is an endotoxin and the most potent immunostimulant. The lipid portion of LPS termed "lipid A" is the portion associated with the Gram-negative bacterial infection such as the endotoxic shock. The LPS released from the gram-negative bacteria associates with LPS binding protein (LBP), an acute phase protein present in the blood stream. The LPS-LBP complex binds to CD14; a glycosylphosphatidylinositol (GPI) linked protein. CD14 is expressed on the cell surface of the phagocytes. The LPS is then transferred to MD-2, which is associated with the extracellular portion of TLR4. These steps are followed by the oligomerization of TLR4, a key component in LPS signaling (Poltorak et al., 1998, Shimazu et al., 1999).

Aβ, is one among the several growing number of endogenous human molecules to activate the human immune response (Kielian, 2006). There is increasing evidence that suggests the involvement of aggregated Aβ in triggering the human innate immune response. Interaction between fibrillar Aβ(1-42) and CD14 resulted in the release of inflammatory products in primary murine microglial cells and human peripheral blood. Also, recent data shows that aggregated Aβ(1-42) induces cytokine production via TLR2 and TLR4, in a human monocytic cell line (Udan et al., 2008). It has been reported earlier that activated microglial cells are typically found clustered around the dense core plaques and not around the diffuse Aβ deposits (Selkoe, 2004). These findings suggest that the activation of the microglial cells is selective to a particular Aβ morphology.

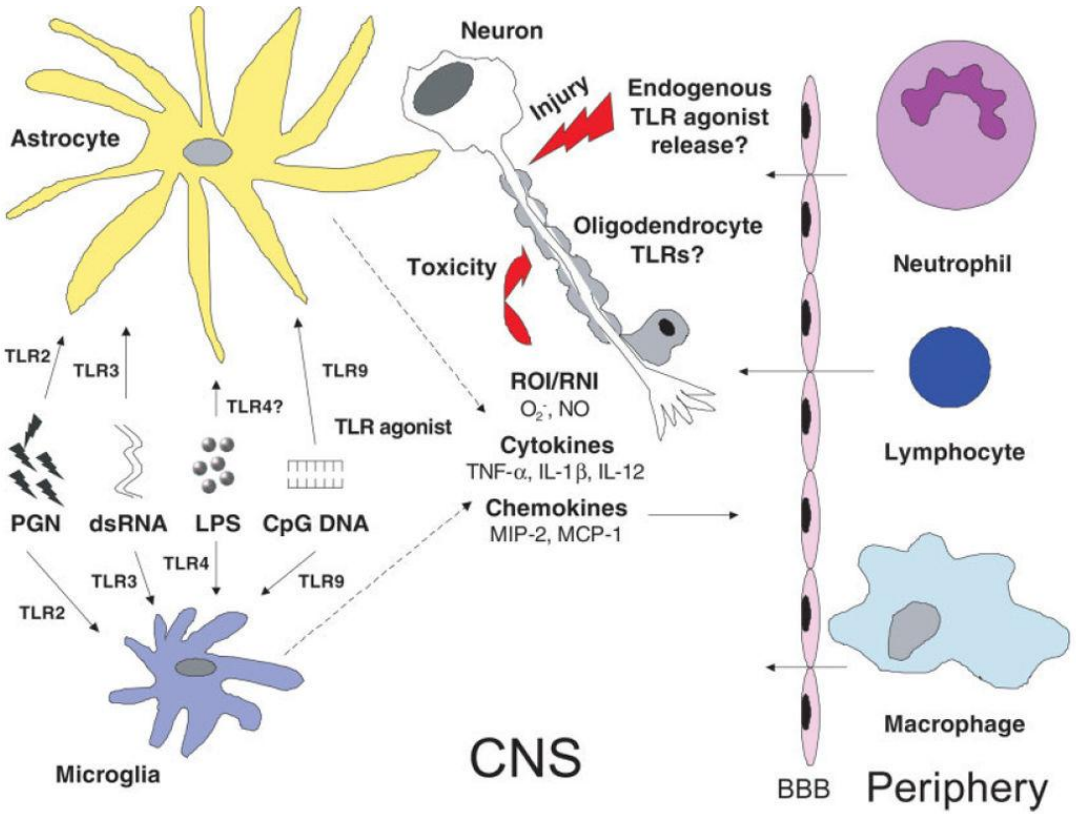

Figure 1.8 Potential roles of TLRs in the CNS response to infection and injury. Microglia and astrocytes respond to numerous PAMPs, including peptidoglycan (PGN; TLR2 agonist), double-stranded RNA (dsRNA; TLR3 agonist), lipopolysaccharide (LPS; TLR4 agonist), and unmethylated CpG oligodeoxynucleotides and/or bacterial DNA (CpG DNA; TLR9 agonist). The stimulation leads to the release of wide array of proinflammatory cytokines (including TNF-α, IL-1β, and IL-12), chemokines [including macrophage inflammatory protein-2 (MIP-2/CXCL2) and monocyte chemoattractant protein-1 (MCP-1)], and reactive oxygen/nitrogen species [ROI/RNI; including superoxide and nitric oxide (NO)]. There is a resultant enhancement of blood–brain barrier (BBB) permeability. Endogenous TLR ligands may be released from injured cells within the CNS parenchyma that may serve to augment neuroinflammation. (Figure adapted from Kielian, T (2004 a) *J Neuroinflamm* 1:16.)

1.12.2 Proinflammatory Cytokine Markers

Ultra structural studies indicate microglia to be closely apposed to extracellular fibrils, and are likely to be involved in a phagocytic response (Wisniewski et al., 1992). Monocytes or macroglia have receptors for Aβ (scavenger type and RAGE) (El Khoury et al., 1996, Yan et al., 1996). In culture conditions the macrophages readily engulf Aβ aggregates, and this interaction is often associated with the release of proinflammatory cytokines, reactive oxygen species, proteases (eg.matrix metalloproteases) (Giulian et al., 1995, Lorton, 1997).

AD brain display immunoreactivity for proinflammatory cytokines IL-1β, TNF-α, IL-6 (Dickson et al., 1993) and IL-1α (Giulian et al., 1995, Mrak et al., 1995). *In vitro* studies have demonstrated that fibrillar Aβ stimulation increases microglial/monocytic TNF-α production (Klegeris et al., 1997, Combs et al., 2000). Increased levels of TNF-α have been reported in the brain and plasma of AD patients (Bruunsgaard et al., 1999, Tarkowski et al., 1999). Transgenic mouse models have shown evidence that inflammation and TNF-α contribute to disease progression. Three month old mice carrying three familial mutations (APP_{Swe}, Tau_{P301L}, and PS1M146V) have shown accumulation of intraneuronal amyloid immunoreactivity in regions that include entorhinal cortex. These studies have also reported the presence of elevated TNF-α mRNA levels in the same regions, and correlated with onset of cognitive deficits in these mice models (Billings et al., 2005, Janelsins et al., 2005). These findings suggest the importance of TNF-α as a valuable proinflammatory marker.

1.13 Therapeutic Approach: Vaccination in AD

Immunotherapy is a very promising approach to target the disease causing Aβ aggregation species. This therapy has been approached in two ways. One is by active Aβ peptide vaccination (Schenk et al., 1999, Bard et al., 2000), and the other is passive infusion of anti-Aβ monoclonal antibodies (Bard et al., 2000). Nasal vaccination with synthetic copolymer used to treat MS was found to decrease senile plaques in mouse model of AD (Frenkel et al., 2005). T-cell based vaccination with glatiramer acetate resulted in decreased plaque formation and induction of neurogenesis in APP mice (Butovsky et al., 2006). There is strong evidence that immune therapy of AD is able to remove Aβ from the CNS, leading to an improvement in the cognitive decline that is associated with AD (Glezer et al., 2007). These data justified the first clinical trial with the active immunization in patients with mild to moderate AD. During the Phase 2 trial of active immunization with Aβ(1-42) in patients with AD, it was observed that about 6 % of the patients developed a T-cell mediated, autoimmune meningoencephalitis, and the treatment had to be stopped (Orgogozo et al., 2003). Autopsy investigations of a few participants showed clearance of parenchymal plaques. Amyloid clearance in these cases was associated with microglia that showed Aβ immunoreactivity, thereby suggesting phagocytosis. A general cognitive-status test revealed a slowing of cognitive decline in these patients (Hock et al., 2003). The passive infusions of anti-Aβ monoclonal antibodies target specific epitopes within the Aβ(1-42) peptide, avoiding a possible harmful binding to normal APP. Since immunotherapy requires repeated infusion of

antibodies over a long period, AD patients will be able to tolerate such antibodies provided they are of human origin (Steinitz, 2008). Immunotherapy has been successful in affecting the Aβ oligomerization and plaque formation. The striking feature was the clearance of early hyperphosphorylated tau in the neurons of mouse models (Oddo et al., 2004). While trials are ongoing, the current hope is that one or more of these approaches can slow down the progression of AD and cognitive impairment.

1.14 Aβ Polymorphism and AD Pathogenic Cascade

Post mortem data suggest that different conformations of Aβ aggregated species, and not one particular Aβ aggregated intermediate, contribute to the disease mechanisms involved in the pathogenic cascade of AD (Hoozemans et al., 2006). Studies have shown that the AD brain has a wide array of polymorphic aggregated Aβ species. Immunocytochemistry studies have shown the presence of diffuse plaques in the limbic and association cortices, and even in the striatum and cerebellum. These diffuse deposits appear loose and granular by light microscopy, and they lack dystrophic neuritis, altered astrocytes and microglia. Abundant diffuse plaques also occur in the brains of neurologically normal elderly humans, and in children with Down's syndrome, leading to the hypothesis that these are precursor lesions to the neuritic plaques. These parenchymal deposits exist as range of species from dense core neuritic plaques containing fibrillar structures to wispy, loose, and granular deposits (Selkoe, 2004). *In vitro* aggregation studies have provided detailed understanding of the fibrillogenesis mechanisms. Many types of Aβ assembly forms have been reported from studies using synthetic Aβ.

Protofibrils (Harper et al., 1997b, Walsh et al., 1997, Hartley et al., 1999, Walsh et al., 1999), annular structures, paranuclei, amyloid derived diffusible ligands (ADDLs) (Lambert et al., 1998, Gong et al., 2003), Aβ*56 (Lesne et al., 2006), secreted soluble Aβ dimers and trimers (Podlisny et al., 1995, Walsh et al., 2000, Walsh et al., 2002a), and amyloid fibrils are the different aggregation species that have been reported. Soluble oligomers are aggregation species that cannot be separated/pelleted from physiological fluids by high speed centrifugation (Dahlgren et al., 2002, Haass and Selkoe, 2007). The conditions that produce these different structures are not well understood. Also, these diverse morphologies have distinct toxic and biologic activity and not do provoke the same *in vivo* response (Dahlgren et al., 2002, Walsh et al., 2002a, Deshpande et al., 2006, Salminen et al., 2009). Significant amount of data suggest that induction of an inflammatory response appeared to favor a fibrillar conformation. The local acidic environment in the brain (endosomes and lysosomes) are believed to promote Aβ fibril formation (McLaurin and Chakrabartty, 1996), thereby inducing the nerurotoxic effects.

The objective of this study was to characterize the different Aβ aggregation species and identify the optimal Aβ aggregation state required for the stimulation of maximal TNF-α response in a human monocytic cell line. It is possible that in the near future the early molecular diagnosis of AD will be based on the correlation of Aβ structural polymorphisms and levels of proinflammatory cytokines. The results of this study will provide further clues to unraveling the complexities of AD, and help find a solution for early diagnosis and treatment of this disorder.

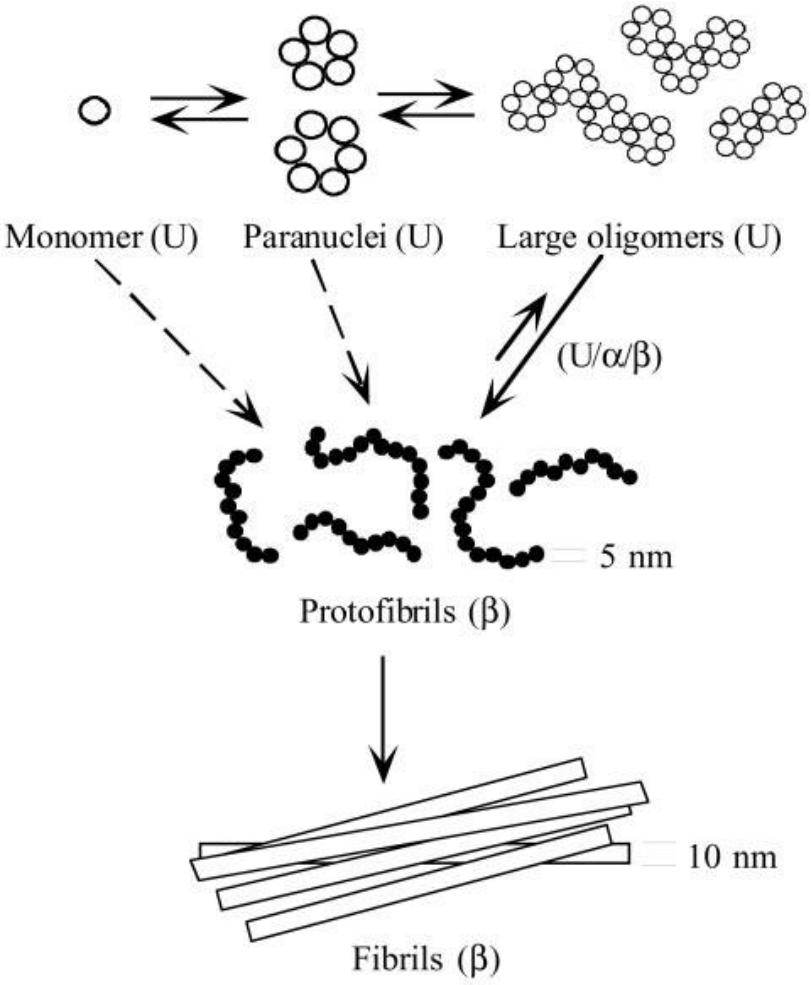

Figure 1.9 Schematic representation of various aggregation species in Aβ(1-42) assembly. The different species reported are annular structures, paranuclei, Amyloid derived diffusible ligands (generally categorized as oligomers). Protofibril formation involves structural rearrangement. The final step is the formation of the mature fibrils.
U (unstructured) α- (alpha helical structure) β (beta sheet). Figure adapted from Bitan et al (2003) *PNAS*,100: 330-335

1.15 Bibliography

Akama, K. T. and Van Eldik, L. J., 2000. Beta-amyloid stimulation of inducible nitric-oxide synthase in astrocytes is interleukin-1beta- and tumor necrosis factor-alpha (TNFalpha)-dependent, and involves a TNFalpha receptor-associated factor- and NFkappaB-inducing kinase-dependent signaling mechanism. J Biol Chem. 275, 7918-7924.

Akira, S. and Takeda, K., 2004. Toll-like receptor signalling. Nat Rev Immunol. 4, 499-511.

Akira, S., Uematsu, S. and Takeuchi, O., 2006. Pathogen recognition and innate immunity. Cell. 124, 783-801.

Akiyama, H., Barger, S., Barnum, S., Bradt, B., Bauer, J., Cole, G. M., Cooper, N. R., Eikelenboom, P., Emmerling, M., Fiebich, B. L., Finch, C. E., Frautschy, S., Griffin, W. S., Hampel, H., Hull, M., Landreth, G., Lue, L., Mrak, R., Mackenzie, I. R., McGeer, P. L., O'Banion, M. K., Pachter, J., Pasinetti, G., Plata-Salaman, C., Rogers, J., Rydel, R., Shen, Y., Streit, W., Strohmeyer, R., Tooyoma, I., Van Muiswinkel, F. L., Veerhuis, R., Walker, D., Webster, S., Wegrzyniak, B., Wenk, G. and Wyss-Coray, T., 2000. Inflammation and Alzheimer's disease. Neurobiol Aging. 21, 383-421.

Allinson, T. M., Parkin, E. T., Turner, A. J. and Hooper, N. M., 2003. ADAMs family members as amyloid precursor protein alpha-secretases. J Neurosci Res. 74, 342-352.

Ancolio, K., Dumanchin, C., Barelli, H., Warter, J. M., Brice, A., Campion, D., Frebourg, T. and Checler, F., 1999. Unusual phenotypic alteration of beta amyloid precursor protein (betaAPP) maturation by a new Val-715 --> Met betaAPP-770 mutation responsible for probable early-onset Alzheimer's disease. Proc Natl Acad Sci U S A. 96, 4119-4124.

Anfinsen, C. B., 1973. Principles that govern the folding of protein chains. Science. 181, 223-230.

Attems, J., 2005. Sporadic cerebral amyloid angiopathy: pathology, clinical implications, and possible pathomechanisms. Acta Neuropathol. 110, 345-359.

Bacskai, B. J., Kajdasz, S. T., Christie, R. H., Carter, C., Games, D., Seubert, P., Schenk, D. and Hyman, B. T., 2001. Imaging of amyloid-beta deposits in brains of living mice permits direct observation of clearance of plaques with immunotherapy. Nat Med. 7, 369-372.

Ballatore, C., Lee, V. M. and Trojanowski, J. Q., 2007. Tau-mediated neurodegeneration in Alzheimer's disease and related disorders. Nat Rev Neurosci. 8, 663-672.

Bamberger, M. E. and Landreth, G. E., 2001. Microglial interaction with beta-amyloid: implications for the pathogenesis of Alzheimer's disease. Microsc Res Tech. 54, 59-70.

Bard, F., Cannon, C., Barbour, R., Burke, R. L., Games, D., Grajeda, H., Guido, T., Hu, K., Huang, J., Johnson-Wood, K., Khan, K., Kholodenko, D., Lee, M., Lieberburg, I., Motter, R., Nguyen, M., Soriano, F., Vasquez, N., Weiss, K., Welch, B., Seubert, P., Schenk, D. and Yednock, T., 2000. Peripherally administered antibodies against amyloid beta-peptide enter the central nervous system and reduce pathology in a mouse model of Alzheimer disease. Nat Med. 6, 916-919.

Bate, C., Veerhuis, R., Eikelenboom, P. and Williams, A., 2004. Microglia kill amyloid-beta1-42 damaged neurons by a CD14-dependent process. Neuroreport. 15, 1427-1430.

Benzing, W. C., Wujek, J. R., Ward, E. K., Shaffer, D., Ashe, K. H., Younkin, S. G. and Brunden, K. R., 1999. Evidence for glial-mediated inflammation in aged APP(SW) transgenic mice. Neurobiol Aging. 20, 581-589.

Bergamaschini, L., Donarini, C., Rossi, E., De Luigi, A., Vergani, C. and De Simoni, M. G., 2002. Heparin attenuates cytotoxic and inflammatory activity of Alzheimer amyloid-beta in vitro. Neurobiol Aging. 23, 531-536.

Bertram, L. and Tanzi, R. E., 2008. Thirty years of Alzheimer's disease genetics: the implications of systematic meta-analyses. Nat Rev Neurosci. 9, 768-778.

Beutler, B., 2004. Inferences, questions and possibilities in Toll-like receptor signalling. Nature. 430, 257-263.

Billings, L. M., Oddo, S., Green, K. N., McGaugh, J. L. and LaFerla, F. M., 2005. Intraneuronal Abeta causes the onset of early Alzheimer's disease-related cognitive deficits in transgenic mice. Neuron. 45, 675-688.

Blacker, D., Wilcox, M. A., Laird, N. M., Rodes, L., Horvath, S. M., Go, R. C., Perry, R., Watson, B., Jr., Bassett, S. S., McInnis, M. G., Albert, M. S., Hyman, B. T. and

Tanzi, R. E., 1998. Alpha-2 macroglobulin is genetically associated with Alzheimer disease. Nat Genet. 19, 357-360.

Blake, C. and Serpell, L., 1996. Synchrotron X-ray studies suggest that the core of the transthyretin amyloid fibril is a continuous beta-sheet helix. Structure. 4, 989-998.

Blake, C. C., Geisow, M. J., Oatley, S. J., Rerat, B. and Rerat, C., 1978. Structure of prealbumin: secondary, tertiary and quaternary interactions determined by Fourier refinement at 1.8 A. J Mol Biol. 121, 339-356.

Blasko, I., Stampfer-Kountchev, M., Robatscher, P., Veerhuis, R., Eikelenboom, P. and Grubeck-Loebenstein, B., 2004. How chronic inflammation can affect the brain and support the development of Alzheimer's disease in old age: the role of microglia and astrocytes. Aging Cell. 3, 169-176.

Borchelt, D. R., Ratovitski, T., van Lare, J., Lee, M. K., Gonzales, V., Jenkins, N. A., Copeland, N. G., Price, D. L. and Sisodia, S. S., 1997. Accelerated amyloid deposition in the brains of transgenic mice coexpressing mutant presenilin 1 and amyloid precursor proteins. Neuron. 19, 939-945.

Bruunsgaard, H., Andersen-Ranberg, K., Jeune, B., Pedersen, A. N., Skinhoj, P. and Pedersen, B. K., 1999. A high plasma concentration of TNF-alpha is associated with dementia in centenarians. J Gerontol A Biol Sci Med Sci. 54, M357-364.

Bu, G., 2009. Apolipoprotein E and its receptors in Alzheimer's disease: pathways, pathogenesis and therapy. Nat Rev Neurosci. 10, 333-344.

Buee, L., Bussiere, T., Buee-Scherrer, V., Delacourte, A. and Hof, P. R., 2000. Tau protein isoforms, phosphorylation and role in neurodegenerative disorders. Brain Res Brain Res Rev. 33, 95-130.

Bukau, B. and Horwich, A. L., 1998. The Hsp70 and Hsp60 chaperone machines. Cell. 92, 351-366.

Busciglio, J., Lorenzo, A., Yeh, J. and Yankner, B. A., 1995. beta-amyloid fibrils induce tau phosphorylation and loss of microtubule binding. Neuron. 14, 879-888.

Butovsky, O., Koronyo-Hamaoui, M., Kunis, G., Ophir, E., Landa, G., Cohen, H. and Schwartz, M., 2006. Glatiramer acetate Fights against Alzheimer's disease by inducing dendritic-like microglia expressing insulin-like growth factor 1. Proc Natl Acad Sci U S A. 103, 11784-11789.

Caughey, B. and Lansbury, P. T., 2003. Protofibrils, pores, fibrils, and neurodegeneration: separating the responsible protein aggregates from the innocent bystanders. Annu Rev Neurosci. 26, 267-298.

Chiti, F. and Dobson, C. M., 2006. Protein misfolding, functional amyloid, and human disease. Annu Rev Biochem. 75, 333-366.

Citron, M., Vigo-Pelfrey, C., Teplow, D. B., Miller, C., Schenk, D., Johnston, J., Winblad, B., Venizelos, N., Lannfelt, L. and Selkoe, D. J., 1994. Excessive production of amyloid beta-protein by peripheral cells of symptomatic and presymptomatic patients carrying the Swedish familial Alzheimer disease mutation. Proc Natl Acad Sci U S A. 91, 11993-11997.

Combs, C. K., Johnson, D. E., Karlo, J. C., Cannady, S. B. and Landreth, G. E., 2000. Inflammatory mechanisms in Alzheimer's disease: inhibition of beta-amyloid-stimulated proinflammatory responses and neurotoxicity by PPARgamma agonists. J Neurosci. 20, 558-567.

Combs, C. K., Karlo, J. C., Kao, S. C. and Landreth, G. E., 2001. beta-Amyloid stimulation of microglia and monocytes results in TNFalpha-dependent expression of inducible nitric oxide synthase and neuronal apoptosis. J Neurosci. 21, 1179-1188.

Cooper, N. R., Bradt, B. M., O'Barr, S. and Yu, J. X., 2000. Focal inflammation in the brain: role in Alzheimer's disease. Immunol Res. 21, 159-165.

Cummings, B. J., Su, J. H. and Cotman, C. W., 1993. Neuritic involvement within bFGF immunopositive plaques of Alzheimer's disease. Exp Neurol. 124, 315-325.

D'Andrea, M. R., Nagele, R. G., Wang, H. Y., Peterson, P. A. and Lee, D. H., 2001. Evidence that neurones accumulating amyloid can undergo lysis to form amyloid plaques in Alzheimer's disease. Histopathology. 38, 120-134.

Dahlgren, K. N., Manelli, A. M., Stine, W. B., Jr., Baker, L. K., Krafft, G. A. and LaDu, M. J., 2002. Oligomeric and fibrillar species of amyloid-beta peptides differentially affect neuronal viability. J Biol Chem. 277, 32046-32053.

Danilova, N., 2006. The evolution of immune mechanisms. J Exp Zoolog B Mol Dev Evol. 306, 496-520.

Davalos, D., Grutzendler, J., Yang, G., Kim, J. V., Zuo, Y., Jung, S., Littman, D. R., Dustin, M. L. and Gan, W. B., 2005. ATP mediates rapid microglial response to local brain injury in vivo. Nat Neurosci. 8, 752-758.

De Strooper, B., Saftig, P., Craessaerts, K., Vanderstichele, H., Guhde, G., Annaert, W., Von Figura, K. and Van Leuven, F., 1998. Deficiency of presenilin-1 inhibits the normal cleavage of amyloid precursor protein. Nature. 391, 387-390.

Deshpande, A., Mina, E., Glabe, C. and Busciglio, J., 2006. Different conformations of amyloid beta induce neurotoxicity by distinct mechanisms in human cortical neurons. J Neurosci. 26, 6011-6018.

Dickson, D. W., 1997. The pathogenesis of senile plaques. J Neuropathol Exp Neurol. 56, 321-339.

Dickson, D. W., Lee, S. C., Mattiace, L. A., Yen, S. H. and Brosnan, C., 1993. Microglia and cytokines in neurological disease, with special reference to AIDS and Alzheimer's disease. Glia. 7, 75-83.

Dobson, C. M., 1999. Protein misfolding, evolution and disease. Trends Biochem Sci. 24, 329-332.

Edison, P., Archer, H. A., Gerhard, A., Hinz, R., Pavese, N., Turkheimer, F. E., Hammers, A., Tai, Y. F., Fox, N., Kennedy, A., Rossor, M. and Brooks, D. J., 2008. Microglia, amyloid, and cognition in Alzheimer's disease: An [11C](R)PK11195-PET and [11C]PIB-PET study. Neurobiol Dis. 32, 412-419.

Eikelenboom, P., Veerhuis, R., Scheper, W., Rozemuller, A. J., van Gool, W. A. and Hoozemans, J. J., 2006. The significance of neuroinflammation in understanding Alzheimer's disease. J Neural Transm. 113, 1685-1695.

El Khoury, J., Hickman, S. E., Thomas, C. A., Cao, L., Silverstein, S. C. and Loike, J. D., 1996. Scavenger receptor-mediated adhesion of microglia to beta-amyloid fibrils. Nature. 382, 716-719.

El Khoury, J. B., Moore, K. J., Means, T. K., Leung, J., Terada, K., Toft, M., Freeman, M. W. and Luster, A. D., 2003. CD36 mediates the innate host response to beta-amyloid. J Exp Med. 197, 1657-1666.

Ellis, R. J., 2001. Macromolecular crowding: an important but neglected aspect of the intracellular environment. Curr Opin Struct Biol. 11, 114-119.

Fassbender, K., Walter, S., Kuhl, S., Landmann, R., Ishii, K., Bertsch, T., Stalder, A. K., Muehlhauser, F., Liu, Y., Ulmer, A. J., Rivest, S., Lentschat, A., Gulbins, E., Jucker, M., Staufenbiel, M., Brechtel, K., Walter, J., Multhaup, G., Penke, B., Adachi, Y., Hartmann, T. and Beyreuther, K., 2004. The LPS receptor (CD14) links innate immunity with Alzheimer's disease. Faseb J. 18, 203-205.

Ferrari, A., Hoerndli, F., Baechi, T., Nitsch, R. M. and Gotz, J., 2003. beta-Amyloid induces paired helical filament-like tau filaments in tissue culture. J Biol Chem. 278, 40162-40168.

Frenkel, D., Maron, R., Burt, D. S. and Weiner, H. L., 2005. Nasal vaccination with a proteosome-based adjuvant and glatiramer acetate clears beta-amyloid in a mouse model of Alzheimer disease. J Clin Invest. 115, 2423-2433.

Games, D., Adams, D., Alessandrini, R., Barbour, R., Berthelette, P., Blackwell, C., Carr, T., Clemens, J., Donaldson, T., Gillespie, F. and et al., 1995. Alzheimer-type neuropathology in transgenic mice overexpressing V717F beta-amyloid precursor protein. Nature. 373, 523-527.

Geula, C., Wu, C. K., Saroff, D., Lorenzo, A., Yuan, M. and Yankner, B. A., 1998. Aging renders the brain vulnerable to amyloid beta-protein neurotoxicity. Nat Med. 4, 827-831.

Giulian, D., 1999. Microglia and the immune pathology of Alzheimer disease. Am J Hum Genet. 65, 13-18.

Giulian, D., Haverkamp, L. J., Li, J., Karshin, W. L., Yu, J., Tom, D., Li, X. and Kirkpatrick, J. B., 1995. Senile plaques stimulate microglia to release a neurotoxin found in Alzheimer brain. Neurochem Int. 27, 119-137.

Giulian, D., Haverkamp, L. J., Yu, J. H., Karshin, W., Tom, D., Li, J., Kirkpatrick, J., Kuo, L. M. and Roher, A. E., 1996. Specific domains of beta-amyloid from Alzheimer plaque elicit neuron killing in human microglia. J Neurosci. 16, 6021-6037.

Glabe, C. C., 2005. Amyloid accumulation and pathogensis of Alzheimer's disease: significance of monomeric, oligomeric and fibrillar Abeta. Subcell Biochem. 38, 167-177.

Glenner, G. G., 1989. The pathobiology of Alzheimer's disease. Annu Rev Med. 40, 45-51.

Glezer, I., Simard, A. R. and Rivest, S., 2007. Neuroprotective role of the innate immune system by microglia. Neuroscience. 147, 867-883.

Goate, A. M., Haynes, A. R., Owen, M. J., Farrall, M., James, L. A., Lai, L. Y., Mullan, M. J., Roques, P., Rossor, M. N., Williamson, R. and et al., 1989. Predisposing locus for Alzheimer's disease on chromosome 21. Lancet. 1, 352-355.

Golde, T. E., Estus, S., Usiak, M., Younkin, L. H. and Younkin, S. G., 1990. Expression of beta amyloid protein precursor mRNAs: recognition of a novel alternatively

spliced form and quantitation in Alzheimer's disease using PCR. Neuron. 4, 253-267.

Gong, Y., Chang, L., Viola, K. L., Lacor, P. N., Lambert, M. P., Finch, C. E., Krafft, G. A. and Klein, W. L., 2003. Alzheimer's disease-affected brain: presence of oligomeric A beta ligands (ADDLs) suggests a molecular basis for reversible memory loss. Proc Natl Acad Sci U S A. 100, 10417-10422.

Gotz, J., Chen, F., van Dorpe, J. and Nitsch, R. M., 2001. Formation of neurofibrillary tangles in P301l tau transgenic mice induced by Abeta 42 fibrils. Science. 293, 1491-1495.

Gouras, G. K., Tsai, J., Naslund, J., Vincent, B., Edgar, M., Checler, F., Greenfield, J. P., Haroutunian, V., Buxbaum, J. D., Xu, H., Greengard, P. and Relkin, N. R., 2000. Intraneuronal Abeta42 accumulation in human brain. Am J Pathol. 156, 15-20.

Greenfield, J. P., Gross, R. S., Gouras, G. K. and Xu, H., 2000. Cellular and molecular basis of beta-amyloid precursor protein metabolism. Front Biosci. 5, D72-83.

Griffin, W. S., 2006. Inflammation and neurodegenerative diseases. Am J Clin Nutr. 83, 470S-474S.

Haass, C. and De Strooper, B., 1999. The presenilins in Alzheimer's disease--proteolysis holds the key. Science. 286, 916-919.

Haass, C. and Selkoe, D. J., 2007. Soluble protein oligomers in neurodegeneration: lessons from the Alzheimer's amyloid beta-peptide. Nat Rev Mol Cell Biol. 8, 101-112.

Halverson, K., Fraser, P. E., Kirschner, D. A. and Lansbury, P. T., Jr., 1990. Molecular determinants of amyloid deposition in Alzheimer's disease: conformational studies of synthetic beta-protein fragments. Biochemistry. 29, 2639-2644.

Hardy, J., 1997. Amyloid, the presenilins and Alzheimer's disease. Trends Neurosci. 20, 154-159.

Hardy, J. and Gwinn-Hardy, K., 1998. Genetic classification of primary neurodegenerative disease. Science. 282, 1075-1079.

Hardy, J. and Selkoe, D. J., 2002. The amyloid hypothesis of Alzheimer's disease: progress and problems on the road to therapeutics. Science. 297, 353-356.

Hardy, J. A. and Higgins, G. A., 1992. Alzheimer's disease: the amyloid cascade hypothesis. Science. 256, 184-185.

Harper, J. D. and Lansbury, P. T., Jr., 1997. Models of amyloid seeding in Alzheimer's disease and scrapie: mechanistic truths and physiological consequences of the time-dependent solubility of amyloid proteins. Annu Rev Biochem. 66, 385-407.

Harper, J. D., Lieber, C. M. and Lansbury, P. T., Jr., 1997a. Atomic force microscopic imaging of seeded fibril formation and fibril branching by the Alzheimer's disease amyloid-beta protein. Chem Biol. 4, 951-959.

Harper, J. D., Wong, S. S., Lieber, C. M. and Lansbury, P. T., 1997b. Observation of metastable Abeta amyloid protofibrils by atomic force microscopy. Chem Biol. 4, 119-125.

Harper, J. D., Wong, S. S., Lieber, C. M. and Lansbury, P. T., Jr., 1999. Assembly of A beta amyloid protofibrils: an in vitro model for a possible early event in Alzheimer's disease. Biochemistry. 38, 8972-8980.

Hartl, F. U. and Hayer-Hartl, M., 2002. Molecular chaperones in the cytosol: from nascent chain to folded protein. Science. 295, 1852-1858.

Hartley, D. M., Walsh, D. M., Ye, C. P., Diehl, T., Vasquez, S., Vassilev, P. M., Teplow, D. B. and Selkoe, D. J., 1999. Protofibrillar intermediates of amyloid beta-protein induce acute electrophysiological changes and progressive neurotoxicity in cortical neurons. J Neurosci. 19, 8876-8884.

Hayashi, H., Kimura, N., Yamaguchi, H., Hasegawa, K., Yokoseki, T., Shibata, M., Yamamoto, N., Michikawa, M., Yoshikawa, Y., Terao, K., Matsuzaki, K., Lemere, C. A., Selkoe, D. J., Naiki, H. and Yanagisawa, K., 2004. A seed for Alzheimer amyloid in the brain. J Neurosci. 24, 4894-4902.

Hendriks, L., van Duijn, C. M., Cras, P., Cruts, M., Van Hul, W., van Harskamp, F., Warren, A., McInnis, M. G., Antonarakis, S. E., Martin, J. J. and et al., 1992. Presenile dementia and cerebral haemorrhage linked to a mutation at codon 692 of the beta-amyloid precursor protein gene. Nat Genet. 1, 218-221.

Hetz, C. and Soto, C., 2003. Protein misfolding and disease: the case of prion disorders. Cell Mol Life Sci. 60, 133-143.

Hilbich, C., Kisters-Woike, B., Reed, J., Masters, C. L. and Beyreuther, K., 1991. Aggregation and secondary structure of synthetic amyloid beta A4 peptides of Alzheimer's disease. J Mol Biol. 218, 149-163.

Hilbich, C., Kisters-Woike, B., Reed, J., Masters, C. L. and Beyreuther, K., 1992. Substitutions of hydrophobic amino acids reduce the amyloidogenicity of Alzheimer's disease beta A4 peptides. J Mol Biol. 228, 460-473.

Hock, C., Konietzko, U., Streffer, J. R., Tracy, J., Signorell, A., Muller-Tillmanns, B., Lemke, U., Henke, K., Moritz, E., Garcia, E., Wollmer, M. A., Umbricht, D., de Quervain, D. J., Hofmann, M., Maddalena, A., Papassotiropoulos, A. and Nitsch, R. M., 2003. Antibodies against beta-amyloid slow cognitive decline in Alzheimer's disease. Neuron. 38, 547-554.

Hoffmann, J. A., 2003. The immune response of Drosophila. Nature. 426, 33-38.

Holcomb, L., Gordon, M. N., McGowan, E., Yu, X., Benkovic, S., Jantzen, P., Wright, K., Saad, I., Mueller, R., Morgan, D., Sanders, S., Zehr, C., O'Campo, K., Hardy, J., Prada, C. M., Eckman, C., Younkin, S., Hsiao, K. and Duff, K., 1998. Accelerated Alzheimer-type phenotype in transgenic mice carrying both mutant amyloid precursor protein and presenilin 1 transgenes. Nat Med. 4, 97-100.

Hoozemans, J. J., Chafekar, S. M., Baas, F., Eikelenboom, P. and Scheper, W., 2006. Always around, never the same: pathways of amyloid beta induced neurodegeneration throughout the pathogenic cascade of Alzheimer's disease. Curr Med Chem. 13, 2599-2605.

Horwich, A. L., Weber-Ban, E. U. and Finley, D., 1999. Chaperone rings in protein folding and degradation. Proc Natl Acad Sci U S A. 96, 11033-11040.

Hsiao, K., Chapman, P., Nilsen, S., Eckman, C., Harigaya, Y., Younkin, S., Yang, F. and Cole, G., 1996. Correlative memory deficits, Abeta elevation, and amyloid plaques in transgenic mice. Science. 274, 99-102.

Hyman, B. T., 1996. Alzheimer's disease or Alzheimer's diseases? Clues from molecular epidemiology. Ann Neurol. 40, 135-136.

Inouye, H., Fraser, P. E. and Kirschner, D. A., 1993. Structure of beta-crystallite assemblies formed by Alzheimer beta-amyloid protein analogues: analysis by x-ray diffraction. Biophys J. 64, 502-519.

Ishii, K., Muelhauser, F., Liebl, U., Picard, M., Kuhl, S., Penke, B., Bayer, T., Wiessler, M., Hennerici, M., Beyreuther, K., Hartmann, T. and Fassbender, K., 2000. Subacute NO generation induced by Alzheimer's beta-amyloid in the living brain: reversal by inhibition of the inducible NO synthase. Faseb J. 14, 1485-1489.

Iwatsubo, T., Odaka, A., Suzuki, N., Mizusawa, H., Nukina, N. and Ihara, Y., 1994. Visualization of A beta 42(43) and A beta 40 in senile plaques with end-specific A beta monoclonals: evidence that an initially deposited species is A beta 42(43). Neuron. 13, 45-53.

Janelsins, M. C., Mastrangelo, M. A., Oddo, S., LaFerla, F. M., Federoff, H. J. and Bowers, W. J., 2005. Early correlation of microglial activation with enhanced tumor necrosis factor-alpha and monocyte chemoattractant protein-1 expression specifically within the entorhinal cortex of triple transgenic Alzheimer's disease mice. J Neuroinflammation. 2, 23.

Jarrett, J. T., Berger, E. P. and Lansbury, P. T., Jr., 1993a. The C-terminus of the beta protein is critical in amyloidogenesis. Ann N Y Acad Sci. 695, 144-148.

Jarrett, J. T., Berger, E. P. and Lansbury, P. T., Jr., 1993b. The carboxy terminus of the beta amyloid protein is critical for the seeding of amyloid formation: implications for the pathogenesis of Alzheimer's disease. Biochemistry. 32, 4693-4697.

Jarrett, J. T. and Lansbury, P. T., Jr., 1993. Seeding "one-dimensional crystallization" of amyloid: a pathogenic mechanism in Alzheimer's disease and scrapie? Cell. 73, 1055-1058.

Jiang, H., Burdick, D., Glabe, C. G., Cotman, C. W. and Tenner, A. J., 1994. beta-Amyloid activates complement by binding to a specific region of the collagen-like domain of the C1q A chain. J Immunol. 152, 5050-5059.

Joachim, C. L., Morris, J. H. and Selkoe, D. J., 1989. Diffuse senile plaques occur commonly in the cerebellum in Alzheimer's disease. Am J Pathol. 135, 309-319.

Kalaria, R. N., 1999. Microglia and Alzheimer's disease. Curr Opin Hematol. 6, 15-24.

Kawarabayashi, T., Shoji, M., Younkin, L. H., Wen-Lang, L., Dickson, D. W., Murakami, T., Matsubara, E., Abe, K., Ashe, K. H. and Younkin, S. G., 2004. Dimeric amyloid beta protein rapidly accumulates in lipid rafts followed by apolipoprotein E and phosphorylated tau accumulation in the Tg2576 mouse model of Alzheimer's disease. J Neurosci. 24, 3801-3809.

Kayed, R., Head, E., Sarsoza, F., Saing, T., Cotman, C. W., Necula, M., Margol, L., Wu, J., Breydo, L., Thompson, J. L., Rasool, S., Gurlo, T., Butler, P. and Glabe, C. G., 2007. Fibril specific, conformation dependent antibodies recognize a generic epitope common to amyloid fibrils and fibrillar oligomers that is absent in prefibrillar oligomers. Mol Neurodegener. 2, 18.

Kehoe, P. G., Russ, C., McIlory, S., Williams, H., Holmans, P., Holmes, C., Liolitsa, D., Vahidassr, D., Powell, J., McGleenon, B., Liddell, M., Plomin, R., Dynan, K., Williams, N., Neal, J., Cairns, N. J., Wilcock, G., Passmore, P., Lovestone, S., Williams, J. and Owen, M. J., 1999. Variation in DCP1, encoding ACE, is associated with susceptibility to Alzheimer disease. Nat Genet. 21, 71-72.

Khachaturian, Z. S., 2002. The challenges of developing and validating molecular and biochemical markers of Alzheimer's disease. Neurobiol Aging. 23, 509-511; discussion 521-502.

Kielian, T., 2006. Toll-like receptors in central nervous system glial inflammation and homeostasis. J Neurosci Res. 83, 711-730.

Kirschner, D. A., Inouye, H., Duffy, L. K., Sinclair, A., Lind, M. and Selkoe, D. J., 1987. Synthetic peptide homologous to beta protein from Alzheimer disease forms amyloid-like fibrils in vitro. Proc Natl Acad Sci U S A. 84, 6953-6957.

Klegeris, A., Walker, D. G. and McGeer, P. L., 1997. Interaction of Alzheimer beta-amyloid peptide with the human monocytic cell line THP-1 results in a protein kinase C-dependent secretion of tumor necrosis factor-alpha. Brain Res. 747, 114-121.

Klein, W. L., Krafft, G. A. and Finch, C. E., 2001. Targeting small Abeta oligomers: the solution to an Alzheimer's disease conundrum? Trends Neurosci. 24, 219-224.

Klunk, W. E., Debnath, M. L. and Pettegrew, J. W., 1994. Development of small molecule probes for the beta-amyloid protein of Alzheimer's disease. Neurobiol Aging. 15, 691-698.

Klunk, W. E., Pettegrew, J. W. and Abraham, D. J., 1989. Quantitative evaluation of congo red binding to amyloid-like proteins with a beta-pleated sheet conformation. J Histochem Cytochem. 37, 1273-1281.

Kojro, E. and Fahrenholz, F., 2005. The non-amyloidogenic pathway: structure and function of alpha-secretases. Subcell Biochem. 38, 105-127.

Koo, E. H., Lansbury, P. T., Jr. and Kelly, J. W., 1999. Amyloid diseases: abnormal protein aggregation in neurodegeneration. Proc Natl Acad Sci U S A. 96, 9989-9990.

Kowalewski, T. and Holtzman, D. M., 1999. In situ atomic force microscopy study of Alzheimer's beta-amyloid peptide on different substrates: new insights into mechanism of beta-sheet formation. Proc Natl Acad Sci U S A. 96, 3688-3693.

Lambert, M. P., Barlow, A. K., Chromy, B. A., Edwards, C., Freed, R., Liosatos, M., Morgan, T. E., Rozovsky, I., Trommer, B., Viola, K. L., Wals, P., Zhang, C., Finch, C. E., Krafft, G. A. and Klein, W. L., 1998. Diffusible, nonfibrillar ligands derived from Abeta1-42 are potent central nervous system neurotoxins. Proc Natl Acad Sci U S A. 95, 6448-6453.

Lansbury, P. T., Jr., 1999. Evolution of amyloid: what normal protein folding may tell us about fibrillogenesis and disease. Proc Natl Acad Sci U S A. 96, 3342-3344.

Lemere, C. A., Blusztajn, J. K., Yamaguchi, H., Wisniewski, T., Saido, T. C. and Selkoe, D. J., 1996. Sequence of deposition of heterogeneous amyloid beta-peptides and APO E in Down syndrome: implications for initial events in amyloid plaque formation. Neurobiol Dis. 3, 16-32.

Lesne, S., Koh, M. T., Kotilinek, L., Kayed, R., Glabe, C. G., Yang, A., Gallagher, M. and Ashe, K. H., 2006. A specific amyloid-beta protein assembly in the brain impairs memory. Nature. 440, 352-357.

Lesne, S., Kotilinek, L. and Ashe, K. H., 2008. Plaque-bearing mice with reduced levels of oligomeric amyloid-beta assemblies have intact memory function. Neuroscience. 151, 745-749.

Leung, E., Guo, L., Bu, J., Maloof, M., Khoury, J. E. and Geula, C., 2009. Microglia activation mediates fibrillar amyloid-beta toxicity in the aged primate cortex. Neurobiol Aging.

Levy, E., Carman, M. D., Fernandez-Madrid, I. J., Power, M. D., Lieberburg, I., van Duinen, S. G., Bots, G. T., Luyendijk, W. and Frangione, B., 1990. Mutation of the Alzheimer's disease amyloid gene in hereditary cerebral hemorrhage, Dutch type. Science. 248, 1124-1126.

Lewis, J., Dickson, D. W., Lin, W. L., Chisholm, L., Corral, A., Jones, G., Yen, S. H., Sahara, N., Skipper, L., Yager, D., Eckman, C., Hardy, J., Hutton, M. and McGowan, E., 2001. Enhanced neurofibrillary degeneration in transgenic mice expressing mutant tau and APP. Science. 293, 1487-1491.

Lomakin, A., Chung, D. S., Benedek, G. B., Kirschner, D. A. and Teplow, D. B., 1996. On the nucleation and growth of amyloid beta-protein fibrils: detection of nuclei and quantitation of rate constants. Proc Natl Acad Sci U S A. 93, 1125-1129.

Lomakin, A., Teplow, D. B., Kirschner, D. A. and Benedek, G. B., 1997. Kinetic theory of fibrillogenesis of amyloid beta-protein. Proc Natl Acad Sci U S A. 94, 7942-7947.

Lorton, D., 1997. beta-Amyloid-induced IL-1 beta release from an activated human monocyte cell line is calcium- and G-protein-dependent. Mech Ageing Dev. 94, 199-211.

Lorton, D., Schaller, J., Lala, A. and De Nardin, E., 2000. Chemotactic-like receptors and Abeta peptide induced responses in Alzheimer's disease. Neurobiol Aging. 21, 463-473.

Maccioni, R. B., Rojo, L. E., Fernandez, J. A. and Kuljis, R. O., 2009. The role of neuroimmunomodulation in Alzheimer's disease. Ann N Y Acad Sci. 1153, 240-246.

Mahley, R. W., 1988. Apolipoprotein E: cholesterol transport protein with expanding role in cell biology. Science. 240, 622-630.

Masters, C. L., Simms, G., Weinman, N. A., Multhaup, G., McDonald, B. L. and Beyreuther, K., 1985. Amyloid plaque core protein in Alzheimer disease and Down syndrome. Proc Natl Acad Sci U S A. 82, 4245-4249.

Mattson, M. P., 1997. Cellular actions of beta-amyloid precursor protein and its soluble and fibrillogenic derivatives. Physiol Rev. 77, 1081-1132.

Mattson, M. P., 2004. Pathways towards and away from Alzheimer's disease. Nature. 430, 631-639.

Mattson, M. P., Cheng, B., Culwell, A. R., Esch, F. S., Lieberburg, I. and Rydel, R. E., 1993. Evidence for excitoprotective and intraneuronal calcium-regulating roles for secreted forms of the beta-amyloid precursor protein. Neuron. 10, 243-254.

McDonald, D. R., Brunden, K. R. and Landreth, G. E., 1997. Amyloid fibrils activate tyrosine kinase-dependent signaling and superoxide production in microglia. J Neurosci. 17, 2284-2294.

McGeer, E. G. and McGeer, P. L., 2001. Innate immunity in Alzheimer's disease: a model for local inflammatory reactions. Mol Interv. 1, 22-29.

McGeer, P. L., Itagaki, S., Tago, H. and McGeer, E. G., 1987. Reactive microglia in patients with senile dementia of the Alzheimer type are positive for the histocompatibility glycoprotein HLA-DR. Neurosci Lett. 79, 195-200.

McGeer, P. L., Rogers, J. and McGeer, E. G., 2006. Inflammation, anti-inflammatory agents and Alzheimer disease: the last 12 years. J Alzheimers Dis. 9, 271-276.

McGeer, P. L., Schulzer, M. and McGeer, E. G., 1996. Arthritis and anti-inflammatory agents as possible protective factors for Alzheimer's disease: a review of 17 epidemiologic studies. Neurology. 47, 425-432.

McGowan, E., Pickford, F., Kim, J., Onstead, L., Eriksen, J., Yu, C., Skipper, L., Murphy, M. P., Beard, J., Das, P., Jansen, K., Delucia, M., Lin, W. L., Dolios, G., Wang, R., Eckman, C. B., Dickson, D. W., Hutton, M., Hardy, J. and Golde, T., 2005. Abeta42 is essential for parenchymal and vascular amyloid deposition in mice. Neuron. 47, 191-199.

McLaurin, J. and Chakrabartty, A., 1996. Membrane disruption by Alzheimer beta-amyloid peptides mediated through specific binding to either phospholipids or gangliosides. Implications for neurotoxicity. J Biol Chem. 271, 26482-26489.

Medzhitov, R. and Janeway, C. A., Jr., 1997. Innate immunity: the virtues of a nonclonal system of recognition. Cell. 91, 295-298.

Mehlhorn, G., Hollborn, M. and Schliebs, R., 2000. Induction of cytokines in glial cells surrounding cortical beta-amyloid plaques in transgenic Tg2576 mice with Alzheimer pathology. Int J Dev Neurosci. 18, 423-431.

Meyer-Luehmann, M., Spires-Jones, T. L., Prada, C., Garcia-Alloza, M., de Calignon, A., Rozkalne, A., Koenigsknecht-Talboo, J., Holtzman, D. M., Bacskai, B. J. and Hyman, B. T., 2008. Rapid appearance and local toxicity of amyloid-beta plaques in a mouse model of Alzheimer's disease. Nature. 451, 720-724.

Mirra, S. S., Heyman, A., McKeel, D., Sumi, S. M., Crain, B. J., Brownlee, L. M., Vogel, F. S., Hughes, J. P., van Belle, G. and Berg, L., 1991. The Consortium to Establish a Registry for Alzheimer's Disease (CERAD). Part II. Standardization of the neuropathologic assessment of Alzheimer's disease. Neurology. 41, 479-486.

Misonou, H., Morishima-Kawashima, M. and Ihara, Y., 2000. Oxidative stress induces intracellular accumulation of amyloid beta-protein (Abeta) in human neuroblastoma cells. Biochemistry. 39, 6951-6959.

Mrak, R. E., Sheng, J. G. and Griffin, W. S., 1995. Glial cytokines in Alzheimer's disease: review and pathogenic implications. Hum Pathol. 26, 816-823.

Mullan, M., Crawford, F., Axelman, K., Houlden, H., Lilius, L., Winblad, B. and Lannfelt, L., 1992. A pathogenic mutation for probable Alzheimer's disease in the APP gene at the N-terminus of beta-amyloid. Nat Genet. 1, 345-347.

Nichols, M. R., Moss, M. A., Reed, D. K., Lin, W. L., Mukhopadhyay, R., Hoh, J. H. and Rosenberry, T. L., 2002. Growth of beta-amyloid(1-40) protofibrils by monomer elongation and lateral association. Characterization of distinct products by light scattering and atomic force microscopy. Biochemistry. 41, 6115-6127.

Nilsberth, C., Westlind-Danielsson, A., Eckman, C. B., Condron, M. M., Axelman, K., Forsell, C., Stenh, C., Luthman, J., Teplow, D. B., Younkin, S. G., Naslund, J. and Lannfelt, L., 2001. The 'Arctic' APP mutation (E693G) causes Alzheimer's disease by enhanced Abeta protofibril formation. Nat Neurosci. 4, 887-893.

Nimmerjahn, A., Kirchhoff, F. and Helmchen, F., 2005. Resting microglial cells are highly dynamic surveillants of brain parenchyma in vivo. Science. 308, 1314-1318.

Nishimoto, I., Okamoto, T., Matsuura, Y., Takahashi, S., Okamoto, T., Murayama, Y. and Ogata, E., 1993. Alzheimer amyloid protein precursor complexes with brain GTP-binding protein G(o). Nature. 362, 75-79.

Nitsch, R. M., Rebeck, G. W., Deng, M., Richardson, U. I., Tennis, M., Schenk, D. B., Vigo-Pelfrey, C., Lieberburg, I., Wurtman, R. J., Hyman, B. T. and et al., 1995. Cerebrospinal fluid levels of amyloid beta-protein in Alzheimer's disease: inverse correlation with severity of dementia and effect of apolipoprotein E genotype. Ann Neurol. 37, 512-518.

Nixon, R. A., Cataldo, A. M., Paskevich, P. A., Hamilton, D. J., Wheelock, T. R. and Kanaley-Andrews, L., 1992. The lysosomal system in neurons. Involvement at multiple stages of Alzheimer's disease pathogenesis. Ann N Y Acad Sci. 674, 65-88.

Nordberg, A., 2008. Amyloid plaque imaging in vivo: current achievement and future prospects. Eur J Nucl Med Mol Imaging. 35 Suppl 1, S46-50.

Oddo, S., Billings, L., Kesslak, J. P., Cribbs, D. H. and LaFerla, F. M., 2004. Abeta immunotherapy leads to clearance of early, but not late, hyperphosphorylated tau aggregates via the proteasome. Neuron. 43, 321-332.

Oddo, S., Caccamo, A., Shepherd, J. D., Murphy, M. P., Golde, T. E., Kayed, R., Metherate, R., Mattson, M. P., Akbari, Y. and LaFerla, F. M., 2003. Triple-transgenic model of Alzheimer's disease with plaques and tangles: intracellular Abeta and synaptic dysfunction. Neuron. 39, 409-421.

Olson, R. E., 1998. Discovery of the lipoproteins, their role in fat transport and their significance as risk factors. J Nutr. 128, 439S-443S.

Orellana, D. I., Quintanilla, R. A., Gonzalez-Billault, C. and Maccioni, R. B., 2005. Role of the JAKs/STATs pathway in the intracellular calcium changes induced by interleukin-6 in hippocampal neurons. Neurotox Res. 8, 295-304.

Orgogozo, J. M., Gilman, S., Dartigues, J. F., Laurent, B., Puel, M., Kirby, L. C., Jouanny, P., Dubois, B., Eisner, L., Flitman, S., Michel, B. F., Boada, M., Frank, A. and Hock, C., 2003. Subacute meningoencephalitis in a subset of patients with AD after Abeta42 immunization. Neurology. 61, 46-54.

Pericak-Vance, M. A., Bass, M. P., Yamaoka, L. H., Gaskell, P. C., Scott, W. K., Terwedow, H. A., Menold, M. M., Conneally, P. M., Small, G. W., Vance, J. M.,

Saunders, A. M., Roses, A. D. and Haines, J. L., 1997. Complete genomic screen in late-onset familial Alzheimer disease. Evidence for a new locus on chromosome 12. Jama. 278, 1237-1241.

Perlmutter, L. S., Barron, E. and Chui, H. C., 1990. Morphologic association between microglia and senile plaque amyloid in Alzheimer's disease. Neurosci Lett. 119, 32-36.

Perlmutter, L. S., Scott, S. A., Barron, E. and Chui, H. C., 1992. MHC class II-positive microglia in human brain: association with Alzheimer lesions. J Neurosci Res. 33, 549-558.

Perry, G., Siedlak, S. L., Richey, P., Kawai, M., Cras, P., Kalaria, R. N., Galloway, P. G., Scardina, J. M., Cordell, B., Greenberg, B. D. and et al., 1991. Association of heparan sulfate proteoglycan with the neurofibrillary tangles of Alzheimer's disease. J Neurosci. 11, 3679-3683.

Petkova, A. T., Ishii, Y., Balbach, J. J., Antzutkin, O. N., Leapman, R. D., Delaglio, F. and Tycko, R., 2002. A structural model for Alzheimer's beta -amyloid fibrils based on experimental constraints from solid state NMR. Proc Natl Acad Sci U S A. 99, 16742-16747.

Pike, C. J., Cummings, B. J. and Cotman, C. W., 1995. Early association of reactive astrocytes with senile plaques in Alzheimer's disease. Exp Neurol. 132, 172-179.

Pimplikar, S. W., 2009. Reassessing the amyloid cascade hypothesis of Alzheimer's disease. Int J Biochem Cell Biol. 41, 1261-1268.

Podlisny, M. B., Ostaszewski, B. L., Squazzo, S. L., Koo, E. H., Rydell, R. E., Teplow, D. B. and Selkoe, D. J., 1995. Aggregation of secreted amyloid beta-protein into sodium dodecyl sulfate-stable oligomers in cell culture. J Biol Chem. 270, 9564-9570.

Poltorak, A., He, X., Smirnova, I., Liu, M. Y., Van Huffel, C., Du, X., Birdwell, D., Alejos, E., Silva, M., Galanos, C., Freudenberg, M., Ricciardi-Castagnoli, P., Layton, B. and Beutler, B., 1998. Defective LPS signaling in C3H/HeJ and C57BL/10ScCr mice: mutations in Tlr4 gene. Science. 282, 2085-2088.

Price, D. L. and Sisodia, S. S., 1998. Mutant genes in familial Alzheimer's disease and transgenic models. Annu Rev Neurosci. 21, 479-505.

Quintanilla, R. A., Orellana, D. I., Gonzalez-Billault, C. and Maccioni, R. B., 2004. Interleukin-6 induces Alzheimer-type phosphorylation of tau protein by deregulating the cdk5/p35 pathway. Exp Cell Res. 295, 245-257.

Radford, S. E. and Dobson, C. M., 1999. From computer simulations to human disease: emerging themes in protein folding. Cell. 97, 291-298.

Rogers, J., 2008. The inflammatory response in Alzheimer's disease. J Periodontol. 79, 1535-1543.

Rogers, J., Cooper, N. R., Webster, S., Schultz, J., McGeer, P. L., Styren, S. D., Civin, W. H., Brachova, L., Bradt, B., Ward, P. and et al., 1992. Complement activation by beta-amyloid in Alzheimer disease. Proc Natl Acad Sci U S A. 89, 10016-10020.

Rogers, J. and Lue, L. F., 2001. Microglial chemotaxis, activation, and phagocytosis of amyloid beta-peptide as linked phenomena in Alzheimer's disease. Neurochem Int. 39, 333-340.

Rogers, J., Lue, L. F., Walker, D. G., Yan, S. D., Stern, D., Strohmeyer, R. and Kovelowski, C. J., 2002a. Elucidating molecular mechanisms of Alzheimer's disease in microglial cultures. Ernst Schering Res Found Workshop, 25-44.

Rogers, J., Strohmeyer, R., Kovelowski, C. J. and Li, R., 2002b. Microglia and inflammatory mechanisms in the clearance of amyloid beta peptide. Glia. 40, 260-269.

Roher, A. E., Lowenson, J. D., Clarke, S., Woods, A. S., Cotter, R. J., Gowing, E. and Ball, M. J., 1993. beta-Amyloid-(1-42) is a major component of cerebrovascular amyloid deposits: implications for the pathology of Alzheimer disease. Proc Natl Acad Sci U S A. 90, 10836-10840.

Rojo, L. E., Fernandez, J. A., Maccioni, A. A., Jimenez, J. M. and Maccioni, R. B., 2008. Neuroinflammation: implications for the pathogenesis and molecular diagnosis of Alzheimer's disease. Arch Med Res. 39, 1-16.

Rozemuller, J. M., Eikelenboom, P., Pals, S. T. and Stam, F. C., 1989. Microglial cells around amyloid plaques in Alzheimer's disease express leucocyte adhesion molecules of the LFA-1 family. Neurosci Lett. 101, 288-292.

Sage, B. H., Jr., O'Connell, J. P. and Mercolino, T. J., 1983. A rapid, vital staining procedure for flow cytometric analysis of human reticulocytes. Cytometry. 4, 222-227.

Saitoh, T., Sundsmo, M., Roch, J. M., Kimura, N., Cole, G., Schubert, D., Oltersdorf, T. and Schenk, D. B., 1989. Secreted form of amyloid beta protein precursor is involved in the growth regulation of fibroblasts. Cell. 58, 615-622.

Salminen, A., Ojala, J., Kauppinen, A., Kaarniranta, K. and Suuronen, T., 2009. Inflammation in Alzheimer's disease: amyloid-beta oligomers trigger innate immunity defence via pattern recognition receptors. Prog Neurobiol. 87, 181-194.

Schenk, D., Barbour, R., Dunn, W., Gordon, G., Grajeda, H., Guido, T., Hu, K., Huang, J., Johnson-Wood, K., Khan, K., Kholodenko, D., Lee, M., Liao, Z., Lieberburg, I., Motter, R., Mutter, L., Soriano, F., Shopp, G., Vasquez, N., Vandevert, C., Walker, S., Wogulis, M., Yednock, T., Games, D. and Seubert, P., 1999. Immunization with amyloid-beta attenuates Alzheimer-disease-like pathology in the PDAPP mouse. Nature. 400, 173-177.

Scheuner, D., Eckman, C., Jensen, M., Song, X., Citron, M., Suzuki, N., Bird, T. D., Hardy, J., Hutton, M., Kukull, W., Larson, E., Levy-Lahad, E., Viitanen, M., Peskind, E., Poorkaj, P., Schellenberg, G., Tanzi, R., Wasco, W., Lannfelt, L., Selkoe, D. and Younkin, S., 1996. Secreted amyloid beta-protein similar to that in the senile plaques of Alzheimer's disease is increased in vivo by the presenilin 1 and 2 and APP mutations linked to familial Alzheimer's disease. Nat Med. 2, 864-870.

Selkoe, D. J., 1999. Translating cell biology into therapeutic advances in Alzheimer's disease. Nature. 399, A23-31.

Selkoe, D. J., 2001. Alzheimer's disease: genes, proteins, and therapy. Physiol Rev. 81, 741-766.

Selkoe, D. J., 2003. Folding proteins in fatal ways. Nature. 426, 900-904.

Selkoe, D. J., 2004. Cell biology of protein misfolding: the examples of Alzheimer's and Parkinson's diseases. Nat Cell Biol. 6, 1054-1061.

Selkoe, D. J. and Podlisny, M. B., 2002. Deciphering the genetic basis of Alzheimer's disease. Annu Rev Genomics Hum Genet. 3, 67-99.

Shankar, G. M., Li, S., Mehta, T. H., Garcia-Munoz, A., Shepardson, N. E., Smith, I., Brett, F. M., Farrell, M. A., Rowan, M. J., Lemere, C. A., Regan, C. M., Walsh, D. M., Sabatini, B. L. and Selkoe, D. J., 2008. Amyloid-beta protein dimers isolated directly from Alzheimer's brains impair synaptic plasticity and memory. Nat Med. 14, 837-842.

Shapira, R., Austin, G. E. and Mirra, S. S., 1988. Neuritic plaque amyloid in Alzheimer's disease is highly racemized. J Neurochem. 50, 69-74.

Shimazu, R., Akashi, S., Ogata, H., Nagai, Y., Fukudome, K., Miyake, K. and Kimoto, M., 1999. MD-2, a molecule that confers lipopolysaccharide responsiveness on Toll-like receptor 4. J Exp Med. 189, 1777-1782.

Sisodia, S. S., Kim, S. H. and Thinakaran, G., 1999. Function and dysfunction of the presenilins. Am J Hum Genet. 65, 7-12.

Sisodia, S. S., Koo, E. H., Beyreuther, K., Unterbeck, A. and Price, D. L., 1990. Evidence that beta-amyloid protein in Alzheimer's disease is not derived by normal processing. Science. 248, 492-495.

Smith, M. A., Richey, P. L., Taneda, S., Kutty, R. K., Sayre, L. M., Monnier, V. M. and Perry, G., 1994. Advanced Maillard reaction end products, free radicals, and protein oxidation in Alzheimer's disease. Ann N Y Acad Sci. 738, 447-454.

St George-Hyslop, P. H., 2000. Genetic factors in the genesis of Alzheimer's disease. Ann N Y Acad Sci. 924, 1-7.

Stefani, M. and Dobson, C. M., 2003. Protein aggregation and aggregate toxicity: new insights into protein folding, misfolding diseases and biological evolution. J Mol Med. 81, 678-699.

Steinitz, M., 2008. Developing injectable immunoglobulins to treat cognitive impairment in Alzheimer's disease. Expert Opin Biol Ther. 8, 633-642.

Streit, W. J., 2004. Microglia and Alzheimer's disease pathogenesis. J Neurosci Res. 77, 1-8.

Strittmatter, W. J., Saunders, A. M., Schmechel, D., Pericak-Vance, M., Enghild, J., Salvesen, G. S. and Roses, A. D., 1993. Apolipoprotein E: high-avidity binding to beta-amyloid and increased frequency of type 4 allele in late-onset familial Alzheimer disease. Proc Natl Acad Sci U S A. 90, 1977-1981.

Sunde, M., Serpell, L. C., Bartlam, M., Fraser, P. E., Pepys, M. B. and Blake, C. C., 1997. Common core structure of amyloid fibrils by synchrotron X-ray diffraction. J Mol Biol. 273, 729-739.

Suzuki, N., Cheung, T. T., Cai, X. D., Odaka, A., Otvos, L., Jr., Eckman, C., Golde, T. E. and Younkin, S. G., 1994. An increased percentage of long amyloid beta protein secreted by familial amyloid beta protein precursor (beta APP717) mutants. Science. 264, 1336-1340.

Tagliavini, F., Giaccone, G., Frangione, B. and Bugiani, O., 1988. Preamyloid deposits in the cerebral cortex of patients with Alzheimer's disease and nondemented individuals. Neurosci Lett. 93, 191-196.

Takahashi, R. H., Almeida, C. G., Kearney, P. F., Yu, F., Lin, M. T., Milner, T. A. and Gouras, G. K., 2004. Oligomerization of Alzheimer's beta-amyloid within processes and synapses of cultured neurons and brain. J Neurosci. 24, 3592-3599.

Takahashi, R. H., Milner, T. A., Li, F., Nam, E. E., Edgar, M. A., Yamaguchi, H., Beal, M. F., Xu, H., Greengard, P. and Gouras, G. K., 2002. Intraneuronal Alzheimer abeta42 accumulates in multivesicular bodies and is associated with synaptic pathology. Am J Pathol. 161, 1869-1879.

Tanzi, R. E. and Bertram, L., 2001. New frontiers in Alzheimer's disease genetics. Neuron. 32, 181-184.

Tarkowski, E., Blennow, K., Wallin, A. and Tarkowski, A., 1999. Intracerebral production of tumor necrosis factor-alpha, a local neuroprotective agent, in Alzheimer disease and vascular dementia. J Clin Immunol. 19, 223-230.

Terry, R. D., Masliah, E., Salmon, D. P., Butters, N., DeTeresa, R., Hill, R., Hansen, L. A. and Katzman, R., 1991. Physical basis of cognitive alterations in Alzheimer's disease: synapse loss is the major correlate of cognitive impairment. Ann Neurol. 30, 572-580.

Thal, D. R., Griffin, W. S., de Vos, R. A. and Ghebremedhin, E., 2008. Cerebral amyloid angiopathy and its relationship to Alzheimer's disease. Acta Neuropathol. 115, 599-609.

Tolnay, M. and Probst, A., 1999. REVIEW: tau protein pathology in Alzheimer's disease and related disorders. Neuropathol Appl Neurobiol. 25, 171-187.

Tycko, R., 2003. Insights into the amyloid folding problem from solid-state NMR. Biochemistry. 42, 3151-3159.

Udan, M. L., Ajit, D., Crouse, N. R. and Nichols, M. R., 2008. Toll-like receptors 2 and 4 mediate Abeta(1-42) activation of the innate immune response in a human monocytic cell line. J Neurochem. 104, 524-533.

van Gool, W. A., Kuiper, M. A., Walstra, G. J., Wolters, E. C. and Bolhuis, P. A., 1995. Concentrations of amyloid beta protein in cerebrospinal fluid of patients with Alzheimer's disease. Ann Neurol. 37, 277-279.

Vassar, R., 2004. BACE1: the beta-secretase enzyme in Alzheimer's disease. J Mol Neurosci. 23, 105-114.

Vassar, R., Bennett, B. D., Babu-Khan, S., Kahn, S., Mendiaz, E. A., Denis, P., Teplow, D. B., Ross, S., Amarante, P., Loeloff, R., Luo, Y., Fisher, S., Fuller, J., Edenson, S., Lile, J., Jarosinski, M. A., Biere, A. L., Curran, E., Burgess, T., Louis, J. C.,

Collins, F., Treanor, J., Rogers, G. and Citron, M., 1999. Beta-secretase cleavage of Alzheimer's amyloid precursor protein by the transmembrane aspartic protease BACE. Science. 286, 735-741.

Vekrellis, K., Ye, Z., Qiu, W. Q., Walsh, D., Hartley, D., Chesneau, V., Rosner, M. R. and Selkoe, D. J., 2000. Neurons regulate extracellular levels of amyloid beta-protein via proteolysis by insulin-degrading enzyme. J Neurosci. 20, 1657-1665.

Villemagne, V. L., Fodero-Tavoletti, M. T., Pike, K. E., Cappai, R., Masters, C. L. and Rowe, C. C., 2008. The ART of loss: Abeta imaging in the evaluation of Alzheimer's disease and other dementias. Mol Neurobiol. 38, 1-15.

Vinters, H. V., Wang, Z. Z. and Secor, D. L., 1996. Brain parenchymal and microvascular amyloid in Alzheimer's disease. Brain Pathol. 6, 179-195.

Vitek, M. P., Bhattacharya, K., Glendening, J. M., Stopa, E., Vlassara, H., Bucala, R., Manogue, K. and Cerami, A., 1994. Advanced glycation end products contribute to amyloidosis in Alzheimer disease. Proc Natl Acad Sci U S A. 91, 4766-4770.

Voet, V. a., 1995. Biochemistry. 191-215.

Walker, L. C. and LeVine, H., 2000. The cerebral proteopathies: neurodegenerative disorders of protein conformation and assembly. Mol Neurobiol. 21, 83-95.

Walsh, D. M., Hartley, D. M., Kusumoto, Y., Fezoui, Y., Condron, M. M., Lomakin, A., Benedek, G. B., Selkoe, D. J. and Teplow, D. B., 1999. Amyloid beta-protein fibrillogenesis. Structure and biological activity of protofibrillar intermediates. J Biol Chem. 274, 25945-25952.

Walsh, D. M., Klyubin, I., Fadeeva, J. V., Cullen, W. K., Anwyl, R., Wolfe, M. S., Rowan, M. J. and Selkoe, D. J., 2002a. Naturally secreted oligomers of amyloid beta protein potently inhibit hippocampal long-term potentiation in vivo. Nature. 416, 535-539.

Walsh, D. M., Klyubin, I., Fadeeva, J. V., Rowan, M. J. and Selkoe, D. J., 2002b. Amyloid-beta oligomers: their production, toxicity and therapeutic inhibition. Biochem Soc Trans. 30, 552-557.

Walsh, D. M., Lomakin, A., Benedek, G. B., Condron, M. M. and Teplow, D. B., 1997. Amyloid beta-protein fibrillogenesis. Detection of a protofibrillar intermediate. J Biol Chem. 272, 22364-22372.

Walsh, D. M. and Selkoe, D. J., 2004. Deciphering the molecular basis of memory failure in Alzheimer's disease. Neuron. 44, 181-193.

Walsh, D. M. and Selkoe, D. J., 2007. Abeta Oligomers - a decade of discovery. J Neurochem.

Walsh, D. M., Tseng, B. P., Rydel, R. E., Podlisny, M. B. and Selkoe, D. J., 2000. The oligomerization of amyloid beta-protein begins intracellularly in cells derived from human brain. Biochemistry. 39, 10831-10839.

Webster, S., Glabe, C. and Rogers, J., 1995. Multivalent binding of complement protein C1Q to the amyloid beta-peptide (A beta) promotes the nucleation phase of A beta aggregation. Biochem Biophys Res Commun. 217, 869-875.

Wekerle, H., 2002. Immune protection of the brain--efficient and delicate. J Infect Dis. 186 Suppl 2, S140-144.

Weldon, D. T., Rogers, S. D., Ghilardi, J. R., Finke, M. P., Cleary, J. P., O'Hare, E., Esler, W. P., Maggio, J. E. and Mantyh, P. W., 1998. Fibrillar beta-amyloid induces microglial phagocytosis, expression of inducible nitric oxide synthase, and loss of a select population of neurons in the rat CNS in vivo. J Neurosci. 18, 2161-2173.

Westermark, P., Benson, M. D., Buxbaum, J. N., Cohen, A. S., Frangione, B., Ikeda, S., Masters, C. L., Merlini, G., Saraiva, M. J. and Sipe, J. D., 2005. Amyloid: toward terminology clarification. Report from the Nomenclature Committee of the International Society of Amyloidosis. Amyloid. 12, 1-4.

Winklhofer, K. F., Tatzelt, J. and Haass, C., 2008. The two faces of protein misfolding: gain- and loss-of-function in neurodegenerative diseases. Embo J. 27, 336-349.

Wirths, O., Multhaup, G. and Bayer, T. A., 2004. A modified beta-amyloid hypothesis: intraneuronal accumulation of the beta-amyloid peptide--the first step of a fatal cascade. J Neurochem. 91, 513-520.

Wisniewski, H. M., Wegiel, J., Wang, K. C., Kujawa, M. and Lach, B., 1989. Ultrastructural studies of the cells forming amyloid fibers in classical plaques. Can J Neurol Sci. 16, 535-542.

Wisniewski, H. M., Wegiel, J., Wang, K. C. and Lach, B., 1992. Ultrastructural studies of the cells forming amyloid in the cortical vessel wall in Alzheimer's disease. Acta Neuropathol. 84, 117-127.

Wisniewski, T., Haltia, M., Ghiso, J. and Frangione, B., 1991. Lewy bodies are immunoreactive with antibodies raised to gelsolin related amyloid-Finnish type. Am J Pathol. 138, 1077-1083.

Wong, P. C., Cai, H., Borchelt, D. R. and Price, D. L., 2002. Genetically engineered mouse models of neurodegenerative diseases. Nat Neurosci. 5, 633-639.

Yan, Q., Zhang, J., Liu, H., Babu-Khan, S., Vassar, R., Biere, A. L., Citron, M. and Landreth, G., 2003. Anti-inflammatory drug therapy alters beta-amyloid processing and deposition in an animal model of Alzheimer's disease. J Neurosci. 23, 7504-7509.

Yan, S. D., Chen, X., Fu, J., Chen, M., Zhu, H., Roher, A., Slattery, T., Zhao, L., Nagashima, M., Morser, J., Migheli, A., Nawroth, P., Stern, D. and Schmidt, A. M., 1996. RAGE and amyloid-beta peptide neurotoxicity in Alzheimer's disease. Nature. 382, 685-691.

Yates, S. L., Burgess, L. H., Kocsis-Angle, J., Antal, J. M., Dority, M. D., Embury, P. B., Piotrkowski, A. M. and Brunden, K. R., 2000. Amyloid beta and amylin fibrils induce increases in proinflammatory cytokine and chemokine production by THP-1 cells and murine microglia. J Neurochem. 74, 1017-1025.

Younkin, S. G., 1995. Evidence that A beta 42 is the real culprit in Alzheimer's disease. Ann Neurol. 37, 287-288.

Zheng, W. H., Bastianetto, S., Mennicken, F., Ma, W. and Kar, S., 2002. Amyloid beta peptide induces tau phosphorylation and loss of cholinergic neurons in rat primary septal cultures. Neuroscience. 115, 201-211.

CHAPTER 2

METHODS

2.1 Disaggregation of Aβ peptides

The main focus of our study was to determine the assembly state of Aβ aggregation species and correlate structure with biological activity. In order to have reproducibility in experimental trials, it was important to start the experiment with a homogenous monomeric solution of Aβ. Commercially purchased peptides may be contaminated with certain levels of preexisting aggregates. These aggregates act as seeds to accelerate the aggregation of monomeric peptides (Evans et al., 1995). Any aggregate seed present in the solution will self assemble and alter the structure of the aggregate being investigated. Studies indicate formation of different conformers of Aβ assemblies from the same peptide sequence (Petkova et al., 2005). Small amounts of preformed aggregates can compromise the experiment. Therefore, protocols that ensure a uniform starting material are very useful when working with synthetic peptides (Chen and Wetzel, 2001).

Aβ(1-42), Aβ(1-40) was purchased from r-Peptide (Bogarth, GA, USA). Aβ(1-42) WT and Aβ(1-42) (L34P) were gifts from Dr Ron Wetzel, University of Pittsburgh. The peptide powder was resuspended in 100% hexafluoroisopropanol (HFIP) to a concentration of 1 mM for one hour to solubilize any preformed aggregates, and also

make smaller aliquots for storage purposes. Further, this treatment allows "normalization" of the properties of different commercial Aβ preparations and also avoids need for subsequent filtration steps. (Wood et al., 1996, Zagorski et al., 1999). The peptide solutions were speed vacuum centrifuged to remove the HFIP. It was important to remove traces of HFIP, since low percentages of it can alter the aggregation pathway (Nichols et al 2005). The speed vacuum centrifuged samples were stored at -20°C.

An alternative method of pretreatment utilized a combination of trifluoroacetic acid (TFA) and HFIP. TFA is known to dissolve the H-bonded protein aggregates and is relatively volatile making its removal from solution easier. Further treatment with HFIP will remove any traces of TFA and ensuring disaggregation of any aggregated material left behind (Zagorski et al., 1999). This protocol was used on crude peptides Aβ(1-42), Aβ(1-40) WT Aβ(1-40) (F4W) and Aβ(1-40) (F19W), synthesized by Dr. Fabio Gallazzi, University of Missouri- Columbia. The peptides were resuspended in 100% TFA to a concentration of 1mM and bath sonicated for 10 minutes, and speed vacuum centrifuged to remove TFA. This was followed by addition of an equal volume of 100% HFIP, followed by incubation in water bath (37°C) for 1 hour, and speed vacuum centrifuged to remove HFIP. The speed vacuum centrifuged peptide samples were stored at -20°C.

2.2 Preparation of Aβ Aggregation Solutions.

Lyophilized peptides were stored as 0.25 mg aliquots. The vials were resuspended in sterile water, phosphate buffered saline (PBS), or Hams F12 medium with

phenol red, as required in the experiment protocol to a final concentration of 100 µM. A more concentrated Aβ aggregation solution of 1.2mM was made in some experiments. For preparations in water, aliquots (0.25 mg) were resuspended in 555 µl sterile water to a final concentration of 100 µM Aβ in a cell culture hood to maintain sterile conditions. The aggregation reactions were initiated, and stored at appropriate temperature conditions as required by the experiment protocol. For a more concentrated Aβ preparation the 0.25 mg vial was resuspended in 46 µl sterile water to a final concentration of 1.2 mM. For preparations in phosphate-buffered saline (PBS), lyophilized Aβ(1-42) peptide (0.25 mg) was resuspended in 500 µl water to a final concentration of 110 µM. The preparation was divided into two aliquots of 250 µl each, and one was supplemented with 25 µl of 10x PBS (Hyclone) to a final Aβ concentration of 100 µM. The pH of the resulting solution was measured using a micro pH electrode (7.1). Alternatively, aggregation reactions in PBS were initiated by resuspending the lyophilized peptide in 100 mM NaOH, (Aβ conc 2 mM, pH 10.2) followed by dilution into PBS (Hyclone,1X) to final Aβ concentration of 100 µM. The measured pH after dilution into PBS was 7.4.

2.3 Preparation of Aβ-Derived Diffusible Ligands (ADDLs)

Lyophilized Aβ(1-42) r-Peptide (0.25 mg) was resuspended in 11µl dimethyl sulfoxide (DMSO,Sigma) to a concentration of 5mM as described in (Dahlgren et al., 2002). Ice cold Ham's F12 medium with phenol red (Hyclone) was added to a final Aβ concentration of 100 µM. The peptide solution was incubated at 4°C for 24 hours, followed by centrifugation at 14,000 x g for 10 minutes. The supernatant after

centrifugation was labeled ADDLs. The only modification made in the protocol was the use of Hams F 12 medium with phenol red.

2.4 Determination of pH of Aggregation Solutions.

The pH of aggregation solutions was measured using a micro pH electrode (Thermo Scientific) connected to pH meter (Accumet^{R} Fisher Scientific). This setup allows pH measurements in microliter volumes. The aggregation studies were done with samples less than 1 ml and volumes as low as 5 µl was sufficient for making pH measurements.

2.5 SDS PAGE / Western Blotting

2.5.1 SDS/PAGE

Aβ samples (100 µM) are prepared and diluted into Laemmli sample buffer (Biorad) 1:1 in the presence of reducing agent β-mercaptoethanol. The samples were boiled for five minutes and 15 µL loaded onto precast 18% Tris- glycine SDS polyacrylamide gels (Biorad). Protein standards (10 µL) (Biorad, Dual color, 10-250 kD) were loaded as control. Aβ aggregation species were separated by electrophoresis in Mini-cell (Mini-Protean, Biorad) using running buffer (25mM Tris, 192 mM glycine, 0.1% SDS, pH 8.3). Electrophoresis was carried out at 200 volts for 40 minutes. After electrophoresis, protein gels were either visualized by Coomassie staining or blotted to membranes for immunoreactivity detection.

2.5.2 Western Blotting

The SDS-PAGE resolved proteins were transferred onto polyvinylidene difluoride (PVDF) membranes (Hybond^{TM}-P, Amersham Biosciences) by electroblotting using the tank system (OWL, Bandit^{TM} VEP-2). The PVDF membrane must be prewetted with methanol in order to enable macromolecules in the aqueous phase to bind to the hydrophobic surface of the membrane (Wetzel, 1999). Electroblotting was carried out at 200 -400 mA for 2 hours in transfer buffer (25mM Tris, 192 mM glycine, 10% methanol, pH 8.3). The nonspecific binding sites on the membranes were blocked by incubating the blots in 5% non-fat dry milk in PBS/T (Phosphate buffer saline; 6.7 mM phosphate, 140mM NaCl, and 0.1% Tween-20, pH 7.5) at 4ºC for at least an hour. In some experiments the blocking was done overnight at 4ºC. The membrane was treated with primary antibody, Ab 9 (gift from Mayo Clinic, Jacksonville) diluted in 5% fat free powdered milk in PBS/T for one hour, followed by wash (three times), each for five minutes with PBS/T. The blots were then incubated with HRP-conjugated secondary antibody, IgG anti-mouse (R&D systems) diluted (1:1000) in 5% fat free powdered milk in PBS/T for one hour, followed by three five minute washes in PBS/T. All incubations and washes were done with rocking. Immunoreactive bands were detected using enhanced chemiluminescence reagent (ECL, Pierce), prepared 5-10 mintes prior to the treating the film. Exposure to (Kodak) was used to measure chemiluminescence, and exposure time depended on strength of the signal.

2.6 Dot Blot Assay

2.6.1 Dot-Blot Procedures

Nitrocellulose membrane was wetted with water and set on a filter paper for 5 minutes. Prior to spotting the sample the surface of the membrane was checked to see if there were any droplets of water. Aβ (1-42) 5 µl (100 µM) was spotted allowed to stand for 20 minutes. The membrane was blocked with 10% milk in PBS-0.2% Tween 20 (PBST) for experiments with OC immune serum and Ab 9. The concentration of Tween was reduced to 0.01% for A11 antibody probing based on recommendations in protocol in (Kayed et al., 2003). The blocking step was done for one hour at 4ºC. The membrane was washed with PBST twice (each 5 minutes), and incubated with OC immune serum (1:5000), Ab 9 antibody (1:5000), or A11 antibody (1:2000) for 1 hr with gentle shaking. Wash procedure was done as mentioned above, and followed by incubation for one hour with secondary antibody which is a 1:1000 dilution of an anti-rabbit IgG [HAF008, R&D systems] for OC immune serum and A11 antibody or anti-mouse IgG [HAF007, R&D systems] for Ab 9. Washed the membrane twice, and incubated with ECL substrate and exposed to film for 30 seconds. All steps were done at 25°C and slight modifications were made to the protocols in (Akiyama et al., 2000, Kayed et al., 2003, Parvathy et al., 2008).

2.6.2 Preparation of Controls for Dot Blot

2.6.2.1 OC Positive Control

0.1 mg of lyophilized Aβ(1-42) was dissolved in 50 µl 100 % HFIP for 10–20 minutes at room temperature. The solution was transferred to a siliconized eppendorf tube and diluted to a concentration of 80 µM in sterile water followed by 10-15 minutes incubation at room temperature. The samples were centrifuged for 15 mins at 14,000 x g. The supernatant was transferred to a new siliconized tube and subjected to a gentle stream of nitrogen for 10 minutes to remove the HFIP. OC positive fibrillar oligomers were generated by stirring sample at ~ 500 RPM using Teflon coated microstir bar for 24 hours at room temperature (Kayed et al., 2007). However, this preparation did not show positive reaction with OC immune serum in the experiments we conducted.

2.6. 2.2 A11 Positive Control

Soluble oligomers were prepared by dissolving 0.1 mg Aβ in 40 µl 100 % HFIP for 10-20 minutes at room temperature as mentioned above. The only difference from above being the final concentration of Aβ (55 µM). 10 µL of monomeric Aβ solution was added to 90 µL sterile water in a siliconized eppendorf tube to a final concentration of 55 µM, and incubated for 10-20 min incubation at room temperature. Following incubation samples were centrifuged for 15 minutes at 14,000 x g and the supernatant fraction (measured pH 3.3) was transferred to a new siliconized tube and subjected to a gentle stream of N_2 for 5-10 minutes to evaporate the HFIP. An aliquot was flash frozen after this step. The samples were stirred at low speed (~ 500 RPM) using a Teflon coated micro stir bar for 24-48 hours at 22 °C (Kayed et al., 2003). An aliquot was taken out and flash frozen after 24 and 48 hours. The flash frozen samples were probed with A11

antibody to test for presence of oligomers. This preparation showed reactivity to A11. Prefibrillar oligomers have also reportedly been prepared by resuspension of Aβ(1-42) in 100 mM NaOH (Aβ conc. 2 mM), followed by bath sonication for 30 seconds. The aggregation reaction was initiated by diluting the solution in phosphate buffered saline (PBS) pH 7.4 and 0.02% sodium azide (Aβ final concentration 45 µM) and incubated at room temperature for up to 96 hours. This method is a slightly modified version of protocol from (Kayed et al., 2007). This preparation was tried as positive control for A11 antibody, but did not show reactivity. However, this preparation showed reactivity when probed with OC immune serum inspite of being a control for oligomers.

2.7 Immunoprecipitation

Aβ aggregation solutions were resuspended to a concentration of 100 µM. Aliquots of 60 µl was incubated with 2 µl (1:10 dilution) OC antisera (2 mg/ml) resulting in ~1:300 dilution. The incubation was done without agitation for 1 hr at 4°C. Protein G-sepharose beads (10 µl) in 20% ethanol suspension (fast flow, Sigma P 3296) was added to the aggregation solution. Protein G beads were tap spun to remove ethanol, and resuspended in same volume of water prior to treatment with aggregation solution. The incubation with Protein-G beads was done with slow mixing for an additional 1 hr at 4°C. Protein G is a cell wall protein isolated from Type G streptococci, and has high binding affinity to the Fc region of immunoglobulin G (IgG) (Akerstrom and Bjorck, 1986). The solution was centrifuged for 15 min at 18,000 x g and the supernatant (45 µl) was used to treat THP-1 monocytes for 6 hours or 24 hours depending on the experiment protocol.

After the incubation period the cells were spun and supernatants tested for TNF-α levels. Another aliquot (5µl) of the 18,000 x g supernatant was used to test for OC immune reactivity by dot blot analysis. AFM image analysis was done with the spin supernatant after dilution to a concentration of 1µM.

2.8 Atomic Force Microscopy (AFM)

An atomic force microscope is optimized for measuring surface features that are extremely small. A Nanoscope III multimode atomic force microscope (Digital Instruments) was used in Tapping Mode. The images were obtained using noncontact high frequency cantilevers (Ted Pella).

2.8.1 Preparation of sample grids for AFM

Aβ(1-42), Aβ(1-40) aggregation solutions (100 µM) were diluted to a concentration of 1 µM. In our earlier trials we used higher concentrations (50 µM) of Aβ and we encountered frequent damage of the cantilever. Samples were allowed to adsorb onto mica which is known to be anatomically flat surface with hydrophilic property. Grade VI mica (Ted Pella, Inc, Redding, CA) was cut into 11mm circles and affixed to 12 mm metal discs. Before application of sample, layers of mica was cleaved by placing a section of one-sided scotch tape on the surface. The tape was then gently pressed and pulled up to reveal a smooth and clean surface. Aliquots (50 µl) were applied to the freshly cleaved mica and allowed to adsorb for 15 minutes. The solution was wicked off from the mica surface with tissue wipe, washed with deionized water twice to remove any unadsorbed sample, and air dried. The prepared mica grids were stored in a

container with desiccant. Images were obtained with a Nanoscope III multimode atomic microscope (Digital Instruments, Santa Barbara, CA) in Tapping Mode ™. Height analysis was performed using the Nanoscope III software on flattened height modes. Alternatively the grids were also prepared by pretreatment with 3 Aminopropyl triethoxy silane (APTES) 99% (Sigma Aldrich). Layers of mica were cleaved as described above and the grids were treated with APTES diluted to 100 fold in 1 mM acetic acid for 10 minutes. The APTES treated grids were washed with water and air dried. The APTES solution is prepared fresh for each treatment. Treated mica grids were placed in disc container overnight and 50 µl Aβ sample was applied the following day and allowed to adsorb for 15 minutes and followed the same steps described above. For SEC fractions, 10 µl from the fractions were applied on APTES treated grids without sample dilution. A small mark was made with a marker adjacent to the sample drop so that the grid could be mounted appropriately for AFM imaging.

2.9 Transmission Electron Microscopy (TEM)

2.9.1 Preparation of Sample Grids for TEM.

Aβ aggregation solutions (100 µM) were diluted to 20 µM in water. Aliquots (10 µl) were applied to 200-mesh formvar-coated copper grids (Ted Pella, Inc.). The coating on the grid gives a shiny surface and hence can be easily identified. Samples are applied on the shiny surface and allowed to adsorb for 10 minutes at room temperature. Excess sample was wicked away with a tissue wipe. The samples grids were washed three times by placing the sample side down on a droplet of water. Heavy metal staining of the samples was done in a similar manner by incubation on a droplet of

2% uranyl acetate (Electron microscopy Sciences, Hatfield, PA) for 5-10 minutes. The excess stain solution was removed and the grids were air dried and stored in desiccated containers. The affixed samples were visualized with a JEOL JEM-2000 FX transmission electron microscope operated at 100 – 200 k eV. The width measurements of aggregation species were done manually.

2.9.2 Preparation of Sample Grids for Immunogold Label Studies.

Aβ aggregation solutions (100 μM) were diluted to 20 μM in water. Aliquots (10 μl) were applied to 200-mesh formvar-coated copper grids with face up (Ted Pella, Inc.). Samples were allowed to adsorb for 10 minutes at room temperature, followed by removal of excess sample solution with a tissue wipe. The samples grids were washed three times by placing the sample side down on a droplet of water. The grids were treated with primary antibody Ab9 which recognizes the amino acids 1-16 in the Aβ peptide. Ab9 was diluted (1:1000) into sample diluent [20 mM Tris pH 7.3, 150mM NaCl, 0.1% BSA, 0.05% Tween 20]. The grids were treated with the diluted Ab 9 preparation with the sample side down and incubated for 1 hour at room temperature, followed by wash with water thrice. This was followed by treatment with secondary antibody which is a solution of goat-anti mouse IgG conjugated to gold particles [Aurion Cat #25129] diluted 1:1000 into sample diluent. Incubation with conjugated gold particles was also done at room temperature with the sample side down. The grids were washed thrice with water and treated with 2% uranyl acetate solution for 5-10 minutes, excess solution removed and the grids were air dried. The affixed samples were

visualized with a JEOL JEM-2000 FX transmission electron microscope operated at 100 – 200 k eV (Yagi et al., 2005, Vicente et al., 2006)

2.10 Cell Culture

2.10.1 THP-1 Monocytes

THP-1 cells are cultured from the blood of patient with acute monocytic leukemia, and have distinct monocytic markers. During culture these cells can maintain the monocytic characteristics for over 14 months (Tsuchiya et al., 1980). THP-1 cells were obtained from ATCC (Manassas, VA) and stored as 1 ml aliquots in liquid nitrogen until they are required for culturing. The cells were maintained in RPMI-1640 culture medium (HyClone, Logan, UT) containing 2 mM L-glutamine, 25 mM HEPES, 1.5 g/L sodium bicarbonate, 10% fetal bovine serum (HyClone), 50 U/ml penicillin, 50 μg/ml streptomycin (HyClone), and 50 μM β-mercaptoethanol at 37^{o}C in 5% CO_2. Prior to experiments, THP-1 monocytes were centrifuged, and the pellet was resuspended in reduced FBS (2%) growth medium (assay medium) followed by centrifugation as mentioned above. Once again pellet was resuspended in assay medium, and cell concentrations were adjusted to 1.0 x 10^6 cells/ml. The cell concentrations were adjusted by counting using a hemocytometer. Depending on the protocol the THP-1 cells (0.255 ml) was added to individual wells of a 48-well sterile culture plate the final volume in the well was 0.3 ml. The Aβ sample (45 μl) and other effectors were added to the wells and incubated at 37°C for 6 or 24 hours as per experiment protocol. For 96-well sterile

culture plate 12 µl Aβ sample was added to individual wells containing 0.068ml cells. The contents of each well were removed, centrifuged at 2500*g* for 10 min, and the supernatant was frozen at −20°C for subsequent TNF-α measurements by ELISA (Enzyme Linked Immunosorbant Assay).

2.10.2 Determination of TNFα levels by ELISA

TNFα levels were measured by using a sandwich enzyme linked immunosorbant assay as described previously in (Udan et al., 2008). Prior to the experiment, 100 µl of 4 µg/ml monoclonal anti-human TNFα/TNFSF1A capture antibody (R&D Systems, Minneapolis, MN) was added to 96-well plates and incubated overnight at room temperature. Wells were washed with PBS (HyClone) containing 0.05% Tween-20 and blocked with 300 µl PBS containing 1% BSA, 5% Sucrose and 0.05% NaN_3 for an hour at room temperature. After washing, 50 µl of sample diluent (20 mM Tris containing 150mM NaCl, 0.1% BSA and 0.05% Tween 20) was added to the wells. This was followed by addition of 50 µl samples, human TNF-α standards, and incubated at room temperature for 2 hours. Following the incubation plates were washed three times, and the wells were next treated with 100 µl biotinylated polyclonal anti-human TNF-α/TNFSF1A detection antibody (R&D Systems) in 20mM Tris with 150 mM NaCl and 0.1% BSA (2 hours at room temperature). In the next step, 100 µL streptavidin-HRP (R&D Systems) diluted 200 times with PBS containing 1% BSA was added and incubated for 20 minutes at room temperature. The wells were washed as described

above followed by addition of substrate which was 100 μl of equal volumes of 3,3',5,5'-tetramethylbenzidine and hydrogen peroxide (KPL, Gaithersburg, MD) for 30 minutes. The reaction was stopped by the addition of 1% H_2SO_4 solution. The optical density of each sample was analyzed at 450nm with a reference reading at 540 nm using a SpectraMax 340 absorbance plate reader (Molecular Devices, Union City, CA). A standard curve was constructed by sequential dilution of a TNF-α standard from 15-2000 pg/ml. The concentration of TNF-α in the experimental samples were calculated from a TNF-α standard curve and the TNF-α levels were normalized by dividing it with the number of cells plated.

2.10.3 Test for Contamination by Lipopolysaccharide (LPS)

Contamination of samples with bacterial lipopolysaccharide (LPS), can give rise to increased signals from the cells. In order to rule out any contamination, and confirm that the proinflammatory signal was not due to LPS contamination, we added polymyxin B sulfate PMX-B (Sigma) to the samples. PMX-B is known to neutralize the pathogenecity of LPS and can be used to detect any trace levels of contaminating LPS in the Aβ(1-42) aggregation preparations (Pristovsek and Kidric, 1999). THP-1 cells were prepared as described above, and plated on 48-well culture plate or 96 well plate. Cells were pretreated with 0.1 μg/ml PMX-B and incubated for 30 minutes at 37°C, 5% CO_2. Following incubation with PMX-B, the cells were treated with 10 ng/ml ultra pure LPS

or Aβ(1-42) (final concentration 15 μM) and incubated for 6 hours at 37°C. The cell supernatants were collected, and stored at −20°C and analysed for TNFα levels.

2.10.4 Monocyte Adhesion Studies

2.10.4.1 Cell adhesion assay

THP-1 monocytes were prepared in reduced FBS growth medium prior to the start of the experiment. THP-1 cells were centrifuged and resuspended in reduced FBS (2%) growth medium, and 0.204 ml was added to individual wells of a 48-well sterile culture plate. Cell adhesion was induced as described in (Crouse et al., 2009), by direct addition of 10 ng/ml phorbol 12-myristate 13-acetate (PMA) (Sigma) or 15 μM Aβ peptides to THP-1 cells. Controls were 0.0005% DMSO for PMA and sterile water for Aβ respectively. Cells were treated with the effectors and incubated at 37°C for 6 hours. After the incubation period, the medium that contains non-adherent cells were removed from the wells. The wells were washed with 200 μl of phosphate buffered saline (PBS) and wash was collected. The cells that adhered to the plate were washed with phosphate buffered saline (PBS, Hyclone). The adherent cells were then removed with 0.25% trypsin-EDTA (HyClone), and counted under a microscope using a standard hemocytometer. Percent adhesion was determined by the adherent cell number divided by the plated cell number. We also coated the surface of 48-well cell culture plates with human fibronectin (Fn) (Sigma). Surface coating was done by addition of 0.1 ml per well of 50 μg/mL Fn in sterile PBS and incubation for 1 hr at 25°C. The plate was covered

and stored at 4°C until needed for an experiment. Before the addition of cells, the excess Fn solution was aspirated from the wells.

2.10.5 XTT Cell Viability Assay

Cell viability was monitored using an XTT (2, 3-bis (2-methoxy-4-nitro-5-sulfophenyl) -2H-tetrazolium-5-carboxanilide) cell assay. XTT is a tetrazolium salt, and is used to measure the cell metabolism of viable cells (Braeckman et al., 2002). The assay is based on the reduction of the colorless XTT tetrazolium salt within the mitochondria of living cells by the enzyme succinate dehydrogenase to form an orange-colored water-soluble formazan. A stock solution of XTT (Sigma) 1mg/ml was prepared in RPMI 1640 without phenol red (Hyclone) supplemented with 2 mM L-glutamine and stored at -20°C. Cells were treated with Aβ for 6 hours or 24 hours followed by further incubation with final concentrations of 0.33 mg/ml XTT and 8.3 µM phenazine methosulfate (PMS) (Acros, Morris Plains, NJ) for 3 hours at 37°C. Cell supernatants were removed from individual wells after incubation and centrifuged at 5000 rpm for 10 minutes. Supernatants were transferred to a fresh 96 well plate. The XTT reduction by viable cells was determined by absorbance measurements of the reduced form of XTT at 467 nm.

2.11 Fast Pressure Liquid Chromatography (FPLC)

The AKTA FPLC is a type of liquid chromatography where the solvent velocity is controlled by pumps to control the constant flow rate of solvents. The standard FPLC consist of one or two high-precision pumps, a control unit, a column, a detection system

(UV spectrophotometer) and a fraction collector. AKTA FPLC is controlled through UNICORN software, which actually controls the run and offers a number of options such as automatic detection and collection of peak fractions. The Superdex 75 HR column was pretreated with 2 mg/ml BSA in running buffer to block non specific binding of Aβ aggregation species to the resin. The column was equilibrated with running buffer. The Aβ preparation was loaded and eluted from a Superdex 75 HR 10/30 column (GE Healthcare) in 50 mM Tris-HCl (pH 8.0) at a flow rate of 0.5 ml/min. Monomeric fractions were isolated by size-exclusion chromatography (SEC). Concentrations of monomeric Aβ isolated from the SEC elution fractions were determined by absorbance using an extinction coefficient of 1450 cm^{-1} M^{-1} at 276 nm for Aβ(1-40) as previously described (Nichols et al., 2002). The percentage recovery of the monomer concentration from the column can be calculated by dividing it by the preload concentration of Aβ. The purified monomer fractions were used to initiate aggregation the aggregation reactions. At the appropriate aggregation time point THP-1 cells were treated with the aggregated fractions for 6 hours and the cell supernatants were tested for TNF-α production. SEC was also used to separate Aβ(1-42) aggregation species. Aβ(1-42) solutions (100 μM) were allowed to aggregate at 4°C for 96 hours, centrifuged for 10 minutes at 18,000 x g, and supernatants were loaded on the column. The fractions were treated with THP-1 monocytes to test for TNF α level. Morphology studies were done using AFM and TEM.

2.12 Thioflavin-T Fluorescence Assay

Thioflavin-T (ThT) is a benzothiazole salt obtained by the methylation of dehydrothiotoluidine with methanol in the presence of hydrochloric acid. ThT

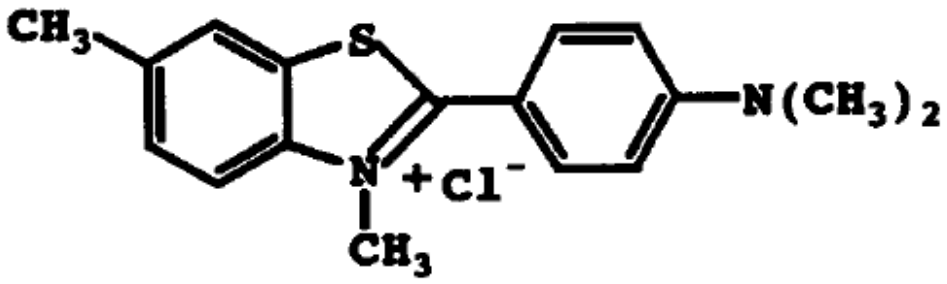

Fig 2.1 Structure of Thioflavin T.

fluorescence intensity is enhanced when bound to enriched β-sheet structure found in amyloid fibrils. This provides a simple fluorometric method for following Aβ aggregation in prepared samples. The dye undergoes a characteristic 120 nm red shift of its excitation spectrum that may be selectively excited at 450 nm, resulting in a fluorescence maximum at 482 nm. The excitation and emission slits of 10 nm were used and all measuremensts were made at room temperature. The fluorescence intensity was monitored by excitation at 450nm and emission scan from 460-520nm using a Cary Eclipse fluorescence spectrophotometer (Naiki et al., 1989, LeVine, 1993). Aβ aggregation solutions were monitored by thioflavin T (ThT) fluorescence as described in (Nichols et al., 2005). Aβ aliquots were removed and diluted 10 fold into water, PBS (pH 7.4), or 50 mM Tris (pH 8.0), or 150mM glycine buffer (pH 8.0) containing 5 μM ThT. The scans were integrated from 470-500 nm to obtain ThT fluorescence values.

2.13 Centrifugation of Aβ Aggregation Solutions to Test Solubility of Aggregation Species

2.13.1 Centrifugation at 18k, 50k, 100 k and 150 k x g

Microfuge^{R} 18 centrifuge, Beckman Coulter^{TM} was moved to 4°C prior to spinning the samples. Aβ(1-42) aggregation solutions were spun for 15 minutes at 18,000 g or 14,000 g as per the experiment protocol. The spun supernatants were treated with THP-1 cells to test for TNFα secretion. Aliquots were removed for AFM and dot blot as per the experiment protocol. The solubility of Aβ(1-42) aggregation species were also tested by high speed ultracentrifugation. Initial centrifugation at 50,000 x g was

done in Sorvall RC 5B plus refrigerated centrifuge using SS-34 rotor. Since we were working with small sample volumes (100 µl), adaptors were used. Aβ(1-42) aggregation solutions were placed in 1.5 ml eppendorf tubes which were in turn placed in adaptors that fit into the SS-34 rotor. The samples were spun for an hour at 50,000 x g, supernatants were collected,and treated with THP-1 cells to measure the proinflammatory response. Simultaneously, samples were diluted to 1µM and applied to mica grids for AFM image analysis. For centrifugation at higher speeds, a refrigerated Beckman Coulter Optima Max ultracentrifuge with TLA-120 rotor was used. The samples were placed in polycarbonate Beckman centrifuge tubes and centrifuged for an hour at 50 k, 100 k, or 150 k x g as per the experiment protocol. The centrifugation supernatants were collected and treated with THP-1 monocytes as described above and the supernatants were tested for TNF-α secretion.

2.13.2 Centrifugation with Centrifugation Filter Devices

Two types of microcentrifugal devices , YM-50 with a nominal molecular weight limit (NMWL) of 50,000 Daltons, and YM-100 with a NMWL of 100,000 Daltons were used. The filter device has a sample reservoir that fits into a vial. The membranes used in the micron filters are anisotrophic, hydrophillic, and has the ability to retain molecules above a specified molecular weight. Aβ aggregation solution was pippeted into the sample reservoir without touching the membrane with the pipette tip. The assembly was placed in Microfuge^{R} 18 centrifuge, Beckman Coulter^{TM} and spun for 15 minutes at 14,000 g. After the run the vial containing the filtrate is seperated from the sample

reservoir. The sample reservoir was turned upside down into a new vial and then spun for 3 minutes at 1000 x g to transfer the retentate into the vial. The supernatant and retentate were treated with THP-1 monocytes for 6 hours. The cell supernatants were tested for TNF-α response. Simultaneously, an aliquot was diluted to 1μM concentration for AFM imaging. We also used centrifugal filter devices with 0.2μm pore size (Millipore Cat # UFC30LG25). Aβ(1-42) was reconstituted in water and allowed to aggregate for 96 hours at 4°C. An aliquot was placed into the filter cup and centrifuged for 3 minutes at 12,000 x g, the filtrate was collected and treated with cells. AFM image analysis, Bradford assay was done with the filtrate and compared to that of the Total (unspun sample).

2.14 Dynamic Light Scattering (DLS)

Light scattering is useful in characterizing macromolecules and colloids. This technique can be divided into two: Static light scattering and dynamic light scattering (DLS). Static light scattering measures the time averaged intensities of the light scattered from a solution of particles and dynamic light scattering which measures the fluctuations of intensities of the scattered light. Using these techniques one can obtain the weight average molecular weight and the radius of gyration from the total intensity (static light scattering) and the hydrodynamic (Stokes) radius (R_H) from DLS (Bloomfield, 2000).

In solution the macromolecules are buffered by the solvent molecules, and the molecules are in random motion called the Brownian motion. As light scatters from the moving macromolecules, this motion imparts randomness to the phase of the scattered

light. This leads to time-dependent fluctuations in the intensity of the scattered light. In DLS the time-dependent fluctuations are measured by a fast photon counter. The fluctuations are directly related to the rate of diffusion of the molecule through the solvent, and can be used to analyze the R_H for the sample

DynaPro Titan Instrument (Wyatt Technology, Santa Barbara, CA) was used to make the R_H measurements. Aβ samples (30 μl) were spun at 18,000 x g for 10 minutes and supernatant was placed directly into a quartz cuvette. The light scattering intensity was collected at 90° angle using a 10-second acquisition time. Particle diffusion coefficients were calculated from auto-correlated light intensity data and converted into R_H with Stokes-Einstein equation. Histograms of percent mass vs. R_H were generated using the Dynamics software (version 6.7.1). The R_H values were calculated from the histogram.

2.15 Bibliography

Akerstrom, B. and Bjorck, L., 1986. A physicochemical study of protein G, a molecule with unique immunoglobulin G-binding properties. J Biol Chem. 261, 10240-10247.

Akiyama, H., Barger, S., Barnum, S., Bradt, B., Bauer, J., Cole, G. M., Cooper, N. R., Eikelenboom, P., Emmerling, M., Fiebich, B. L., Finch, C. E., Frautschy, S., Griffin, W. S., Hampel, H., Hull, M., Landreth, G., Lue, L., Mrak, R., Mackenzie, I. R., McGeer, P. L., O'Banion, M. K., Pachter, J., Pasinetti, G., Plata-Salaman, C., Rogers, J., Rydel, R., Shen, Y., Streit, W., Strohmeyer, R., Tooyoma, I., Van Muiswinkel, F. L., Veerhuis, R., Walker, D., Webster, S., Wegrzyniak, B., Wenk, G. and Wyss-Coray, T., 2000. Inflammation and Alzheimer's disease. Neurobiol Aging. 21, 383-421.

Bloomfield, V. A., 2000. Static and dynamic light scattering from aggregating particles. Biopolymers. 54, 168-172.

Braeckman, B. P., Houthoofd, K. and Vanfleteren, J. R., 2002. Assessing metabolic activity in aging Caenorhabditis elegans: concepts and controversies. Aging Cell. 1, 82-88; discussion 102-103.

Chen, S. and Wetzel, R., 2001. Solubilization and disaggregation of polyglutamine peptides. Protein Sci. 10, 887-891.

Crouse, N. R., Ajit, D., Udan, M. L. and Nichols, M. R., 2009. Oligomeric amyloid-beta(1-42) induces THP-1 human monocyte adhesion and maturation. Brain Res. 1254, 109-119.

Dahlgren, K. N., Manelli, A. M., Stine, W. B., Jr., Baker, L. K., Krafft, G. A. and LaDu, M. J., 2002. Oligomeric and fibrillar species of amyloid-beta peptides differentially affect neuronal viability. J Biol Chem. 277, 32046-32053.

Evans, K. C., Berger, E. P., Cho, C. G., Weisgraber, K. H. and Lansbury, P. T., Jr., 1995. Apolipoprotein E is a kinetic but not a thermodynamic inhibitor of amyloid formation: implications for the pathogenesis and treatment of Alzheimer disease. Proc Natl Acad Sci U S A. 92, 763-767.

Kayed, R., Head, E., Sarsoza, F., Saing, T., Cotman, C. W., Necula, M., Margol, L., Wu, J., Breydo, L., Thompson, J. L., Rasool, S., Gurlo, T., Butler, P. and Glabe, C. G., 2007. Fibril specific, conformation dependent antibodies recognize a generic epitope common to amyloid fibrils and fibrillar oligomers that is absent in prefibrillar oligomers. Mol Neurodegener. 2, 18.

Kayed, R., Head, E., Thompson, J. L., McIntire, T. M., Milton, S. C., Cotman, C. W. and Glabe, C. G., 2003. Common structure of soluble amyloid oligomers implies common mechanism of pathogenesis. Science. 300, 486-489.

LeVine, H., 3rd, 1993. Thioflavine T interaction with synthetic Alzheimer's disease beta-amyloid peptides: detection of amyloid aggregation in solution. Protein Sci. 2, 404-410.

Naiki, H., Higuchi, K., Hosokawa, M. and Takeda, T., 1989. Fluorometric determination of amyloid fibrils in vitro using the fluorescent dye, thioflavin T1. Anal Biochem. 177, 244-249.

Nichols, M. R., Moss, M. A., Reed, D. K., Cratic-McDaniel, S., Hoh, J. H. and Rosenberry, T. L., 2005. Amyloid-beta protofibrils differ from amyloid-beta aggregates induced in dilute hexafluoroisopropanol in stability and morphology. J Biol Chem. 280, 2471-2480.

Nichols, M. R., Moss, M. A., Reed, D. K., Lin, W. L., Mukhopadhyay, R., Hoh, J. H. and Rosenberry, T. L., 2002. Growth of beta-amyloid(1-40) protofibrils by monomer elongation and lateral association. Characterization of distinct products by light scattering and atomic force microscopy. Biochemistry. 41, 6115-6127.

Parvathy, S., Rajadas, J., Ryan, H., Vaziri, S., Anderson, L. and Murphy, G. M., Jr., 2008. Abeta peptide conformation determines uptake and interleukin-1alpha expression by primary microglial cells. Neurobiol Aging.

Petkova, A. T., Leapman, R. D., Guo, Z., Yau, W. M., Mattson, M. P. and Tycko, R., 2005. Self-propagating, molecular-level polymorphism in Alzheimer's beta-amyloid fibrils. Science. 307, 262-265.

Pristovsek, P. and Kidric, J., 1999. Solution structure of polymyxins B and E and effect of binding to lipopolysaccharide: an NMR and molecular modeling study. J Med Chem. 42, 4604-4613.

Tsuchiya, S., Yamabe, M., Yamaguchi, Y., Kobayashi, Y., Konno, T. and Tada, K., 1980. Establishment and characterization of a human acute monocytic leukemia cell line (THP-1). Int J Cancer. 26, 171-176.

Udan, M. L., Ajit, D., Crouse, N. R. and Nichols, M. R., 2008. Toll-like receptors 2 and 4 mediate Abeta(1-42) activation of the innate immune response in a human monocytic cell line. J Neurochem. 104, 524-533.

Vicente, R., Escalada, A., Villalonga, N., Texido, L., Roura-Ferrer, M., Martin-Satue, M., Lopez-Iglesias, C., Soler, C., Solsona, C., Tamkun, M. M. and Felipe, A., 2006.

Association of Kv1.5 and Kv1.3 contributes to the major voltage-dependent K+ channel in macrophages. J Biol Chem. 281, 37675-37685.

Wetzel, R., 1999. Methods in Enzymology. 309, 333-349.

Wood, S. J., Maleeff, B., Hart, T. and Wetzel, R., 1996. Physical, morphological and functional differences between ph 5.8 and 7.4 aggregates of the Alzheimer's amyloid peptide Abeta. J Mol Biol. 256, 870-877.

Yagi, H., Kusaka, E., Hongo, K., Mizobata, T. and Kawata, Y., 2005. Amyloid fibril formation of alpha-synuclein is accelerated by preformed amyloid seeds of other proteins: implications for the mechanism of transmissible conformational diseases. J Biol Chem. 280, 38609-38616.

Zagorski, M. G., Yang, J., Shao, H., Ma, K., Zeng, H. and Hong, A., 1999. Methodological and chemical factors affecting amyloid beta peptide amyloidogenicity. Methods Enzymol. 309, 189-204.

CHAPTER 3

CORRELATION OF Aβ AGGREGATION STATE WITH ABILITY TO INDUCE PROINFLAMMATORY RESPONSE IN HUMAN THP-1 MONOCYTIC CELL MODEL SYSTEM

3.1 Introduction

AD is the most frequent form of senile dementia, and is characterized by extracellular senile plaques, and intracellular neurofibrillary tangles. The extracellular plaques consist primarily of aggregated amyloid beta (Aβ), a 40-42 amino acid peptide derived by the proteolysis of amyloid precursor protein (APP). Although only two amino acids longer, Aβ(1-42) polymerizes into amyloid fibrils more rapidly than the biologically abundant Aβ(1-40) form of the peptide (Jarrett et al., 1993b, Harper et al., 1997a). In addition to deposition of Aβ peptides into extracellular plaques, there is also evidence for the presence of intracellular Aβ that is believed to be initially involved in the disease process (LaFerla et al., 2007). *In vitro* studies have shown that Aβ monomer will undergo non-covalent self-assembly to form a mixture of diverse Aβ assemblies that ultimately form insoluble fibrils (Harper et al., 1997b, Walsh et al., 1997, Harper et al., 1999). It is assumed that the same aggregation process occurs *in vivo*, and these wide ranges of morphologies appear to stimulate different types of biological responses *in vivo*. Cell culture studies have demonstrated the neurotoxicity of Aβ fibrils (Pike et al.,

1993, Lorenzo and Yankner, 1994, Seilheimer et al., 1997). Recent studies now suggest that soluble oligomeric Aβ species may be more potent than the mature fibrils (Lambert et al., 1998, Hartley et al., 1999, Walsh et al., 2005). Furthermore, a strong positive correlation has been demonstrated between soluble oligomeric Aβ and severity of dementia in humans (Lue et al., 1999).

One of the proposed mechanisms underlying progressive neurodegeneration in AD is a chronic inflammatory response to aggregated Aβ involving production of toxic cytokines such as tumor necrosis factor alpha (TNFα). Pathology studies have shown the presence of inflammatory markers like activated microglia and proinflammatory cytokines surrounding the Aβ lesions in the human AD brain (McGeer et al., 1987). TNFα is a crucial mediator of the inflammatory response. Overexpression of TNFα in the central nervous system of transgenic mouse models results in inflammation of the CNS and neurodegeneration (Probert et al., 1995). *In vitro* studies have shown that TNFα stimulation of neuronal cell lines leads to increased expression of inducible nitric oxide synthase that leads to apoptosis (Heneka et al., 1999). TNFα levels are elevated in the post mortem AD brain sections (Dickson et al., 1993) and micro vessels compared to non AD micro vessels (Grammas and Ovase, 2001). TNFα levels are also significantly elevated in the cerebrospinal fluid (CSF) of clinically diagnosed AD patients (Tarkowski et al., 2003). These findings suggest TNFα levels as a valuable marker for proinflammatory response.

Though there are several Aβ lesions, not all of them have surrounding inflammatory pathology (Walsh and Selkoe, 2007). The exact mechanism by which Aβ

causes neurodegeneration is still not clear. Understanding the molecular structure of amyloid fibrils has attracted tremendous attraction over the past several years. These studies have shed light on issues such as the nature of the intermolecular interactions that stabilize amyloid structures (Tycko, 2004). Moreover, *in vitro* aggregation studies have provided useful information regarding fibrillogenesis mechanisms. These studies have provided information about the various Aβ species that are formed along the aggregation pathway, and how they vary in size, length, solubility and morphology (Harper et al., 1997b, Walsh et al., 1997, Harper et al., 1999, Walsh et al., 1999, Stine et al., 2003). Further characterization of Aβ aggregation species will therefore enable identification of the particular Aβ assembly state that triggers the inflammatory mechanisms in AD.

Our objective in this study was to investigate the Aβ structure-function relationship through modulation of Aβ aggregation conditions by varying several factors including peptide concentration, peptide length and temperature. Synthetic Aβ peptides. were used, and characterization of the aggregation species were done using biophysical and biochemical techniques in an effort to identify the Aβ assembly state that induces maximum proinflammatory response in human THP-1 cell line. Our data indicate that an intermediate fibrillar oligomeric aggregation species is optimal for inducing maximum proinflammatory response in THP-1 immune cell model system. These data will provide additional information towards understanding the relationship between inflammation and AD. The data from this study will subsequently provide clues to the development of therapeutic strategies to treat AD patients. This work was done in collaboration with Maria Udan, University of Missouri, Saint Louis.

3.2 Cell Model System for Inflammatory Studies

THP-1 human monocyte cells were used as a model system to study the proinflammatory response. THP-1 cells attain a microglia-like morphology when treated with lipopolysaccharide (LPS), a bacterial toxin (Yates et al., 2000), and hence, serves as a model of primary human microglial cells. Human microglial cells are very difficult to obtain in large quantities, while the THP-1 cells are easy to grow and can be obtained in large quantities. Previous studies have shown that both LPS and Aβ are capable of activating THP-1 cells, and stimulate cytokine production (Klegeris et al., 1997, Yates et al., 2000, Combs et al., 2001).

3.3 Probing Aβ Aggregation State that Induces Maximum Proinflamamtory Response

3.3.1 TNFα Production is Influenced by Aβ(1-42) Aggregation State

Deposition of Aβ(1-40) and Aβ(1-42) peptides in the form of senile plaques is a neuropathological hallmark of AD. Aβ(1-42) in the fibrillar form is abundant in the senile plaques. Aβ(1-40) also has the tendency to form fibrils, but to a lesser extent (Iwatsubo et al., 1994). We wanted to test the ability of Aβ(1-42) to stimulate the THP-1 cells for proinflammatory response. Aβ(1-42) forms aggregates very quickly and hence it was important to control the rate of aggregation in order to study the various species

along the fibril formation pathway. The initial phase of Aβ(1-42) oligomerization involves the formation of pentamer units, hexamer units, and paranuclei. These associate to form large oligomers and protofibrils that elongate to form mature fibrils (Bitan et al., 2003)

In our initial studies, Aβ(1-42) reconstituted in DMSO was used and aggregation reactions were followed by ThT fluorescence measurements. Though ThT fluorescence values confirmed the progress of aggregation, there was inconsistency in the biological activity. Some Aβ(1-42) preparations in DMSO were able to induce considerable activity while the others did not (data not shown). A different protocol capable of generating monomeric starting material was employed. The commercially available Aβ(1-42) peptide was treated with HFIP, vacuum centrifuged and stored as described in Methods. Aβ(1-42) aggregation reactions were set up by reconstituting the vacuum centrifuged peptide film in sterile water to a concentration of 100 µM and incubated at 4°C. Aliquots were removed periodically at 48, 72, 96, 120, 144, 168, 192 and 216 hours and treated with THP-1 monocytes with cell concentration of 1 $x10^6$ cells/ml for 6 hours as described in Methods. The cell supernatants were tested for the ability to stimulate TNFα production. We observed that freshly reconstituted Aβ(1-42) induced secretion of very small amounts of TNFα. The TNFα levels in the freshly reconstituted Aβ(1-42) varied amongst trials, but the levels were consistently low. However, we found a significant increase in TNFα levels at the intermediate time points (48-72hours) of the aggregation reaction (Fig 3.1). Continued aggregation at 4°C showed a decrease in the proinflammatory response after 96 hours, and the signal diminished by 216 hours (Fig 3.1).

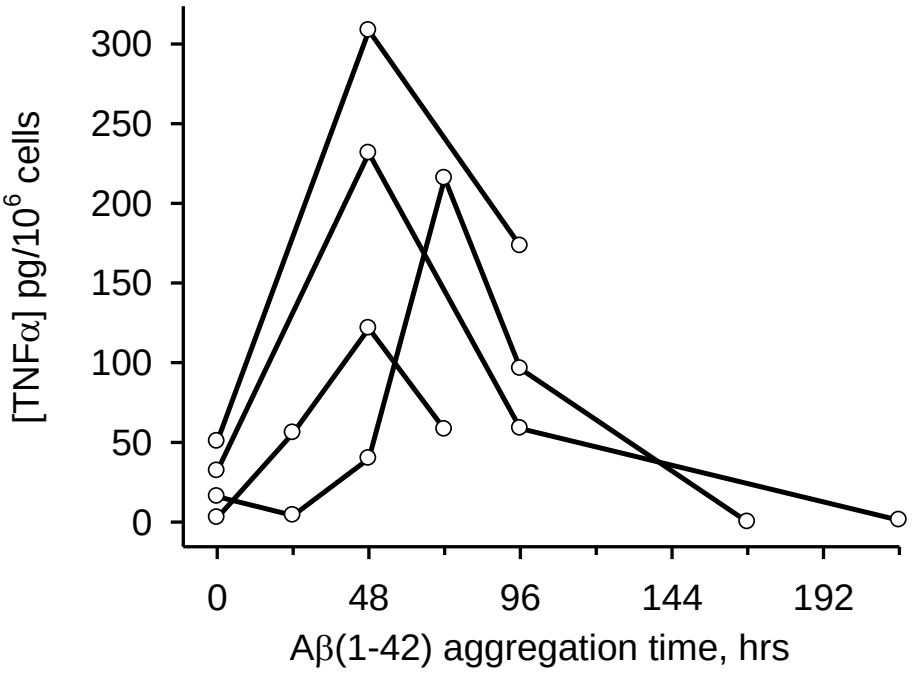

Figure 3.1 Proinflammatory activity of Aβ(1-42). Aβ(1-42) was reconstitued in water to a concentration of 100 μM and stored at 4°C, as described in the Methods. THP-1 monocytes were incubated with Aβ(1-42) to a final concentration of 15 μM. Aliquots were removed immediately after reconstitution, and at 48, 96 and 216 hours of incubation at 4°C, treated with THP-1 cells, incubated for 6 hours at 37°C, 5% CO_2. After 6 hours incubation, supernatants were collected and TNFα production was measured by ELISA. Each line in the figure corresponds to a separate experiment. The peak response lies between 48-96 hours of aggregation at 4°C. Courtesy Maria Udan, University of Missouri, Saint Louis.

The data from multiple experiments led us to hypothesize that an intermediate aggregation species may be responsible for inducing TNFα production in THP-1 monocytes.

3.3.2 An Intermediate Aggregation State Induces Maximum Proinflammatory Response

The morphology of the aggregation species was studied using AFM. Analysis of Aβ(1-42) aggregation time course was done in order to correlate the morphology with ability to induce TNFα production in THP-1 cells. As reported earlier (Udan et al., 2008), we noticed small punctuate species with heights < 2 nm immediately upon reconstitution of Aβ(1-42) (Fig 3.2, zero hour). Dynamic light scattering (DLS) measurements of the freshly reconstituted Aβ(1-42) showed a major peak with an R_H of 1.0 nm. This peak (95% mass) represents the monomeric Aβ and ensures that the starting material is monomeric. AFM imaging of the aggregation reaction showed presence of flexible fibrillar structures by 48 hours (Fig 3.2). These intermediate fibrillar structures correlated with maximal TNFα production by THP-1 cells. Height analyses of the fibers were done using the Nanoscope software as described in the Methods. The fibers formed after 48 hours of aggregation have a mean height and standard deviation (SD) of 4.2 +/- 1.4 nm. The lengths of the fibers ranged from 1-3 μm. Height analyses of the fibers made at corresponding time points of cell treatment indicate no significant change in the heights of the fibers as the aggregation proceeds from 48 hours to 216 hours. The fibers formed at 216 hours time point had a mean height of 4.5 +/- 1.4 nm. However, the length of the fibrils changed as the aggregation proceeds, especially fibers formed by 216 hours

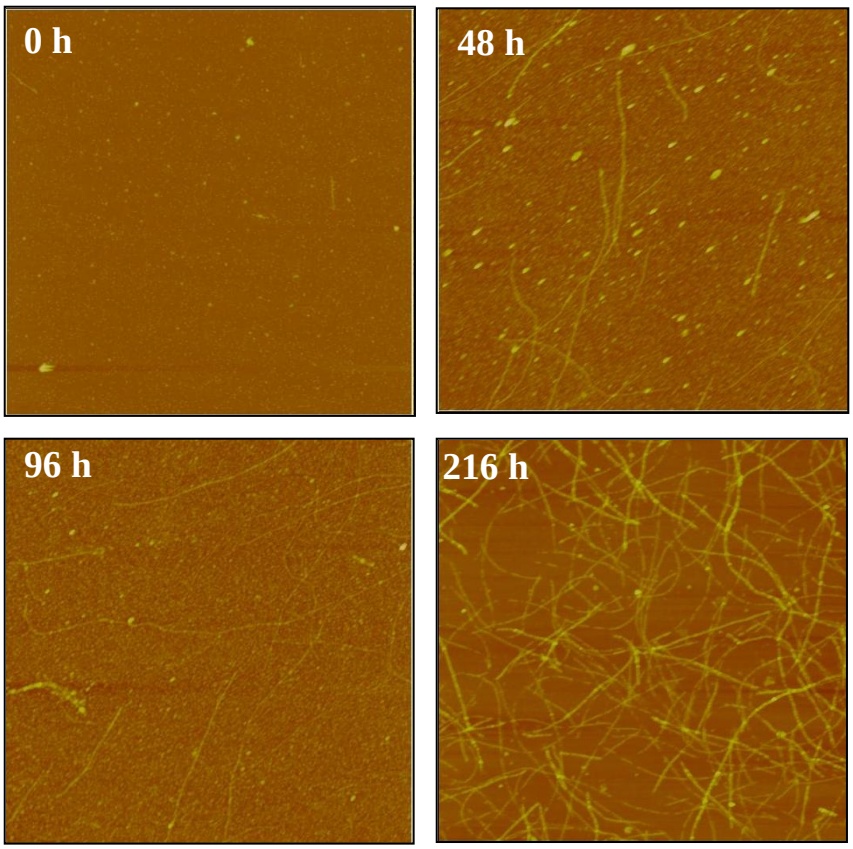

Figure 3.2. Morphology analyses of Aβ(1-42) aggregation species by AFM. Aβ(1-42) aggregation solutions (100 μM) in water was prepared as described in Methods, and allowed to aggregate at 4°C. Aliquots were removed at 0, 48, 96 and 216 hours, diluted to 1 μM with water and applied on to mica grids as described in Methods, and imaged by AFM. Image panels are 5μm x 5μm and are shown in 'height' mode. The heights were measured using the Nanoscope III soft ware.

of incubation (< 3 μm). There was a significant difference in the density of fibers. The calculated values of the density of fibers are 1 fiber/μm^2 at 48 hours of incubation and 6 fibers/μm^2 at 216 hours of incubation. ThT fluorescence measurements of the aggregation reactions were made in order to monitor the progression of the aggregation in the reactions as mentioned in Methods. Measurements at the zero hour time point of Aβ(1-42) solution showed no ThT fluorescence, indicating absence of aggregated structures with β-sheet at the time of reconstitution. ThT fluorescence intensity increased as the aggregation progressed indicating formation of β-sheet structures, and by 216 hours of incubation there was nearly 25 fold increase in the fluorescence intensities compared to the values at start of the reaction (Fig 3.3). This correlates with the AFM images that show formation of increased fibrillar structures by 216 hours (Fig 3.2).

3.4 Modulation of Aggregation Reaction Conditions

Aggregation of Aβ proceeds by a multistep, nucleation-dependent, process (Jarrett et al., 1993a). In the absence of preformed fibril seed there is a significant lag period for the formation of Aβ fibrils. Once the seeds are generated, there is rapid fibril elongation phase. The lag time for the fibrils can be shortened by the addition of preformed fibril seeds to monomer solutions (Jarrett et al., 1993a). The rate of Aβ fibril formation is controlled by both fibril seed concentration and monomer concentration (Naiki and Nakakuki, 1996). Aβ aggregation is also dependent on temperature (Harper et al., 1999) and pH (Wood et al., 1996). The calculated pI of Aβ is 5.5, and rapid aggregation of this peptide at pH 5.5-6.0 may be mediated by non-specific interactions of the highly

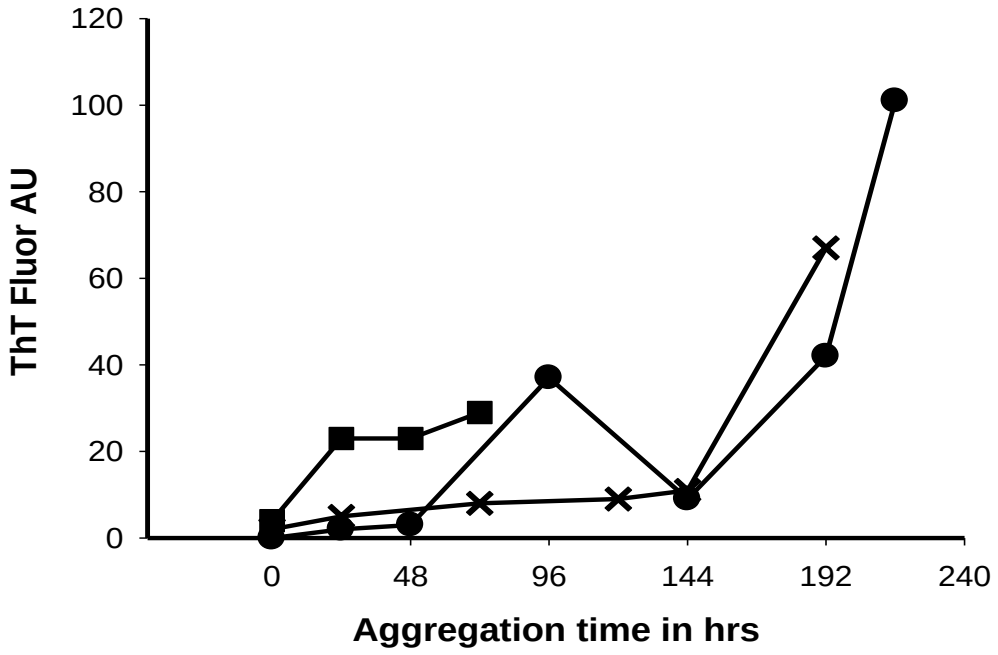

Figure 3.3. **ThT fluorescence scans of Aβ(1-42) aggregation time course.** Each plot represents a separate 100 μM Aβ(1-42) aggregation reaction. Aβ(1-42) aggregation reactions (100 μM) in sterile water, and incubated at 4°C as described in Methods. At specific time points aliquots of Aβ(1-42) aggregation solutions were removed and mixed with ThT diluted into water (5 μM) in a cuvette (final Aβ concentration 10 μM). ThT fluorescence was measured as described in Methods.

hydrophobic neutral molecules (Wood et al., 1996). In order to study the intermediates in the slow and controlled aggregation pathway, Aβ aggregation must occur outside of this rapid aggregation pH range. Small changes in the organelle pH, or the peptide secretion rates might control the efficiency of fibril formation i*n vivo* (Wood et al., 1996).

3.4.1 Increased Peptide Concentration Diminishes the Proinflammatory Signal

In Fig 3.1, we have seen that Aβ(1-42) aggregation species formed at the later time points were not effective in inducing a proinflammatory response, suggesting that continued aggregation diminishes the response. We increased the peptide concentration by 12 fold in order to increase the aggregation kinetics so that the lag time for nucleation is shortened. This step will cause rapid polymerization and fibril formation. The more concentrated solution of Aβ(1-42) (1.2 mM) was incubated at 25 °C and the cells were treated with the same final concentration of 15μM of Aβ(1-42). The Aβ(1-42) solution at zero hour was able to induce a very small level of TNFα. However, there was no induction of proinflammatory response at 24 hours and 48 hours even though the cells were treated with the same final concentration of 15 μM Aβ (Fig 3.4 A). The results were very different from the 100 μM preparation wherein we were able to see the peak response at 48 hours. AFM imaging of the concentrated samples showed the formation of small fibrillar structures at the time of reconstitution (Fig 3.4 B) and by 24 hours there was rapid fiber formation. Height analyses of the concentrated Aβ(1-42) fibers were not possible due to severe overlapping of fibers. However, the density was calculated to be 6

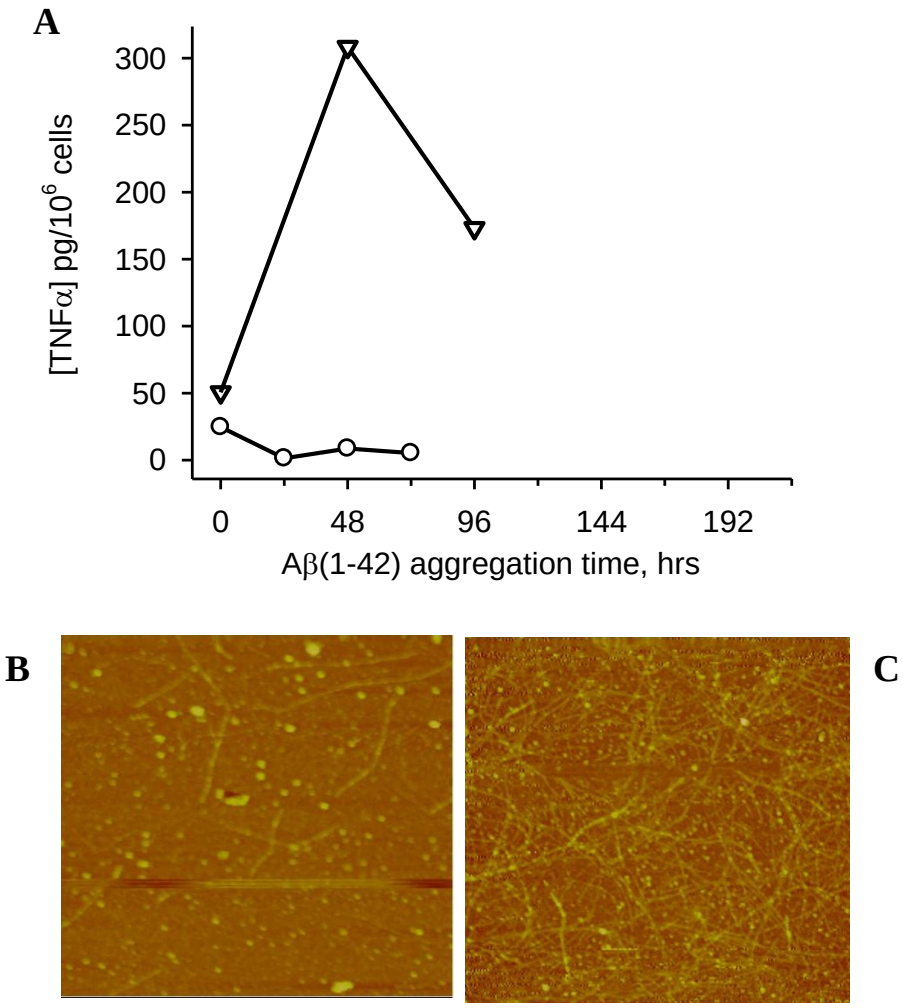

Figure 3.4. **Increase in Aβ(1-42) peptide concentration decreases TNF-α signal**
Panel A. Two Aβ(1-42) aggregation reactions were set up. Aβ(1-42), 100 µM (triangles) was incubated at 4°C, and the concentrated Aβ(1-42) 1.2 mM (circles), was incubated at 25°C. At specific time points aliquots were removed from the two samples and treated with THP-1 cells with final Aβ concentration of 15 µM. Courtesy Maria Udan. **Panel B-C**. Representative AFM images of the concentrated 1.2 mM Aβ(1-42) sample. At specific time points aliquots were removed and diluted to final concentration of 1 µM and applied to grids as described in Methods. **B**. Aβ(1-42), 1.2 mM sample aliquot taken shortly after reconstitution and **C**, Aβ(1-42), 1.2 mM sample after 24 hours incubation at 25°C.

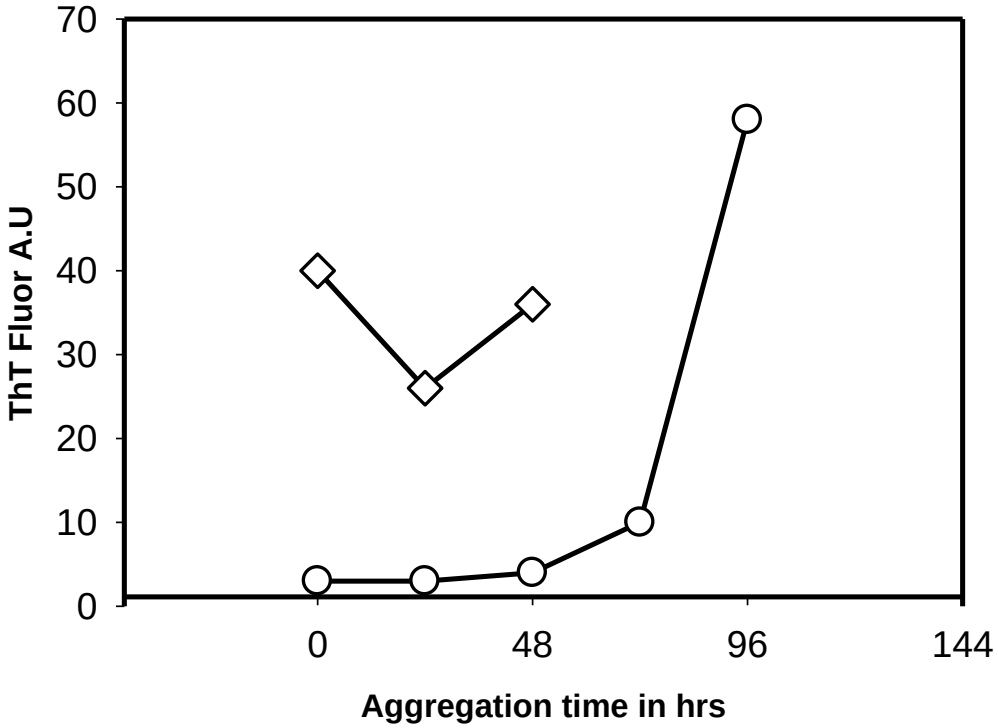

Figure 3.5 Concentrated peptide solutions show high ThT fluorescence. Two lyophilized aliquots of Aβ(1-42) were reconstituted to 0.1 mM incubated at 4°C (circles) or 1.2 mM incubated at room temperature (diamonds). ThT fluorescence was measured at different time points by mixing Aβ(1-42) (10 μM) with ThT (5 μM) as described in Methods.

fibers per square micron after 24 hours incubation. This was comparable to the fiber density at 216 hours aggregation of Aβ(1-42) (100 μM). We have already seen from Fig 3.1 that the 216 hour sample with the same density of fibers did not stimulate the cells for a response. It is possible that an increase in the peptide concentration caused rapid aggregation so that the transient intermediate species were either not formed, or were immediately converted into the higher aggregated form. ThT fluorescence measurements were 10 times higher in the 1.2 mM solutions than in the 100 μM solutions indicating rapid formation of β-sheet structures in the 1.2 mM sample compared to the less concentrated peptide solution (Fig 3.5).

3.4.2 Incubation of Aβ(1-42) at Higher Temperatures Diminishes Proinflammatory Response

Previous studies have shown that elongation rates of Aβ fibrils vary dramatically with temperature (Kusumoto et al., 1998). The aggregation rate of 100 μM sample was accelerated by incubation at higher temperatures. Three aggregation reactions of 100 μM Aβ(1-42) were prepared and incubated at 4°C, 25°C, or 37°C. Aliquots were taken from the reactions, treated with cells at final Aβ(1-42) concentration of 15 μM, and tested for ability to induce proinflammatory response. Only the reaction set up at 4°C stimulated the cells for a response, while the reactions set up at 25°C or 37°C significantly diminished the ability to stimulate THP-1 cells for TNFα production (Fig 3.6 A). The aggregation reactions were monitored by ThT fluorescence measurements (Fig 3.6 B). ThT fluorescence values were high for the aggregation at 37°C with a peak at 96 hour

.

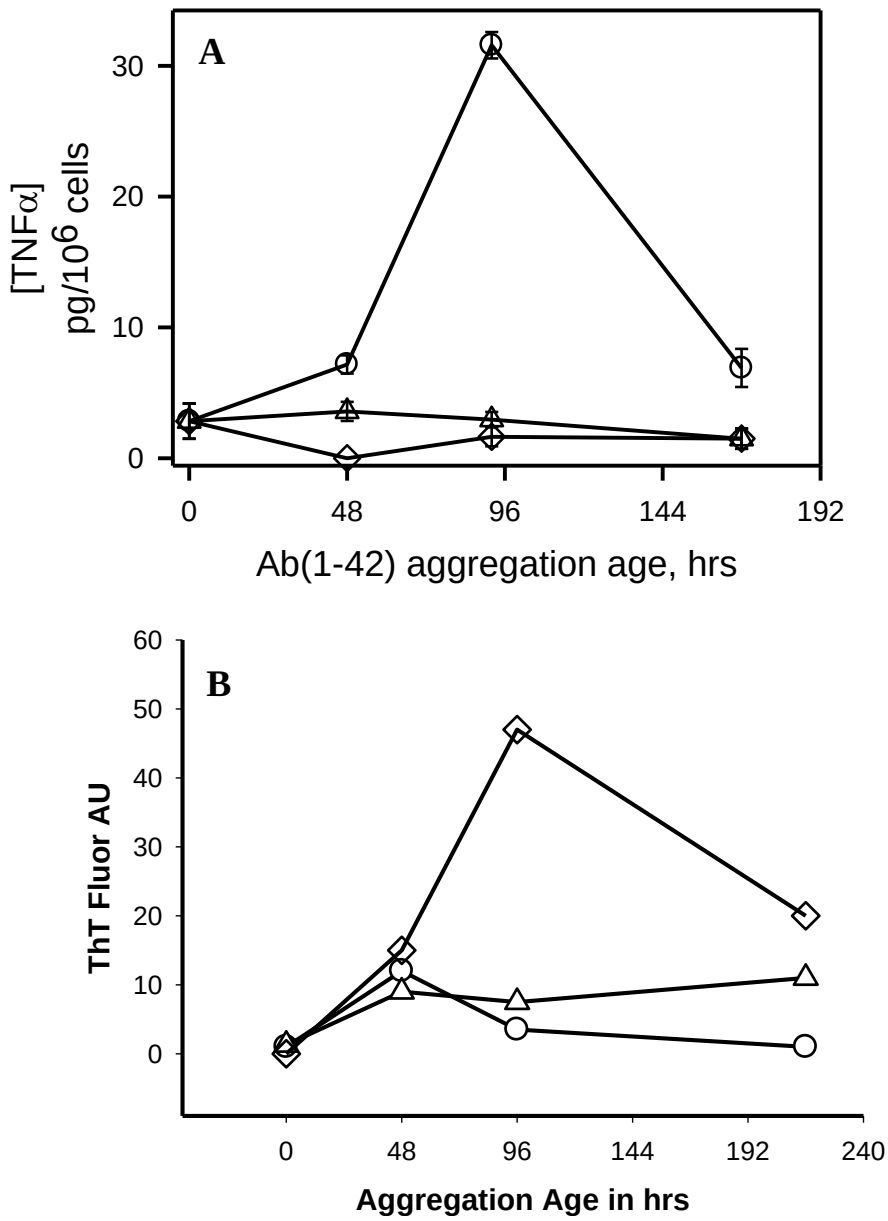

Figure 3.6 Incubation at higher temperatures accelerates aggregation, but diminishes proinflammatory activity. **Panel A.** A solution of Aβ(1-42), 100 μM was separated into three tubes and incubated at three different temperatures 4°C (circles), 25°C (triangles) and 37°C (diamonds). At various time points aliquots were removed for treatment with THP-1 monocytes. Secreted TNFα measurements for each time point were determined by ELISA. Courtesy Maria Udan. **Panel B.** ThT fluorescence measurements were made at specific time points as described in Figure 3.3.

time point. The ThT fluorescence values did not correlate with TNFα levels. In Fig 3.6 (Panel B) the highest ThT fluorescence intensities were recorded for the sample incubated at 37°C. However, the same sample did not stimulate the cells for high TNFα secretion. AFM images of the aggregation time course showed differences in the extent of aggregation. The peak TNFα response form the cells was at 96 hours, hence, we obtained the height analyses of the fibrils incubated at different temperature for this time point. The images of Aβ(1-42) at 4°C contained long flexible fiber structures with a mean height of 5.5 +/- 1.6 nm (SD) along with the globular species (Fig 3.7 E). The sample at 25°C displayed increased number of fibers with a mean height of 6.9 +/- 2.1 nm. There was disparity in the measured fibrils heights. Also, there was an increase in fibers with height < 5 nm (Fig 3.7 F). The AFM image of sample incubated at 37°C showed less number of fibrils, and the average height of the fibrils were 6.1+/- 1.6 nm (Fig 3.7 G). The heights were not very different from the 25°C aggregation reaction. However, the striking feature was the absence of globular species. The fibrils formed at 37°C had a twisted appearance, and shorter than the ones formed at the other two temperatures. The decrease in the number of fibrils could possibly be due to decreased adsorption to the mica surface. These data suggest that the proinflammatory response corresponded with the formation of the initial intermediate fibrillar structures of Aβ(1-42) solution that was incubated at 4°C. This finding was further strengthened by the observation that continued, accelerated, or increased fibril formation abolished the ability of Aβ(1-42) to stimulate the THP-1 monocytes to induce TNFα production.

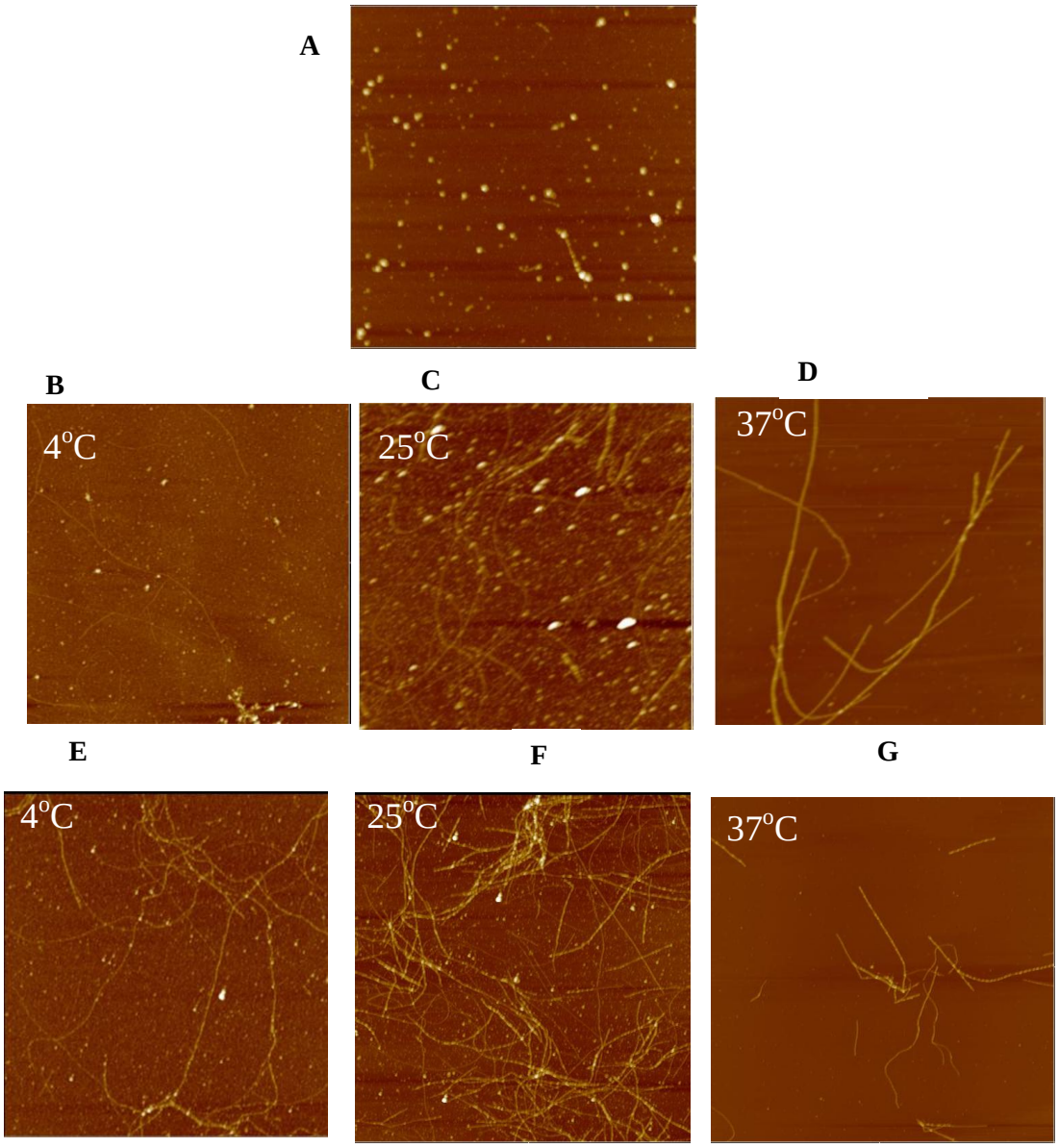

Figure 3.7. Increasing the temperature of aggregation reactions failed to invoke TNFα response in THP-1 monocytes. 100 μM Aβ(1-42) was prepared in water (100 μM), and incubated at 4°C, 25°C or 37°C. **A-G.** Representative AFM images of freshly prepared (A), 48 hours (B-D) or 96-hours (E-G) aggregation. B and E are the images of Aβ(1-42) aggregation solution incubated at 4°C, (C and F) are images of 25°C incubation, and (D and G) are images of 37°C incubation. Heights were determined using the Nanoscope software as described in Methods.

3.4.3 Proinflammatory Activity is Dependent on Peptide Length

Aβ is formed from APP by the action of α- β- γ- secretases. The action of γ-secretases results in the formation of Aβ peptides of different fragments of 39-42 amino acids long (Selkoe, 2001). Among the fragments formed, the most abundant is Aβ(1-40) fragment. Among others, Aβ(25-35) fragment is the shortest peptide sequence that retains the biological activity comparable to Aβ(1-42) and exhibits β-sheet aggregated structures (Pike et al., 1995, D'Ursi et al., 2004). Aβ-(25-35) is present in plaques and degenerating hippocampus neurons in the AD brains and not in age matched control subjects. Aβ(25-35) has a high tendency to quickly assemble into insoluble aggregates (Clementi et al., 2005). Our results so far indicate that Aβ(1-42) incubated at 4°C formed a species that induces maximum proinflamamtory stimulus. We wanted to test if length of the peptide is crucial for the proinflammatory stimulus. Aβ(1-40), Aβ(25-35) peptide fragments were selected for the experiment and compared to the response from Aβ(1-42) under similar conditions. Three separate reactions (100 μM) of these three peptides were set up and allowed to aggregate at 4°C. The aggregation reaction was monitored by making ThT fluorescence measurements at specific time points. At specified time intervals the cells were treated separately with each of the three peptides and tested for TNFα production. ThT measurements indicate that under similar conditions Aβ(1-40) and Aβ(25-35) did not aggregate as fast as the longer peptide Aβ(1-42) (Fig 3.8). The supernatants from the THP-1 cells treatment indicated that only Aβ(1-42) aggregation solution incubated at 4°C stimulated the cells and were consistent with our previous data.

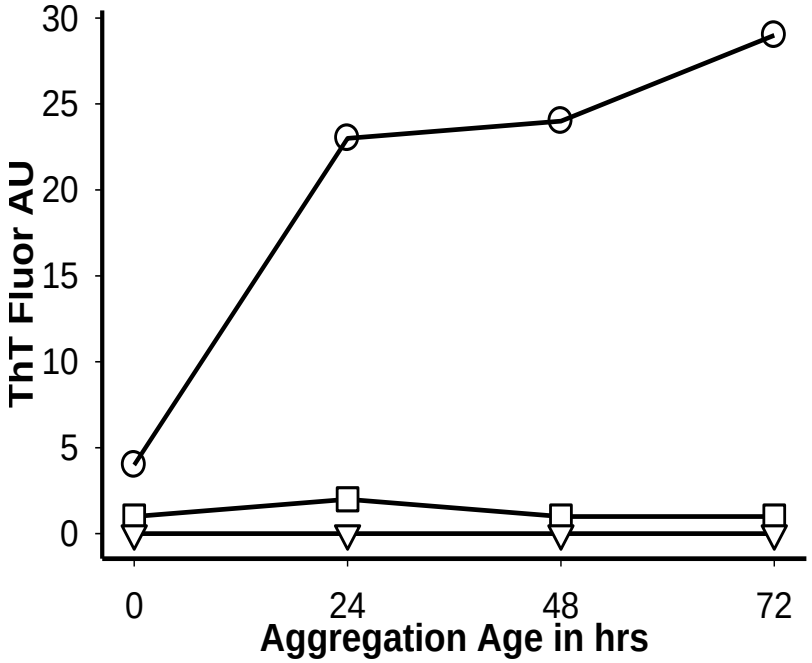

Figure 3.8. **Shorter Aβ peptide aggregates at a slower rate under similar conditions**. Three aggregation reactions were set up by reconstituting Aβ(1-42) (circles), Aβ(1-40) (squares) and Aβ-(25-35) (inverted triangles) in water to a concentration of 100 µM. The aggregation reactions were allowed to incubate at 4°C. At specific time points ThT fluorescence was measured by mixing Aβ (10 µM) with ThT (5 µM) as described in Methods.

Aβ(1-40) and Aβ(25-35) aggregation reactions were not able to induce TNFα production in THP-1 cells under similar conditions (data not shown). Therefore, to probe further we used Aβ(1-40) aggregation reactions set up at different temperatures. Solutions of Aβ(1-42) and Aβ(1-40) (100 μM) were prepared. The Aβ(1-42) solution was incubated at 4°C while Aβ(1-40) was incubated at 4°C, 25°C, or 37°C. THP-1 monocytes were treated with aliquots from the aggregation solutions with final Aβ concentration at 15 μM. Only Aβ(1-42),aggregation reaction set up at 4°C effectively stimulated the cells for TNFα production (Fig 3.9). AFM (Fig 3.10) images indicate fibril formation by Aβ(1-40) sample incubated at the three different temperatures (Fig 3.10 A-C), but at a much slower rate compared to Aβ(1-42) (Fig 3.7 E-G). Height analyses of these images indicate that fibrils were longer (> 5 μm) and only one or two fibrils could be located in a 5 μm x 5 μm image panel. The heights of these fibrils were slightly greater than Aβ(1-42) fibrils, measuring 5.9 +/- 1.7 nm (SD) at 96 hours (Fig 3.10 D). There was very little change in the fibril heights from 96 hours to 216 hours, but they were slightly longer at 216 hours (Fig 3.10 G). TEM images of the same Aβ(1-40) aggregation reactions also displayed fibril formation at the different temperatures (Fig 3.11). Increased temperature resulted in the formation of large number of fibrils as seen in the AFM images, yet these aggregation species did not induce proinflammatory activity. Aβ(1-40) and Aβ(1-42) oligomerize through different pathways (Bitan et al., 2003), and it is possible that Aβ(1-42) with the extra two amino acids forms a distinct intermediate species that is able to stimulate a proinflammatory response. AFM and TEM image analyses indicate the

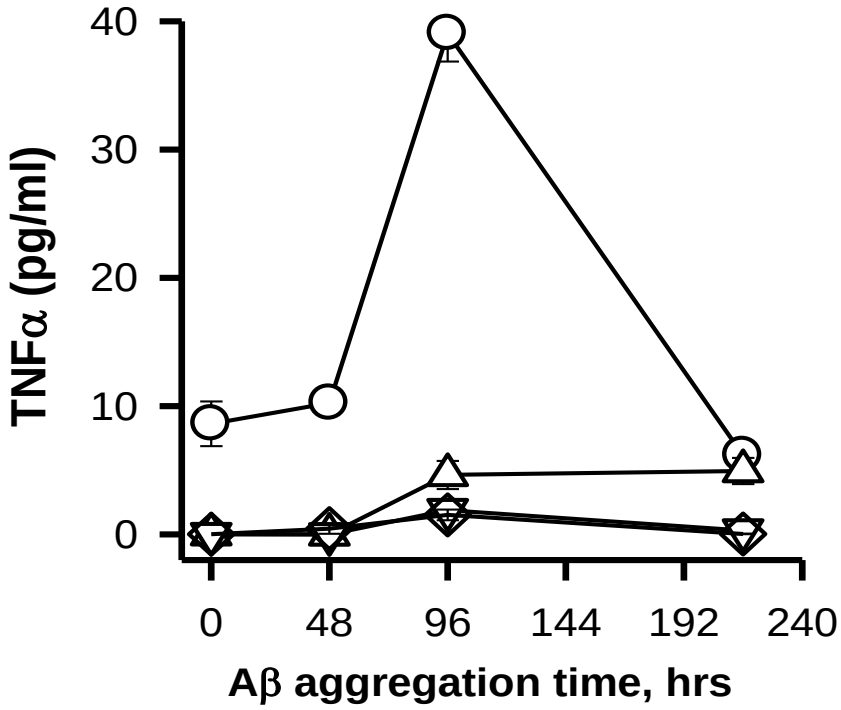

Figure 3.9. Aβ(1-40) failed to induce proinflammatory activity on THP-1 cells. Aβ(1-40) (100 μM) was resuspended in sterile water, and incubated at 4°C (triangle), 25°C (inverted triangle) and 37°C (diamond), as described in Methods. Aliquots from the respective aggregation solutions were used to treat the THP-1 monocytes to a final Aβ concentration of 15 μM for 6 hours; supernatants were collected and analyzed for TNFα production. Aβ(1-42) 100 μM incubated at 4°C was used as a control (circles). Courtesy Maria Udan, Universit of Missouri, St-Louis.

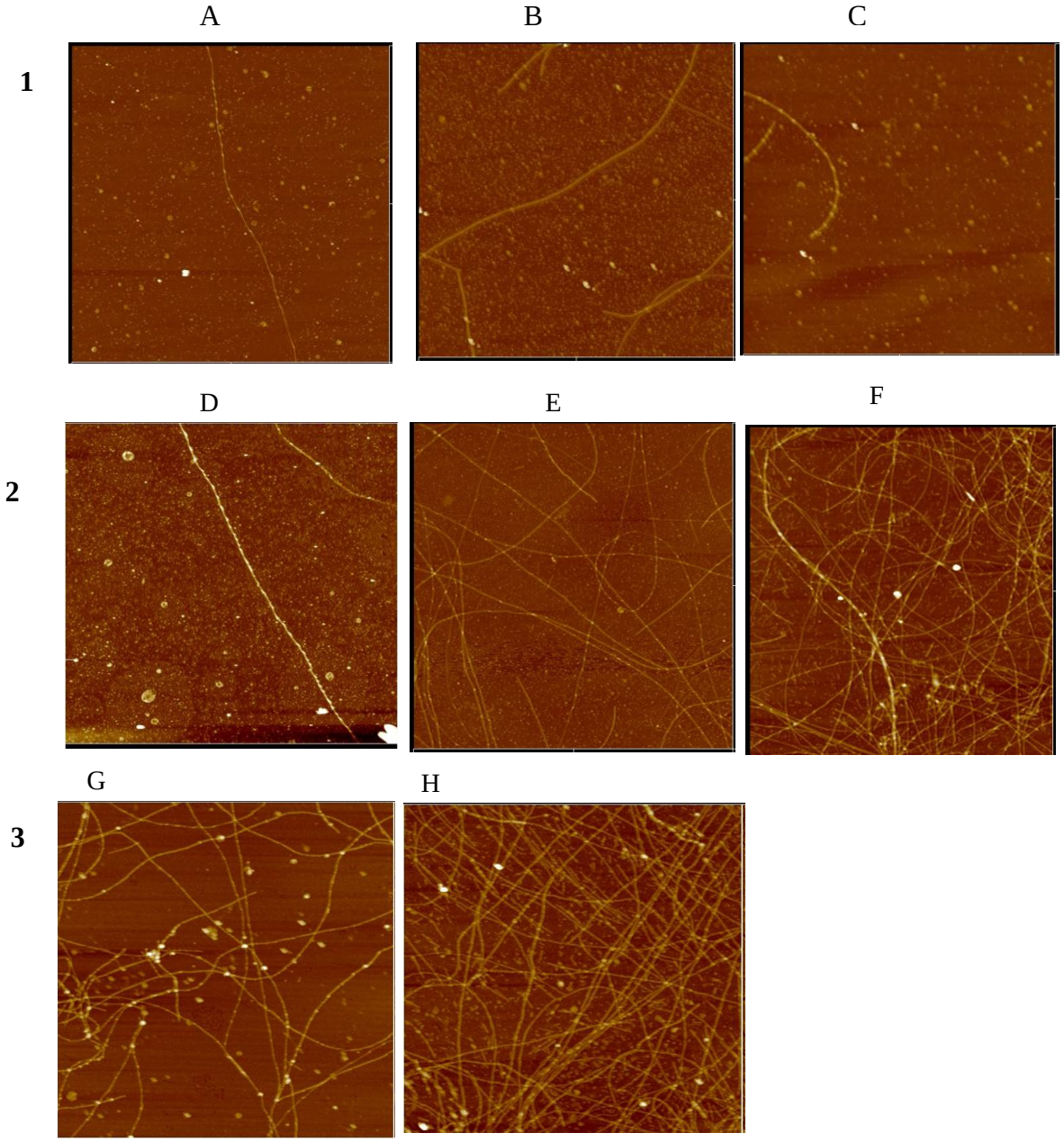

Figure 3.10. Increased temperature induces formation of diverse fibrils, but fails to stimulate inflammatory response. Aβ(1-40) (100 μM) was diluted to 1 μM and applied on the surface of freshly cleaved mica as described in Methods. The images shown above are representative AFM images of Aβ (1-40) samples. **Panel 1 (A-C)** are images after 48 hours at 4^{o}C (A), 25^{o}C (B) and 37^{o}C (C). **Panel 2 (D-E)** are images after 96 hours at 4^{o}C (D), 25^{o}C (E) and 37^{o}C (F) and **Panel 3 (G-H)** images after 216 hours at 4^{o}C (G), 25^{o}C (H) AFM images panels are 5 μm x 5μm.

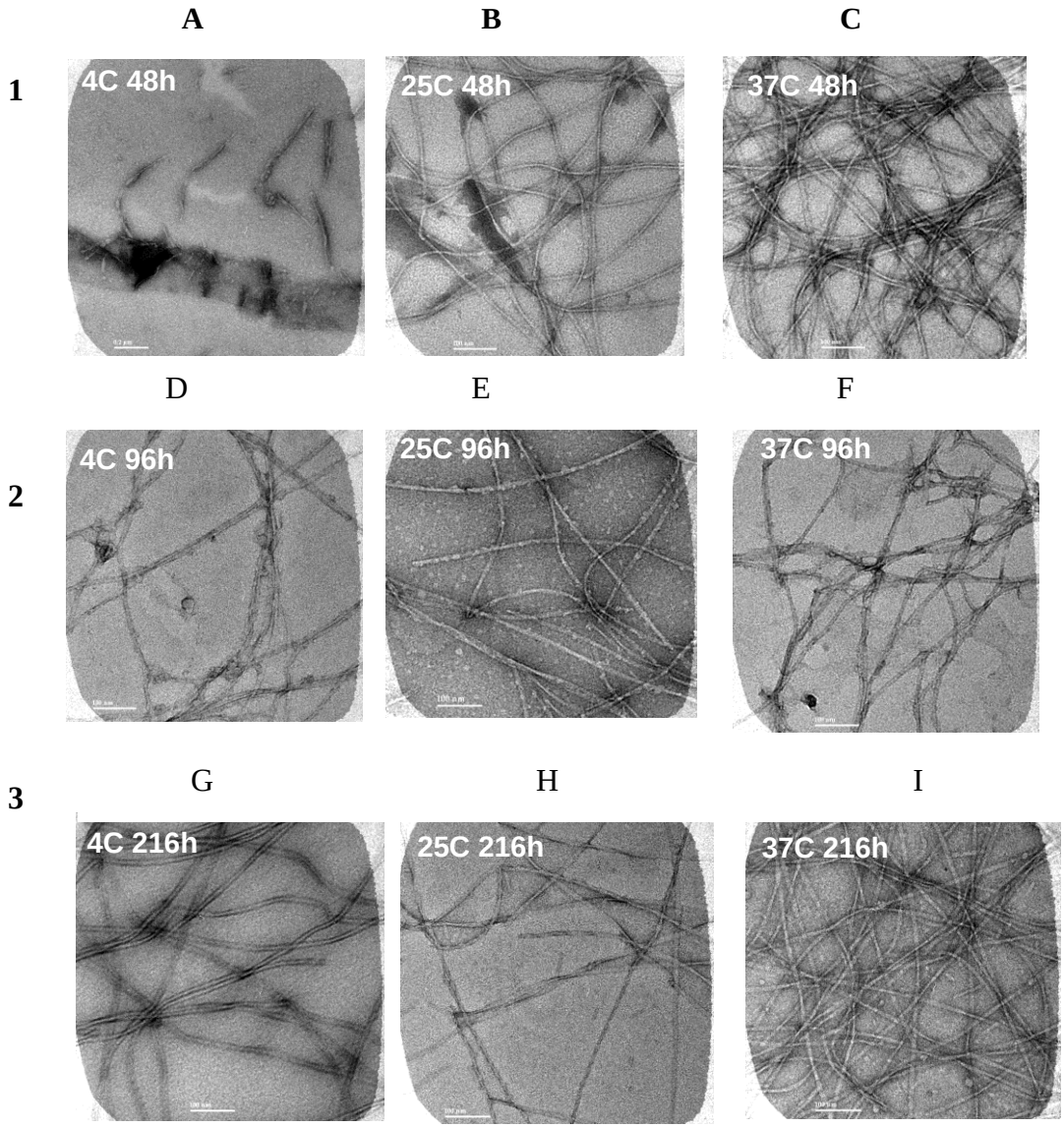

Figure 3.11. Aβ(1-40) forms diverse fibrils upon incubation at different temperatures. Representative TEM images of Aβ(1-40)) samples from the same experiment as mentioned in Figure 3.9. Aβ(1-40) (100 µM) solutions were diluted to a concentration of 20 µM and applied to formvar coated copper grids as described in Methods. **Panel 1 (A-C)** are images after 48 hours at 4^{o}C (A), 25^{o}C (B) and 37^{o}C (C**). Panel 2 (D-E)** are images after 96 hours incubation at 4^{o}C (D), 25^{o}C (E) and 37^{o}C (F) and **Panel 3 (G-E)** images after 216 hours 4^{o}C (G), 25^{o}C (H) and 37^{o}C (I). The scale bars represent 100 nm.

formation of different diverse fibrillar forms of Aβ(1-40), but none of these aggregation species were able to stimulate a proinflammatory response when treated with THP-1 monocytes.

3.4.4 Effect of pH, Ionic strength, and Buffer Type on Aβ(1-42) Aggregation and Proinflammatory Activity

The morphology of Aβ aggregation species alters under varying conditions of pH and ionic strength (Fraser et al., 1991, Harper et al., 1999). Previous studies indicate that fibrillization of Aβ(1-40) in 0.1M HCl was highly reproducible, and was free from fibril-fibril association (Lomakin et al., 1996). The fibrils formed were also found to be morphologically indistinguishable from those formed *in vivo* (Lomakin et al., 1996). In our experiments, pH measurements of Aβ(1-42) aqueous solutions in water were done using a microelectrode, and measured pH was 3.6. Aggregation conditions were modulated by preparing Aβ(1-42) aggregation solution in the physiological pH 7.4. We hypothesized that Aβ(1-42) at higher ionic strength and neutral pH will form different structures that may stimulate proinflammatory activity in a different way. Aβ(1-42) was reconstituted in water (100 μM), and another preparation was made wherein Aβ(1-42) was reconstituted in 100 mM NaOH to a concentration of 2mM Aβ, followed by dilution into PBS to a final concentration of 100 μM. The measured pH of the solution in PBS was 7.4. The aggregation reactions were monitored by ThT fluorescence measurements. In all previous ThT fluorescence measurements, the aggregation of Aβ(1-42)/water solutions were monitored by ThT solution prepared in water which maintained the acidic

pH. We followed this protocol inorder to rule out any change in Aβ morphology due to change in pH. The ThT values were very low and did not correlate with the corresponding AFM images of the same sample which showed formation of fibrils (data not shown). However, we observed that the same Aβ(1-42)/water solution when mixed with ThT prepared in PBS (pH 7.4), or 50 mM Tris buffer (pH 8.0) had higher ThT fluorescence values compared to measurements made with ThT/water. We analysed ThT fluorescence of an aggregated solution of Aβ(1-42)/water (100 μM), incubated at 4°C for 96 hours with ThT solutions prepared in water, 50 mM Tris buffer (pH 8.0) and 150 mM glycine buffer (pH 8.0) (Fig 3.12). We observed that ThT prepared in glycine and Tris produced similar ThT fluorescence values that were significantly higher than ThT/water solution (Fig 3.12). For subsequent experiments with Aβ(1-42)/water, ThT measurements were made with ThT prepared in Tris (pH 8.0) (Fig 3.13 A circles). Further investigations need to be done to probe the pH dependence of ThT fluorescence measurements. The Aβ(1-42)/PBS solutions did not stimulate the THP-1 cells for TNFα production (Fig 3.13 B, triangles) compared to the aqueous Aβ(1-42) solution (Fig 3.13 B circles). The PBS samples did not adhere to the mica discs for AFM imaging, therefore,TEM was used for morphology analyses. TEM analyses of both preparations of Aβ(1-42) showed presence of fibrillar content (Fig 3.14). However, there were differences in the alignment of the fibrils. The fibrils formed in the aqueous solutions were thin and were more or less isolated (Fig 3.14 A, C), while the fibrils formed by incubation in PBS showed lateral association (Fig 3.14 B, D). Also, there was an increase in the number of fibrils in the PBS preparations. This may be the reason for the

increase in ThT fluorescence values for the Aβ(1-42) solution in PBS (Fig 3.13, triangles).

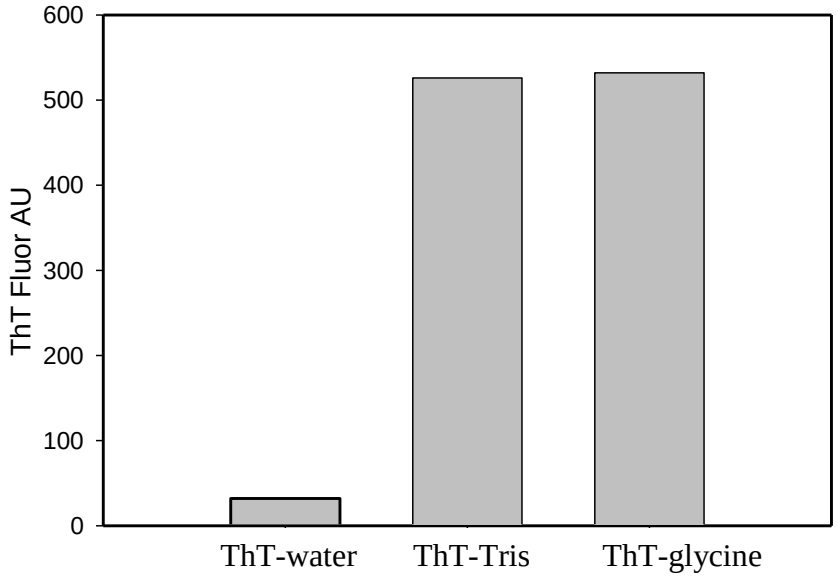

Figure 3.12 ThT fluorescence values were significantly higher at higher pH. Aβ(1-42) was resuspended in water to a concentration of 100 µM and incubated at 4°C. After 96 hours of incubation at 4°C, aliquots (7 µl) were removed from the aggregation solution and mixed with (63µl) ThT solutions that were prepared in water, 50 mM Tris buffer (pH 8.0), and 150 mM Glycine buffer (pH 8.0). ThT fluorescence measurements were recorded as mentioned in the Methods

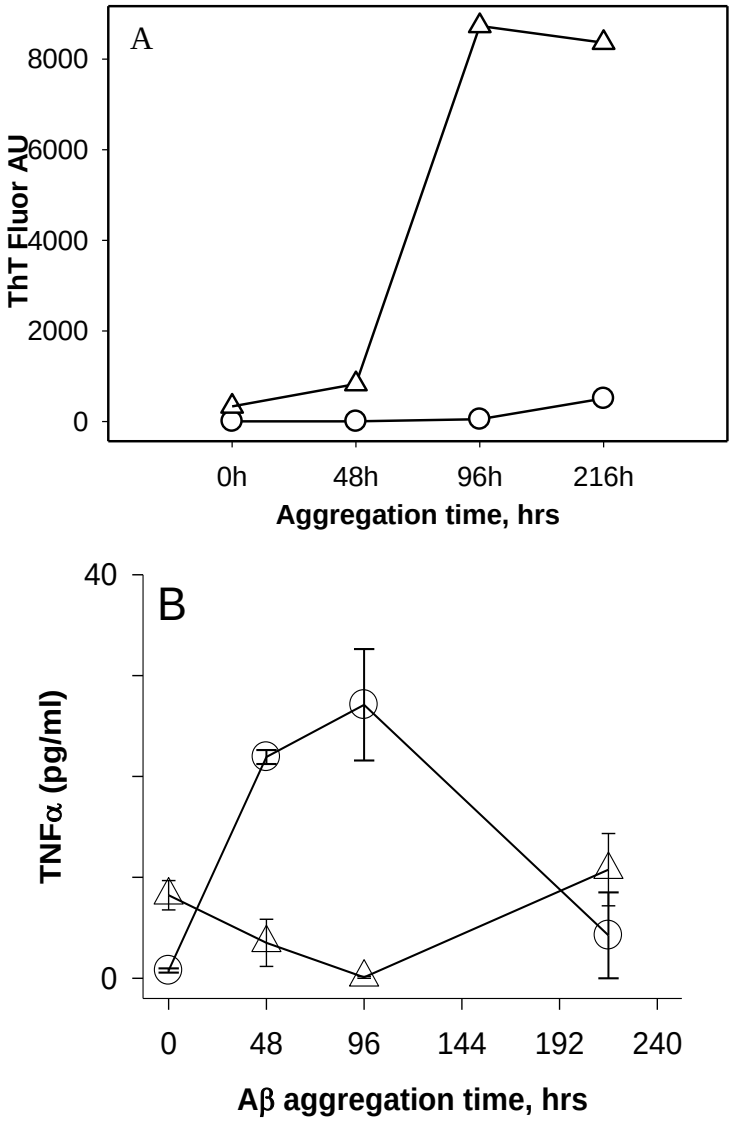

Figure 3.13. pH and ionic strength of aggregation solution influences rate of aggregation and Aβ(1-42) proinflammatory activity. Two lyophyllized Aβ(1-42) aliquots were reconstituted in either sterile water (circles) or 100 mM NaOH followed by dilution into sterile phosphate-buffered saline (PBS) (triangles) to a concentration of 100 µM and incubated at 4°C. **(Panel A)** ThT-fluorescence measurements for both Aβ(1-42)

solutions were made at specific time points as mentioned in the Methods. **(Panel B)** At the above time points, aliquots from the two aggregation solutions were treated with THP-1 cells to a final concentration of 15 μM Aβ(1-42). The secreted TNFα levels in cell supernatants were measured by ELISA.

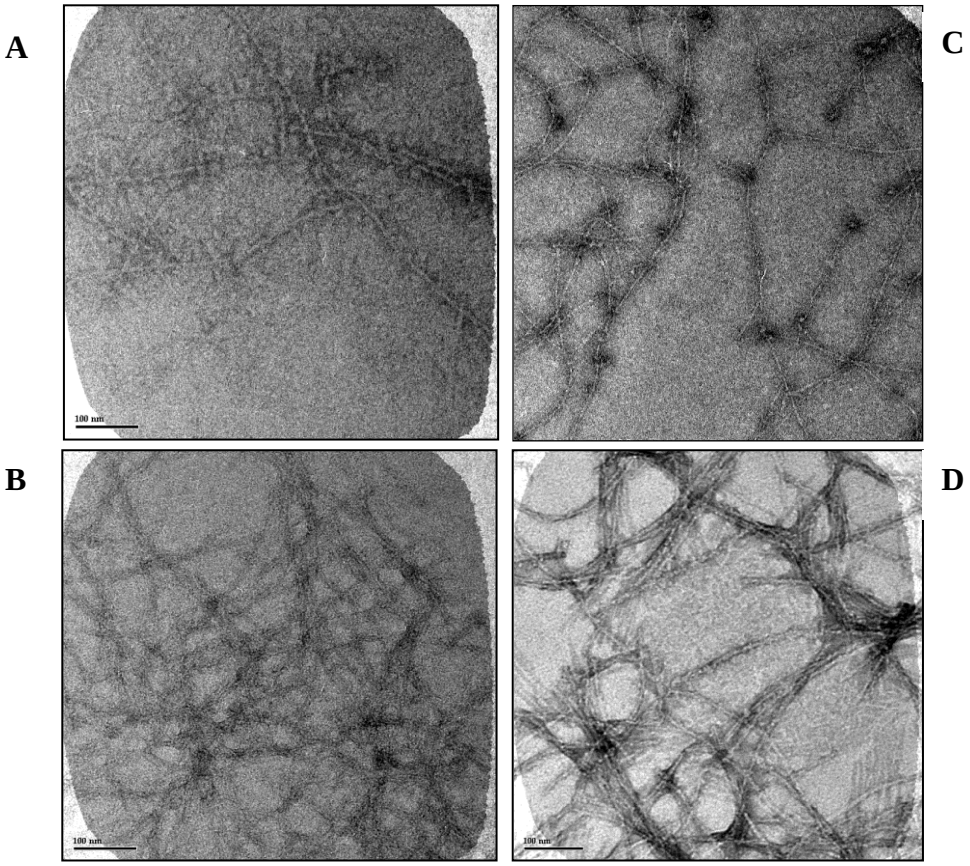

Figure 3.14. **Modulation of pH and ionic strength results in formation of fibrils that diminish proinflammatory activity**. Two Aβ(1-42) aggregation solutions were prepared in either sterile water, or, in 100 mM NaOH followed by dilution into sterile phosphate-buffered saline (PBS) at a concentration of 100 μM and incubated at 4°C. At specific time points aliquots were removed, diluted to 20 μM and applied on formvar coated grids as described in Methods. (**Panel A)** Aβ(1-42) in water after 48 hours and **(Panel C)** Aβ(1-42) 96 hours of incubation at 4°C. (**Panel B and D)** Aβ(1-42) in PBS after 48 hours and 96 hours incubation at 4°C. The scale bar represents 100 nm.

3.5 Fibrils Formed in Aqueous Solutions are Soluble and Non Toxic to THP-1 Cells

3.5.1 Test for Solubility of Proinflammatory Aggregation Species

The observations made from the aggregation modulation experiments confirm that Aβ(1-42) prepared in aqueous solutions and stored at 4°C formed a species that stimulated the THP-1 monocytes for a proinflammatory response. Our data also indicate that the proinflammatory activity diminished as the aggregation progressed (216 hours). The loss of stimulatory response was based on two assumptions. One was the reasoning that the late stage fibrils precipitated out of the solution, and hence the loss of signal. We tested the solubility of Aβ(1-42) aggregation species prepared in aqueous solutions at specified time points. Aβ(1-42) was resuspended in water and an aliquot was separated and centrifuged at 18,000 x g for 10 minutes. The resultant supernatant and the unspun (total) sample were treated with cells to test for TNFα production as described in the Methods (Fig 3.15 A). AFM images show that fibrils were present in the supernatant after centrifugation at 18,000 x g, indicating that fibrils do not precipitate out of solution even at the later time points of aggregation (Fig 3.15 B). Insoluble fibrils will precipitate when spun at 18,000 x g. Our findings confirm that fibrillar structures that stimulate the cells for proinflammatory response were soluble since the centrifugation supernatants were still able to activate the cells for a response (Fig 3.15 A).

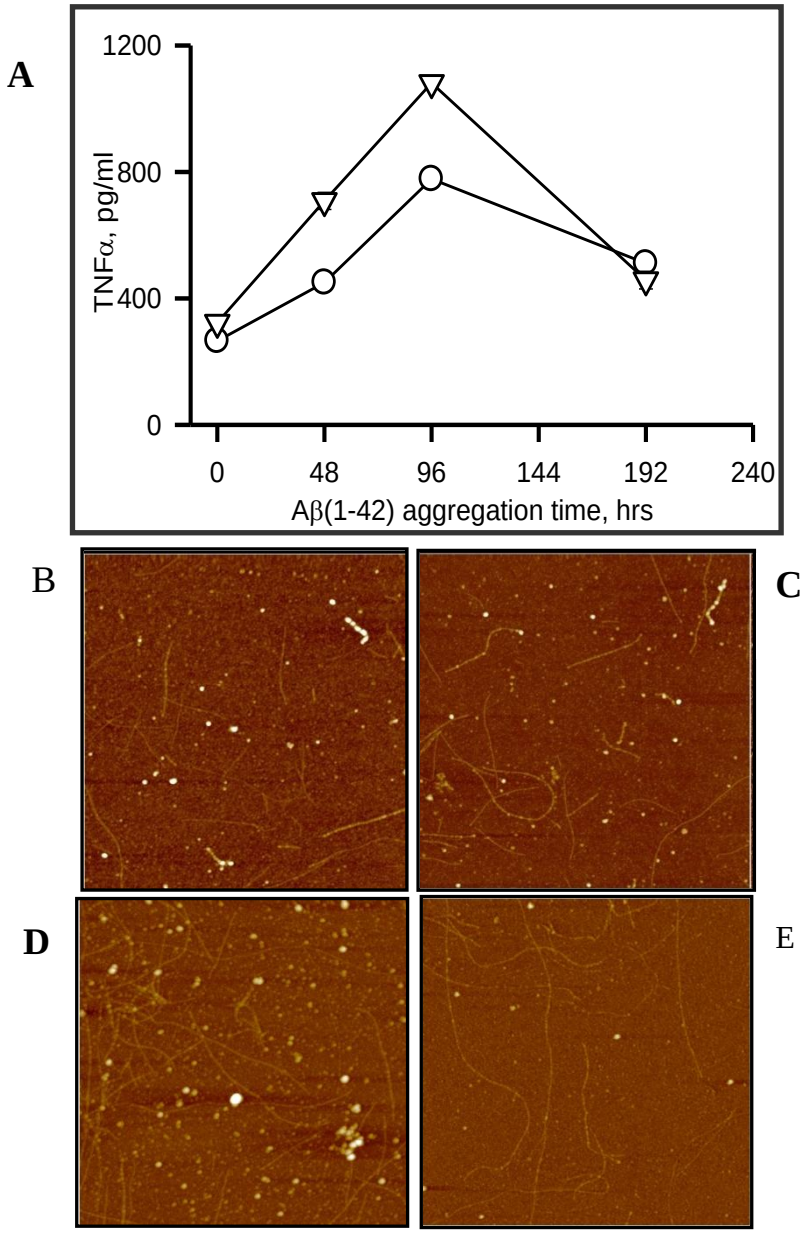

Figure 3.15. Proinflammatory response is not affected by centrifugation of aggregation solutions at 18,000 x g. (A) Aβ (1-42) solution (100 μM) were prepared in water and incubated at 4°C. At specific time points aliquots were removed, centrifuged at 18,000 x g for 10 minutes at 4°C. The spun supernatant (inverted triangles) and unspun (total) (circles) were treated with THP-1 cells for 6 hours and TNFα measured in cell supernatants Courtesy Maria Udan. At the same time points, aliquots were removed before and after centrifugation at 18,000 x g for 10 minutes, diluted to 1 μM, and imaged by AFM. Images are 5 μm x 5 μm. The AFM images above (B, C) correspond to total and spun supernatant sample after 96h, and (D, E) represent total and spun supernatant after 216 hour incubation at 4°C.

3.5.2 Test for Toxicity of Proinflammatory Aggregation Species

Toxicity of fibrils could be a reason for the loss of inflammatory response. It was assumed that the fibrils, especially the ones formed in the later stages, were toxic to the cells. We tested the toxicity of Aβ(1-42) prepared in aqueous solutions at the intermediate and the later time points using XTT assay. The data indicates that the intermediate and the late stage fibrils are not toxic to the cells since the mitochondrial mediated reduction of XTT was not affected in both the samples (data not shown).

3.6 Characterization of Aβ(1-42) Proinflammatory Species

The observations made from the above experiments indicate more clearly that when Aβ(1-42) prepared in aqueous solutions is incubated at 4°C there is a specific time period for the formation of an aggregation species that is capable of inducing a proinflammatory response. From the cumulative data it is clear that the time period for formation of the proinflammatory species ranges from 48-96 hours. The shift in the peak response is attributed to variation in the Aβ(1-42) peptide lots that were purchased from r-Peptide. These findings indicate that an intermediate Aβ(1-42) species was optimal for inducing proinflammatory response. In order to characterize these species further we separated the samples by SDS PAGE followed by immunoblotting with Ab 9 antibody. Ab 9 binds to amino acid residues 1-16 of the Aβ peptide. Aβ(1-42) prepared in aqueous solution was incubated at 4°C, and aliquots of samples were snap frozen at specific time

points and separated by SDS PAGE. The SDS PAGE resolved sample was subjected to immunoblotting. There was no clear cut separation of aggregation species (data not shown).

Previous studies have shown that Aβ(1-42) aggregates were soluble after centrifugation at 16,000 x g and 100,000 x g for 30 minutes (Stine et al., 2003). Our data clearly indicate that the fibrillar structures were soluble after centrifugation at 18,000 x g for 15 minutes. We tested the solubility of Aβ(1-42) prepared in aqueous solutions by ultracentrifugation at higher speeds. The peak proinflammatory response for the Aβ(1-42) peptide lot was at 72 hours of incubation at 4°C. Hence, Aβ(1-42) solution was reconstituted in sterile water and allowed to aggregate for 72 hours, centrifuged at high speeds ranging from 50,000 x g to 150,000 x g for an hour at 4°C. The centrifugation supernatants were treated with THP-1 monocytes and evaluated for TNFα production. The centrifugation supernatants at 50,000 (Fig 3.16 A) and 100,000 x g (Fig 3.16B) induced TNFα production in THP-1 cells and were almost similar to the unspun sample (total). There was small decrease in the signal for 150,000 x g spin supernatant. Analyses of AFM images showed that high speed ultracentrifugation at 150,000 x g was effective in removing some fibrils from the solution (Fig 13.17 D). Overall, the ultracentrifugation data further strengthened our hypothesis that intermediate fibrillar forms that elicited maximum proinflammatory response in THP-1 monocytes were soluble. The data also suggests that the fibrils may spin down if spun at speeds higher than 150,000 x g. Therefore spinning at 200-300 k for an hour could be done to confirm the above hypothesis.

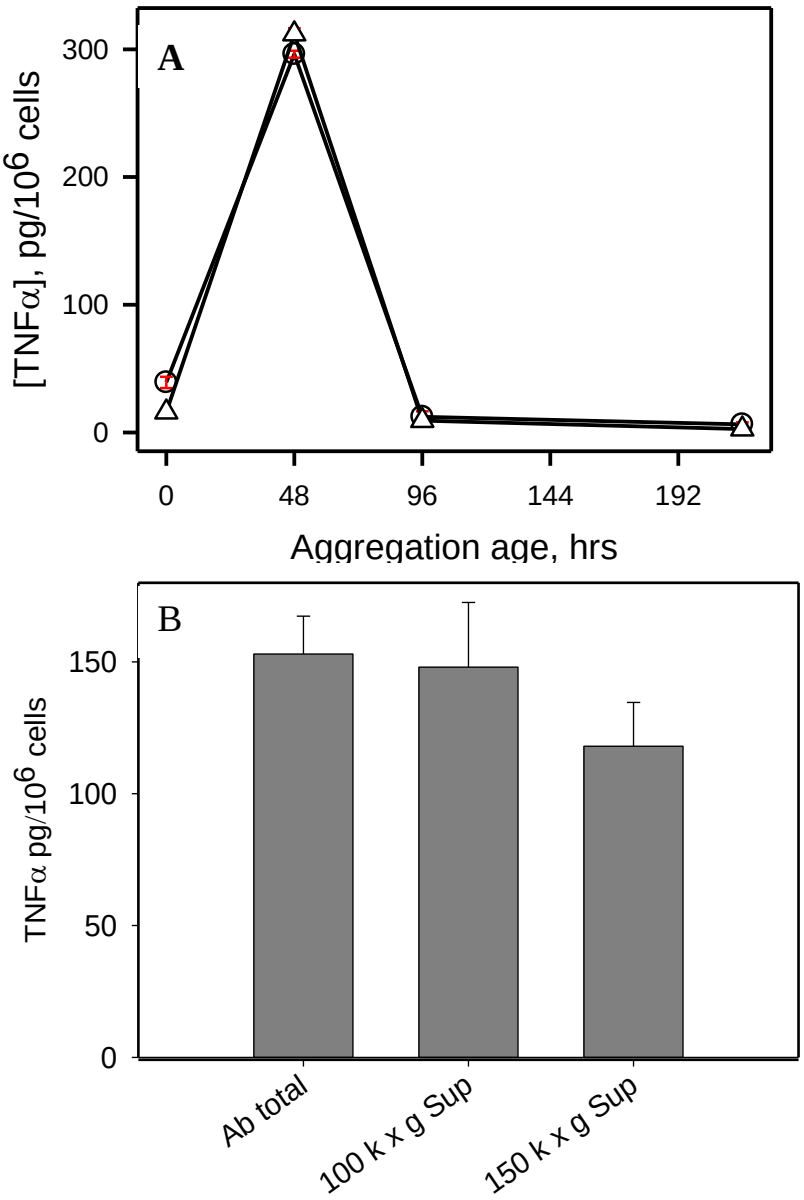

Figure 3.16 Fibrillar structures are soluble after high speed ultracentrifugation. (**A**) Aβ(1-42) was reconstituted in water (100 µM) and incubated at 4°C. At specific time points two aliquots were removed, and one was centrifuged at 50,000 x g for 1 hour at 4°C. The centrifugation supernatant and total (circles) were treated with THP-1 cells as described in Methods. (**B**) Aβ(1-42) was reconstituted in water (100 µM) and incubated at 4°C for 72 hours. Separate aliquots of the same solution were centrifuged for 1 hour at 4°C. at 10,000 x g and 150,000 x g. The pre-centrifuge sample (Total) and the supernatants were incubated with THP-1 cells for 24 hours. The secreted TNF α level was measured as described in Methods. Courtesy Maria Udan

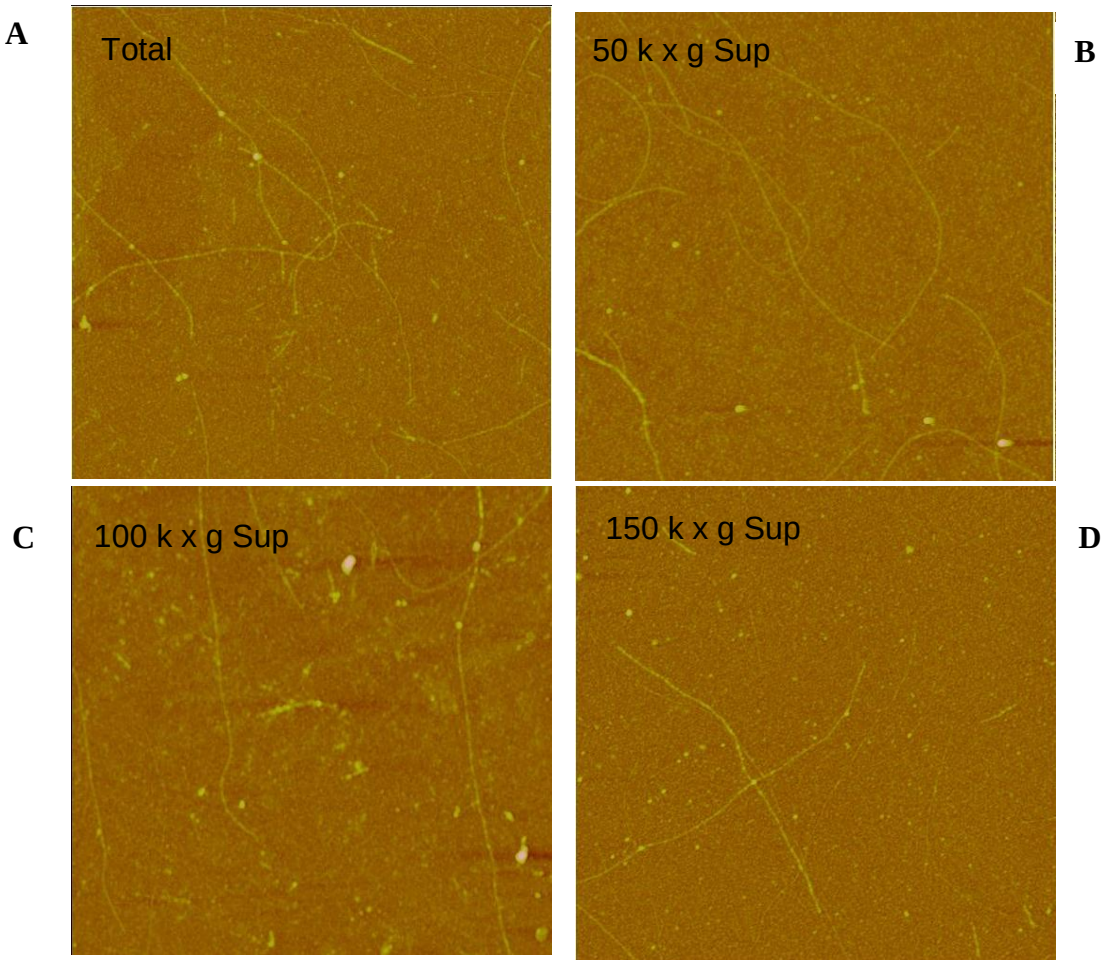

Figure 3.17 Fibrillar species are soluble even after high speed ultracentrifugation of Aβ(1-42) aggregation solutions. Aβ(1-42) was reconstituted in water (100 µM) and incubated at 4°C for 72 hours as described in Fig 3.15. Aliquots of the supernatant after centrifugation at 50,000 x g, (Panel B) 100,000 x g (Panel C), and 150,000 x g (Panel D) were diluted to 1 µM and applied onto mica grids as described in Methods. (Panel A) Aβ(1-42), (total) after 72 hours at 4°C. The AFM image panels are 5µm x 5µm.

In order to confirm that proinflammatory response was due to intermediate fibrillar forms, it was necessary to remove fibrils from the aggregation solution, and test the ability of the solution without fibrils to evoke a response when treated with THP-1 cells. Centrifugal filter devices with 0.2 µm membrane pore have been reported to filter out Aβ (1-40) protofibrils from the aggregation solution (Lashuel and Grillo-Bosch, 2005). We used centrifugal filter units with 0.2 µm PTFE membrane for our experiments. Aβ (1-42) was reconstituted in water as described in Methods to a concentration of 100 µM and allowed to incubate at 4°C for 72-96 hours. An aliquot was centrifuged at 12,000 x g for 3 minutes using 0.2 µm centrifugal filter devices. The filtrate was tested for the ability to stimulate proinflammatory response and compared to the prefiltering sample (Fig 3.18 A). AFM images indicated that the filtrate was devoid of fibrils, but at the same time there were some globular species present (Fig 3.18 C). The unfiltered sample had both fibrillar and globular species. Bradford assay was done to determine the protein concentration in the pre and post filter samples. The data showed about 35 % of Aβ remaining in the filtrate compared to the prefiltered sample. In a separate experiment using the 0.2 µm filter, we collected the filtrate and the retentate. The retentate was recovered from the filter cup and imaged by AFM. The images showed the presence of both fibrillar and globular species (data not shown). Treatment of THP-1 cells with the filtrate resulted in complete wipe out of proinflammatory response compared to unfiltered Aβ (1-42) solution. ThT fluorescence of the filtrate was significantly reduced (75 A.U) in comparison to the unfiltered sample (870 A.U). Results from this experiment suggest that the filter device is capable of removing fibrils from the aggregation solution and at the same time the filtrate does have some nonfibrilar Aβ. The data also confirms that

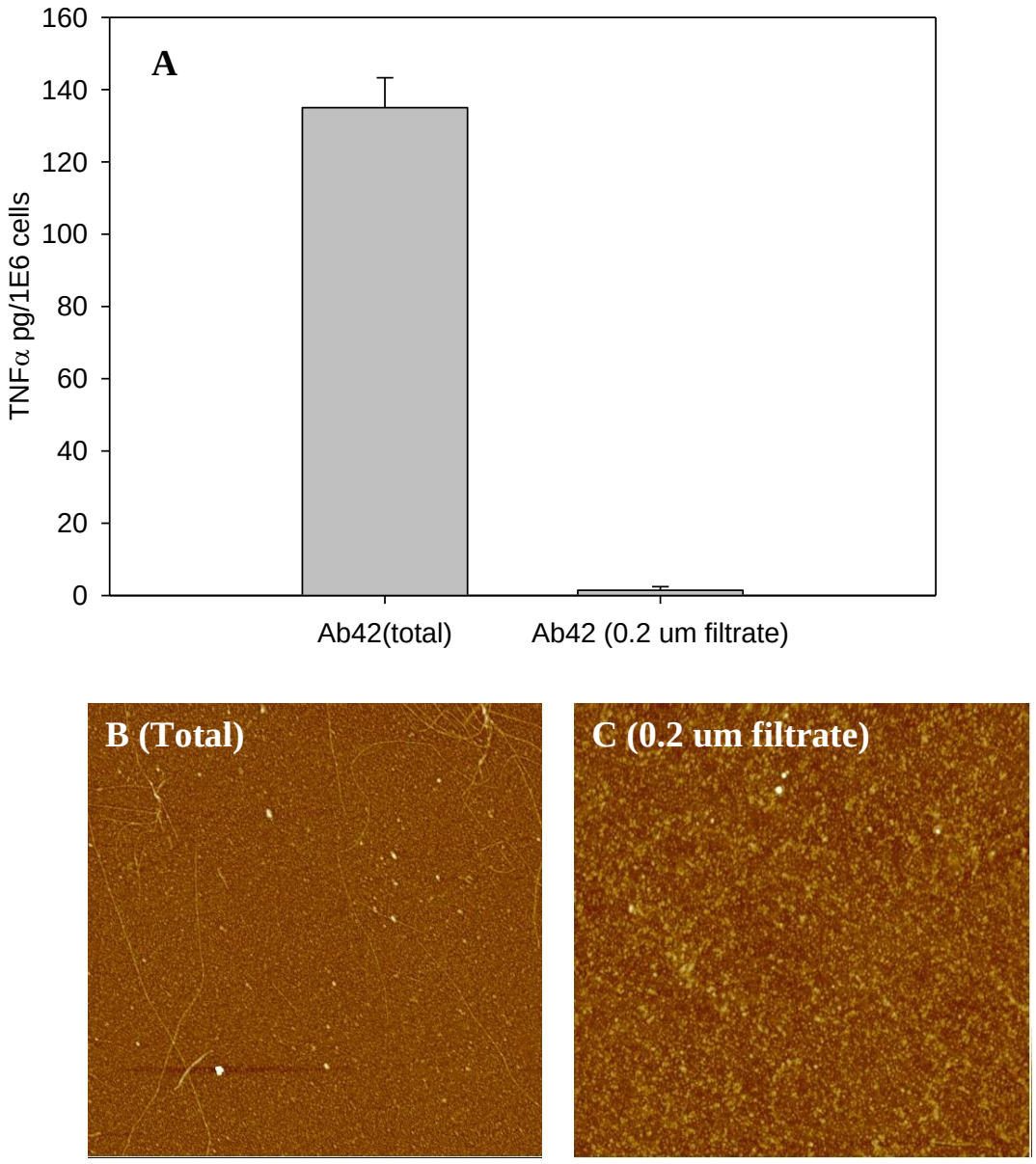

Figure 3.18 Aβ(1-42) was reconstituted in water (100 µM) and incubated at 4°C for 72 or 96 hours as described in methods. An aliquot was removed from the aggregation solution and centrifuged using 0.2 µm PTFE membrane filters at 12,000 x g for 3 minutes. **(Panel A)**. The unspun sample (Total) and the centrifugation filtrate were treated with THP-1 cells at a final concentration of 15 µM as described in Methods. The cell supernatants were tested for TNFα levels by ELISA. The same samples were diluted and applied on to mica grids at a final concentration of 1 µM for AFM imaging.**C-D**. AFM images of Total (C), and 0.2 µm centrifugation filtrate (D). The images are 5 µm x 5 µm panels.

early fibrillar forms are required for inducing a proinflammaotry response and these fibrillar species were soluble even after ultracentrifugation at high speed.

3.7 Proinflammatory Aβ(1-42) Aggregation Species can be Recognized by Antibodies Specific for Fibrillar Conformation

At present not much is known about the high resolution oligomeric structural studies. Conformation-dependent antibodies and antisera that specifically recognize amyloid fibrils (O'Nuallain and Wetzel, 2002, Kayed et al., 2007, Moretto et al., 2007) or prefibrillar oligomers (Kayed et al., 2003) have been reported. These antibodies have the unusual property of recognizing generic epitopes that are associated with specific aggregation states regardless of their amino acid sequence (Glabe, 2008). Fibrils have been defined as insoluble material that sediments at 100,000 x g. and data indicate existence of small soluble oligomers that can react with fibril-specific antibodies (Kayed et al., 2007). These studies discuss the possibility of presence of oligomers with structural organization as that of insoluble fibrils (Glabe, 2008). These oligomers are termed fibrillar oligomers (Kayed et al., 2007). Since fibril assembly is known to be nucleation dependent process, it is possible that small "seed" aggregates exist in which the peptide is organized in the same lattice structure as that of fibrils (Glabe, 2008). (Kayed et al., 2007) used fibrillar specific antibody (OC) to distinguish between fibrillar and the other oligomeric species. We used OC immune serum to investigate if the aggregation species capable of inducing maximum proinflammatory response belong to fibrillar oligomer category. Aβ(1-42) solution was allowed to age for 72 hours at 4°C following which they were subjected to immunodepletion of OC positive material as

described in Methods. The immunodepleted supernatant (OC sup) was simultaneously reprobed with OC immune serum and also with Ab 9 antibody, using dot blot assay. Ab 9 is a sequence specific antibody and is not dependent on the conformation. Dot blot showed significant Aβ remaining in the supernatant probed by Ab 9. There was very little reaction to OC immune serum (Fig 3.19 C & D). AFM image analyses showed a significant decrease in the fibrillar and diffuse material (Fig 3.19 B) compared to total (Fig 3.19A). We wanted to probe the OC sensitivity of Aβ(1-42) aggregation species throughout the time course of our experiment. Aβ(1-42) solution in water was prepared as described in Methods, and an aliquot was removed immediately upon reconstitution and snap frozen. The remaining solution was incubated at 4°C. At specific time points aliquots were removed and probed for OC sensitivity. The samples were also probed with Ab 9 antibody as control since it is sequence specific (Fig 3.19 E). Once we confirmed the presence of OC sensitive species in our Aβ(1-42) aggregation solutions, we performed immunodepletion experiment, and supernatants were treated with the cells as described in the Methods. The ability of OC supernatant to stimulate TNFα production in THP-1 cells was assessed. An aliquot of the same Aβ(1-42) solution (untreated) and Aβ(1-42) treated with rabbit IgG serum was used as control. Rabbit IgG serum was used in order to rule out any non specific binding to fibrils. Immunodepletion of OC-positive material in the Aβ(1-42) solution diminished the proinflammatory activity when compared to the untreated 18,000 x g spun sample or supernatants after IP with rabbit IgG and centrifugation at 18,000 x g (Fig 3.20 A). The same samples were probed again with OC immune serum. The dot blot showed a reduction in the OC positive material in the OC-immunodepleted material

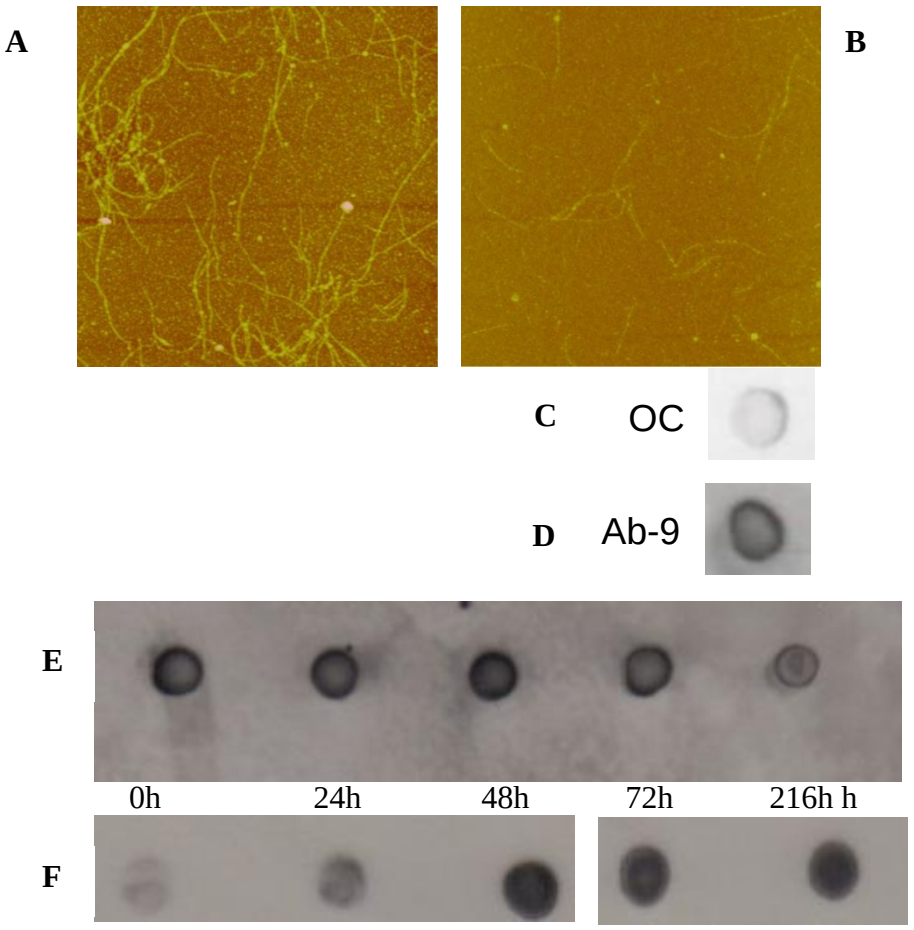

Figure 3.19. Immunoprecipitation with OC antisera depletes fibrillar oligomers and fibrils. Aβ(1-42) was reconstituted in sterile water (100 µM) and stored at 4°C for 72 hours. The solution was immunodepleted with OC antisera as described in the Methods. **(A-B)** AFM Images of the untreated (total) and the immunodepleted supernatant (OC Sup). **C-D**. OC Supernatant probed again with OC antisera (C) and Ab-9 (D) by Dot blot assay. **E-F** Aβ(1-42) was reconstituted in sterile water (100 µM) and stored at 4°C. At the above mentioned time points aliquots were removed and probed with Ab 9 and OC antisera by Dot blot.

.

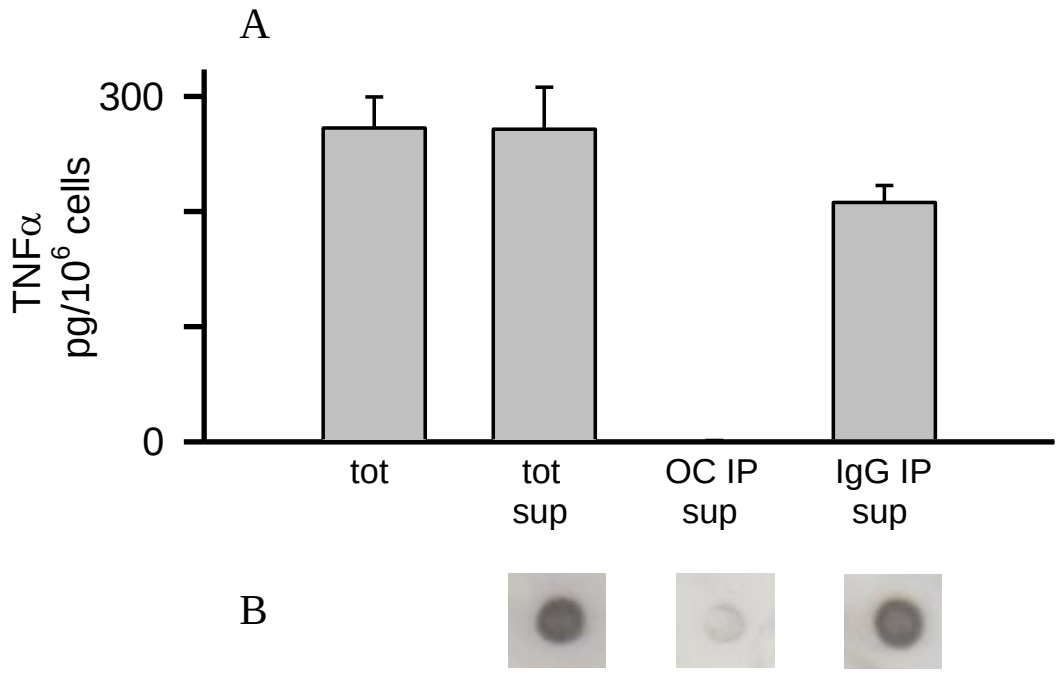

Figure 3.20. Immunoprecipitation with OC antisera reduces Aβ(1-42) induced proinflammatory response. Aβ(1-42) was reconstituted in sterile water and incubated at 4°C for 72 hours. Aliquots of Aβ(1-42) solution were treated with OC antisera or rabbit IgG as described in Methods. The immunodepleted Aβ(1-42) supernatants were reprobed with OC antisera to test for OC sensitivity by dot blot. Simultaneously aliquots were also treated with THP-1 cells and tested for TNFα secretion. (**Panel A**) Aβ(1-42) untreated solution (tot), Aβ(1-42) untreated, but centrifuged at 18,000 x g and supernatant collected (tot sup), OC immunodepletion supernatant (OC IP Sup) and rabbit IgG immunodepleted supernatant (IgG IP Sup) were incubated with THP-1 cells for 24 hours and the secreted TNFα was measured as described in Methods. (**Panel B**) Dot blot of tot sup, OC/IP Sup and IgG IP Sup probed with OC antisera.

compared to the 18,000 x g spun supernatants or the supernatants after IP treatment with the rabbit IgG (Fig 3.20 B).

3.8 Size Exclusion Chromatography(SEC) of Aβ(1-42) Aggregation Species

The AFM images from ultracentrifugation experiments showed loss of fibrillar structures in the supernatant after centrifugation at both 100,000 x g and 150,000 x g. The loss of fibrils in the supernatants was higher in the case of centrifugation at 150,000 x g. In spite of this decrease in the fibrils, the cellular activity did not show a drastic decrease in the proinflammatory signal. It has been discussed earlier that insoluble fibrils sediment when centrifuged at 100,000 x g (Stine et al., 2003). Therefore, it is possible that during high speed centrifugation the insoluble fibrils were the ones that separated out of the solution, hence, there was no significant loss of cellular activity. (Kayed et al., 2007)) reported that SEC fractions of Aβ(1-42) showed a broad distribution of oligomer sizes from 8 kDa to 200 kDa, and they were recognized by OC. In our experiments peak proinflammatory activity was around 72-96 hours of Aβ(1-42) incubation at 4°C. For further characterization, Aβ(1-42) solution was reconstituted in sterile water and allowed to incubate for 96 hours at 4°C. After 96 hours, the solution was centrifuged at 18,000 x g for 10 minutes and supernatant was loaded on to Superdex 75 column for separation of aggregation species as described in Methods. The elution profile showed four peaks by UV absorbance one of them being the void volume peak, an included volume that comprised of peaks 2 and 3 and the monomer peak (Fig 3.21 A). The peak fractions (11,

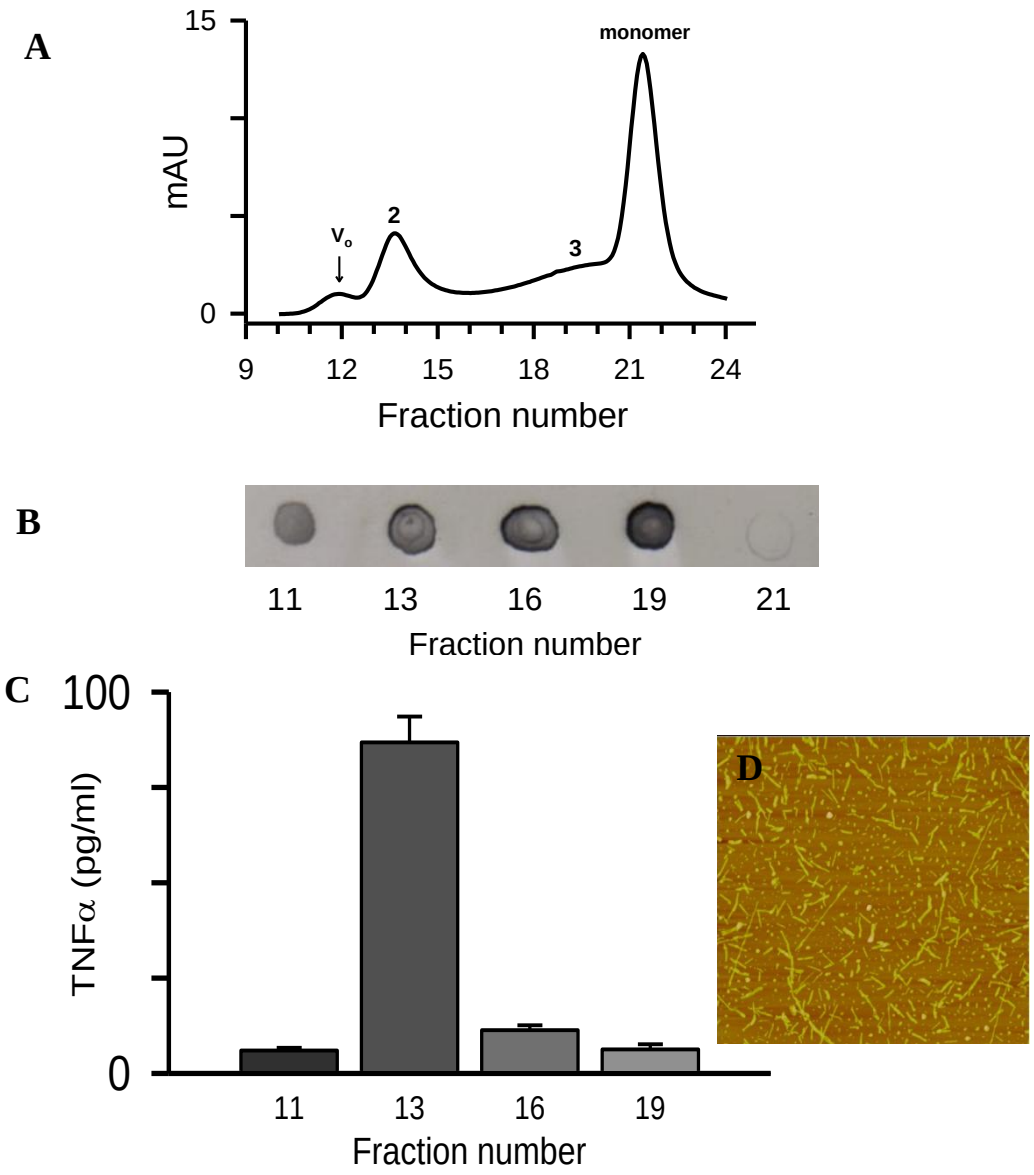

Figure 3.21 Characterization of aggregated Aβ(1-42) by SEC. Aβ(1-42) reconstituted in sterile water was allowed to incubate at 4°C for 96 hours. The solution was centrifuged at 18,000 x g for 10 minutes and the supernatant was loaded on to Superdex 75 column. (**Panel A**) 280 nm absorbance elution profiles show four peaks indicated by arrows, (1) (Vo) Void Volume, and the peaks labeled 2, 3, and monomer are the peaks for the included volumes. The absorbance maximum for the peaks are 1.4 µM for the void, and 5.7 µM, 3.7 µM , 18.3 µM, for the included volume. **(Panel B**) Select peak fractions were probed for OC sensitivity by Dot Blot. Fractions were used for dot blot without dilution. (**Panel C)** The OC positive fractions were treated with THP-1 monocytes for 6 hours, and TNFα was measured as described in Methods. **(Panel D)** AFM image analysis of the peak fraction that gave maximum proinflammatory response. The image panels are 3 µm x 3 µm.

13, 16, 19 and 21) were assessed for OC reactivity by dot-blot analysis (3.21 B). All of the selected fractions, with the exception of the monomer, showed OC-positive material. Selected peak fractions were treated with THP-1 monocytes to test their ability to induce proiflammatory response. The included peak 2 (Frac 13) showed the highest levels of TNFα secretion (Fig 3.21 C). The peak fraction that gave maximum proinflammatory signal was analysed by AFM. Images showed the presence of large number of short fibrillar structures which were in the range of 100-200 nm in length, and average height (diameter) of 5.4 nm +/- 1.6 SD for n= 116 measurements.

3.9 Discussion

AD accounts for about two-thirds of the cases of progressive dementia in elderly people (Golde, 2002). The exact sequence of events that lead to AD is still debated. However, there is lot of evidence that supports the hypothesis that accumulation of Aβ in the brain triggers a complex pathological cascade leading to neuronal damage and ultimately dementia (Selkoe, 2001). One of the events within this pathological cascade is an inflammatory response. A key finding that signals the presence of neuroinflammation is the accumulation of reactive microglia in the degenerating areas of the brain (McGeer and McGeer, 2004, McGeer et al., 2005). Clumps of activated microglia appear on the senile plaques found in AD brains and also in the surrounding tissue (McGeer and McGeer, 2004). However, very few, if any, were found in similar regions of control brains. AD-relevant inflammation has been investigated by studying the interactions of human brain microglia with synthetic or brain derived Aβ peptides. These studies were

based on the pathological observations that activated microglia in the AD-affected brains are associated with aggregated, thioflavin S-reactive, Aβ plaques (Walker and Lue, 2005). These studies indicate that microglia upon interaction with fibrillar amyloid plaques become activated. Fibrillar Aβ aggregates cause a limitation in the phagocytosis that leads to cell activation in a proinflammatory manner (Walker and Lue, 2005). Studies also indicate the involvement of cytokines (Dickson et al., 1993) in signaling for activation. Dystrophic neurites, activated microglia and proinflammatory cytokines are the inflammatory markers that are found surrounding the Aβ lesions in the human brain. An array of different aggregate morphologies ranging from dense core neuritic plaques to granular diffuse wispy Aβ deposits are observed in the human brain. However, only the plaques seem to provoke the inflammatory response (Selkoe, 2004), and microglia were observed surrounding only the dense core plaques and not diffuse plaques.

In this study we used THP-1 monocytes to investigate the Aβ-induced proinflammatory response. These cells have been used extensively in such studies since they display a similar pattern of activation to that of microglial cells (Klegeris et al., 1997, Yates et al., 2000, Combs et al., 2001). Aβ solution was allowed to aggregate over a time period and monitored for the ability to induce a proinflammatory response from THP-1 monocytes. Earlier studies have used Aβ(1-40) preparations in acidic pH to monitor the fibrillization of Aβ and also to quantitate the nucleation and elongation rate constants (Lomakin et al., 1996). The fibrils formed were morphologically identical to the ones formed *in vivo* (Lomakin et al., 1996). We observed that an intermediate Aβ(1-42) species formed in aqueous solutions (pH 3.6-4) was optimal in inducing a

proinflammatory response. The peak activity correlated with the formation of short fibrillar structures that appeared early on in the time course. There was slight shift in the peak cellular response due to the variation in the Aβ lots but nevertheless the peak was in the intermediate time points (48-96 hours) during the course of aggregation (Fig 3.1). The proinflammatory activity diminished with the appearance of fibril structures (216 hour). Modulation of aggregation of Aβ(1-42) and Aβ(1-40), by increasing the temperature of the reaction conditions, resulted in the formation of different types of aggregates (Fig 3.9-11), but they did not provoke a proinflammatory response. Aβ(1-42) fibrils formed at neutral pH in PBS were also not effective in inducing a proinflammatory response (Fig 3.13). In fact, the aggregation at neutral pH, and increased ionic strength promotes aggregation as shown in the TEM images and ThT fluorescence data (Fig 3.13-3.14). The data indicates that acceleration in the aggregation process may have by-passed the formation of the transient fibrillar structures that induces the maximum proinflammatory response. The OC-immunodepletion studies suggest that the active Aβ(1-42) aggregation species is reminiscent of fibrillar oligomers previously reported (Kayed et al., 2007). There is evidence for the formation of Aβ in acidic conditions. The build up of intracellular Aβ may be an early event in the pathogenesis of AD and Downs Syndrome (LaFerla et al., 2007). Accumulation of intracellular Aβ precedes formation of extracellular deposits (Mori et al., 2002). AD and Downs syndrome brains were analyzed along with the control brains and the data indicates that most of the intracellular Aβ ends at residue 42 (Takahashi et al., 2002). Further, it is suggested that endosomes are the likely sites of Aβ generation due to their acidic nature, and the enzymes BACE-1 and β-secretase have optimal activity at the acidic pH. There is also evidence showing the

interaction of BACE-1 and APP by FRET (Kinoshita et al., 2003). The link between extracellular and intracellular Aβ is still under investigation. However, immunotherapy studies show that removal of extracellular plaques are slowly followed by the removal of intracellular plaques (Oddo et al., 2004). These findings suggest that extracellular Aβ may be formed from the intraneuronal pools and there exists a dynamic equilibrium between the pools, such that when the extracellular pools are removed the intraneuronal pools are forced out of the cell. At present not much is known about the morphology of the intraneuronal Aβ. We have seen that Aβ(1-42) in aqueous solution (pH 3.6-4) form short fibrillar structures that are capable of inducing proinflammatory response (Fig 3.2). It is possible that these fibrillar precursors may form intraneuronally and when secreted lead to the activation of the microglial cells that in turn induces the proinflammatory response. Freshly reconstituted Aβ solutions have punctuate species <2 nm, and DLS measurements of freshly reconstituted Aβ showed a predominant peak of 1nm species that corresponds to monomer. AFM image analyses have shown that the proinflamamtory species have a mean height and standard deviation (SD) of 4.2 +/- 1.4 nm respectively. AFM imaging of Aβ aggregation species over time was helpful in providing information regarding the dimensions and morphology of the aggregated Aβ.

Modulation of aggregation conditions like change in pH, temperature and mode of aggregation (quiescent/agitation) have indicated a change in the fibril structure and neuronal toxicity. Solid state structural studies indicate the presence of in register-parallel β-sheets for full length Aβ(1-40), Aβ(1-42) and shorter fragment Aβ-(10-35) (Benzinger et al., 2000, Tycko, 2003). Our studies show that changing the pH and ionic

strength of aggregation solutions altered the fibril morphology and diminished the proinflammatory response (Fig 3.13). Aβ(1-40) and the shorter peptide Aβ-25-35 failed to stimulate the THP-1 monocytes for a proinflammatory response under similar aggregation conditions. This may perhaps be due to the slow nucleation propensity of Aβ(1-40) thereby resulting in the formation of a very low concentration of fibrillar oligomers. Aβ-25-35 is supposed to aggregate fast and the biological activity can be compared to that of Aβ(1-42), but in our studies this shorter peptide failed to stimulate the proinflammatory response. It is possible that the last two amino acids in Aβ(1-42) are very important for the formation of the active proinflammatory species.

The intermediate fibrillar species in Aβ(1-42) aqueous solution was the most active in inducing a proinflammatory response. We tried to further characterize the aggregation species by separating out fibrils from solution by ultracentrifugation (100,000 x g and 150,000 x g). Our results indicate that fibrillar structures are soluble and centrifugation supernatants are able to stimulate the cells for TNFα production (Fig 3.16-17). AFM image analysis showed a decrease in fibrils in the supernatant. But this decrease did not cause a drastic change in the proinflammatory signal. In order to characterize the aggregation species further, we used conformation-specific antibodies. These conformation-specific antibodies have the ability to distinguish between fibrillar and oligomeric species (Kayed et al., 2007). OC antisera can bind fibrillar species and precursors to fibrils that have already formed a fibrillar core structure. In fact, (Kayed et al., 2007) reported the existence of prefibrillar oligomers that were found to be different from fibrillar oligomers. Since the OC sera can detect any fibrillar species, we chose the

time point of aggregation that gave the maximum proinflamamtory activity to conduct immunodepletion studies. The data indicate that the selective removal of fibrillar oligomers from the aggregation solution resulted in lowering the proinflammatory signal (Fig 3.20). AFM imaging of the SEC fraction that eilicited the maximum proinflammatory response showed the presence of short rod like fibrillar structures (Fig 3.21D). These findings substantiate our hypothesis that small units of the intermediate fibrillar precursors are optimal for inducing proinflammatory response. The small units are crucial since we have observed that continued aggregation, and accelerated aggregation resulted in fibrils that failed to stimulate the cells. These active proinflammatory species seem to be transient and appear simultaneously with the fibrils. From the time course of aggregation it is evident that these transient small units disappear to form bigger units mostly due to elongation. The intermediate species bound well to OC sera indicating presence of fibrillar species. These fibrillar oligomers may be similar to "seed" aggregates in which the peptide is organized in the same lattice structure as that of the fibrils (Glabe, 2008). Further investigations will help decipher if these fibrillar oligomers are precursors to protofibrils.

Soluble Aβ(1-42) oligomeric species have been implicated as primary toxic species in many neurodegenerative diseases. In fact, large fibrillar plaques provide much less Aβ surface area to neuronal membranes compared to a number of small oligomers. It is possible that a group of small oligomers can diffuse into synaptic clefts and these assemblies are better candidates for inducing synaptic dysfunction (Haass and Selkoe, 2007). Amongst the several unresolved questions, one question raised is the possible role of soluble oligomers in triggering a proinflammatory cascade. It is possible that these

species could activate the local microglia and astrocytes either directly or indirectly that could lead to synaptic dysfunction (Haass and Selkoe, 2007). Our findings indicate that the soluble prefibrillar oligomeric species formed during the intermediate stage of the aggregation pathway are optimal for inducing a proinflammatory response. This could be the partial answer to the question raised above, although a thorough characterization of the proinflammatory aggregation species will answer the question completely. The plaque core contains fibrillar Aβ, and there are reports that indicate plaques to be a reservoir of bioactive molecules (Meyer-Luehmann et al., 2008). These studies also discuss about the presence of soluble oligomeric Aβ around the plaques. These oligomeric Aβ contribute to synapse loss in a mouse model of AD (Koffie et al., 2009). Their studies indicate presence of polymorphic Aβ species not only in the brain parenchyma, but also within the plaque area. According to our findings, the soluble pre-fibrillar Aβ(1-42) species are optimal for triggering a proinflammatory response in human THP-1 monocytes. These studies provide additional information into the complexities of Aβ aggregation morphology and may help in deciphering treatment strategies. Identification of the favorable conformation of Aβ(1-42) that triggers a proinflammatory response opens up avenues to further probe into the interaction of Aβ with cell surface receptors.

3.10 Bibliography

Benzinger, T. L., Gregory, D. M., Burkoth, T. S., Miller-Auer, H., Lynn, D. G., Botto, R. E. and Meredith, S. C., 2000. Two-dimensional structure of beta-amyloid(10-35) fibrils. Biochemistry. 39, 3491-3499.

Bitan, G., Kirkitadze, M. D., Lomakin, A., Vollers, S. S., Benedek, G. B. and Teplow, D. B., 2003. Amyloid beta -protein (Abeta) assembly: Abeta 40 and Abeta 42 oligomerize through distinct pathways. Proc Natl Acad Sci U S A. 100, 330-335.

Clementi, M. E., Marini, S., Coletta, M., Orsini, F., Giardina, B. and Misiti, F., 2005. Abeta(31-35) and Abeta(25-35) fragments of amyloid beta-protein induce cellular death through apoptotic signals: Role of the redox state of methionine-35. FEBS Lett. 579, 2913-2918.

Combs, C. K., Karlo, J. C., Kao, S. C. and Landreth, G. E., 2001. beta-Amyloid stimulation of microglia and monocytes results in TNFalpha-dependent expression of inducible nitric oxide synthase and neuronal apoptosis. J Neurosci. 21, 1179-1188.

D'Ursi, A. M., Armenante, M. R., Guerrini, R., Salvadori, S., Sorrentino, G. and Picone, D., 2004. Solution structure of amyloid beta-peptide (25-35) in different media. J Med Chem. 47, 4231-4238.

Dickson, D. W., Lee, S. C., Mattiace, L. A., Yen, S. H. and Brosnan, C., 1993. Microglia and cytokines in neurological disease, with special reference to AIDS and Alzheimer's disease. Glia. 7, 75-83.

Fraser, P. E., Nguyen, J. T., Surewicz, W. K. and Kirschner, D. A., 1991. pH-dependent structural transitions of Alzheimer amyloid peptides. Biophys J. 60, 1190-1201.

Glabe, C. G., 2008. Structural classification of toxic amyloid oligomers. J Biol Chem. 283, 29639-29643.

Golde, T. E., 2002. Inflammation takes on Alzheimer disease. Nat Med. 8, 936-938.

Grammas, P. and Ovase, R., 2001. Inflammatory factors are elevated in brain microvessels in Alzheimer's disease. Neurobiol Aging. 22, 837-842.

Haass, C. and Selkoe, D. J., 2007. Soluble protein oligomers in neurodegeneration: lessons from the Alzheimer's amyloid beta-peptide. Nat Rev Mol Cell Biol. 8, 101-112.

Harper, J. D., Lieber, C. M. and Lansbury, P. T., Jr., 1997a. Atomic force microscopic imaging of seeded fibril formation and fibril branching by the Alzheimer's disease amyloid-beta protein. Chem Biol. 4, 951-959.

Harper, J. D., Wong, S. S., Lieber, C. M. and Lansbury, P. T., 1997b. Observation of metastable Abeta amyloid protofibrils by atomic force microscopy. Chem Biol. 4, 119-125.

Harper, J. D., Wong, S. S., Lieber, C. M. and Lansbury, P. T., Jr., 1999. Assembly of A beta amyloid protofibrils: an in vitro model for a possible early event in Alzheimer's disease. Biochemistry. 38, 8972-8980.

Hartley, D. M., Walsh, D. M., Ye, C. P., Diehl, T., Vasquez, S., Vassilev, P. M., Teplow, D. B. and Selkoe, D. J., 1999. Protofibrillar intermediates of amyloid beta-protein induce acute electrophysiological changes and progressive neurotoxicity in cortical neurons. J Neurosci. 19, 8876-8884.

Heneka, M. T., Feinstein, D. L., Galea, E., Gleichmann, M., Wullner, U. and Klockgether, T., 1999. Peroxisome proliferator-activated receptor gamma agonists protect cerebellar granule cells from cytokine-induced apoptotic cell death by inhibition of inducible nitric oxide synthase. J Neuroimmunol. 100, 156-168.

Iwatsubo, T., Odaka, A., Suzuki, N., Mizusawa, H., Nukina, N. and Ihara, Y., 1994. Visualization of A beta 42(43) and A beta 40 in senile plaques with end-specific A beta monoclonals: evidence that an initially deposited species is A beta 42(43). Neuron. 13, 45-53.

Jarrett, J. T., Berger, E. P. and Lansbury, P. T., Jr., 1993a. The C-terminus of the beta protein is critical in amyloidogenesis. Ann N Y Acad Sci. 695, 144-148.

Jarrett, J. T., Berger, E. P. and Lansbury, P. T., Jr., 1993b. The carboxy terminus of the beta amyloid protein is critical for the seeding of amyloid formation: implications for the pathogenesis of Alzheimer's disease. Biochemistry. 32, 4693-4697.

Kayed, R., Head, E., Sarsoza, F., Saing, T., Cotman, C. W., Necula, M., Margol, L., Wu, J., Breydo, L., Thompson, J. L., Rasool, S., Gurlo, T., Butler, P. and Glabe, C. G., 2007. Fibril specific, conformation dependent antibodies recognize a generic epitope common to amyloid fibrils and fibrillar oligomers that is absent in prefibrillar oligomers. Mol Neurodegener. 2, 18.

Kayed, R., Head, E., Thompson, J. L., McIntire, T. M., Milton, S. C., Cotman, C. W. and Glabe, C. G., 2003. Common structure of soluble amyloid oligomers implies common mechanism of pathogenesis. Science. 300, 486-489.

Kinoshita, A., Fukumoto, H., Shah, T., Whelan, C. M., Irizarry, M. C. and Hyman, B. T., 2003. Demonstration by FRET of BACE interaction with the amyloid precursor protein at the cell surface and in early endosomes. J Cell Sci. 116, 3339-3346.

Klegeris, A., Walker, D. G. and McGeer, P. L., 1997. Interaction of Alzheimer beta-amyloid peptide with the human monocytic cell line THP-1 results in a protein kinase C-dependent secretion of tumor necrosis factor-alpha. Brain Res. 747, 114-121.

Koffie, R. M., Meyer-Luehmann, M., Hashimoto, T., Adams, K. W., Mielke, M. L., Garcia-Alloza, M., Micheva, K. D., Smith, S. J., Kim, M. L., Lee, V. M., Hyman, B. T. and Spires-Jones, T. L., 2009. Oligomeric amyloid beta associates with postsynaptic densities and correlates with excitatory synapse loss near senile plaques. Proc Natl Acad Sci U S A. 106, 4012-4017.

Kusumoto, Y., Lomakin, A., Teplow, D. B. and Benedek, G. B., 1998. Temperature dependence of amyloid beta-protein fibrillization. Proc Natl Acad Sci U S A. 95, 12277-12282.

LaFerla, F. M., Green, K. N. and Oddo, S., 2007. Intracellular amyloid-beta in Alzheimer's disease. Nat Rev Neurosci. 8, 499-509.

Lambert, M. P., Barlow, A. K., Chromy, B. A., Edwards, C., Freed, R., Liosatos, M., Morgan, T. E., Rozovsky, I., Trommer, B., Viola, K. L., Wals, P., Zhang, C., Finch, C. E., Krafft, G. A. and Klein, W. L., 1998. Diffusible, nonfibrillar ligands derived from Abeta1-42 are potent central nervous system neurotoxins. Proc Natl Acad Sci U S A. 95, 6448-6453.

Lashuel, H. A. and Grillo-Bosch, D., 2005. In vitro preparation of prefibrillar intermediates of amyloid-beta and alpha-synuclein. Methods Mol Biol. 299, 19-33.

Lomakin, A., Chung, D. S., Benedek, G. B., Kirschner, D. A. and Teplow, D. B., 1996. On the nucleation and growth of amyloid beta-protein fibrils: detection of nuclei and quantitation of rate constants. Proc Natl Acad Sci U S A. 93, 1125-1129.

Lorenzo, A. and Yankner, B. A., 1994. Beta-amyloid neurotoxicity requires fibril formation and is inhibited by congo red. Proc Natl Acad Sci U S A. 91, 12243-12247.

Lue, L. F., Kuo, Y. M., Roher, A. E., Brachova, L., Shen, Y., Sue, L., Beach, T., Kurth, J. H., Rydel, R. E. and Rogers, J., 1999. Soluble amyloid beta peptide concentration as a predictor of synaptic change in Alzheimer's disease. Am J Pathol. 155, 853-862.

McGeer, E. G., Klegeris, A. and McGeer, P. L., 2005. Inflammation, the complement system and the diseases of aging. Neurobiol Aging. 26 Suppl 1, 94-97.

McGeer, P. L., Itagaki, S., Tago, H. and McGeer, E. G., 1987. Reactive microglia in patients with senile dementia of the Alzheimer type are positive for the histocompatibility glycoprotein HLA-DR. Neurosci Lett. 79, 195-200.

McGeer, P. L. and McGeer, E. G., 2004. Inflammation and the degenerative diseases of aging. Ann N Y Acad Sci. 1035, 104-116.

Meyer-Luehmann, M., Spires-Jones, T. L., Prada, C., Garcia-Alloza, M., de Calignon, A., Rozkalne, A., Koenigsknecht-Talboo, J., Holtzman, D. M., Bacskai, B. J. and Hyman, B. T., 2008. Rapid appearance and local toxicity of amyloid-beta plaques in a mouse model of Alzheimer's disease. Nature. 451, 720-724.

Moretto, N., Bolchi, A., Rivetti, C., Imbimbo, B. P., Villetti, G., Pietrini, V., Polonelli, L., Del Signore, S., Smith, K. M., Ferrante, R. J. and Ottonello, S., 2007. Conformation-sensitive antibodies against alzheimer amyloid-beta by immunization with a thioredoxin-constrained B-cell epitope peptide. J Biol Chem. 282, 11436-11445.

Mori, C., Spooner, E. T., Wisniewsk, K. E., Wisniewski, T. M., Yamaguch, H., Saido, T. C., Tolan, D. R., Selkoe, D. J. and Lemere, C. A., 2002. Intraneuronal Abeta42 accumulation in Down syndrome brain. Amyloid. 9, 88-102.

Naiki, H. and Nakakuki, K., 1996. First-order kinetic model of Alzheimer's beta-amyloid fibril extension in vitro. Lab Invest. 74, 374-383.

O'Nuallain, B. and Wetzel, R., 2002. Conformational Abs recognizing a generic amyloid fibril epitope. Proc Natl Acad Sci U S A. 99, 1485-1490.

Oddo, S., Billings, L., Kesslak, J. P., Cribbs, D. H. and LaFerla, F. M., 2004. Abeta immunotherapy leads to clearance of early, but not late, hyperphosphorylated tau aggregates via the proteasome. Neuron. 43, 321-332.

Pike, C. J., Burdick, D., Walencewicz, A. J., Glabe, C. G. and Cotman, C. W., 1993. Neurodegeneration induced by beta-amyloid peptides in vitro: the role of peptide assembly state. J Neurosci. 13, 1676-1687.

Pike, C. J., Walencewicz-Wasserman, A. J., Kosmoski, J., Cribbs, D. H., Glabe, C. G. and Cotman, C. W., 1995. Structure-activity analyses of beta-amyloid peptides: contributions of the beta 25-35 region to aggregation and neurotoxicity. J Neurochem. 64, 253-265.

Probert, L., Akassoglou, K., Pasparakis, M., Kontogeorgos, G. and Kollias, G., 1995. Spontaneous inflammatory demyelinating disease in transgenic mice showing central nervous system-specific expression of tumor necrosis factor alpha. Proc Natl Acad Sci U S A. 92, 11294-11298.

Seilheimer, B., Bohrmann, B., Bondolfi, L., Muller, F., Stuber, D. and Dobeli, H., 1997. The toxicity of the Alzheimer's beta-amyloid peptide correlates with a distinct fiber morphology. J Struct Biol. 119, 59-71.

Selkoe, D. J., 2001. Alzheimer's disease: genes, proteins, and therapy. Physiol Rev. 81, 741-766.

Selkoe, D. J., 2004. Cell biology of protein misfolding: the examples of Alzheimer's and Parkinson's diseases. Nat Cell Biol. 6, 1054-1061.

Stine, W. B., Jr., Dahlgren, K. N., Krafft, G. A. and LaDu, M. J., 2003. In vitro characterization of conditions for amyloid-beta peptide oligomerization and fibrillogenesis. J Biol Chem. 278, 11612-11622.

Takahashi, R. H., Milner, T. A., Li, F., Nam, E. E., Edgar, M. A., Yamaguchi, H., Beal, M. F., Xu, H., Greengard, P. and Gouras, G. K., 2002. Intraneuronal Alzheimer abeta42 accumulates in multivesicular bodies and is associated with synaptic pathology. Am J Pathol. 161, 1869-1879.

Tarkowski, E., Andreasen, N., Tarkowski, A. and Blennow, K., 2003. Intrathecal inflammation precedes development of Alzheimer's disease. J Neurol Neurosurg Psychiatry. 74, 1200-1205.

Tycko, R., 2003. Insights into the amyloid folding problem from solid-state NMR. Biochemistry. 42, 3151-3159.

Tycko, R., 2004. Progress towards a molecular-level structural understanding of amyloid fibrils. Curr Opin Struct Biol. 14, 96-103.

Udan, M. L., Ajit, D., Crouse, N. R. and Nichols, M. R., 2008. Toll-like receptors 2 and 4 mediate Abeta(1-42) activation of the innate immune response in a human monocytic cell line. J Neurochem. 104, 524-533.

Walker, D. G. and Lue, L. F., 2005. Investigations with cultured human microglia on pathogenic mechanisms of Alzheimer's disease and other neurodegenerative diseases. J Neurosci Res. 81, 412-425.

Walsh, D. M., Hartley, D. M., Kusumoto, Y., Fezoui, Y., Condron, M. M., Lomakin, A., Benedek, G. B., Selkoe, D. J. and Teplow, D. B., 1999. Amyloid beta-protein

fibrillogenesis. Structure and biological activity of protofibrillar intermediates. J Biol Chem. 274, 25945-25952.

Walsh, D. M., Klyubin, I., Shankar, G. M., Townsend, M., Fadeeva, J. V., Betts, V., Podlisny, M. B., Cleary, J. P., Ashe, K. H., Rowan, M. J. and Selkoe, D. J., 2005. The role of cell-derived oligomers of Abeta in Alzheimer's disease and avenues for therapeutic intervention. Biochem Soc Trans. 33, 1087-1090.

Walsh, D. M., Lomakin, A., Benedek, G. B., Condron, M. M. and Teplow, D. B., 1997. Amyloid beta-protein fibrillogenesis. Detection of a protofibrillar intermediate. J Biol Chem. 272, 22364-22372.

Walsh, D. M. and Selkoe, D. J., 2007. Abeta Oligomers - a decade of discovery. J Neurochem.

Wood, S. J., Maleeff, B., Hart, T. and Wetzel, R., 1996. Physical, morphological and functional differences between ph 5.8 and 7.4 aggregates of the Alzheimer's amyloid peptide Abeta. J Mol Biol. 256, 870-877.

Yates, S. L., Burgess, L. H., Kocsis-Angle, J., Antal, J. M., Dority, M. D., Embury, P. B., Piotrkowski, A. M. and Brunden, K. R., 2000. Amyloid beta and amylin fibrils induce increases in proinflammatory cytokine and chemokine production by THP-1 cells and murine microglia. J Neurochem. 74, 1017-1025.

CHAPTER 4

DIVERSE Aβ AGGREGATION ASSEMBLIES AND THEIR ROLE IN ACTIVATION OF DIFFERENT BIOCHEMICAL PATHWAYS

4.1 Introduction

The neuropathological features of AD include amyloid deposits, neurofibrillary tangles and selective neuronal loss (Selkoe, 1991). Amyloid deposits contain Aβ, a 40-42 residue peptide produced by the endoproteolytic cleavage of amyloid precursor protein (APP) (Selkoe, 1993). Microglia are the immune cells of the brain. Aβ deposits attract the microglia and activate them to produce inflammatory mediators, some of which will act as a feed back to induce further chemotaxis and activation. Once at the site of Aβ deposition, the activated microglia attempt to phagocytose and clear the substance, thereby leading to more activation (Rogers and Lue, 2001). The plaques in AD brain are surrounded by activated microglial cells (Heneka and O'Banion, 2007). Microglia may be responsible for the phagocytosis and removal of Aβ under normal conditions (Wisniewski et al., 1991). In AD, it is argued that the microglia clustered around Aβ deposits become dysfunctional and incapable of removing Aβ (Rogers et al., 2002).

The limbic and association cortices of AD brain are surrounded by dead or dying neurons, activated microglial cells and reactive astrocytes (Selkoe, 1989, Mrak and Griffinbc, 2001). Aβ induced neurotoxicity has been demonstrated in numerous cell culture studies (Pike et al., 1993, Lorenzo and Yankner, 1994, Simmons et al., 1994). Transgenic mice expressing mutant human APP develop neuropathological lesions similar to those found in AD patients. Immunization of these mice with Aβ(1-42) aggregates reverses the neuropathology significantly (Janus et al., 2000, Morgan et al., 2000). This effect could be due to two possibilities. One is that the antibodies generated by the host will neutralize Aβ in a restricted compartment, or it may deplete some soluble form of Aβ. The other possibility could be that the microglia get activated due to the immunization and this clears the deposited Aβ. These lead to reversal of cognitive imbalance (Janus et al., 2000, Morgan et al., 2000). The proposed hypothesis is that the immune system acts as a peripheral sink, traps Aβ, and depletes it from CNS (Matsuoka et al., 2003, Heneka and O'Banion, 2007). When there is an overwhelming production of Aβ(1-42), the levels exceed the rate at which the macrophage machinery clears the amyloid deposits resulting in the plaque core found within the AD brain. Also, the clearance mechanisms become less efficient as one ages and this causes severe deposition of Aβ aggregates. These data indicate the significant contribution of Aβ(1-42) to neurotoxicity in AD.

Extensive biophysical studies reveal that full length and fragments of Aβ peptides form intermolecular parallel β-sheet structures in amyloid fibrils (Serpell, 2000, Antzutkin et al., 2002, Balbach et al., 2002). In addition to β-sheets, turn structures or

bend structures were also present at positions 24-27 in Aβ(1-40) aggregates (Whittemore et al., 2005), and positions 26-27 in Aβ(1-42) aggregates (Olofsson et al., 2006). However, the precise positions of these turn or bend structures in Aβ aggregates are still under investigation. The relationship between the turn position and its impact on inflammatory response is not known. A detailed investigation into Aβ aggregation profile may provide clues into the structure-function relationship.

We investigated the relationship between Aβ aggregation state and its role in the activation of monocytes and their maturation into macrophages. We identified that a rapidly formed oligomeric aggregation species is responsible for the maturation of monocytes into macrophages, and an intermediate fibrillar oligomer elicits proinflammatory response via TLR2 and TLR4 receptors.

4.2 Role of Aβ Aggregation State in Monocyte Recruitment

This study was done in collaboration with Nikkilina Crouse, and the work is published in (Crouse et al., 2009). The cell surface represents the first site of interaction between extracellular Aβ and neurons. Therefore the cell surface may be the location where the neurotoxic cascade is initiated (Bateman et al., 2007). Neurotoxicity studies of Aβ indicate that aggregated Aβ is generally more toxic than monomeric Aβ (Pike et al., 1993, Simmons et al., 1994, Podlisny et al., 1998, Walsh et al., 1999, Walsh et al., 2002).

Blood monocytes represent a large pool of scavenger and potential effector cells inside blood vessels both in homeostasis, as well as, during inflammatory processes (Auffray et al., 2007). In mammals, monocytes also represent the accessory cells that

link inflammation and innate defense against microorganisms to adaptive immune responses (Auffray et al., 2009). Aβ is believed to play roles in monocyte migration (Yan et al., 1996, Giri et al., 2000, Le et al., 2001), adhesion and differentiation into macrophages (Yan et al., 1996). Aβ assemblies exhibit a wide range of morphologies that appear to stimulate different types of biologic responses *in vivo.* The type of aggregation species or the receptor mechanisms that causes the monocyte/microglia recruitment, monocyte differentiation, and microglial activation are not fully understood. We investigated the ability of Aβ aggregation species to induce monocyte maturation into an adherent form.

4.3. Aβ(1-42) Induces THP-1 Monocyte Adhesion and Maturation

THP-1 monocytes cell model system was used for studying the monocyte recruitment and differentiation process since they are non-adherent and have a round morphology (Tsuchiya et al., 1980). They normally circulate in the blood. In the event of a proinflammatory, or immune stimuli in the periphery, the monocytes are recruited to the site and are differentiated into macrophages. The differentiation process is an attempt to round up and destroy the foreign pathogen, and prevent further damage to the body. THP-1 monocytes can be induced to differentiate along the monocytic pathway. These cells can be converted into mature cells with functions of macrophages by treatment with phorbol diesters (Tsuchiya et al., 1982). Phorbol-12-myristate-13-acetate (PMA) is known to induce cell differentiation. (Schwende et al., 1996) have reported that PMA

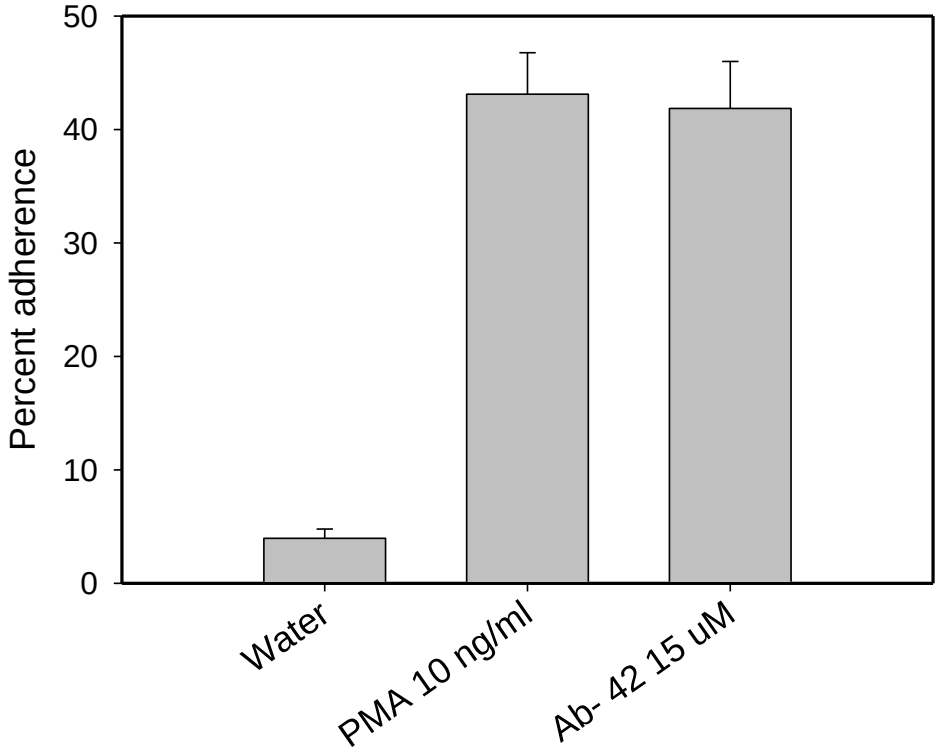

Fig 4.1 Aβ(1-42) induces monocyte adherence comparable to PMA. THP-1 monocytes were treated with 10 ng/ml PMA or 15 μM Aβ(1-42) from a freshly reconstituted 100 μM water solution and incubated for 6 hours at 37°C. Percent adherence was determined by direct cell counting as described in the methods. Standard error bars were calculated from n=17 trials for PMA and n=22 trials for Aβ(1-42). Water (n=15) controls induced 5 ± 1% adherence. Courtesy Nikkilina Crouse

induces adherence, and their reports also show a decrease in cell proliferation when treated with PMA. We used PMA as a control to monitor the differentiation in cells.

When THP-1 cells were incubated with PMA for 6, 24 and 48 hours respectively,there was monocyte differentiation. The ability to differentiate the monocytes was evaluated by measuring monocyte adhesion, a marker for cell maturation. Freshly reconstituted Aβ(1-42) in water (100 μM) induced 41.85 +/- 4.14 % adherence, and it was comparable to the 43.11+/- 3.65 % induction by PMA (10 ng/ml) (Fig. 4.1). The monocyte adhesion ability was dependent on the concentration of Aβ. When cells were treated with different Aβ(1-42) concentrations (5, 10, 15 μM), the 15 μM Aβ(1-42) induced maximum adherence. (data not shown). We used this concentration for further experiments.

4.4 Freshly solubilized Aβ(1-42) Induces Maximum Monocyte Maturation Compared to Aggregated Aβ(1-42).

The influence of Aβ(1-42) aggregated state in inducing the monocyte maturation was tested by incubating Aβ(1-42) for longer incubation time. Aβ(1-42) was reconstituted in water, an aliquot was treated with the cells immediately, and the remaining solution was allowed to aggregate at 4°C. At specific time points of aggregation (0, 48, 72, 96, 120, 144, 216 hours), aliquots of Aβ(1-42) aggregation solution were treated with cells, and the ability to induce the monocyte adhesion was monitored. The maximum adhesion occurred at zero and 48 hours of aggregation, and the ability to induce adhesion was lost with increase in the duration of aggregation. AFM images of samples at the correlating time points showed presence of small globular species for the freshly reconstituted solution of Aβ(1-42). Small fibrillar structures were

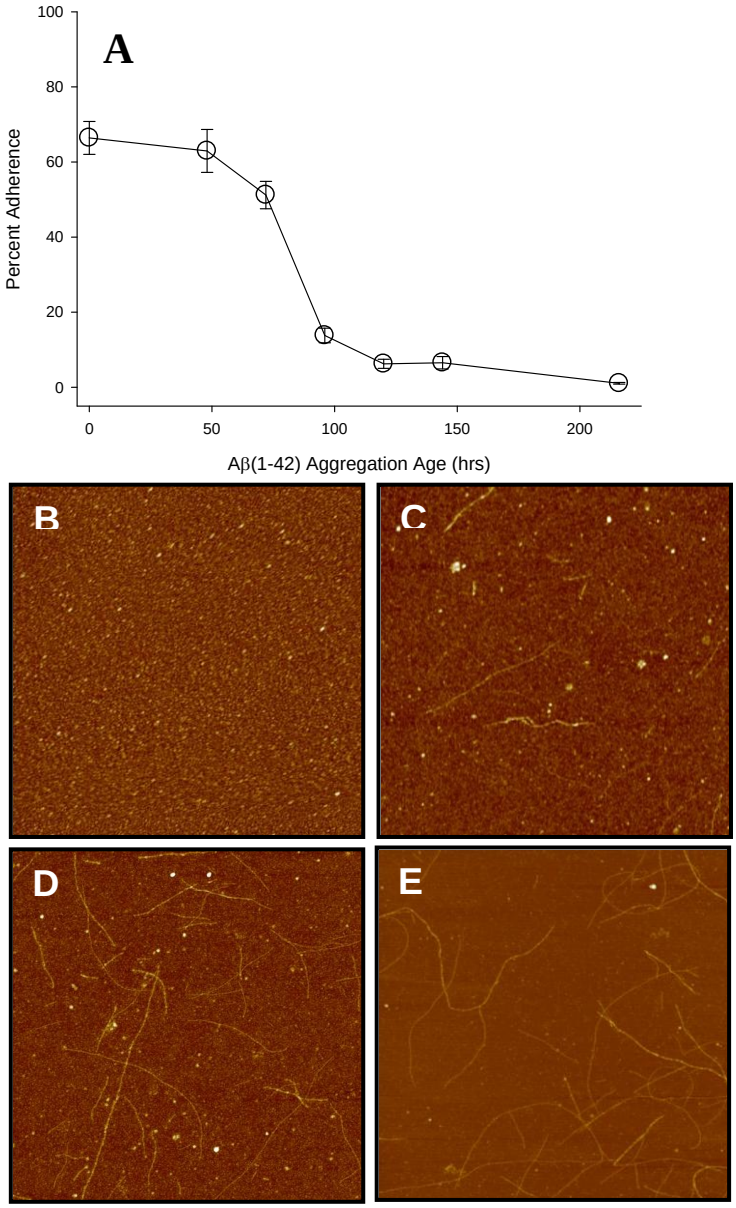

Fig. 4.2 Aβ(1-42) aggregates in freshly reconstituted solution induce monocyte adherence. Aβ(1-42)) was reconstituted in sterile water to 100 µM and incubated at 4°C. (**A)** At the given times, cells were treated with 15 µM Aβ for 6 hours and adherence was measured by direct counting as described in the Methods. Error bars represent standard error for n trials of 19 (0 h), 17 (48 h), 4 (72 h), 5 (96 h), 7 (120 h), 3 (144 h), and 7 (216 h) Courtesy Nikkilina Crouse. (**B-E)** Representative AFM images of Aβ(1-42) aggregation at 4°C taken at 0, 48, 96 and 216 hours respectively. Aβ(1-42) was diluted a concentration of 1 µM and applied on mica grids as described in Methods. Images are 5 µm x 5µm panels.

observed after 48 hours along with the small globular species, and by 96 hours, there was an increase in the number of fibrils, and a significant loss of ability to induce cell adherence. The data clearly suggest that aggregation species present in the freshly reconstituted Aβ(1-42) was the most effective in inducing monocyte maturation. Height analysis of the AFM images showed presence of diffuse material < 1nm in height in the freshly reconstituted Aβ(1-42). Short rod like structures averaging 4-5 nm appeared by 48 hours and these were able to induce monocyte adhesion but was slightly less than the zero hour sample. As the aggregation progressed there was an increase in the number of fibrils. The heights of the fibrils averaged between 5-6 nm. There was significant increase in the fibril numbers with heights greater than 6 nm after 216 hours aggregation. We observed the disappearance of the diffuse aggregation species as the aggregation progressed. The data from this experiment suggests that fibrillar aggregates were unable to induce maturation of THP-1 monocytes to an adherent form. Several trials of the experiment showed consistency in this trend although the percent adhesion levels showed a variation depending on the Aβ(1-42) lot numbers.

4.5 Increase in Peptide Concentration Affects the Ability to Induce Monocyte Maturation

Data from section 4.3 suggests that increased Aβ(1-42) aggregation decreases the monocyte maturation process. The maximum activity was exhibited by Aβ(1-42) species present at the time of reconstitution. We modulated the aggregation conditions by increasing the starting concentration of the monomer. We hypothesized that, there will be an increase in the rate of the species that forms immediately after reconstitution. Aβ

aggregation proceeds by multistep, nucleation-dependent process (Jarrett and Lansbury, 1993). Formation of the nucleation seed is the rate limiting step, so that, in the absence of preformed seeds, there is a significant lag time for the formation of fibrils. The rate of monomer incorporation to form fibrils increases as concentrations of monomer and seed increases (Naiki and Nakakuki, 1996).

We increased the monomer concentration by 10 fold (1 mM) and compared activity to the 100 μM Aβ(1-42) solution that was used for the experiment in Fig 4.2. Increased monomer concentration will alter the rate of formation of the early species. The cells were however treated with the same final concentration of 15μM Aβ(1-42). The more concentrated 1 mM Aβ(1-42) solution showed a decrease in the ability to induce monocyte adhesion (Fig 4.3 A). AFM images showed presence of fibers with heights ranging 2-3 nm immediately upon reconstitution in the 1 mM Aβ(1-42) solution. Aliquots of the same preparation was analysed by TEM, and the fibril widths were 6-10 nm. Further incubation of 1mM Aβ(1-42) solution for 24 hours resulted in increased fibril formation compared to Aβ(1-42) 100 μM sample. The fibrils were longer and the heights were 4-5nm, but the monocyte adhesion inducing activity was diminished (Fig 4.3). The treatment of 1 mM Aβ(1-42) with the cells produced 67 % of monocyte maturation induced by the 100 μM sample. It is possible that accelerated aggregation depleted the Aβ species capable of inducing monocyte maturation. The depletion is due to the rapid aggregation into the fibrillar forms as seen in the AFM images (Fig 4.3 B-C). These findings suggest that the maturation of monocytes was induced by either a monomeric, or, oligomeric species that was formed early in the aggregation reaction of 100 μM Aβ(1-42) that was reconstituted in water.

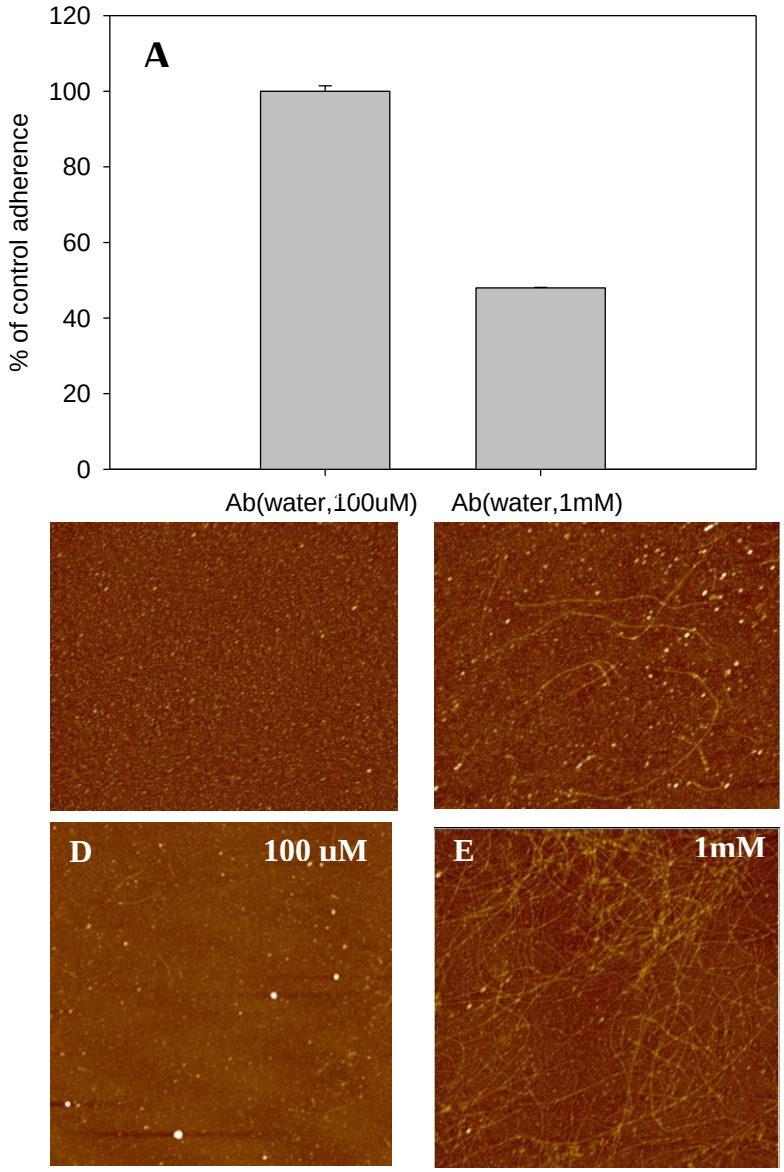

Fig 4.3. Increased peptide concentration decreases monocyte adherence. Two aggregations were set up by reconstituting Aβ(1-42) in sterile water to 100 µM and 1 mM and incubated at 4°C. **A**. Cells were treated with 15 µM Aβ for 6 hours and adherence was measured by direct counting as described in the Methods (Courtesy Nikkilina Crouse). **B-E.** Representative AFM images of Aβ(1-42) aggregation. B and D) Aβ(1-42), 100 µM, at zero and 24 hours incubation at 4°C, C and E) Aβ(1-42), 1 mM at zero and 24 hours incubation at 4°C respectively. Images are 5 µm x 5µm panels.

4.6 Monocyte Maturation is Induced by Aβ(1-42) and not Aβ(1-40)

The maximum monocyte adherence was found when THP-1 cells were treated with freshly reconstituted Aβ(1-42). We hypothesized that the monomeric species may be potent. Studies of the kinetics of Aβ fibril formation have shown that Aβ(1-42) forms fibrils significantly faster than Aβ(1-40) (Jarrett et al., 1993). The initial oligomerization and assembly of Aβ(1-40) and Aβ(1-42) indicate that these peptides have distinct behaviors at the earlier stages in the assembly, monomer oligomerization (Bitan et al., 2003). The shorter peptide, Aβ(1-40), is believed to remain in the monomer state for a longer time than Aβ(1-42) (Walsh et al., 1997). In order to further clarify the Aβ aggregation species responsible for monocyte maturation, we compared the reactions between Aβ(1-40) and Aβ(1-42). We tested the ability of Aβ(1-40) to induce monocyte maturation. Since the aggregation propensity of Aβ(1-40) is much slower we reasoned that the monomer would remain the solution longer, and we could test our hypothesis to see if monomer species, or, early oligomeric species was actually inducing the maturation of monocytes. We investigated the time-dependent aggregation of Aβ(1-40) (100 μM) reconstituted in sterile water and incubated at three temperatures 4°C, 25°C, 37°C. The activity was compared to Aβ(1-42) (100 μM) incubated at 4°C. Significant difference was observed in the two peptide solutions immediately after reconstitution. Aβ(1-42) (100 μM) was able to induce 57% monocyte adhesion while Aβ(1-40) under similar conditions did not (Fig 4.4 A). Accelerating the Aβ(1-40) kinetics by increasing the temperature did not induce any monocyte adherence. Continued aggregation of Aβ(1-40) showed fibrils formation by 216 hours, but none of the intermediates formed had

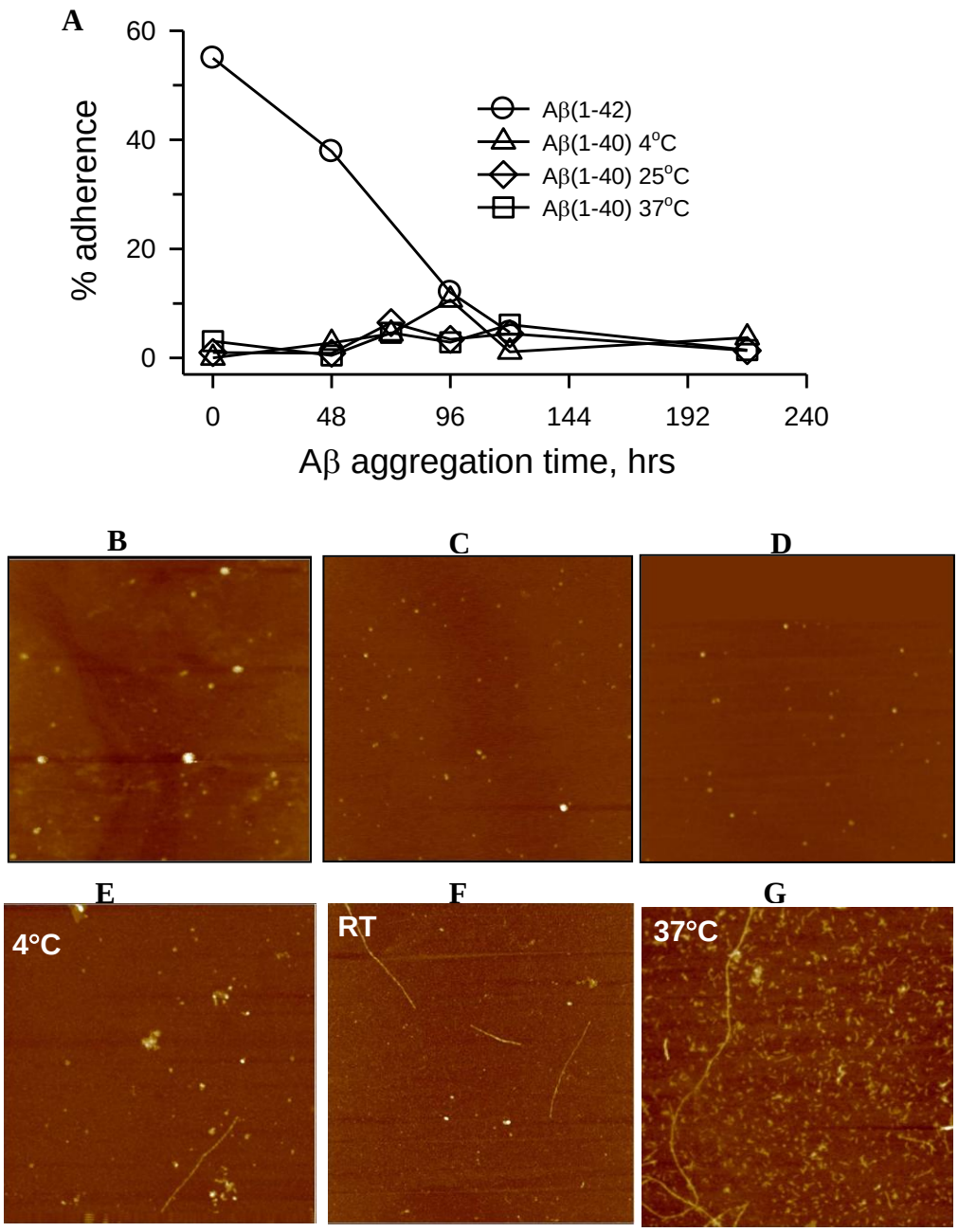

Fig.4.4 Aβ(1-40) aggregated at different temperatures does not induce THP-1 adherence. Aβ(1-40) was reconstituted in sterile water to 100 µM and incubated at 4°C, 25 or 37°C. **Panel A**. At the given times, cells were treated with 15 µM Aβ(1-40) for 6 hours and adherence was measured by direct counting as described in the Methods. Aβ(1-42) incubated at 4°C was used as the control, Panel A (circles). Error bars represent standard error for n trials of 3. Courtesy Nikkilina Crouse. **B-D.** Representative AFM images of Aβ(1-40) aggregation taken at 0 hours at the three different temperatures. **E-G.** AFM images of Aβ(1-40) aggregation taken at 216 hours at 4, 25 or 37°C, respectively. Images are 5 µm x 5 µm. The images are in the height mode.

the ability to induce monocyte maturation. The results suggest that adhesion-inducing activity was mediated by an aggregation species that was formed in the Aβ(1-42) pathway, but was not formed by any of the aggregation species formed by Aβ(1-40). These data led us to hypothesize that the two extra amino acids in Aβ(1-42) may be important in the formation of species responsible for monocyte maturation process.

4.7 Oligomeric Aβ(1-42) Induces Monocyte Maturation

From the results discussed above, we hypothesized that monomer could still be the active species, but the activity was dependent on the two additional amino acids in Aβ(1-42). The extra two amino acids may be crucial for the monomer induced monocyte adhesion. We have seen in Section 4.5 that the lag phase in nucleation–dependent polymerization process can be altered by a change in concentration of monomer. Two Aβ(1-42) aggregation solutions were initiated, one at 50 µM concentration and the other at a concentration of 100 µM. We were of the opinion that in the 50 µM aggregation solution the available starting monomer concentration is low and therefore the aggregation reaction will be slower. Also, there would be availability of high monomer compared to oligomers due to slower aggregation. On the other hand the 100 µM Aβ(1-42) solution has more concentration of the monomer thereby driving the reaction towards oligomer formation. We assumed that this would result in a decrease in the monomer compared to oligomer. The cells were treated with the same final concentration of 15µM Aβ(1-42). Cells treated with freshly reconstituted 100 µM Aβ(1-42) induced 58+/- 4% adhesion while there was only 16+/- adhesion for the cells treated with 50 µM Aβ(1-42)

(Fig 4.5 A). If monomer was responsible for inducing adhesion then the 50 µM Aβ(1-42) aggregation solution with a high monomer:oligomer ratio should have induced a high monocyte adhesion property. Upon additional incubation for 24 hours the activity reduced in both aggregation reactions to 41+/- 5 and 12+/-3% adhesion for 100 µM and 50 µM Aβ(1-42) respectively. There was further decrease in the adhesion levels as the aggregation progressed to 48 hours. AFM images of the freshly reconstituted solutions of 50 µM and 100 µM solutions did not show any distinct morphological species that could differentiate between the two preparations (Fig 4.5 B). However, the 48 hour images showed a difference in the extent of aggregation (Fig 4.5 C and D). The images showed the formation of fibrillar species in the 100 µM preparation that correlated with a drop in the cell adhesion. The 50 µM sample at the same time did not have any fibrillar aggregates, but was not able to stimulate cell adhesion. Though AFM images could not provide additional information regarding the morphology of the species that induces adherence in the cells, it was evident that the monomer was not involved in inducing adherence in the THP-1 cells.

4.8 Mutated Aβ(1-42) (L34P) Does not Induce Monocyte Maturation

The data so far indicated that an active Aβ(1-42) aggregation species was capable of inducing cell adherence. These active species were formed in freshly reconstituted solutions of Aβ(1-42) indicating that the species is formed early in the aggregation, and the role of monomer in the maturation process was ruled out at this point. We wanted to try a mutational approach to get further clarification of the species that was active in the

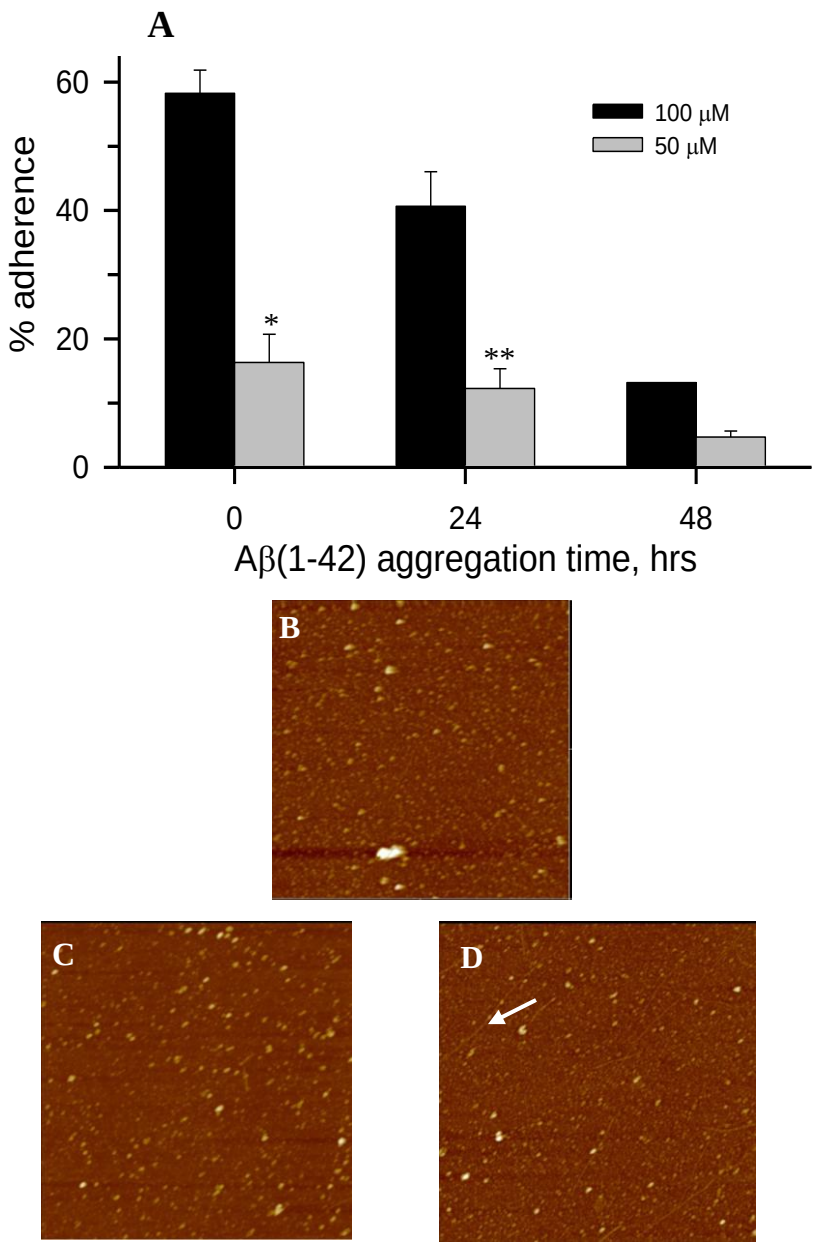

Fig 4.5 Lowering the initial Aβ(1-42) concentration decreases monocyte adherence. Aβ(1-42) was reconstituted in sterile water to either 100 µM or 50 µM and aggregated at 4°C. (Panel A) At the times indicated, THP-1 cells were treated with 15 µM of either solution for 6 hours at 37°C. The percent adherence was determined as described in the Methods. SE was determined for n trials of 3 (0 hours) and 2 (24 hours and 48 hours, 50 µM). Only 1 trial was done for 100 µM at 48 hours. Water-induced adherence controls (2.8 ± 0.4 %) were subtracted from final percent adherence presented. Differences between 100 µM and 50 µM treatments were significant at 0 (* $p<0.0005$) and 24 hours (** $p<0.005$) of aggregation. Courtesy Nikkilina Crouse. (Panel B-D) Representative AFM images of the same experiment B) 50 µM sample after 24 h, D) 100 µM sample after 24 hours.

maturation of monocytes. Single mutations in proteins can cause aggregation to switch from one pathway to the other. Systematic replacement with proline in peptides is a reliable method for predicting the secondary structure (Wood et al., 1995). Proline residues are rarely present in the β- sheets, but can easily be accommodated in the turns and bends (Chou and Fasman, 1978, Lifson and Sander, 1979). Hence, proline residues can be introduced into peptides to slow down the aggregation process. Liu et al., (2004) investigated the aggregation of Aβ using different Aβ fragments and concluded that residues 17-20 and 30-35 are the important regions for aggregation. Introduction of proline into Aβ peptide sequence can improve the solubility and also block or reduce aggregation (Wood et al., 1995) We tried a mutated Aβ(1-42) L34P peptide for further probing. If the last two amino acids in Aβ(1-42) were responsible for transformation of monocytes into macrophages, the Aβ(1-42) L34P should also be able to form the active species. The leucine to proline mutation at residue 34 slows down aggregation and destabilizes the fibrils (Williams et al., 2004). This mutation enables the peptide to remain in the non fibrillar form for a longer time. However, Aβ(1-42) L34P prepared under similar conditions failed to induce monocyte adhesion after reconstitution in sterile water. The cells responded to differentiation by PMA in these experiments (data not shown). Even prolonged incubation up to 168 hours failed to induce monocyte adhesion. Aβ(1-42) L34P did not produce any fibrillar structures as seen in the AFM images. These data suggest that a rapidly forming Aβ(1-42) oligomeric species was active in inducing monocyte cell adhesion. These results clearly indicated the monomer was not involved in inducing differentiation in monocytes.

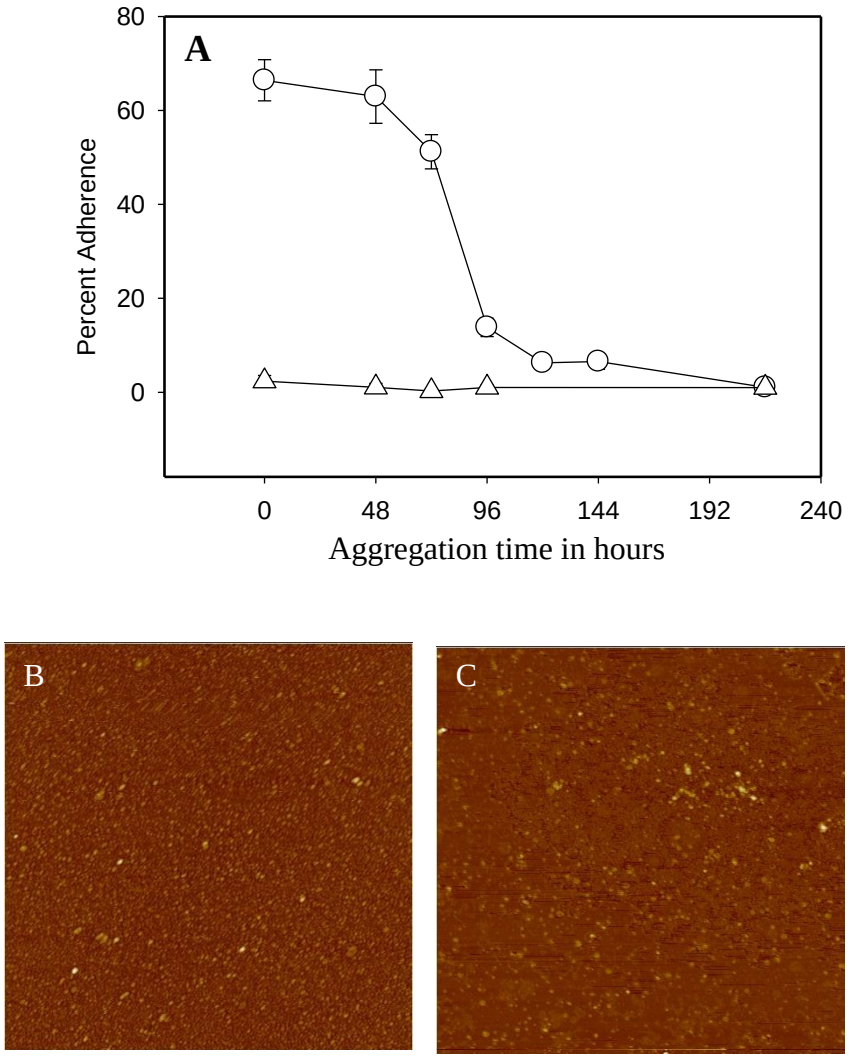

Fig. 4.6 Aβ(1-42) L34P does not induce THP-1 monocyte adherence
Aβ(1-42) (L34P) was reconstituted in sterile water to 100 µM and incubated at 4°C. **A.** At the given times, cells were treated with 15 µM Aβ L34P (triangles) for 6 hours and adherence was measured by direct counting as described in the Methods. Error bars represent standard error for n trials of 5 for Aβ(1-42) L34P. The time course for Aβ(1-42) (circles) from Fig 4.2 is shown for comparison. Courtesy Nikkilina Crouse. **B-C.** Representative AFM images of Aβ(1-42) L34P aggregation at 4°C taken at 0 (B) and 168 hours (C), respectively. Images are 5 µm x 5 µm and taken as described in Methods.

However, there was rapid aggregation when Aβ(1-42) (L34P) was reconstituted in water and incubated at 37°C. The measured pH of Aβ(1-42) (L34P) solution was 3.4. This pH was close to the measured pH of Aβ(1-42) solutions reconstituted in water. Dense fibrils formed upon incubation at 37°C for 24 hours. The fibril density increased as the aggregation progressed (Fig 4.7). We also noticed less diffuse structures at the start of the aggregation reaction (Fig 4.7 A). Upon prolonged incubation at 37°C, fibrils were sheared (Fig 4.7 F-G). It is clear that these morphologies failed to induce maturation in THP-1 monocytes. However, the ability of these aggregates to induce a proinflammatory response is yet to be probed. Aβ(1-42) (17-35) fragment contained a high ratio of β-sheet structure, and was comparable to full length Aβ(1-42) (45% and 41%) (Liao et al., 2007). The mutation at position 34 may alter the β-sheet structure and may have a different effect on the proinflammatory-stimulating activity. These findings may provide important information towards the correlation of structure and biological activity.

4.9 Amyloid Derived Diffusible Ligands (ADDLs) Not Effective Inducers of Monocyte Adhesion

We wanted to investigate the effect of oligomers on monocyte maturation process. Lambert et al., (1998), reported the detection of small globular structures ~ 5-6 nm in diameter which they referred to as ADDLs. These structures were free of large protofibrils or fibrils (Walsh et al., 1997, Harper et al., 1999). Also, Aβ(1-42) appear to populate these structures to a higher degree than Aβ(1-40) (Walsh et al., 1997, Stine et al., 2003). ADDLs cause neuronal cell death, block LTP (Lambert et al., 1998) and

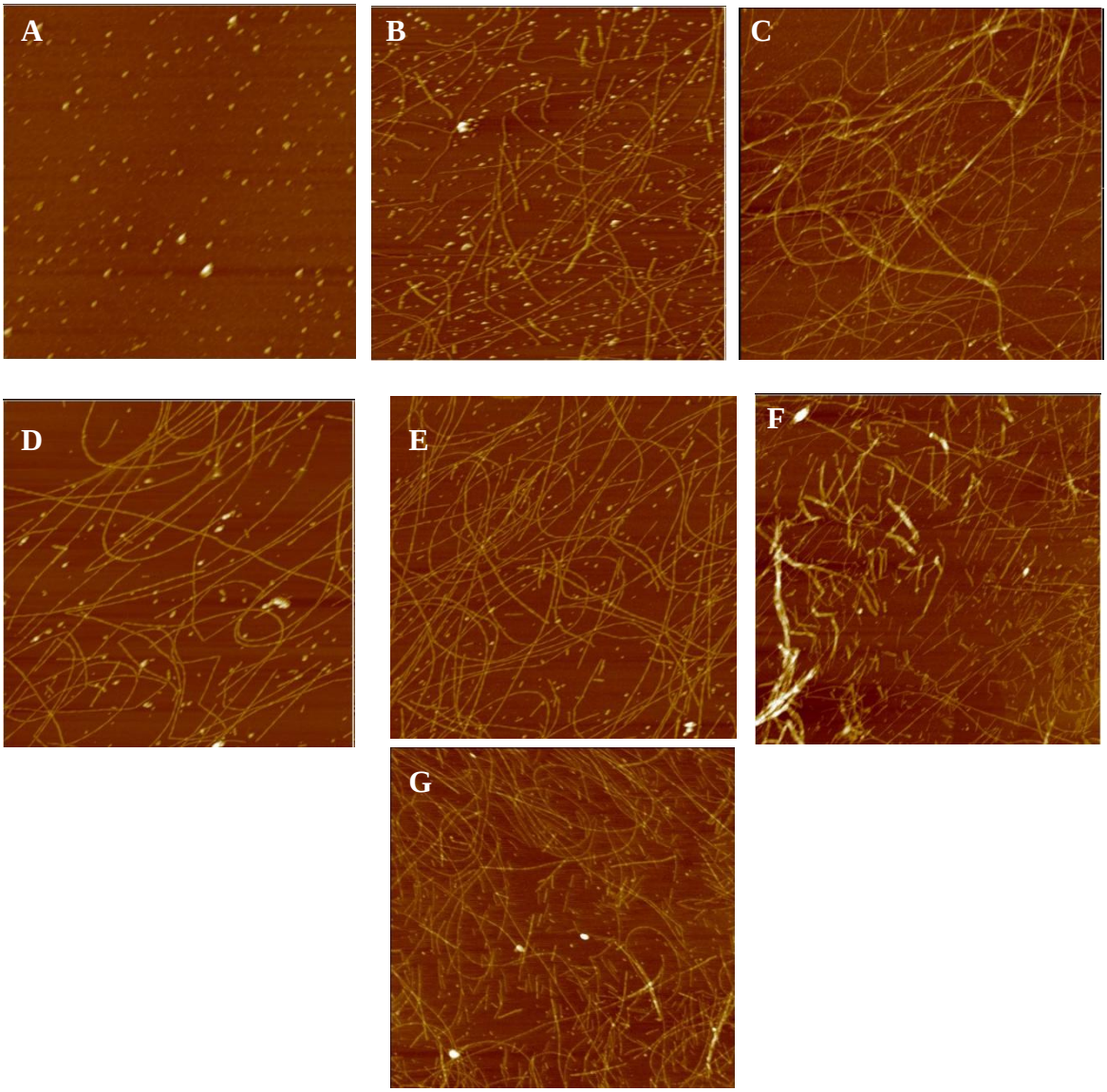

Fig 4.7. Aβ(1-42) (L34P) aggregates rapidly at high temperatures. Aβ(1-42)(L34P) was reconstituted to 100 μM in water and allowed to aggregate at 37°C. At specific time points an aliquot was removed, diluted to 1μM and grids were prepared for AFM imaging as described in Methods. **A-G.** AFM images at zero (A), 24 hours (B), 48 hours (C), 72 hours (D), 96 hours (E), 168 hours (F), and 216 hours (G). The image panels are 5μm x 5μm and are in the "height" mode

inhibit reduction of 3-(4,5-dimethylthiazol-2-yl)-2,5-diphenyltetrazolium bromide (MTT) in neural cell lines, which is an indication of cell death (Dahlgren et al., 2002, Wang et al., 2002, Kim et al., 2003) When low concentrations of ADDLs (5 nM) were incubated with organo typic mouse brain culture slices for 24 hours there was a 20 % loss in cell number. However, at higher concentrations (500 nM), and incubation for shorter periods resulted in complete loss of LTP (Lambert et al., 1998, Wang et al., 2002). Since our data indicates that Aβ(1-42) oligomeric species was causing monocyte adhesion, we wanted to see if ADDLs had any effect on THP-1 monocyte adhesion. The preparation of ADDLs was different from the regular Aβ(1-42) aggregation reactions. The protocol includes an incubation step for 24 hours, and the centrifugation supernatant after 24 hours was called ADDLs. For our experiments, we tested the pre-centrifugation solution (total) and the ADDLs. The pre-centrifugation solution induced 6+/-3% and ADDLs induced 7 +/- 2% adhesion respectively (Fig 4.8 A).

AFM images showed the presence of small oligomeric species ranging from 1-6 nm (mean = 3.0 +/- 1.3 nm SD) respectively (Fig 4.8 C). The morphological aspects of the spherical aggregates correlated with earlier reports of ADDLs (Dahlgren et al., 2002). However, the cellular data suggest that Aβ(1-42) oligomeric species that induces cell adhesion was different from ADDLs. Moreover, ADDLs are prepared in a different solution, and we have seen in Chapter 3 that change in solution conditions alter the aggregation morphology, and biologic activity. It is possible that the active Aβ(1-42) species are different and are generated before the ADDLs-like conformation is formed.

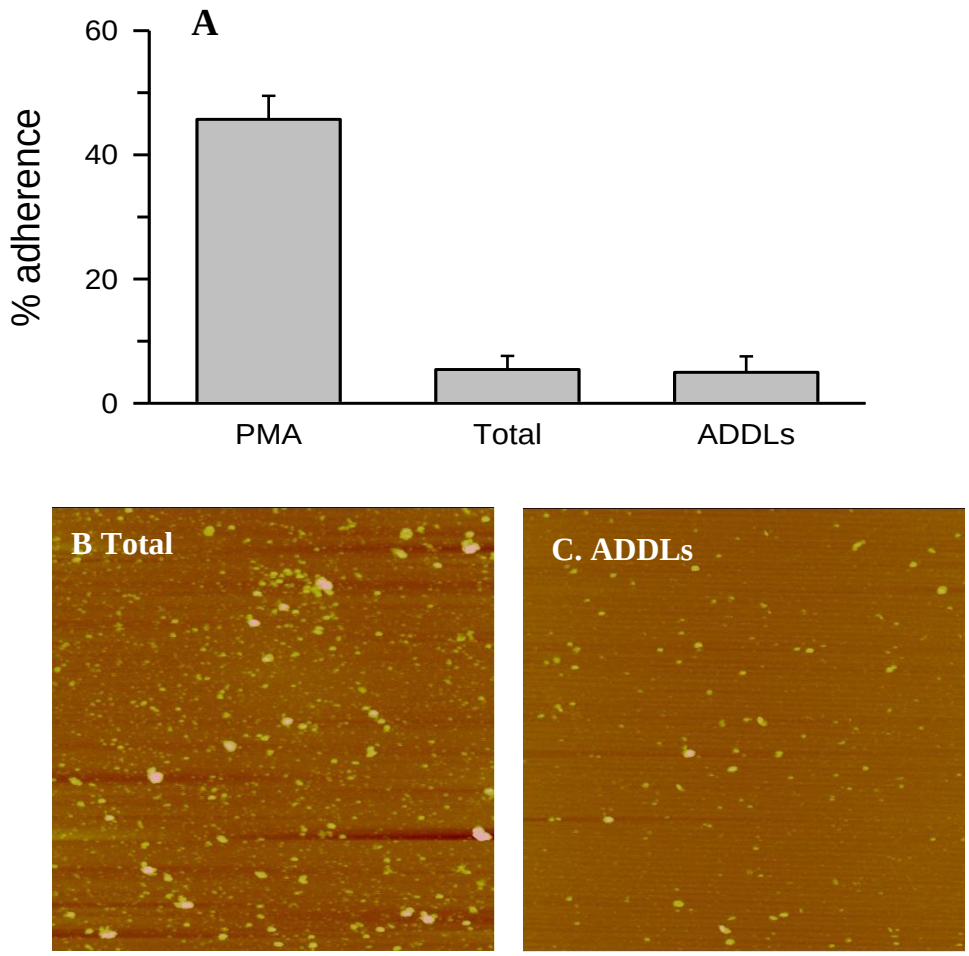

Fig 4.8 ADDLs failed to induce monocyte adherence. ADDLs were prepared in DMSO/ice cold Ham's F12 medium with phenol red as described in Methods. **Panel A** Cells were treated with the Aβ(1-42) aggregation solution prior to centrifugation (Total) or ADDLs at a final concentration of 15 μM Aβ(1-42). PMA (10 ng/ml was included as control. Adherence is presented as the average ± SE for n=2 trials for PMA and n=4 trials for Total and ADDLs over two separate experiments. Courtesy Nikkilina Crouse, University of Missouri, St Louis. **Panel B-C.** AFM images of Total (Panel B), and ADDLs preparation (Panel C) that were used to treat THP-1 cells. The images are 5 μm x 5 μm panels and are shown in the "height" mode.

4.10 Intermediate fibrillar Aβ(1-42) Aggregation Species Activate Innate Immune Response in THP-1 Cells via Toll-like Receptors (TLRs) 2 and 4

This work was done in collaboration with Maria Udan and is published in (Udan et al., 2008). TLRs are known to comprise a family of 10 proteins (Akira, 2003). TLRs are often considered to be the staring point of immunity. They function in continuous sampling of extracellular environment, and informing the cell to respond to infection. These cellular responses are facilitated via signaling pathways (Parker et al., 2007). One of the earliest phagocytes to respond to infection is the tissue macrophage. These originate as monocytes in the peripheral blood system. TLR stimulation activates numerous genes in the human monocytes, leading to the release of cytokines, chemokines and growth factors that exert potent autocrine and paracrine inflammatory responses. (Kopydlowski et al., 1999, Wang et al., 2000, Ritter et al., 2005).

Human THP-1 monocytes produce significant proinflammatory response when treated with aggregated Aβ (Klegeris et al., 1997, Yates et al., 2000). Aβ(1-42) peptides were prepared by reconstitution in water and incubated at 4°C as described in Methods, and the aggregation was monitored by AFM. The freshly reconstituted Aβ(1-42) solution showed a dense population of punctuate species that had very little stimulatory effect on the cells for a proinflammatory response. Continued aggregation produced thin flexible fiber like structures. Over the time course of aggregation, we identified that the fibers formed at 48 hours was able to induce maximum proinflammatory response. AFM height analysis indicated the presence of fibrils that fell into two populations. One was the most

populated peak that had a mean height of 4.4 nm +/- 0.1 nm and the other was a population of fibers that had a mean height of 7.9 +/- 0.6 nm respectively. Prolonged incubation beyond 96 hours incubation at 4°C resulted in the loss of cell stimulation. From Chapter 3 we have seen that fibrillar oligomers were optimal to stimulate maximum response. The objective of the study was to determine which transmembrane TLR plays a functional role in transducing the Aβ-induced innate immune signal through the membrane.

A TLR neutralization assay was developed to probe the TLRs that mediate the Aβ(1-42) induced proinflammatory response. The assay was initially tested on the TLR agonists LPS and Pam_3CSk_4 in order to determine the sensitivity of the assay (Udan et al., 2008) (data not included). Once we determined the sensitivity of the assay, we conducted the neutralization studies against the Aβ(1-42) proinflammatory response. In Chapter 3, we have already seen that aggregated Aβ(1-42) that has been incubated at 4°C for 48 hours or 72 hours stimulated maximum proinflammatory response. Hence, we used Aβ(1-42) that has been aggregated for 48-72 hours for the neutralization assays. Both TLR2 and TLR4 neutralizaton resulted in the attenuation of the Aβ(1-42) induced proinflammatory signal, with the TLR2 showing a greater degree of blocking activity. The antibody neutralization experiments indicated that multiple TLRs mediate the Aβ-induced activity. When the cells were neutralized by a combination of TLR2 and TLR4 antibodies, there was increased blocking of the Aβ(1-42) induced proinflammatory signal (Fig 4.9). These data indicate that both TLR2 and TLR4 have active roles in mediating the Aβ(1-42) induced innate immune response.

The interaction between Aβ- aggregates, TLRs and innate immunity will provide some more details into the complexities of the AD etiology. From chapter 3 we have identified that small intermediate Aβ(1-42) fibrillar oligomers are optimal for inducing proinflammatory response. We will be extending the studies to get more information regarding the interaction of Aβ with the cells. We have done preliminary studies to label the Aβ(1-42) with immunogold label antibodies (Fig 4.10). We will be extending the investigations to study the interaction between Aβ and the cell membranes using the immunogold label studies

4.11 Discussion

The role of macrophages in the innate immune system has gained lot of importance, and it has been established that they are crucial for defense against microbes and removal of cellular debris (Fiala et al., 2007). Brain amyloidosis is hypothesized as a very crucial mechanism in the AD brain. Accumulation of Aβ either in fibrillar, soluble or oligomeric conformations, is toxic to neurons. (Lambert et al., 1998, Hardy and Selkoe, 2002, Oddo et al., 2006). Neuropahological study of AD and control brains showed penetration of blood derived monocytes across brain microvessels, excessive engorgement of macrophages with Aβ. Also, there was retention of these macrophages in the wall of congophillic vessels (Fiala et al., 2002). Despite data suggesting the recruitment of non resident cells into the CNS, there is still no clear picture of how the transformation from monocytes to macrophages occurs. Human monocytes from

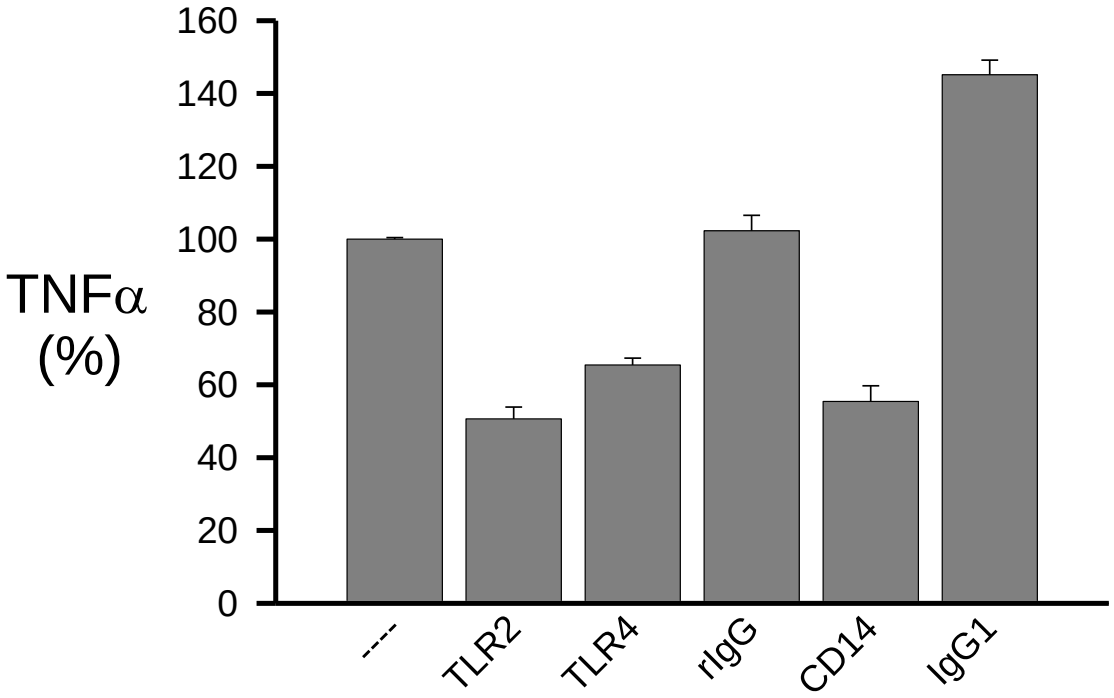

Fig 4.9 TLR2, TLR4 play an active role in Aβ-induced innate immune response activation. Aβ(1-42) 100 μM was prepared in sterile water and incubated at 4°C for 48-72 hours depending on the peptide lot as described in Methods. THP-1 monocytes were pre-incubated with 10 μg/ml of TLR2, TLR4 CD14(InvivoGen) antibodies, or IgG isotype controls, as described in Methods. Isotype controls were rat IgG (Sigma) for TLR2 and TLR4 and IgG1 for CD14. After incubation, THP-1 cells were stimulated with 15 μM of Aβ(1-42) for 6 hours. TNFα was measured using ELISA.Courtesy Maria Udan.

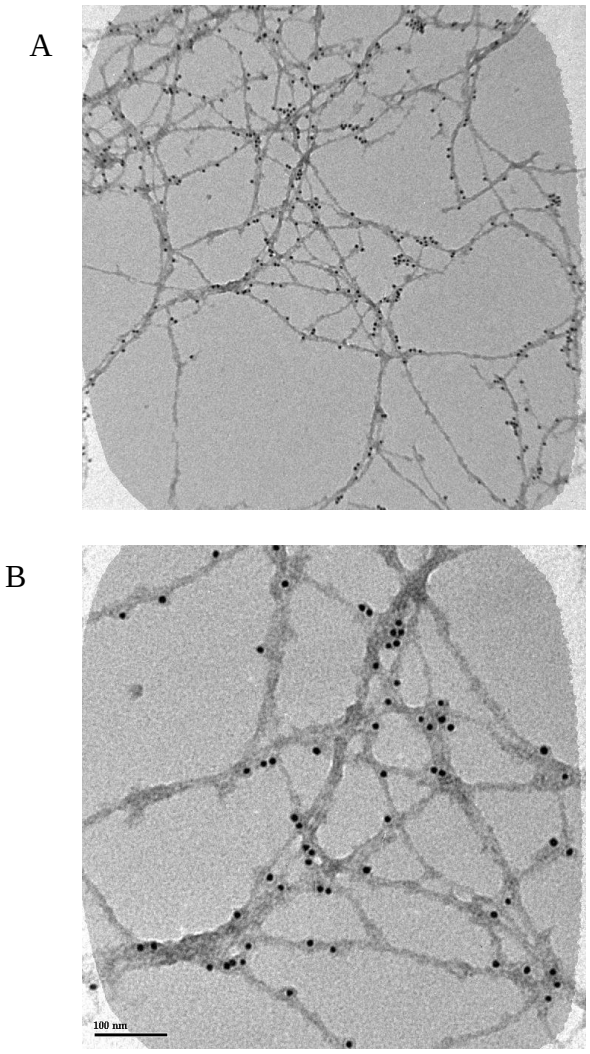

Fig 4.10. Immugold labeling of Aβ(1-42) fibrils. Aggregated Aβ(1-42) (100 µM) was diluted to concentration of 20 µM and applied on to formvar coated copper grids as described in Methods. The grids were incubated with Aβ sequence specific antibody Ab 9 for an hour, followed by incubation with secondary antibody conjugated to 10 nm gold particles. The grids are stained with 2% uranyl acetate and imaged using JOEL TEM microscope. (**Panel A)** TEM image with a magnification of 10 k.The scale bar represents 200 nm. (**Panel B)** TEM image with a magnification of 25 k. Scale bar represents 100 nm.

different donors were tested for their ability to differentiate into macrophages. These studies have shown that in the presence of Aβ(1-42), the monocytes differentiate into macrophages and also have the ability to secrete cytokines and chemokines (Fiala et al., 1998). The aggregation state of Aβ plays a crucial role in the ability to interact with cells. Structural polymorphism is a prominent feature in Aβ aggregation. Aβ that is found in the parenchyma of the brain have been shown to be a continuum of structures, and is not limited to a specific aggregation species.(Selkoe, 2004). We have identified that an early oligomeric form of Aβ(1-42) can transform the monocytes into an adherent form. The adherence induced by this oligomeric Aβ(1-42) is comparable to a known differentiating agent, PMA (Fig 4.1). We also observed that the ability to induce monocyte maturation is lost as Aβ(1-42) aggregates into fibrils. The AFM images indicate that small globular species were predominant at the time of reconstitution (Fig 4.6 B). As aggregation proceeds, fibrillar structures are formed that led to a decrease in the ability to convert the monocytes into the adherent form. The shorter peptide Aβ(1-40) did not induce cell adherence in spite of increasing the aggregation temperature (Fig 4.4). This confirms that the active species was formed in the Aβ(1-42) aggregation pathway. The mutational study with Aβ(1-42)(L34P) was done since this peptide does aggregate well due to the presence of proline at residue 34 (Williams et al., 2004). We hypothesized that there would be high monomer to oligomer ratio due to the reduced potential to aggregate. AFM images confirmed that the aggregation was not rapid, but could not specifically identify the specific species (Fig 4.6). Decreasing the amount of

starting monomer concentration, could increase the possibility of a large monomer to oligomer ratio. Decreasing the monomer concentration to 50 μM extended the lag phase of aggregation compared to 100 μM Aβ(1-42) (Fig 4.5). The fact that the 50 μM Aβ(1-42) preparation induced less cell adherence than the 100 μM sample clearly rules out the role of monomer in monocyte maturation. Therefore it is clear that specific Aβ(1-42) oligomeric species stimulates the monocyte adherence. ADDLs are oligomeric species, yet, were not able to induce monocyte adhesion (Fig 4.8). ADDLs are species that are formed after 24 hours incubation. The active species in our experiments are formed at the time of reconstitution of Aβ(1-42) solution. It is possible that the active Aβ(1-42) oligomeric species are smaller than ADDLs . The data from this part of the study indicate that Aβ(1-42) is able to induce adherence in the non adherent THP-1 monocytes. These data may provide further information in understanding the recruitment and transformation of non-resident monocytes into the CNS in AD.

We have seen that an early oligomeric species induces adherence in monocytes (Crouse et al., 2009). The data clearly indicates that the Aβ(1-42) aggregation progresses to form fibrillar structures that diminished the ability to induce cell adhesion, but induces a proinflammatory response in THP-1 cells. Here we see the influence of Aβ aggregation state in eliciting a biological response. It is possible that the early oligomeric species induces the recruitment of monocytes from blood. The activation of microglia may be separate process from that of monocyte recruitment or differentiation. From our data we see that as the aggregation progresses into formation of the intermediate fibrillar species it triggers the proinflammatory response. These fibrillar forms triggers the microglial activation. Our data also shows that an intermediate fibrillar oligomeric species of Aβ(1-

42) triggers the proinflammatory response that is mediated via receptors TLR2 and TLR4 (Udan et al., 2008). We have also seen that neutralization of TLR2 and TR4 results in attenuating the fibrillar oligomeric Aβ(1-42) induced signal (Fig 4.9). However, blocking the TLR2 and TLR4 did not attenuate the oligomeric Aβ(1-42) induced monocyte adherence (data not shown). These data further clarify the significance of Aβ aggregation state and its involvement in different biochemical pathways. These data may provide important clues into the different stages in the inflammatory pathway.

4.12 Bibliography

Akira, S., 2003. Mammalian Toll-like receptors. Curr Opin Immunol. 15, 5-11.

Antzutkin, O. N., Leapman, R. D., Balbach, J. J. and Tycko, R., 2002. Supramolecular structural constraints on Alzheimer's beta-amyloid fibrils from electron microscopy and solid-state nuclear magnetic resonance. Biochemistry. 41, 15436-15450.

Auffray, C., Fogg, D., Garfa, M., Elain, G., Join-Lambert, O., Kayal, S., Sarnacki, S., Cumano, A., Lauvau, G. and Geissmann, F., 2007. Monitoring of blood vessels and tissues by a population of monocytes with patrolling behavior. Science. 317, 666-670.

Auffray, C., Sieweke, M. H. and Geissmann, F., 2009. Blood monocytes: development, heterogeneity, and relationship with dendritic cells. Annu Rev Immunol. 27, 669-692.

Balbach, J. J., Petkova, A. T., Oyler, N. A., Antzutkin, O. N., Gordon, D. J., Meredith, S. C. and Tycko, R., 2002. Supramolecular structure in full-length Alzheimer's beta-amyloid fibrils: evidence for a parallel beta-sheet organization from solid-state nuclear magnetic resonance. Biophys J. 83, 1205-1216.

Bateman, D. A., McLaurin, J. and Chakrabartty, A., 2007. Requirement of aggregation propensity of Alzheimer amyloid peptides for neuronal cell surface binding. BMC Neurosci. 8, 29.

Bitan, G., Kirkitadze, M. D., Lomakin, A., Vollers, S. S., Benedek, G. B. and Teplow, D. B., 2003. Amyloid beta -protein (Abeta) assembly: Abeta 40 and Abeta 42 oligomerize through distinct pathways. Proc Natl Acad Sci U S A. 100, 330-335.

Chou, P. Y. and Fasman, G. D., 1978. Empirical predictions of protein conformation. Annu Rev Biochem. 47, 251-276.

Crouse, N. R., Ajit, D., Udan, M. L. and Nichols, M. R., 2009. Oligomeric amyloid-beta(1-42) induces THP-1 human monocyte adhesion and maturation. Brain Res. 1254, 109-119.

Dahlgren, K. N., Manelli, A. M., Stine, W. B., Jr., Baker, L. K., Krafft, G. A. and LaDu, M. J., 2002. Oligomeric and fibrillar species of amyloid-beta peptides differentially affect neuronal viability. J Biol Chem. 277, 32046-32053.

Fiala, M., Cribbs, D. H., Rosenthal, M. and Bernard, G., 2007. Phagocytosis of amyloid-beta and inflammation: two faces of innate immunity in Alzheimer's disease. J Alzheimers Dis. 11, 457-463.

Fiala, M., Liu, Q. N., Sayre, J., Pop, V., Brahmandam, V., Graves, M. C. and Vinters, H. V., 2002. Cyclooxygenase-2-positive macrophages infiltrate the Alzheimer's disease brain and damage the blood-brain barrier. Eur J Clin Invest. 32, 360-371.

Fiala, M., Zhang, L., Gan, X., Sherry, B., Taub, D., Graves, M. C., Hama, S., Way, D., Weinand, M., Witte, M., Lorton, D., Kuo, Y. M. and Roher, A. E., 1998. Amyloid-beta induces chemokine secretion and monocyte migration across a human blood--brain barrier model. Mol Med. 4, 480-489.

Giri, R., Shen, Y., Stins, M., Du Yan, S., Schmidt, A. M., Stern, D., Kim, K. S., Zlokovic, B. and Kalra, V. K., 2000. beta-amyloid-induced migration of monocytes across human brain endothelial cells involves RAGE and PECAM-1. Am J Physiol Cell Physiol. 279, C1772-1781.

Hardy, J. and Selkoe, D. J., 2002. The amyloid hypothesis of Alzheimer's disease: progress and problems on the road to therapeutics. Science. 297, 353-356.

Harper, J. D., Wong, S. S., Lieber, C. M. and Lansbury, P. T., Jr., 1999. Assembly of A beta amyloid protofibrils: an in vitro model for a possible early event in Alzheimer's disease. Biochemistry. 38, 8972-8980.

Heneka, M. T. and O'Banion, M. K., 2007. Inflammatory processes in Alzheimer's disease. J Neuroimmunol. 184, 69-91.

Janus, C., Pearson, J., McLaurin, J., Mathews, P. M., Jiang, Y., Schmidt, S. D., Chishti, M. A., Horne, P., Heslin, D., French, J., Mount, H. T., Nixon, R. A., Mercken, M., Bergeron, C., Fraser, P. E., St George-Hyslop, P. and Westaway, D., 2000. A beta peptide immunization reduces behavioural impairment and plaques in a model of Alzheimer's disease. Nature. 408, 979-982.

Jarrett, J. T., Berger, E. P. and Lansbury, P. T., Jr., 1993. The carboxy terminus of the beta amyloid protein is critical for the seeding of amyloid formation: implications for the pathogenesis of Alzheimer's disease. Biochemistry. 32, 4693-4697.

Jarrett, J. T. and Lansbury, P. T., Jr., 1993. Seeding "one-dimensional crystallization" of amyloid: a pathogenic mechanism in Alzheimer's disease and scrapie? Cell. 73, 1055-1058.

Kim, H. J., Chae, S. C., Lee, D. K., Chromy, B., Lee, S. C., Park, Y. C., Klein, W. L., Krafft, G. A. and Hong, S. T., 2003. Selective neuronal degeneration induced by soluble oligomeric amyloid beta protein. Faseb J. 17, 118-120.

Klegeris, A., Walker, D. G. and McGeer, P. L., 1997. Interaction of Alzheimer beta-amyloid peptide with the human monocytic cell line THP-1 results in a protein kinase C-dependent secretion of tumor necrosis factor-alpha. Brain Res. 747, 114-121.

Kopydlowski, K. M., Salkowski, C. A., Cody, M. J., van Rooijen, N., Major, J., Hamilton, T. A. and Vogel, S. N., 1999. Regulation of macrophage chemokine expression by lipopolysaccharide in vitro and in vivo. J Immunol. 163, 1537-1544.

Lambert, M. P., Barlow, A. K., Chromy, B. A., Edwards, C., Freed, R., Liosatos, M., Morgan, T. E., Rozovsky, I., Trommer, B., Viola, K. L., Wals, P., Zhang, C., Finch, C. E., Krafft, G. A. and Klein, W. L., 1998. Diffusible, nonfibrillar ligands derived from Abeta1-42 are potent central nervous system neurotoxins. Proc Natl Acad Sci U S A. 95, 6448-6453.

Le, Y., Gong, W., Tiffany, H. L., Tumanov, A., Nedospasov, S., Shen, W., Dunlop, N. M., Gao, J. L., Murphy, P. M., Oppenheim, J. J. and Wang, J. M., 2001. Amyloid (beta)42 activates a G-protein-coupled chemoattractant receptor, FPR-like-1. J Neurosci. 21, RC123.

Liao, M. Q., Tzeng, Y. J., Chang, L. Y., Huang, H. B., Lin, T. H., Chyan, C. L. and Chen, Y. C., 2007. The correlation between neurotoxicity, aggregative ability and secondary structure studied by sequence truncated Abeta peptides. FEBS Lett. 581, 1161-1165.

Lifson, S. and Sander, C., 1979. Antiparallel and parallel beta-strands differ in amino acid residue preferences. Nature. 282, 109-111.

Liu, R., McAllister, C., Lyubchenko, Y. and Sierks, M. R., 2004. Residues 17-20 and 30-35 of beta-amyloid play critical roles in aggregation. J Neurosci Res. 75, 162-171.

Lorenzo, A. and Yankner, B. A., 1994. Beta-amyloid neurotoxicity requires fibril formation and is inhibited by congo red. Proc Natl Acad Sci U S A. 91, 12243-12247.

Matsuoka, Y., Saito, M., LaFrancois, J., Saito, M., Gaynor, K., Olm, V., Wang, L., Casey, E., Lu, Y., Shiratori, C., Lemere, C. and Duff, K., 2003. Novel therapeutic approach for the treatment of Alzheimer's disease by peripheral administration of agents with an affinity to beta-amyloid. J Neurosci. 23, 29-33.

Morgan, D., Diamond, D. M., Gottschall, P. E., Ugen, K. E., Dickey, C., Hardy, J., Duff, K., Jantzen, P., DiCarlo, G., Wilcock, D., Connor, K., Hatcher, J., Hope, C., Gordon, M. and Arendash, G. W., 2000. A beta peptide vaccination prevents memory loss in an animal model of Alzheimer's disease. Nature. 408, 982-985.

Mrak, R. E. and Griffinbc, W. S., 2001. The role of activated astrocytes and of the neurotrophic cytokine S100B in the pathogenesis of Alzheimer's disease. Neurobiol Aging. 22, 915-922.

Naiki, H. and Nakakuki, K., 1996. First-order kinetic model of Alzheimer's beta-amyloid fibril extension in vitro. Lab Invest. 74, 374-383.

Oddo, S., Caccamo, A., Tran, L., Lambert, M. P., Glabe, C. G., Klein, W. L. and LaFerla, F. M., 2006. Temporal profile of amyloid-beta (Abeta) oligomerization in an in vivo model of Alzheimer disease. A link between Abeta and tau pathology. J Biol Chem. 281, 1599-1604.

Olofsson, A., Sauer-Eriksson, A. E. and Ohman, A., 2006. The solvent protection of alzheimer amyloid-beta-(1-42) fibrils as determined by solution NMR spectroscopy. J Biol Chem. 281, 477-483.

Parker, L. C., Prince, L. R. and Sabroe, I., 2007. Translational mini-review series on Toll-like receptors: networks regulated by Toll-like receptors mediate innate and adaptive immunity. Clin Exp Immunol. 147, 199-207.

Pike, C. J., Burdick, D., Walencewicz, A. J., Glabe, C. G. and Cotman, C. W., 1993. Neurodegeneration induced by beta-amyloid peptides in vitro: the role of peptide assembly state. J Neurosci. 13, 1676-1687.

Podlisny, M. B., Walsh, D. M., Amarante, P., Ostaszewski, B. L., Stimson, E. R., Maggio, J. E., Teplow, D. B. and Selkoe, D. J., 1998. Oligomerization of endogenous and synthetic amyloid beta-protein at nanomolar levels in cell culture and stabilization of monomer by Congo red. Biochemistry. 37, 3602-3611.

Ritter, M., Mennerich, D., Weith, A. and Seither, P., 2005. Characterization of Toll-like receptors in primary lung epithelial cells: strong impact of the TLR3 ligand poly(I:C) on the regulation of Toll-like receptors, adaptor proteins and inflammatory response. J Inflamm (Lond). 2, 16.

Rogers, J. and Lue, L. F., 2001. Microglial chemotaxis, activation, and phagocytosis of amyloid beta-peptide as linked phenomena in Alzheimer's disease. Neurochem Int. 39, 333-340.

Rogers, J., Lue, L. F., Walker, D. G., Yan, S. D., Stern, D., Strohmeyer, R. and Kovelowski, C. J., 2002. Elucidating molecular mechanisms of Alzheimer's disease in microglial cultures. Ernst Schering Res Found Workshop, 25-44.

Schwende, H., Fitzke, E., Ambs, P. and Dieter, P., 1996. Differences in the state of differentiation of THP-1 cells induced by phorbol ester and 1,25-dihydroxyvitamin D3. J Leukoc Biol. 59, 555-561.

Selkoe, D. J., 1989. The deposition of amyloid proteins in the aging mammalian brain: implications for Alzheimer's disease. Ann Med. 21, 73-76.

Selkoe, D. J., 1991. The molecular pathology of Alzheimer's disease. Neuron. 6, 487-498.

Selkoe, D. J., 1993. Physiological production of the beta-amyloid protein and the mechanism of Alzheimer's disease. Trends Neurosci. 16, 403-409.

Selkoe, D. J., 2004. Alzheimer disease: mechanistic understanding predicts novel therapies. Ann Intern Med. 140, 627-638.

Serpell, L. C., 2000. Alzheimer's amyloid fibrils: structure and assembly. Biochim Biophys Acta. 1502, 16-30.

Simmons, L. K., May, P. C., Tomaselli, K. J., Rydel, R. E., Fuson, K. S., Brigham, E. F., Wright, S., Lieberburg, I., Becker, G. W., Brems, D. N. and et al., 1994. Secondary structure of amyloid beta peptide correlates with neurotoxic activity in vitro. Mol Pharmacol. 45, 373-379.

Stine, W. B., Jr., Dahlgren, K. N., Krafft, G. A. and LaDu, M. J., 2003. In vitro characterization of conditions for amyloid-beta peptide oligomerization and fibrillogenesis. J Biol Chem. 278, 11612-11622.

Tsuchiya, S., Kobayashi, Y., Goto, Y., Okumura, H., Nakae, S., Konno, T. and Tada, K., 1982. Induction of maturation in cultured human monocytic leukemia cells by a phorbol diester. Cancer Res. 42, 1530-1536.

Tsuchiya, S., Yamabe, M., Yamaguchi, Y., Kobayashi, Y., Konno, T. and Tada, K., 1980. Establishment and characterization of a human acute monocytic leukemia cell line (THP-1). Int J Cancer. 26, 171-176.

Udan, M. L., Ajit, D., Crouse, N. R. and Nichols, M. R., 2008. Toll-like receptors 2 and 4 mediate Abeta(1-42) activation of the innate immune response in a human monocytic cell line. J Neurochem. 104, 524-533.

Walsh, D. M., Hartley, D. M., Kusumoto, Y., Fezoui, Y., Condron, M. M., Lomakin, A., Benedek, G. B., Selkoe, D. J. and Teplow, D. B., 1999. Amyloid beta-protein fibrillogenesis. Structure and biological activity of protofibrillar intermediates. J Biol Chem. 274, 25945-25952.

Walsh, D. M., Klyubin, I., Fadeeva, J. V., Cullen, W. K., Anwyl, R., Wolfe, M. S., Rowan, M. J. and Selkoe, D. J., 2002. Naturally secreted oligomers of amyloid beta protein potently inhibit hippocampal long-term potentiation in vivo. Nature. 416, 535-539.

Walsh, D. M., Lomakin, A., Benedek, G. B., Condron, M. M. and Teplow, D. B., 1997. Amyloid beta-protein fibrillogenesis. Detection of a protofibrillar intermediate. J Biol Chem. 272, 22364-22372.

Wang, H. W., Pasternak, J. F., Kuo, H., Ristic, H., Lambert, M. P., Chromy, B., Viola, K. L., Klein, W. L., Stine, W. B., Krafft, G. A. and Trommer, B. L., 2002. Soluble oligomers of beta amyloid (1-42) inhibit long-term potentiation but not long-term depression in rat dentate gyrus. Brain Res. 924, 133-140.

Wang, Z. M., Liu, C. and Dziarski, R., 2000. Chemokines are the main proinflammatory mediators in human monocytes activated by Staphylococcus aureus, peptidoglycan, and endotoxin. J Biol Chem. 275, 20260-20267.

Whittemore, N. A., Mishra, R., Kheterpal, I., Williams, A. D., Wetzel, R. and Serpersu, E. H., 2005. Hydrogen-deuterium (H/D) exchange mapping of Abeta 1-40 amyloid fibril secondary structure using nuclear magnetic resonance spectroscopy. Biochemistry. 44, 4434-4441.

Williams, A. D., Portelius, E., Kheterpal, I., Guo, J. T., Cook, K. D., Xu, Y. and Wetzel, R., 2004. Mapping abeta amyloid fibril secondary structure using scanning proline mutagenesis. J Mol Biol. 335, 833-842.

Wisniewski, T., Haltia, M., Ghiso, J. and Frangione, B., 1991. Lewy bodies are immunoreactive with antibodies raised to gelsolin related amyloid-Finnish type. Am J Pathol. 138, 1077-1083.

Wood, S. J., Wetzel, R., Martin, J. D. and Hurle, M. R., 1995. Prolines and amyloidogenicity in fragments of the Alzheimer's peptide beta/A4. Biochemistry. 34, 724-730.

Yan, S. D., Chen, X., Fu, J., Chen, M., Zhu, H., Roher, A., Slattery, T., Zhao, L., Nagashima, M., Morser, J., Migheli, A., Nawroth, P., Stern, D. and Schmidt, A. M., 1996. RAGE and amyloid-beta peptide neurotoxicity in Alzheimer's disease. Nature. 382, 685-691.

Yates, S. L., Burgess, L. H., Kocsis-Angle, J., Antal, J. M., Dority, M. D., Embury, P. B., Piotrkowski, A. M. and Brunden, K. R., 2000. Amyloid beta and amylin fibrils induce increases in proinflammatory cytokine and chemokine production by THP-1 cells and murine microglia. J Neurochem. 74, 1017-1025.

CHAPTER 5

Conclusion

Data from our studies indicate that Aβ(1-42) has the ability to stimulate the THP-1 monocytes for a proinflammatory response. We have also shown the significance of the Aβ(1-42) aggregation state in eliciting this response from the cells. By using a combination of biophysical and cellular assays we have identified that an intermediate fibrillar species in Aβ(1-42) aggregation pathway is capable of eliciting maximum proinflammatory response. Our data also indicate that only intermediate species formed from Aβ(1-42) aggregation solution incubated at 4°C could activate the cells for a response. Aggregation of Aβ(1-40) under similar conditions did not elicit stimulatory activity. Furthermore, high speed centrifugation of Aβ(1-42) aggregation solution established the solubility of the proinflammatory species. The centrifugation supernatant was active in stimulating the cells. Using conformation-specific antibodies, we were able to categorize the proinflammatory species as fibrillar oligomers. Our immunoprecipitation (IP) protocol, using fibril-specific antibody (OC immune serum), depleted the active species from aggregation solution, which was confirmed by depletion of proinflammatory response by the IP supernatant. Characterization of Aβ(1-42) aggregation solution by SEC enabled isolation of the peak fraction that gave maximum proinflammatory response. These studies strengthen our earlier findings (Udan et al., 2008) where we had shown the involvement of toll-like receptors, particularly TLR4 and TLR2, in Aβ-induced response. We have also shown that an early oligomeric species in

the Aβ(1-42) aggregation pathway has the ability to transform monocytes into an adherent form that look like macrophage cells. Here again we were able to display the exclusive property of Aβ(1-42) to form an early oligomeric assembly that was not formed by the oligomeric Aβ(1-42) ADDLs and the mutated Aβ(1-42) (L34P) (Crouse et al., 2009). Overall, our data displays the correlation between Aβ and the human immune response, and also pinpoints the assembly state that is involved in activating the different stages of inflammatory pathway. This study provides further clues into understanding the mechanism of Aβ induced inflammatory response and may be useful in designing therapeutic strategies towards the treatment of AD.

5.1 Bibliography

Crouse, N. R., Ajit, D., Udan, M. L. and Nichols, M. R., 2009. Oligomeric amyloid-beta(1-42) induces THP-1 human monocyte adhesion and maturation. Brain Res. 1254, 109-119.

Udan, M. L., Ajit, D., Crouse, N. R. and Nichols, M. R., 2008. Toll-like receptors 2 and 4 mediate Abeta(1-42) activation of the innate immune response in a human monocytic cell line. J Neurochem. 104, 524-533.

6. VITA

Deepa was born in Chennai, India, on January 29, 1971. She obtained her bachelor's degree in chemistry from Bharathiar University, Coimbatore, India in 1991. She earned her MS in Clinical Biochemistry from Kasturba Medical College, India, in 1994. The same year she joined PSG Institute of Medical Sciences and Research as a faculty member. In 2004 she enrolled into the graduate program at University of Missouri-St Louis (UMSL), and joined the laboratory of Dr. Michael R. Nichols. She earned her MS in Chemistry and Biochemistry from UMSL in 2006. Upon completion of requirements for the PhD program in fall 2009, she accepted a post doctoral position with Dr. Gary A. Weisman at University of Missouri-Columbia. She is married to Ajit Kumar Vasudevan, and has two children Aditi and Tejazaditya.